

**The essential iron-sulphur protein Rli1
is a key determinant of oxidative stress
resistance in *Saccharomyces cerevisiae***

Alawiah Mohammad Alhebshi, MBIoSci

Thesis submitted to the University of Nottingham for
the degree of Doctor of Philosophy

September 2013

The University of Nottingham
School of Biology

Abstract

Reactive oxygen species (ROS) are linked to a range of degenerative conditions in humans, and may cause damage to an array of cellular components. However, it is unclear which cellular target(s) of ROS may primarily account for toxicity during oxidative stress. The sensitivity of iron-sulphur (Fe-S) clusters to ROS makes these candidate determinants of ROS mediated cell killing. Ribonuclease L inhibitor (Rli1p) is a highly conserved protein that is essential in all tested eukaryotes and archaea, but requires Fe-S clusters for its crucial functions in protein synthesis. Herein, the novel hypothesis that ROS toxicity is caused by loss of Rli1p function was tested. Rli1p activity (in nuclear export of ribosomal subunits) was impaired during mild oxidative stress in yeast. In addition, resistance to pro-oxidants was decreased by *RLI1* repression and increased by *RLI1* overexpression. This Rli1p-dependency was abolished during anaerobicity and accentuated in cells expressing the Fe-S cluster defective Rli1p construct, *rli1^{C58A}*. The effects appeared specific to Rli1p as overexpression of other essential Fe-S proteins did not increase stress resistance. Methionine sulphoxide reductases (MSRs) and the Mn-superoxide dismutase (Sod2p) are known to help preserve the integrity of Fe-S clusters in cells. Here, these proteins' antioxidant actions were shown to be at least partly mediated through Rli1p. Resistance to both chronic and acute oxidative stress was Rli1p-dependent. Further experiments indicated that Rli1p-dependent protein synthesis could be a critical target of ROS and, specifically, that Rli1p function may help to protect against ROS-induced mRNA mistranslation. The study indicated that Rli1p function is a primary biological target of ROS action, owing to its essential nature but dependency on ROS-labile Fe-S clusters. Such insights could offer new approaches for combating oxidative stress-related disease.

Published Papers

Alhebshi, A., Sideri, T. C., Holland, S. L., Avery, S. V. (2012). The essential iron-sulfur protein Rli1 is an important target accounting for inhibition of cell growth by reactive oxygen species. *Mol. Biol. Cell.* 23. 18: 3582-3590.

Acknowledgements

Firstly, I would like to thank my supervisor Dr Simon Avery for his guidance and advice throughout this project. My sincere thank to king Abdul-Aziz University in Jeddah for funding and supporting my study in Nottingham. I would also like to thank all members of my lab, in particular, Dr Sara Holland and Lee Shunburne. I gratefully acknowledge Paul Dyer and Gary Jones for their helpful discussion and advice.

Most importantly, I would like to give my greatest thanks to my dear husband Hamzah Alhebshi Alhashemi, my sons Alhasan, Alhussian, Mohesien, Jawad and my lovely daughter Fatmah-Alzahra for their love, patience, as none of this would have been possible without their support, encouragement and appreciate my effort throughout my entire education journey.

My great thanks to my dear parents (father: Mohammad Alhebshi Alhashemi and a great mother kadejja Alhebshi Alhashemi) for their prayers, encouragement and support throughout my studying. I would like especially to thank my lovely sister Eman and my dear friend Huda Aljeilani for their prayers and support.

Table of Contents

Chapter 1– Introduction	10
1.1 Reactive Oxygen Species (ROS) In Biological Systems	11
1.2 The yeast <i>Saccharomyces cerevisiae</i> as eukaryotic model to study oxidative stress	13
1.3 Generation of oxidative stress in organisms	14
1.4 Antioxidant defence systems in eukaryotes	16
1.4.1 <i>Non-enzymatic defence systems</i>	16
1.4.1.1 <i>Glutathione</i>	16
1.4.1.2 <i>Polyamines</i>	17
1.4.1.3 <i>Lipid-soluble antioxidants</i>	18
1.4.1.4 <i>Metallothioneins</i>	19
1.4.1.5 <i>Glutaredoxins</i>	20
1.4.2 <i>Enzymatic defence systems</i>	21
1.4.2.1 <i>Superoxide dismutase</i>	21
1.4.2.2 <i>Catalase</i>	22
1.4.2.3 <i>Glutathione peroxidase</i>	22
1.4.2.4 <i>Methionine sulphoxide reductase</i>	23
1.5 Molecular targets of oxidative stress	26
1.5.1 <i>Loss of essential function by ROS action</i>	26
1.5.1.1 <i>Lipid peroxidation and membrane function</i>	26
1.5.1.2 <i>DNA oxidation</i>	29
1.5.1.3 <i>Protein oxidation</i>	30
1.5.1.4 <i>Protein synthesis as a ROS target</i>	33
1.6 The iron-sulphur clusters in proteins and ROS-mediated targeting	34
1.6.1 <i>Importance of Fe-S clusters in protein functions</i>	34
1.6.2 <i>Structural and chemical properties of Fe-S clusters</i>	35
1.6.3 <i>Fe-S clusters and oxidative conditions</i>	39
1.7 The biogenesis of Fe-S proteins in eukaryotes	41
1.8 Diseases linked to Fe-S proteins and their biosynthesis	45
1.9 The essential Fe-S protein Rli1	46
1.9.1 <i>Ribosome biogenesis requires the Fe-S protein Rli1</i>	49
1.9.2 <i>Rli1p and translation initiation</i>	50

1.9.3 <i>Rli1p</i> and translation termination and ribosome recycling	51
1.10 Aims of the current work.....	54
Chapter 2 - Materials and Methods	55
2.1 Strains and plasmids.....	56
2.1.1 Construction of <i>pCM10-tetATM1</i>	61
2.2 Growth conditions	64
2.3 Isolation of DNA	65
2.3.1 Genomic DNA extraction from <i>S. cerevisiae</i>	65
2.3.2 Plasmid DNA extraction from <i>E. coli</i>	66
2.3.3 Plasmid DNA extraction from <i>S. cerevisiae</i>	67
2.4 Polymerase Chain Reaction (PCR)	67
2.4.1 <i>Phusion</i> [®] High-Fidelity DNA polymerase PCR reaction.....	68
2.4.2 <i>Taq</i> DNA polymerase PCR Reaction.....	68
2.4.3 Yeast Colony PCR	69
2.4.4 Bacterial Colony PCR	69
2.5 DNA Sequencing	69
2.6 Digestion of DNA with Restriction Enzymes	70
2.7 DNA Agarose Gel Electrophoresis	70
2.8 DNA Purification from Agarose Gel	71
2.9 DNA Ligations	73
2.9.1 Ethanol Precipitation.....	74
2.10 Transformations	74
2.10.1 Transformation of plasmid DNA into Yeast.....	74
2.10.2 Preparation of Electro-competent <i>E. coli</i> XLI Blue cells	75
2.10.2.1 Transformation of plasmid DNA into <i>E. coli</i>	76
2.11 Measurement of protein synthesis rate.....	76
2.11.1 Metabolic labelling with ³⁵ S-methionine	76
2.11.2 Protein extraction from <i>S. cerevisiae</i> cells	77
2.11.3 Protein quantification with the Bradford assay	77
2.11.4 Quantification of incorporated [³⁵ S] methionine.....	78
2.12 RNA Extraction.....	78
2.13 First-strand cDNA synthesis	79
2.14 Quantitative RT-PCR (q RT-PCR)	80

2.14.1 Calculation of DNA copy number for q RT-PCR standard curves	80
2.15 Yeast culture and toxicity assays.....	81
2.15.1 Growth curve assays in broth media	81
2.15.2 Growth assays on agar	81
2.15.3 Short-term killing assays	82
2.16 Assay of nuclear Rps2p-eGFP export.....	83
2.16.1 Doubling time determination	84
2.17 Qualitative mRNA mistranslation assay	84
2.18 Quantitative mRNA mistranslation assay	85
2.19 Statistical Analysis	85
Chapter 3- Rli1p-dependent resistance to oxidative stress.....	86
3.1 Introduction	87
3.2 Doxycycline controls the expression levels of <i>RLI1</i> through tetO promoter.....	90
3.3 Rli1p-dependent resistance to oxidative stress.....	92
3.3.1 <i>RLI1</i> expression level determines the level of copper resistance in wild type cells.....	92
3.3.2 <i>RLI1</i> expression level determines the level of chromate resistance in wild type cells.....	93
3.3.3 <i>RLI1</i> expression level determines the level of H ₂ O ₂ resistance in wild type cells	96
3.3.4 <i>RLI1</i> overexpression confers a very slight effect on paraquat resistance	96
3.4 Stress resistance is specific to Rli1p, among essential Fe-S proteins.....	99
3.5 <i>RLI1</i> overexpression confers resistance to acute short-term killing by copper.....	102
3.6 Discussion.....	111
Chapter 4- Mild pro-oxidant stress and Rli1p activity.....	115
4.1 Introduction	116
4.2 Mild pro-oxidant stress perturbs Rli1p function in nuclear export of Rps2-GFP	119
4.2.1 Nuclear accumulation of Rps2p-GFP as an indicator of defective Rli1p function.....	119

4.2.2 ROS sensitivity of Rli1p function in nuclear export of ribosomal subunits.....	121
4.3 ATM1 overexpression restores Rli1p activity in nuclear Rps2-GFP export during copper stress.....	126
4.4 The integrity of Fe-S clusters is required for Rli1p activity during mild oxidative stress	128
4.4.1 Expression of an iron-sulphur cluster mutant, <i>rli1</i> ^{C58A} , heightens cellular ROS sensitivity	128
4.4.2 Expression of <i>rli1</i> ^{C58A} in place of Rli1 decreases nuclear Rps2 GFP export during copper stress	130
4.5 Oxygen-requirement in Rli1p-dependent stress resistance	130
4.6 Oxygen requirement for the stress sensitivity of <i>rli1</i> ^{C58A} -expressing cells.....	133
4.7 Discussion.....	135
Chapter 5- Influence of specific gene deletion and essential metals on Rli1p function in stress resistance	139
5.1 Introduction	140
5.2 Genes that help preserve Rli1p function during oxidative stress	142
5.2.1 MSRs have a role in Rli1p-dependent nuclear export of ribosomal subunits.....	142
5.2.2 Sod2 activity is required for Rli1p-dependent pro-oxidant resistance	144
5.2.2.1 Copper sensitivity phenotype of Sod2 defective cells....	144
5.2.2.2 Manganese treatment confers Cu-resistance in <i>sod2Δ</i> cells	144
5.2.2.3 RLI1 overexpression enhances Cu-resistance in Sod2 defective cells	146
5.3 Restoration of Rli1p-dependent stress resistance under conditions that promote Fe-S cluster reconstitution	149
5.4 Discussion.....	153
Chapter 6- Role of RLI1 expression level on translation fidelity during ROS-induced mRNA mistranslation.....	156
6.1 Introduction	157

6.2 <i>RLI1</i> overexpression confers resistance to certain agents that cause mRNA mistranslation.....	160
6.2.1 <i>RLI1</i> overexpression protects against mistranslation-causing agents.....	160
6.2.2 <i>RLI1</i> overexpression protects against synergistic toxicity of paromomycin and CrO ₃	160
6.3 <i>RLI1</i> overexpression corrects mRNA mistranslation.....	163
6.3.1 <i>RLI1</i> overexpression protects against paromomycin and CrO ₃ -induced mRNA mistranslation: qualitative assay	163
6.3.2 <i>RLI1</i> overexpression protects against ROS-induced mRNA mistranslation: qualitative assay.....	164
6.3.3 <i>RLI1</i> overexpression decreased the rate of mRNA mistranslation induced by ROS and paromomycin: quantitative assay	168
6.4 Discussion.....	173
Chapter 7- Concluding Remarks	176
7.1 Concluding Remarks.....	177
References.....	183

List of Figures

Figure 1.1- Diastereomeric structure of methionine sulfoxide: Met-S-(O) and Met-R-(O)	25
Figure 1.2- Mechanism of lipid peroxidation	28
Figure 1.3- [2Fe-2S] cluster structure of ferredoxin	38
Figure 1.4- [4Fe-4S] cluster structure.....	38
Figure 1.5- A model of Fe-S protein biogenesis in eukaryotes	44
Figure 1.6- The iron-sulphur domains of Rli1p.....	48
Figure 2.1- Maps of key plasmids utilised during this study.....	57
Figure 2.2- Construction of <i>pCM190-tetATM1</i>	63
Figure 2.3- DNA ladders 1kb and 100 bp used in agarose gel electrophoresis.....	72
Figure 2.4- Map of pJET1.2/blunt Vector	74
Figure 3.1- qRT-PCR analysis of <i>RLI1</i> expression	91
Figure 3.2- <i>RLI1</i> expression level determines cellular copper resistance	94
Figure 3.3- <i>RLI1</i> expression level determines cellular chromium resistance	95
Figure 3.4- <i>RLI1</i> expression level determines cellular H ₂ O ₂ resistance	97
Figure 3.5- <i>RLI1</i> expression level determines cellular paraquat resistance	98
Figure 3.6- Overexpression of essential Fe-S proteins other than Rli1 does not increase stress resistance	100
Figure 3.7- Overexpression of essential Fe-S proteins other than Rli1 does not increase stress resistance	101
Figure 3.8- Killing concentrations of copper detected by colony forming unit (CFU) counts.....	103
Figure 3.9- <i>RLI1</i> overexpression protects against cell killing by Cu	104
Figure 3.10- <i>RLI1</i> overexpression protects against cell killing by Cu... ..	106
Figure 3.11- Cycloheximide inhibits protein synthesis in a short term exposure.....	107

Figure 3.12- <i>RLI1</i> overexpression protects against cell killing by cycloheximide	108
Figure 3.13- <i>RLI1</i> overexpression alters protein synthesis rate	110
Figure 4.1- Rli1p is required for nuclear export of ribosomal subunits	120
Figure 4.2- Rli1p activity in Rps2p-GFP export is sensitive to mild copper stress	123
Figure 4.3- Rli1p-dependent activity in ribosomal subunit Rps2p export is decreasing during mild pro-oxidant stress	124
Figure 4.4- Rli1p-dependent activity in ribosomal subunit Rps2p export is decreased during mild copper stress of <i>S. cerevisiae</i> BY4741	125
Figure 4.5- <i>ATM1</i> overexpression restores Rli1p function during mild copper stress	127
Figure 4.6- Expression of an iron-sulphur (Fe-S) cluster Rli1 mutant (<i>rli1^{C58A}</i>) heightens cellular ROS sensitivity.....	129
Figure 4.7- Expression of the Fe-S cluster mutant <i>rli1^{C58A}</i> heightens defective Rli1p function during copper stress	131
Figure 4.8- Rli1p-dependent resistance to pro-oxidants requires oxygen.....	132
Figure 4.9- Sensitivity of <i>rli1^{C58A}</i> -expressing cell to pro-oxidants is suppressed during anaerobicity	134
Figure 5.1- Exacerbation of defective Rli1p function in <i>msrΔ</i> mutant cells during mild copper stress.....	143
Figure 5.2- Copper sensitivity phenotype of <i>sod2Δ</i> mutant cells	145
Figure 5.3- Manganese treatment protects against Cu toxicity	147
Figure 5.4- <i>RLI1</i> overexpression rescues Cu-sensitivity of Sod2p depleted cells.....	148
Figure 5.5- Restoration of cellular copper resistance by supplementation with Fe ³⁺	151
Figure 5.6- Restoration of cellular H ₂ O ₂ resistance by supplementation with Fe ³⁺	152
Figure 6.1- <i>RLI1</i> overexpression protects against mRNA mistranslation agents	161
Figure 6.2- <i>RLI1</i> overexpression protects against synergistic toxicity of paromomycin and CrO ₃	162

Figure 6.3- *RLI1* overexpression protects against paromomycin and CrO₃-induced mRNA mistranslation 166

Figure 6.4- *RLI1* overexpression protects against copper-induced mRNA mistranslation 167

Figure 6.5- *RLI1* overexpression does not appear to protect against paraquat-induced mRNA mistranslation, and H₂O₂ does not cause UGA codon readthrough..... 169

Figure 6.6- Mild effect on yeast growth at concentrations of agents used in short-term dual-luciferase assays 170

Figure 6.7- *RLI1* overexpression suppresses mRNA mistranslation caused by various stressors 172

List of Tables

Table 1- <i>S. cerevisiae</i> strains used in this study.....	58
Table 2- Primers used to generate <i>ATM1</i> fragment for insertion in pCM190	62
Table 3- Amino Acid and Antibiotic Concentrations.....	65
Table 4- Phusion® High-Fidelity DNA Polymerase PCR Reaction Mixture	68
Table 5- Taq DNA Polymerase PCR Reaction Mixture.....	69
Table 6- Sequencing Primers.....	70
Table 7- qRT-PCR primers.....	80
Table 8- Concentrations of stressors and chemical compounds used during this study.....	83

Chapter 1- Introduction

1.1 Reactive oxygen species (ROS) in Biological systems

Reactive oxygen species (ROS) are a compulsory evil of aerobic life and unavoidable in aerobic organisms which depend on oxidative processes for life (Manda et al., 2009). Reactive oxygen species are chemically reactive, unstable molecules containing oxygen. They are generally perceived as toxicants that readily react with various biological targets such as lipids, proteins, and DNA to cause oxidative deterioration, and alter their normal functions (Avery, 2011). Moreover, ROS can be generated as secondary products of various metabolic pathways localized in different cellular compartments, such as β -oxidation in peroxisomes, prostaglandin synthesis and detoxification reactions by cytochrome P450 (Trachootham et al., 2009). Furthermore, ROS generation is elevated by environmental perturbation, with oxidative stress being common to the effects of diverse natural (e.g. radiation) and anthropogenic (e.g. chemical pollutant) stresses (Avery, 2001; Limon-pacheco & Gonsebatt, 2009). Oxidative damage by ROS in biological systems depends on the delicate equilibrium between ROS production, and their scavenging (Sharma et al., 2012).

Oxygen-derived pro-oxidants, which can cause damage to biological targets, and are generally referred to as ROS can be classified into two types of ROS: radicals and non-radicals. The radical type encompasses oxygen metabolites (compounds) such as superoxide radical anion ($O_2^{\cdot-}$), nitric oxide radical (NO^{\cdot}), peroxy (ROO^{\cdot}), hydroxyl radical (OH^{\cdot}), and alkoxy radicals (RO^{\cdot}) (Kohen et al., 2003). These species are radicals since they contain one or more unpaired electron(s) in their outer molecular orbital (Halliwell & Gutteridge, 1999., Rice-Evans & Burdon, 1994). The availability of unpaired electron(s) results in high reactivity of these species by their affinity to donate or acquire another electron to achieve stability (Halliwell & Gutteridge, 1999). The non-radical ROS have paired electron(s) but are chemically reactive and can be transformed in to radical ROS. There are a large variety of non-radical ROS include hydrogen peroxide (H_2O_2), ozone (O_3), singlet oxygen (1O_2), and

hypochlorous acid (HClO) (Trachootham et al., 2009). Even though hydrogen peroxide molecules are considered reactive oxygen metabolites, they are not radicals; they can, nevertheless, cause damage to the cell at a comparatively low concentration (10 μ M). They are freely dissolved in aqueous solution and can simply penetrate biological membranes. Their damaging chemical effects can be direct or indirect. Direct activity derives from their innate oxidizing characteristics which can cause oxidation of DNA, lipid, -SH groups, and keto acids, in addition to degradation of haem proteins, release of iron and inactivation of enzymes. When acting indirectly, they serve as a source of more damaging species, such as OH $^-$ or HClO (Halliwell et al., 2000).

ROS damage is linked to serious diseases in humans (Roberts et al., 2009). ROS that are produced by normal mitochondrial respiration can damage mitochondrial DNA (mtDNA), and have been implicated in degenerative diseases including cancer and aging (Doudican et al., 2005). Reactive oxygen species that are generated by deposition of amyloid beta (A β) peptides in the brain, which is a peptide of 36–43 amino acids that is processed from the Amyloid precursor protein, are implicated in Alzheimer's inflammatory and neurodegenerative pathology (Shen et al., 2010).

A range of carcinogens may also exert their effect by generating ROS during metabolism (Waris & Ahsan, 2006). In addition, Parkinson's disease is due to the degeneration of dopaminergic neurotransmission in the substantia nigra region of the brain. In the cell cytosol, dopamine metabolism results in the generation of hydrogen peroxide (H $_2$ O $_2$), which in turn can be turned to highly reactive ROS such as hydroxyl radicals. These hydroxyl radicals can damage dopaminergic neurons. Patients suffering from this disease show elevated lipid peroxidation, increased production of ROS, decreased levels of glutathione and elevated levels of iron (Friedlich et al., 2009). Furthermore, Friedreich's ataxia (FRDA) is an autosomal recessive neurodegenerative disorder related to deficiency of the mitochondrial protein frataxin (Tracey & Tong, 2008). Frataxin deficiency appears to be always associated with increased sensitivity

to ROS (Bayot et al., 2011). Damage of cellular organelles and enzymes, increased lipid peroxidation, and development of insulin resistance can be results of high ROS levels and the simultaneous decline in antioxidant defence mechanisms. These consequences of oxidative stress can enhance the development of complications in diabetes mellitus (Maritim et al., 2003).

1.2 The yeast *Saccharomyces cerevisiae* as eukaryotic model to study oxidative stress

Saccharomyces cerevisiae is extensively used as an ideal eukaryotic organism model to study the regulation of gene expression in response to oxidative stress, metal transport, and metal homeostasis. Several features of this organism make it appropriate for genetic, biochemical and cell biological studies. The completion of the *S. cerevisiae* genome sequence in 1996 which has a size of 12 million base pairs and about 6,275 genes, closely organized on 16 chromosomes, where 18.2% of the genes are essential for cells viability, made it the first eukaryotic model enabling genome-wide assignment of gene function (Altmann et al., 2007). Furthermore, *S. cerevisiae* can be cultured easily in inexpensive media and has a short generation time (less than 2hr under ideal conditions). *S. cerevisiae* is used as an ideal model system to describe the basic molecular mechanism of mitochondrial DNA damage because it is a facultative anaerobe. Therefore, cells which suffer loss of mitochondrial respiration can still proliferate and be studied when a fermentable carbon source (glucose) is provided (Shadel, 1999). Furthermore, many expression vectors, including episomal ones, which behave as extrachromosomal without causing any disruption of host genome, (Parent & Bostian, 1995), and other useful tools such as reporter genes, immunotags, and genetically selectable markers (Gueldener et al., 2002; Gueldener et al., 1996; Janke et al., 2004; Sheff & Thorn, 2004) are available for *S. cerevisiae*. The availability of highly efficient transformation methods has aided *S. cerevisiae* genetic engineering (Gietz & Woods, 2001). The extraordinary high efficiency of homologous recombination in this species has facilitated targeted

manipulations within chromosomes (Klinner & Schafer, 2004). As was mentioned previously 18.2% of yeast genes are required for viability, imposing some limitation on genetic analysis with knockouts. However, promoter-shut off/on (TetO promoter) strains as well as heterozygous mutants have been created to facilitate analysis of essential yeast genes (Mnaimneh et al., 2004).

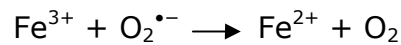
As a result of the limitations of the experimentation with animal and plant systems, *S. cerevisiae* is considered to be a useful eukaryotic model in many studies, including investigation of the mechanisms of metal toxicity (Avery, 2001). *S. cerevisiae* also exhibits considerable protein sequence conservation with humans, such that 40% of cloned single-gene determinants of human heritable disease are thought to have a functional orthologue in yeast (Foury, 1997). Furthermore, many yeast genes related to cell-defence responses are related to human diseases (Bolotin-Fukuhara et al., 2010) such as the Cu-Zn SOD (Sod1p), which is required for defence against superoxide anion through its activity in conversion $O_2^{\cdot-}$ to hydrogen peroxide and oxygen, is involved in amyotrophic lateral sclerosis (Morimoto et al., 2012), in addition, the antioxidant enzyme catalase, which protects yeast cells against H_2O_2 toxicity, is related to intestinal cancers and inflammatory intestines diseases (Calinescu et al., 2012). As a result of that, experiments with *S. cerevisiae* may support our understanding of such genetic disease in humans. Yeast has been used to study hypoxic and oxidative stress as these may relate to aging or diseases such as cancer due to many of the proteins involved in such disorders and associated pathways being functionally conserved between yeasts and humans (Bharadwaj et al., 2010). Functional description of human genes is commonly achieved by their heterologous expression in mutant yeasts, testing for functional complementation.

1.3 Generation of oxidative stress in organisms

Oxidative stress describes a state in which cellular antioxidant defence mechanisms are insufficient to scavenge or inactivate ROS, or excessive ROS are produced, or both. An imbalance

between pro-oxidants and antioxidant defences in a biological system is thought to be involved in the pathogenesis of more than a hundred diseases (Djordjevic, 2004). The balance between generation and elimination of ROS maintains the proper function of redox-sensitive signalling proteins under physiological conditions, which ensures that the cells respond properly to endogenous and exogenous stimuli. When redox homeostasis is disturbed, oxidative stress may lead to cell death (Trachootham et al., 2008). For example, the metabolic abnormalities of diabetes are associated with overproduction of mitochondrial superoxide ($O_2^{\cdot-}$) in endothelial cells, and in the myocardium (Giacco & Brownlee, 2010). Also, increased glucose flux enhances oxidant production and impairs antioxidant defences by multiple interacting non-enzymatic, enzymatic and mitochondrial pathways (Mehta et al., 2006; King & Loeken, 2004). Cellular metabolism may produce ROS either by means of energy transfer which can trigger molecular oxygen to form singlet oxygen (1O_2), or by electron transfer that forms superoxide anion radicals ($O_2^{\cdot-}$) from molecular oxygen (Mohora et al., 2007). Moreover, between 0.4 and 4% of all oxygen consumed is reduced to $O_2^{\cdot-}$ by the mitochondrial electron transport chain through normal oxidative phosphorylation, which is essential for producing ATP (Boveris, 1984). Also, in normal conditions, superoxide ($O_2^{\cdot-}$) can be converted into other ROS such as H_2O_2 by the mitochondrial enzyme, manganese superoxide (Mn-SOD) within the mitochondria and by copper and zinc (CuZn-SOD) in the cytosol (Mendez et al., 2005; Faraci & Didion, 2004). H_2O_2 is then either detoxified to H_2O and O_2 by cellular enzymatic defence systems such as glutathione peroxidases in combination with glutathione reductase, or by catalases. However, H_2O_2 can be transformed to the highly reactive hydroxyl radical (HO^{\cdot}) in the presence of reduced transition metals such as Cu or Fe generating oxidative stress (Mohora et al., 2007). Catalysis of free radical production by metal is well known for iron and copper, and to a lesser extent for metals like chromium and cobalt. Metals can generate free radicals through various mechanisms, the Fenton and Haber-Weiss type reactions being the most common leading to generation of the hydroxyl radicals (OH^{\cdot})

(Jomova & Valko, 2011) from H_2O_2 and $\text{O}_2^{\bullet-}$. Reduction of ferric ion (Fe^{3+}) to ferrous ion (Fe^{2+}) is the first step of the catalytic reaction as following:



Net reaction:



1.4 Antioxidant defence systems in eukaryotes

Continuous exposure to different types of oxidative stress from many sources has led organisms to develop mechanisms for defence against oxidative stress. Cellular redox balance is preserved by antioxidant defence systems that neutralize ROS (Manda et al., 2009). Cells have both enzymatic and nonenzymatic defence systems to preserve cellular redox state and to defend their cellular components (Jamieson, 1998). The responses invoked by organisms to counter oxidative stress have received considerable research attention over the last two decades. These include the up-regulation of ROS-scavenging proteins, or enzymes that reverse oxidative damage. Oxidative stress responses are now well characterized in a diverse range of organisms (Imlay, 2008).

1.4.1 Non-enzymatic defence systems

Non-enzymatic defence system includes low molecular weight compounds which act generally as radical scavengers, being oxidized by ROS and thus eliminating oxidants from solution to maintain cellular redox balance and protecting various cell components against oxidation. These molecules may be soluble in aqueous or lipid surroundings (Jamieson, 1998). Several non-enzymatic antioxidants are present in biological systems such as:

1.4.1.1 Glutathione

Glutathione (GSH) is a tripeptide with a gamma peptide linkage between the amine group ($-\text{NH}_2$) of cysteine and the carboxyl group ($-\text{COOH}$) of the glutamate side-chain. Moreover, glutathione is a low-molecular-weight antioxidant, thiol-containing tripeptide termed

glutamic acid-cysteine-glycine (GSH) in its reduced form and glutathione disulfide (GSSG) in its oxidized form; the GSSG form arises when two GSH molecules join via the oxidation of the -SH groups of the cysteine residue to form a disulphide bridge (Halliwell & Gutteridge, 1999). Reduced glutathione (GSH) has essential roles as a non-enzymatic defence system in maintaining redox homeostasis by acting as a direct scavenger of ROS such as singlet oxygen, hydroxyl radicals and superoxide radicals. In addition, GSH is a co-substrate for peroxide detoxification by glutathione peroxidases (GPx) and for conjugation by glutathione S-transferases. Thus, GSH can help reduce protein disulphides and regulate the thiol/disulphide status of the cell via disulphide exchange reactions. The oxidized form of glutathione (GSSG) is formed during these reactions and converted back to reduced glutathione by glutathione disulphide reductase (Schafer & Buettner, 2001). *S. cerevisiae* glutathione-deficient mutants have been shown to be hypersensitive to oxidants (Stephen & Jamieson, 1996).

1.4.1.2 Polyamines

Polyamines are a group of aliphatic amines, having two or more primary amino groups -NH₂ and as a result of their anion- and cation-binding properties they could act as antioxidants which involve radical scavenging (Bors et al, 1989). They have been shown to inhibit both lipid peroxidation and metal-catalysed oxidative stress (Kitada et al., 1979; Tadolini, 1988). Elevated cellular polyamines inhibit oxidative stress induced by exposure to arsenite (Zou et al., 2012). Several studies have shown that polyamines may play a role in protecting the cells of a wide range of organisms from oxidative damage caused by elevated ROS concentrations (Chattopadhyay et al., 2002; Rider et al., 2007; Burritt, 2008). Nayvelt et al. (2010) showed that both natural and synthetic polyamines can protect DNA from damage caused by oxidative stress and enhance the stability of DNA. It has been suggested that polyamines can scavenge directly ROS, especially hydroxyl radicals that readily target DNA. Furthermore, due to their positive charges, polyamines are able to

bind by electrostatic linkage to many cellular macromolecules with a negative charge such as proteins, RNA and DNA (Kusano et al., 2008). Vijayanathan et al. (2002) showed that when 89-90% of the charges associated with DNA can be neutralized through binding with polyamines. DNA compaction is induced, limiting the accessibility of hydroxyl radicals to target sites within the DNA, and therefore protecting against oxidative stress.

1.4.1.3 Lipid-soluble antioxidants

Antioxidants that are soluble in lipid are known as lipid-soluble antioxidants; they are localized to cellular membranes and lipoproteins, and protect cell membranes from lipid peroxidation (Sies, 1997; Krinsky, 1998). The most abundant lipid-soluble antioxidant is alpha-tocopherol (vitamin E) which is present in all cells in human tissues, and is described as the first line of defence against lipid peroxidation (Pekmezci, 2011). Dam et al. (2003) showed that alpha-tocopherol protects cultured endothelial cells against H₂O₂-induced lipid peroxidation via its reaction with radicals such as lipid peroxy radical (ROO⁻). In addition, it has been suggested that vitamin E primarily neutralizes H₂O₂ by raising the intracellular level of glutathione (Shimpuku et al., 2000). Furthermore, based on studies in animal cell-derived membranes, tocopherols were shown to quench singlet oxygen (¹O₂) and scavenge a variety of radicals (Bramley et al., 2000). A mechanism of alpha-tocopherol action involves reducing radicals by donating a single electron, leading to the creation of a relatively stable tocopheroxyl radical. Following donation of a second electron from the tocopheroxyl radical the non-radical product tocopherol quinone is formed (Stoyanovsky et al., 1995; May et al., 1998). Alpha-tocopherol scavenges ROS and lipid peroxides such as those generated during stress from ultraviolet radiation (Yuen & Halliday, 1997).

Another example of lipid-soluble antioxidant is ubiquinol, which is the reduced form of ubiquinone and also termed coenzyme Q. It holds electrons rather loosely, so it donates its electrons to stabilizing unstable ROS, and therefore acts as an antioxidant. It is

located in plasma lipoprotein, all membranes and in the inner membrane system of the mitochondria, where it is an essential electron carrier in the mitochondrial respiratory chain (Maroz et al., 2009).

1.4.1.4 Metallothioneins

A cadmium binding protein was the first metallothionein (MT) isolated, from horse kidney (Margoshes & Vallee, 1957). There are two major isoforms MT-I and MT-II, which are low-molecular-weight (6-7 kDa), non-enzymatic proteins usually consisting of a single polypeptide chain of 61 amino acids characterized by a high content of sulphur (present as cysteine), and metals such as zinc (Zn) and copper (Cu) (Kagi & Vallee, 1960; Margoshes & Vallee, 1957). Several studies have suggested that MT has a role in the homeostasis of essential metals such as zinc and copper, detoxification of toxic metals such as cadmium and mercury, and in protecting against oxidative stress (Oliver & Eva, 2009). MT has the capacity to bind a number of essential and non-essential metal ions and these binding interactions are thermodynamically stable as a result of the affinity of sulphur for transition metals (Kang, 2006). MT is ubiquitous and accumulates under states of oxidative stress (Penkowa et al., 2005). *In vitro*, metallothioneins showed oxyradical scavenging ability, indicating that they may particularly neutralize hydroxyl radicals (OH[•]). Such antioxidant properties of MTs originate from sulphhydryl nucleophilicity (Viarengo et al., 2000), since most metals have a strong affinity for nucleophilic ligands (Flora et al., 2007), as well as from metal complexation. A Cu-MT exhibits antioxidant activity in yeast by sequestration of copper (Viarengo et al., 2000). Shestivska et al. (2011) showed that insertion of MT gene into the DNA of tobacco plants considerably enhances their antioxidant properties in comparison with the non transgenic plants. In yeast, increased MT-I and MT-II (Cu-MT) levels can functionally compensate for deficiency of Cu/Zn-superoxide dismutase (Cu/Zn-SOD) in the defence against oxidative stress (Tamai et al., 1993).

1.4.1.5 Glutaredoxins

Glutaredoxins (GRXs) are thiol oxidoreductases required for maintaining thiol/disulphide equilibrium in cell proteins (Holmgren, 1989) and regulating the redox state of cysteine thiol groups, major targets of protein oxidants, through utilizing GSH as reductant (Lillig et al., 2008). Preservation of cellular redox homeostasis and protection against oxidative stress are important cellular functions of glutaredoxins (Kalinina et al., 2008). Grx's have antioxidant properties by virtue of the reducing power of their active site (CXXC), which catalyzes the transfer of electrons from reduced glutathione to disulphides (Holmgren, 1989). The active site (CXXC) is a fragment of amino acid sequence (commonly Cys-Pro-Tyr-Cys) with two functionally active thiols in the active center (Bushweller et al., 1994; Nordstrand et al., 1999). Grx's are found in all taxonomic groups including prokaryotes, and eukaryotes from yeasts to plants and humans (Fernandes & Holmgren, 2004). Furthermore, glutaredoxins preserve functional SH-groups from oxidation and re-establish functionally active thiols by catalyzing S-glutathionylation of proteins, which is an important regulatory mechanism due to the reversible modification of protein thiols (Daily et al., 2001; Klatt et al., 1999), and deglutathionylation of proteins, affecting structure and function and preserving the redox-dependent thiol/disulphide state of proteins (Kalinina et al., 2008). Formation of mixed disulphides from protein thiols and glutathione (GSH) is a key event in regulation of cell response to oxidative stress. Eight glutaredoxins have been characterized in *S. cerevisiae*, described as Grx1 to Grx8 (Grant, 2001; Herrero & de la Torre-Ruiz, 2007; Lillig & Holmgren, 2007; Mesecke et al., 2008; Eckers et al., 2009). Similar to humans, yeast Grx5 is involved in maintenance of iron homeostasis (Wingert et al., 2005; Rodriguez-Manzaneque et al., 2002). *GRX5* knockout in yeasts leads to oxidative stress as a result of iron accumulation in the cell, and inactivation of enzymes containing [Fe-S] clusters (Rodriguez-Manzaneque et al., 2002). Mesecke et al. (2008) showed that Grx6 and Grx7 are essential for cell resistance to oxidative stress.

1.4.2 Enzymatic defence systems

Antioxidant enzymes provide protection within the cell against reactive oxygen species (ROS) by catalysing the neutralization of ROS, or repairing oxidative damage (Szaleczky et al., 1999). Enzymatic defence systems include a variety of proteins which differ from each other in their intracellular distribution, structure or mode of defence against ROS:

1.4.2.1 Superoxide dismutase

Some intracellular antioxidant defence is provided by superoxide dismutases (SODs), which catalyze the conversion of superoxide anion to hydrogen peroxide and oxygen and can be required to sustain life in aerobic conditions (McCord et al., 1971). Several classes of the enzyme have since been specified and the proteins in this family differ in their cofactors and structure, each containing a transition metal cofactor in its catalytic centre. The Cu-Zn SOD (Sod1p) requires copper and zinc for its activity. Cu-Zn SOD is widely localized in the cytoplasm and intermembrane space, and protects *S. cerevisiae* cells against copper toxicity due to the metal binding activity of the protein (Culotta et al., 1995). Addition of potassium superoxide (KO_2), which generates superoxide (O_2^-), gave increased Cu-Zn SOD (Sod1) levels (Rao et al., 2008). On the other hand, Mn-SOD (Sod2) can be found in prokaryotic cells and eukaryotic mitochondria (Halliwell & Cuttidge, 1999). Mn-SOD was also found in the chloroplasts of the marine diatom *Thalassiosira pseudonana* to minimize oxidative stress associated with photosynthesis (Wolfe-Simon et al., 2006). Mn-SOD is a major mitochondrial antioxidant enzyme which acts as superoxide scavenger in mitochondria (Weisiger & Fridovich, 1973). The ability of Sod2 to reduce ROS levels and increase resistance to oxidative stress is strongly induced by the action of a mitochondrial deacetylase, Sirt3 action which deacetylates two critical lysine residues on Sod2 and enhances its antioxidant activity (Qiu et al., 2010). The fungal pathogen *Histoplasma capsulatum* has the ability to survive under oxidative stress conditions where superoxide dismutase (Sod3p) is produced for extracellular

protection from exogenous superoxide (O_2^-), while intracellular protection occurs by Sod1 (Youseff et al., 2012). Yeasts lacking both mitochondrial and cytosolic SOD grow very weakly in aerobic conditions, but relatively well under anaerobic conditions (Longo et al., 1996).

1.4.2.2 Catalase

The antioxidant enzyme catalase (CAT) has a vital function in protection against damage caused by reactive oxygen species due to its role in catalyzing the breakdown of H_2O_2 into water (H_2O) and oxygen (O_2) molecules (Ahn *et al.* 2006). Catalase is expressed in almost all types of eukaryotic cell, and is considered to be the most important regulator of H_2O_2 metabolism. Iron is essential for its activity and attached to the active site of the enzyme (Kirkman & Gaetani, 2007; Chelikani et al., 2004). Catalases in yeast are encoded by *CTA1* and *CTT1* genes; Cta1p is localized in the peroxisomes (Susani et al., 1976) and is thought to detoxify peroxide generated by fatty acid β -oxidation (Skoneczny et al., 1988). On the other hand, Ctt1p is localized in the cytosol and plays a role in scavenging H_2O_2 (Marchler et al., 1993). Moreover, Abbott et al. (2009) showed that cytosolic catalase (Ctt1) overexpression in *S. cerevisiae* decreases lactic acid-induced oxidative stress, and increases aerobic growth levels. In addition, elevated superoxide dismutase and catalase levels allowed the evolution of *S. cerevisiae* in medium with high concentrations of copper (Adamo et al., 2012).

1.4.2.3 Glutathione peroxidase

Since mitochondria do not have catalase, an alternative defence against the potentially toxic properties of H_2O_2 is glutathione peroxidase (GPX) activity (Chance et al., 1979). GPXs are considered key essential intracellular antioxidant enzymes in defence against ROS-mediated damage to proteins, nucleic acids and membrane lipids. They reduce a variety of hydroperoxides ranging from H_2O_2 to complex organic hydroperoxides (ROOH) (ji & La et al., 2000). Gpx enzymes in mammals require reduced glutathione (GSH) or in some cases thioredoxin (Trx) or glutaredoxin (Grx) as electron donor to reduce

H₂O₂ or organic hydroperoxide (ROOH) to water (H₂O) and alcohol (ROH) (Bjornstedt et al., 1997; Bjornstedt et al., 1994; Holmgren et al., 2005; Martins et al., 2005).

In humans, glutathione peroxidase was identified as an erythrocyte enzyme defending hemoglobin from oxidative damage (Mills, 1957). Most human Gpxs are selenoenzymes which contain a highly reactive selenocysteine (Se-Cys) residue in their active site (Flohe et al., 1973). By contrast, seleno-independent GPXs were found in yeast and named non selenium Gpx (NS-Gpx), where the Se-Cys residue of the active site is replaced by a cysteine (Herbette et al., 2007). It was found that NS-GPXs are not reduced by GSH in *S. cerevisiae* but are efficiently reduced by thioredoxins (Tanaka et al., 2005). Avery & Avery (2001) discovered a phospholipid hydroperoxidase (PHGPx) function for the yeast GPXs that protects against phospholipid hydroperoxides and consequently lipid peroxidation. A peroxisomal glutathione peroxidase (Pmp20) has been found to be the primary scavenger of ROS such as H₂O₂ that are produced via methanol metabolism by the yeast *Pichia pastoris* during its growth on methanol; the growth defect observed in the *pppmp20Δ* mutant resulted from a failure to detoxify ROS (Taisuke et al., 2009).

1.4.2.4 Methionine sulfoxide reductase

The side chains of the amino acid residues that contain sulphur (cysteine and methionine) are especially susceptible to oxidation by ROS. Methionine is oxidized to methionine sulfoxide (MetO) by the addition of an oxygen atom to its reactive sulphur atom (Weissbach et al., 2005). Such modifications may change protein function or modulate protein activity (Stadtman, 2001). The product of methionine oxidation is a diastereomeric mixture of methionine S-sulfoxide (Met-S-SO) and methionine R-sulfoxide (Met-R-SO) residues in protein (Sharov et al., 1999; Sharov & Schoneich, 2000) (Fig 1.1).

Methionine sulfoxide reductases (MSRs) are crucial repair enzymes that protect cells by repairing oxidized methionine residues in proteins through catalysis of the reduction of MetO to methionine (Weissbach et al., 2002; Kim & Gladyshev, 2007). Two forms of these

enzymes exist, MsrA and MsrB, which reduce free and protein-bound Met-(S)-SO and Met-(R)-SO, respectively (Weissbach et al., 2005). Recently, a new class of MSR, named free methionine-(R)-sulfoxide reductase (fRMSR), has been identified and characterized in *S. cerevisiae* which is specific for repairing free Met-(R)-SO but inactive with protein-based Met-(R)-SO (Lee et al., 2008). Depletion of MSRs increases sensitivity to oxidative stress by ROS. Calcium regulatory proteins such as Calmodulin (CaM) are functionally sensitive to methionine oxidation, which causes helix destabilization leading to the non-productive connection between oxidized CaM and target proteins. However, repair of oxidized methionine by MSRs restores their cellular function (Bigelow & Squier, 2005). *S. cerevisiae* mutants that lack the *MSRA* show delayed growth in the presence of H₂O₂ (1mM) (Moskovitz et al., 1997).

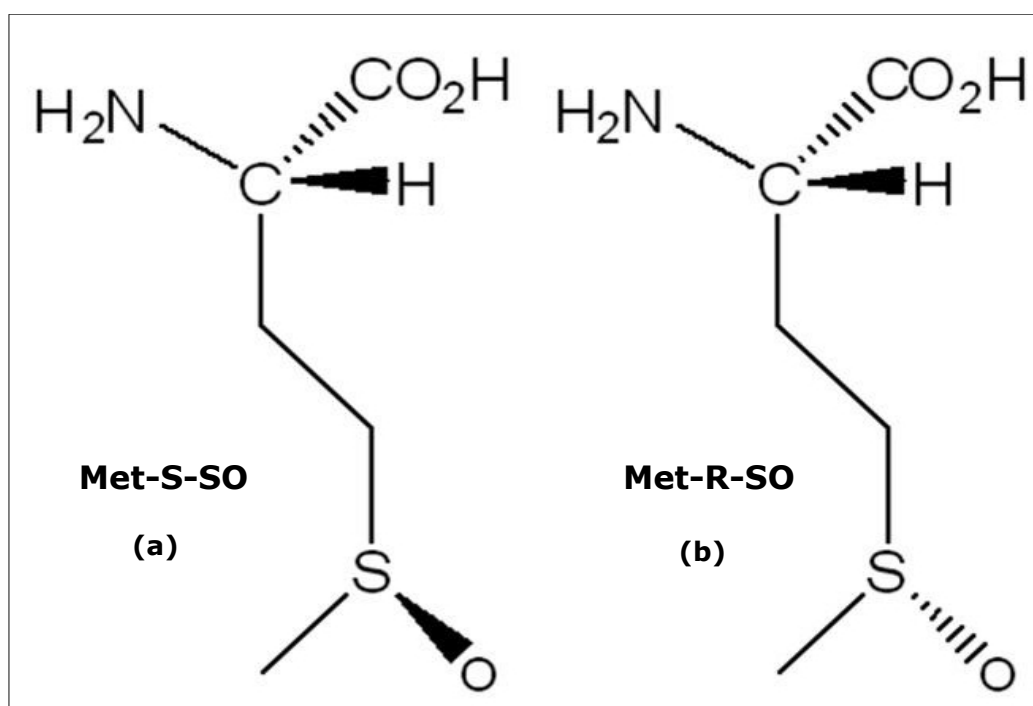


Figure 1.1- Diastereomeric structure of methionine sulfoxide: Met-S-(O) and Met-R-(O). (a) Met-S-SO denotes the diastereomer with the (S) configuration at the alpha carbon and (S) configuration at the sulphur. (b) Met-R-SO shows the (S) configuration at the alpha carbon and (R) configuration at the sulphur. It is slightly modified from (Khor et al., 2010).

In addition, a greater resistance to oxidative stress caused by paraquat was observed in *MsrA*-overexpressing *S. cerevisiae* (Moskovitz et al., 1998; Ruan et al., 2002). Mutations that lead to a loss of MsrA activity in yeast lead to reduced life span (Koc et al., 2004). MsrA and MsrB are fused into one protein MsrBA, which is a bifunctional methionine sulfoxide reductase enzyme, in bacterial pathogens. MsrBA has essential role in the preservation of protein activity required for bacterial survival under highly oxidizing conditions linked with pathogenesis or bioremediation (Chen et al., 2007).

1.5 Molecular targets of oxidative stress

Despite the above systems to counter oxidative stress, ROS-mediated toxicity does occur. Increased attention is now concentrating on identifying the key cellular targets of ROS when defences are overwhelmed. Whereas oxidative damage to cellular macromolecules is very widely reported, two types of general effect are thought potentially to cause ROS toxicity: loss of essential cellular function or gain of toxic function (Avery, 2011). Gain-of-function mechanisms could include accumulation of toxic oxidized-protein aggregates (Holland et al., 2007) or apoptotic cell death (Circu & Aw, 2010). Oxidative damage to essential targets has been linked causally to loss of cell integrity and/or viability by using models which permit the types of manipulation required to establish such causal associations.

1.5.1 Loss of essential function by ROS action

1.5.1.1 Lipid peroxidation and membrane function

Lipid peroxidation refers to oxidative degradation of lipids, key constituents of cell membranes. In this process, free radicals take electrons from the lipids in cell membranes, in particular from polyunsaturated fatty acids (PUFAs) since these have multiple double bonds between the methylene -CH₂ groups that have particularly reactive hydrogens bound to a carbon atom. Subsequently, via a chain of reactions, lipid hydroperoxides are formed. These species can lead to increased membrane fluidity, loss of cell membrane impermeability (with efflux of cytosolic solutes) and loss of the activities of proteins within membranes (Priault et al., 2002). The lipid peroxidation process

occurs in three major steps: initiation, propagation, and termination (Fig 1.2).

Highly reactive ROS such as hydroxyl radical and superoxide anion can initiate the process of lipid peroxidation (Halliwell & Cutler, 1999). In addition, numerous agents such as transition metals can catalyze lipid peroxidative processes, in particular, iron which is a major catalyst of lipid peroxidation (Ahn et al., 1993). A high concentration of polyunsaturated fatty acids in membrane lipids makes biological membranes especially susceptible to lipid peroxidation, involving the interaction of oxygen-derived free radicals with PUFAs (Reed, 2011). Membrane lipid peroxidation and a decline in membrane function are common observations in oxidatively stressed organisms. For example, in plant cells, considerable increases in electrolyte leakage and membrane permeability were observed during treatment with nickel (50 and 100 μ M) and this was accompanied by increased lipid peroxidation, as well as altered fatty acid composition and decreased degree of unsaturation (Gajewska et al., 2012). A role for such lipid peroxidation in ROS-mediated killing has been suggested by tests showing increased resistance in organisms treated with α -tocopherol (vitamin E), which acts as a lipid peroxidation inhibitor (Bansal & Bilaspuri, 2009; Mattie & Freedman, 2001). Moreover, *S. cerevisiae* cells with PUFA-enriched membrane, showed hypersensitivity to cadmium toxicity, which was mediated by lipid peroxidation (Howlett & Avery, 1997).

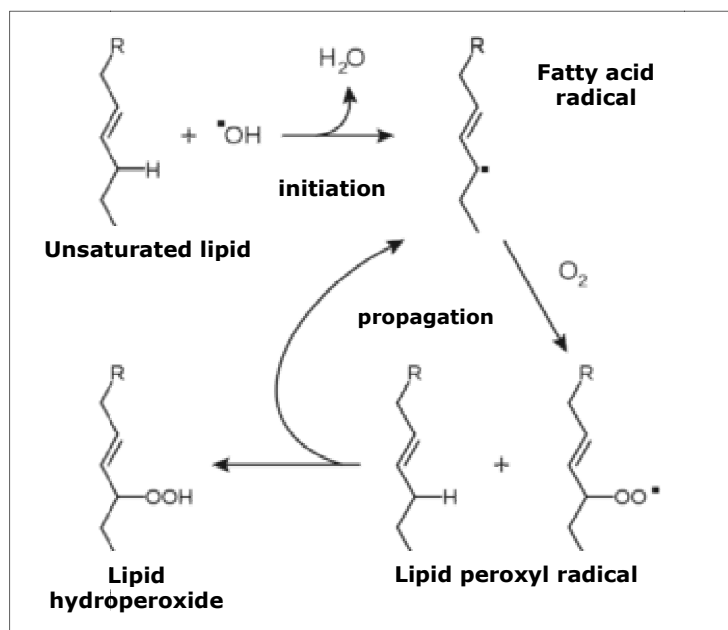


Figure 1.2- Mechanism of lipid peroxidation. **Initiation:** ROS initiators in living cells such as OH^\cdot react with a hydrogen atom of unsaturated lipid to produce H_2O and an unstable fatty acid radical. **Propagation:** Fatty acid radicals combine with molecular oxygen, producing unstable peroxy-fatty acid radicals, which react with another free fatty acid, producing a different fatty acid radical and lipid peroxide. New fatty acids continue this cycle in the same way. **Termination:** The radical reaction terminates when two radicals combine to generate a non-radical species and that occurs just when the concentration of radicals is sufficiently high for there to be a high possibility of collision of two radicals. It is slightly modified from (Young & McEneny, 2001).

In addition, lipid peroxidation was linked with H₂O₂-induced cell death where lipid peroxidation breakdown products accumulated to a higher rate following H₂O₂ exposure (Reekmans et al., 2005). Increased lipid peroxidation caused by menadione led to the breakdown of cellular redox homeostasis and negatively affected yeast cell viability (Kim et al., 2011). Lipid membranes are damaged oxidatively by copper and that has been identified as one mechanism of copper action in *S. cerevisiae* (Avery et al., 1996; Howlett & Avery, 1997).

1.5.1.2 DNA oxidation

Various types of pro-oxidants may cause oxidative DNA damage via production of hydroxyl radical and singlet oxygen which are the principal ROS directly targeting DNA (Dawes, 1999). The highly reactive hydroxyl radical reacts directly with double bonds of DNA bases and by abstraction of an H atom from the methyl group of thymine (Sonntag, 1987). In addition, H₂O₂ itself can not directly oxidize DNA, but its reactivity with transition metals (such as Fe²⁺) leads to damage via hydroxyl radicals production. These actions involve oxidative sugar fragmentation, strand scission, and base adducts (Hutchinson, 1985). The death of *E. coli* exposed to H₂O₂ was associated primarily with DNA damage (Hagensee & Moses, 1989; Imlay & Linn, 1986). Reaction of iron with the phosphodiester backbone leads to hydroxyl radical production. However, EPR (electron paramagnetic resonance) spectroscopy studies suggested that oxidative DNA damage by copper is limited as most of the H₂O₂-oxidizable copper is located in the periplasm, removed from the DNA (Macomber et al., 2007). DNA damage itself can cause increased ROS production (Salmon et al., 2004), with the possibility of targeting other biological molecules which may be more crucial for cell viability. Moreover, superoxide accelerates oxidative DNA damage by increasing the free iron content of cells through its ability to damage a subset of iron-sulphur clusters and therefore elevating the free iron levels (Keyer & Imlay, 1996).

Nuclear DNA lesions were observed in frataxin-deficient yeast cells (*Δyfh1*) after oxygen exposure, that is oxidized DNA bases and single-strand breaks. The Apn1 AP-endonuclease of the base excision repair pathway is required for DNA repair and cell survival. The *Δyfh1 Δapn1* double mutant showed growth impairment, increased mutagenesis and severe sensitivity to H₂O₂. Overexpression of the *APN1* gene in *Δyfh1* mutant cells decreased spontaneous and induced mutagenesis, suggesting that oxidative DNA damage and repair could be significant characteristics in the progression of Friedreich's ataxia (Lefevre et al., 2012). Studies to date indicate that DNA oxidation may play a more important role in ROS toxicity in certain types of organism (e.g., bacteria) than others. Among the DNA bases, guanine is a very sensitive base because it has the ability to mispair with DNA bases during DNA replication which leads to form mutagenic lesion known as 8-oxoguanine (8-oxoG) (Hazra et al., 2001). Furthermore, 8-oxoG is one of the most characteristic markers of oxidative stress and plays an essential role in the process of carcinogenesis *in vivo* (Tudek & Speina, 2012; Tudek et al., 2010). There are two types of DNA repair enzymes: the major enzyme is 8-oxoguanine DNA N-glycosylase (OGG1), which plays an important role in repairing 8-oxoG in the nonreplicating genome via excises 8-oxoG when paired with C, T, and G but not often with A. The second type is OGG2 which repairs 8-oxoG in emerging or transcriptionally active DNA (Hazra et al., 2001).

1.5.1.3 Protein oxidation

Damage to protein structure and impairment of function can be caused by protein oxidation (Zhang, 2010). There are certain proteins are more susceptible than others to oxidative attack. The factors determining such selectivity include the relative content of amino acids such as Cys and Met which are sensitive to oxidation due to the presence of sulphur, the existence of metal-binding sites, the localization of protein in the cell, and molecular conformation. Moreover, increasing evidence suggests that proteins that are newly synthesized are the most susceptible to oxidative damage, demonstrating that complete folding and integration into protein

complexes may provide protection from oxidative attack (Holland et al., 2007; Medicherla & Goldberg, 2008).

Protein damage by oxidation has received particular attention due to its implication in disease and aging (Davies, 2005; Stadtman et al., 2005). Proteins can be targeted by ROS in cells either via oxidation of their amino acid side chains to hydroxy or carbonyl derivatives, or by a shearing of their peptide bonds (Cabiscol et al., 2000; Costa et al., 2002). Nevertheless, oxidation of proteins can also have a regulatory role, additional to modifications like phosphorylation, glycosylation, acetylation, ubiquitination and others, which may reflect an approach of organisms to deal with continually changing development status and environmental conditions. Altering the chemical properties of amino acid side chains by oxidation leads to alterations of protein structure and folding. These changes, in many cases, cause protein impairment, while in others they may lead to activation of protein function and associated metabolic pathways (Levine et al., 2000). Furthermore, carbonylation is the most frequent type of protein modification in response to oxidative stress which induces protein degradation (England & Cotter, 2005). Untimely disruptions of essential pathways of energy metabolism due to protein oxidation are implicated in a number of human diseases (Martinez et al., 2010).

Oxidation of some amino acids in proteins such as Lys, His, Tyr and Trp can be irreversible and when oxidized, the affected proteins are permanently modified. In contrast, the two sulphur-containing residues (Cys and Met) are very prone to oxidation but in biological systems this reaction is reversible (Davies, 2005; Vogt, 1995; Zhang & Weissbach, 2008). Nearly all organisms can reverse the oxidation of methionine by expressing methionine sulfoxide reductase enzymes. Oxidation products of cysteine thiols that comprise cysteine-sulphenic acids and disulphides are reduced by thioredoxin or glutathione in biological systems whereas the reduction of stable cysteine-sulphinic acid is catalyzed by *S. cerevisiae* sulphiredoxin which is crucial for the antioxidant action of peroxiredoxins in ATP-dependent reduction (Biteau et al., 2003).

Reversible oxidation of cysteine and methionine residues has implications for protein function (Zhang, 2010). Protein tyrosine phosphatases are one group of proteins whose activity is commonly suppressed by this modification, affecting dephosphorylation of their target kinase proteins (Tonks, 2006). However, reduction of the oxidized cysteine reinstates the kinase phosphorylation state and enzyme activity (Humphries et al., 2005). Oxidation of Met may have regulatory roles in cellular signal transduction, growth and developmental processes. For example, formation of MetO as a result of Met oxidation in alpha-1-proteinase inhibitor (α 1-antitrypsin) leads to loss of proteinase inhibiting activity (Johnson & Travis, 1979), but reducing MetO to Met by human MSR can reinstate the activity of the oxidized α 1-antitrypsin *in vitro* (Carp et al., 1983). Furthermore, a number of proteins have been proven to be inactivated during oxidative conditions and/or by oxidative damage, such as a number of Fe-binding proteins (Drake et al., 2002), Crm1p which is required for nuclear export of HeLa cells (Crampton et al., 2009), and alcohol dehydrogenase (Matuszewska et al., 2008).

Metabolic processes are central to cell vitality, but their relative importance may vary according to environmental circumstance. Therefore, some proteins that are sensitive to oxidation may be dispensable in some conditions, but required under others. That can be illustrated in metabolic enzymes such as dehydratases. The presence of iron-sulphur (Fe-S) clusters, which are highly susceptible to oxidative targeting yet required for enzymatic activity, predisposes these enzymes and the metabolic process that they perform to oxidative inactivation (Imlay, 2006). Furthermore, biosynthesis of some amino acids (such as valine, lysine and isoleucine) in yeast and bacteria depends on the activity of Fe-S enzymes, and during oxidative stress their effect on cell vitality becomes observable in media lacking these affected amino acids (Carlioz & Touati, 1986; Wallace et al., 2004). To date, these examples provide the primary evidence that impairment of protein function by oxidation may cause ROS toxicity.

1.5.1.4 Protein synthesis as a ROS target

The rate of translation initiation and protein synthesis decreases as part of the normal response to mild oxidative stress. In *S. cerevisiae*, in response to hydroperoxides (such as H₂O₂), inhibition of translation initiation occurs in a manner dependent on phosphorylation of the α subunit of the translation initiation factor eIF2 (eukaryotic initiation factor2) by the Gcn2 (general control non-repressed 2) kinase. This leads to decreased formation of the ternary complex (TC) consisting of eIF2, GTP and the initiator Met-tRNA required for translation initiation (Mascarenhas et al., 2008). This response is thought to assist in preventing the potentially harmful effects of continuing mRNA translation under the error-prone conditions of oxidative stress, while giving time for a reprogramming of the proteins being expressed by the cell after stress is sensed (Shenton et al., 2006).

The approach seems to be effective in the case of mild H₂O₂ stress, which was not linked with increased errors during translation in yeast (Holland et al., 2007). On the other hand, mRNA mistranslation was caused by the redox-active metal chromate in a manner dependent on oxygen. This effect, a primary mechanism of Cr (VI) toxicity, was associated with protein carbonylation induced by chromium and the production of toxic protein aggregates (Sumner et al., 2005; Holland et al., 2007). Moreover, there is a competition between chromate and sulphate for uptake into cells because chromate transport into yeast cells is partly mediated by the sulphate transporters, Sul1p and Sul2p, and a resultant decreased availability of S-containing amino acids (S-starvation) is a reason for mistranslation induced by chromium (Holland et al., 2010).

Certain pro-oxidants may affect the process of mRNA translation by targeting certain proteins which are critical for the fidelity of this process. This did not appear to be the case for chromium-induced mistranslation. However, the toxic metal cadmium was found to target the critical eIF4E factor required for eukaryotic translation initiation in human cell lines. The mechanism was proposed to be ROS-mediated. Cytotoxicity and cell death were observed as a

result of cadmium exposure, following ubiquitination and subsequent proteolysis of the eIF4E protein, which leads to decrease cellular levels of cyclinD1, a protein that regulates cell cycle and growth (Othumpangat et al., 2005). A more recent study of Ling & Soll, (2010) showed that decreased editing activity of threonyl-tRNA synthetase (ThrRS) was induced by H₂O₂ (200µM), which caused oxidation of the crucial Cys¹⁸² editing site of the protein. This resulted in the production of Ser-tRNA^{Thr} and protein mistranslation that impaired the growth of *E. coli*. Mistranslation was also associated with protein misfolding.

To summarize, it is known that lipids, DNA and protein may all be oxidized during oxidative stress, and some specific examples of protein oxidation have been studied. However, it remains unknown which putative target(s) first accumulates damage of severity that precludes cell recovery, i.e., what target(s) primarily accounts for growth inhibition and/or loss of viability during oxidative stress? Oxidative impairment of protein(s) that is essential for viability provides one of the most plausible models to address this. In order to establish the identity of an essential protein that is a major ROS target, key criteria that need to be met are that the protein should be modified in an oxidation-dependent manner and exhibit decreased function (which cannot be accounted for by decreased expression) during oxidative stress. Furthermore, knock-down of the relevant protein should produce a ROS sensitive phenotype and, moreover, overexpression should confer resistance (Avery, 2011). Protein activities most likely to be affected by oxidative stress include those that depend on ROS-labile components, like Fe-S clusters.

1.6 The Iron-Sulphur clusters in proteins and ROS-mediated targeting

1.6.1 Importance of Fe-S clusters in protein functions

Iron-sulphur (Fe-S) clusters are essential inorganic cofactors of many bacterial and eukaryotic proteins which best known for their role in the oxidation/reduction reactions of the mitochondrial electron transport chain (Beinert et al., 1997; Meyer, 2008). These Fe-S

clusters are among the most ROS-sensitive structures in biology, yet they have been conserved through evolution and required for diverse protein functions (Imlay, 2006; Lill, 2009; Py et al., 2011). Fe-S clusters are amongst the most versatile prosthetic groups due to their redox properties, which also accounts for their primary role in electron transfer involving the mitochondrial respiratory chain complexes (complexes I, II and III) (Fontecave, 2006; Sheftel et al., 2010). Furthermore, Fe-S clusters have electrochemical features and structural flexibility, assisting their roles in substrate binding and activation, for instance in the dehydratases (Ruzicka & Beinert, 1978). Fe-S clusters can also act as sensors for environmental or intracellular conditions. Therefore, these clusters can regulate gene expression (Barras et al., 2005), functioning as “molecular switches” at both the transcriptional and translational levels owing to their sensitivity to cellular redox conditions (Kiley & Beinert, 2003), iron-sulphur storage and protein activity (Johnson et al., 2005). More recently, several essential nuclear proteins involved in DNA replication or repair have been shown to require Fe-S metallocenters (Rudolf et al., 2006; Klinge et al., 2007; Netz et al., 2012).

1.6.2 Structural and chemical properties of Fe-S clusters

Fe atoms provide the basic structure of Fe-S clusters, linked to sulphur atoms of cysteine residues and inorganic sulphide. Depending on the number of Fe atoms, a cluster can be as uncomplicated as a Fe (Cys)₄ centre, which is one Fe atom with four cysteine residues, or can be a more complex construct such as [8Fe-7S] and/or where other metals are incorporated into the cluster. Fe-S clusters consist of ferrous (Fe²⁺) and/or ferric (Fe³⁺) iron, inorganic sulphide (S²⁻) ions (Beinert, 2000), and in rare cases additional metals such as molybdenum in bacterial nitrogenase or nickel in various hydrogenases cofactors (Volbeda et al., 1995; Chan et al., 1993). *In vitro*, the assembly of Fe-S clusters occurs spontaneously on proteins that have the correct number and arrangement of Cys ligands (Malkin & Rabinowitz, 1966). However, because both Fe²⁺ and S²⁻ in their free forms are highly reactive and toxic *in vivo*, coordination in the delivery

of both of them is required to produce intracellular Fe-S clusters. This means that assembly of Fe-S clusters does not happen spontaneously in living cells but it is a catalysed process which requires coordinated biosynthetic machineries. This became clear from genetic, biochemical and cell biological studies in the 1990s. Three distinct types of Fe-S biosynthetic machinery have been identified, and all of these are mechanistically unified. They share common core functions comprising a cysteine desulfurase as the ultimate source of sulphur, and scaffold proteins which act as sulphur and iron acceptors and which transfer preformed clusters into recipient apo protein (Johnson et al., 2005). As mentioned briefly above, there are several forms of Fe-S clusters which are grouped into three main structural types based on their atomic content: [2Fe-2S], [3Fe-4S], [4Fe-4S], and other metal mixed types. [2Fe-2S] and [4Fe-4S] are the most abundant Fe-S clusters in eukaryotes. These are created by tetrahedrally coordinated iron atoms with bridging sulphides, usually linked to the protein through cysteine residues (Tracey et al., 2008). Cysteine residues act as axial ligands, where the iron atom is coordinated to the protein by forming covalent bonds with thiolate sulphur atoms of cysteine residues (Freeman, 1975), and thereby cysteine thiolate ligands are formed (Johnson et al., 2005).

The simplest form of Fe-S cluster is [2Fe-2S], which exists in ferredoxins (Fig 1.3) and Rieske protein (Ferraro et al., 2005; Schneider & Schmidt, 2005). [4Fe-4S] clusters (Fig 1.4) comprise a cubic structure with Fe and S filling corners of the cube, producing decreased space between the Fe atoms (Lill & Muhlenhoff, 2006). This type of cluster is found in many proteins, such as aconitase (Kennedy & Stout, 1992), the ABC protein Rli1 (Karcher et al., 2008), and in the transcription factor FNR (Fumarate nitrate reduction) of *E. coli* (Khoroshilova et al., 1995; Green et al., 1996). Some proteins of the respiratory chain such as Sdh2 in the inner membrane of yeast mitochondria contain [3Fe-4S] clusters. In addition, various protein structural folds have been identified to coordinate these simple Fe-S clusters (Meyer, 2008).

Electron transfer is the most important function of Fe-S clusters due to the tendency of iron ions of Fe-S clusters in proteins to switch between a reduced ferrous (Fe^{2+}) and oxidized ferric (Fe^{3+}) state (Beinert et al., 1997).

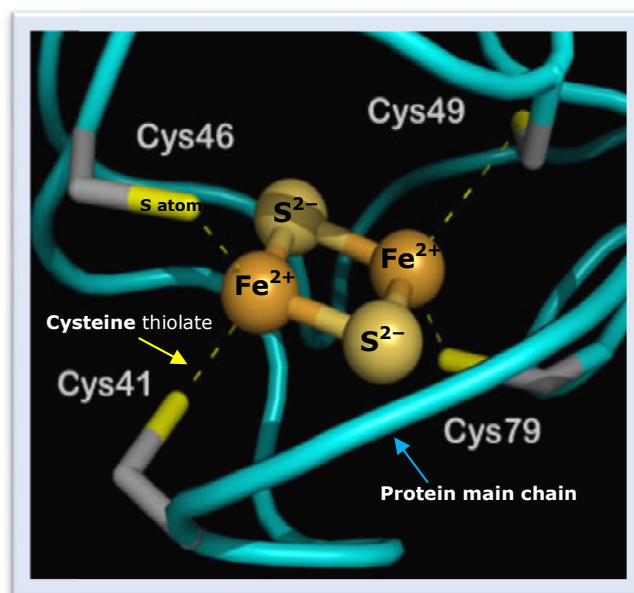


Figure 1.3- [2Fe-2S] cluster structure of ferredoxin. The side chains of the cysteine residues that coordinate to the iron atoms are shown as sticks, with the β carbon in grey and the γ sulphur atoms yellow, where iron atoms are coordinated to the protein by thiolate sulphur atoms of cysteine residues. The blue tubes represent the protein main chain. Image slightly modified from (Rypniewski et al., 1991).

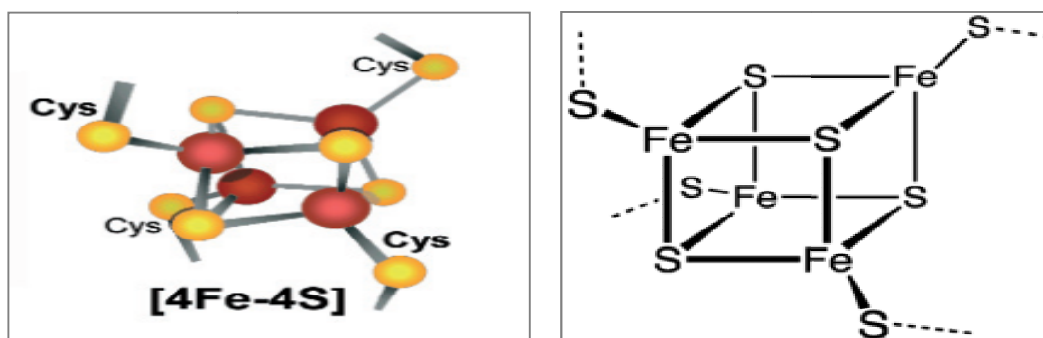


Figure 1.4- [4Fe-4S] cluster structure. Four iron atoms coordinated by four cysteine thiolates. Taken from (Lill, 2007).

1.6.3 Fe-S clusters and oxidative conditions

The extreme ROS sensitivity of Fe-S clusters leads to their being easily degraded, which may lead to further toxic ROS production (Imlay, 2006). ROS to which Fe-S clusters are susceptible include H₂O₂ and O₂^{•-} (Lill et al., 2006). Studies of ROS sensitivity to date have focused on Fe-S proteins which are usually non-essential, such as dehydratases. These have [4Fe-4S]²⁺ clusters in which one iron atom is solvent-exposed making them susceptible to oxidation by ROS (Flint et al., 1993; Park et al., 2005). The study of Varghese et al. (2003) showed that aconitase B activity was reduced by more than 50% in superoxide dismutase (SOD) mutants compared to wild type cells. The proposed inactivation mechanism of dehydratases is that O₂^{•-} attacks the solvent-exposed iron in a [4Fe-4S]²⁺ cluster. The transfer of one electron to O₂^{•-}, producing H₂O₂, converts the [4Fe-4S]²⁺ cluster to the unstable [4Fe-4S]³⁺ state that releases one Fe²⁺ to produce a [3Fe-4S]¹⁺ cluster and thus an inactive enzyme (Flint et al., 1993). Furthermore, the released ferrous iron atom (Fe²⁺) can bind DNA and/or react with H₂O₂ via the Fenton reaction (Reaction 1), which produces the highly reactive hydroxyl radical (OH[•]) that can attack and damage DNA (Keyer & Imlay, 1996).



Macomber & Imlay (2009) showed that exposure of *E. coli* to copper quickly caused inactivation of dehydratase Fe-S enzymes. This inactivation of dehydratases occurred as a result of damage to their Fe-S clusters, causing toxicity via displacement of Fe atoms from the solvent-exposed clusters and binding of Cu (I) to the coordinating sulphur atoms.

Fe-S enzymes also represent targets for cobalt. In one study, three selected Fe-S enzymes, tRNA methylthio-transferase, aconitase and ferrichrome reductase, were found to be targeted by intracellular cobalt in *E. coli*, resulting in the loss of their activities (Ranquet et al., 2007). In addition, elevated iron uptake was observed

in cells exposed to cobalt. *In vitro* experiments showed that cobalt reacted with labile Fe-S clusters, not fully assembled but present in scaffold proteins (ISCU, SUFA) implicated in Fe-S cluster biogenesis, by substituting for Fe in clusters (Ranquet et al., 2007). Protein isolated from cobalt exposed cells was shown to contain cobalt atoms and to exhibit cluster degradation. It was proposed that cobalt ions (Co^{2+}) compete with iron ions for the particular binding sites in iron-sulphur proteins (Ranquet et al., 2007). In *Bacillus subtilis*, effects of copper on the expression of *suf* genes, which encode proteins required for biogenesis of Fe-S clusters, as well as expression of genes involved in cysteine biosynthesis and others encoding Fe-S proteins were discovered by microarray analysis with copper stressed cells (Chillappagari et al., 2010). Because of a proposed relationship between copper and Fe-S cluster maturation, a mutant with a conditional mutation in SufU, which is the major scaffold protein used for cluster assembly and transfer in *B. subtilis*, was used to study copper sensitivity. This mutant was hyper-sensitive to copper stress. By investigating the effect of copper on clusters within SufU *in vitro*, it was observed that copper at submicromolar doses destabilizes cluster formation at the scaffold. Consequently, by affecting Fe-S cluster formation, expression of *SufU* and its target proteins in addition to proteins involved in iron and sulphur acquisition was enhanced by copper stress, suggesting these to be adaptations to help restore cluster biogenesis (Chillappagari et al., 2010).

Fe-S cluster integrity is also extremely sensitive to oxidative stress in *S. cerevisiae*. This was illustrated by ^{55}Fe -labelling studies in MSR-deficient cells (Sideri et al., 2009). These studies showed that Fe-S cluster turnover was accelerated in the *mxr* Δ (MSR deficient) mutant versus the wild type. This elevated oxidative targeting of clusters in MSR-deficient cells indicated that MSR enzymes protect Fe-S clusters from oxidative damage (Sideri et al., 2009).

1.7 The biogenesis of Fe-S proteins in eukaryotes

Despite the comparative simplicity of Fe-S clusters with regard to their structure and composition, Fe-S clusters require a highly complicated and coordinated process to be assembled and integrated into apoproteins in living cells (Johnson et al., 2005; Bandyopadhyay et al., 2008). There are three proteinaceous systems which contribute in the production of Fe-S proteins in eukaryotes (Lill & Muhlenhoff, 2006; Lill et al., 2006; Lill & Muhlenhoff, 2008; Kispal et al., 1999).

The biogenesis of Fe-S proteins in the eukaryotic cytosol and nuclei needs the participation of both mitochondrial Fe-S cluster (ISC) assembly machinery as well as a mitochondrial ISC export system. In *S. cerevisiae*, Fe-S clusters are formed within mitochondria, and are exported into the cytosol by the ABC transporter Atm1p (Kispal et al., 1999). In addition, essential cytosolic Fe-S protein assembly (CIA) machinery is required for the maturation of Fe-S proteins, and this system exists in almost all eukaryotes (Lill & Muhlenhoff, 2006; Lill & Muhlenhoff, 2008) (Fig 1.5). The first details of the complex biosynthesis processes in eukaryotes have been established by using the yeast *S. cerevisiae* as a model organism. Moreover, the pathway is highly conserved from lower to higher eukaryotes (Muhlenhoff & Lill, 2000), and that was demonstrated by recent studies in human cell culture and other model systems such as *E. coli* and *Azotobacter vinelandii* (Tong & Rouault, 2006; Fontecave & Ollagnier-de-Choudens, 2008; Ayala-Castro et al., 2008).

Most components of the ISC assembly, ISC export and CIA machineries are encoded by essential genes in yeast (Lill et al., 2005). The biogenesis process can be divided into two main steps: In the mitochondrial ISC assembly system, the transient Fe-S cluster is assembled initially on scaffold proteins su1p/Isu2p, which contains three conserved Fe-S cluster-coordinating cysteine residues (Muhlenhoff et al., 2003; Raulfs et al., 2008). Then, the Fe-S cluster is released and transferred to recipient apoproteins for integration by coordination with specific amino acid residues (Unciuleac et al., 2007;

Chandramouli et al., 2007). Every stage of these steps includes the involvement of some proteins and cofactors, which perform specific function in the biosynthetic process, such as: a cysteine desulphurase complex (termed Nfs1-Isd11 in mitochondria) which serves as sulphur donor by releasing the sulphur required for Fe-S cluster synthesis from cysteine, thus converting cysteine to alanine and creating an enzyme-bound persulphide. This persulphide (-SSH) is transferred to Isu1/2 by direct interaction between Nfs1 and Isu1/2, facilitating the new assembly of the Fe-S cluster on a conserved cysteine residue of this protein (Wiedemann et al., 2006; Adam et al., 2006). Owing to the physiological toxicity of Fe²⁺ in its free form, its accurate delivery to scaffold protein is important. Therefore, the iron-binding protein frataxin (Yfh1) serves as an iron donor by stimulating interaction of iron with Isu1-Nfs1) (Gerber et al., 2003; Bencze et al., 2006; Wang & Craig, 2008). In addition, electrons are required for the reduction of sulphur (present in cysteine) to sulphide S²⁻, which exists in Fe-S clusters. Therefore, the [2Fe-2S] ferredoxin (Yah1) performs this function by receiving electrons from the mitochondrial ferredoxin reductase (Arh1) and NADH (Muhlenhoff et al., 2003) (Fig 1.5).

The second main step of biosynthesis requires specific cofactors including some from the chaperone system such as Ssq1 and Jac1 as well as the nucleotide exchange factor Mge1 and the monothiol glutaredoxin Grx5. These facilitate cluster dissociation from scaffolds and transfer the susceptible Fe-S clusters to recipient apoproteins (Schilke et al., 2006; Andrew et al., 2006). After that, the ABC transporter Atm1p (ABCB7 in humans) of the mitochondrial inner membrane, which is a member of the ISC export machinery, is required to transfer Fe-S cluster precursors that were synthesized by mitochondrial proteins to the cytosol to participate in the generation of cytosolic Fe-S proteins (Kispal et al., 1999; Cavadini et al., 2007). In addition, there is another required component for the export process named sulphhydryl oxidase Erv1, situated in the intermembrane space of mitochondria to catalyse the formation of disulphide bridges during Mia40-dependent protein import, and therefore achieving a dual function (Mesecke et al., 2005). The cytosolic Fe-S protein assembly

(CIA) machinery is involved in the maturation of cytosolic and nuclear Fe-S proteins, and this process can be split into two major partial reactions (Netz et al., 2007). Firstly, the transient assembly of Fe-S clusters occurs on the P-loop NTPases Cfd1 and Nbp35. Then a heterotetrameric complex Cfd1-Nbp35 is formed which serves as a scaffold (Roy et al., 2003; Hausmann et al., 2005). This complex participates in the maturation of Nar1 (nuclear architecture related), which is a component of the CIA machinery, by supporting the assembly of two Fe-S clusters on Nar1. Then, the Nar1 holoprotein interacts with Cia1, a WD40 repeat protein that acts as a harbour platform for binding Nar1, to assist in transfer and incorporation of Fe-S clusters to target cytosolic and nuclear apoprotein, yielding Fe-S holoproteins (Srinivasan et al., 2007) (Fig 1.5).

The two mitochondrial ISC systems and the CIA machinery are required for the maturation of Fe-S clusters of essential nuclear Fe-S proteins such as Rad3, which has a function in nucleotide excision repair and Pri2, which has a function in RNA primer synthesis for DNA replication (Rudolf et al., 2006; Klinge et al., 2007). This gives a strong association between mitochondria and the primary processes of life. Muhlenhoff et al. (2003) demonstrated that depletion of some components implicated in Fe-S protein biogenesis in yeast was lethal under any growth condition tested; these components are the proteins cysteine desulphurase (Nfs1p), ferredoxin reductase (Arh1p), ferredoxin (Yah1p) and the scaffold protein pair Isu1p/Isu2p. With the exception of Yah1p, which seems to be involved in its own maturation, none of the mitochondrial proteins known to be Fe-S proteins in their own right are essential for cell viability (Lange et al., 2000). In contrast, essential nuclear (see above) and cytosolic (below) Fe-S proteins are known.

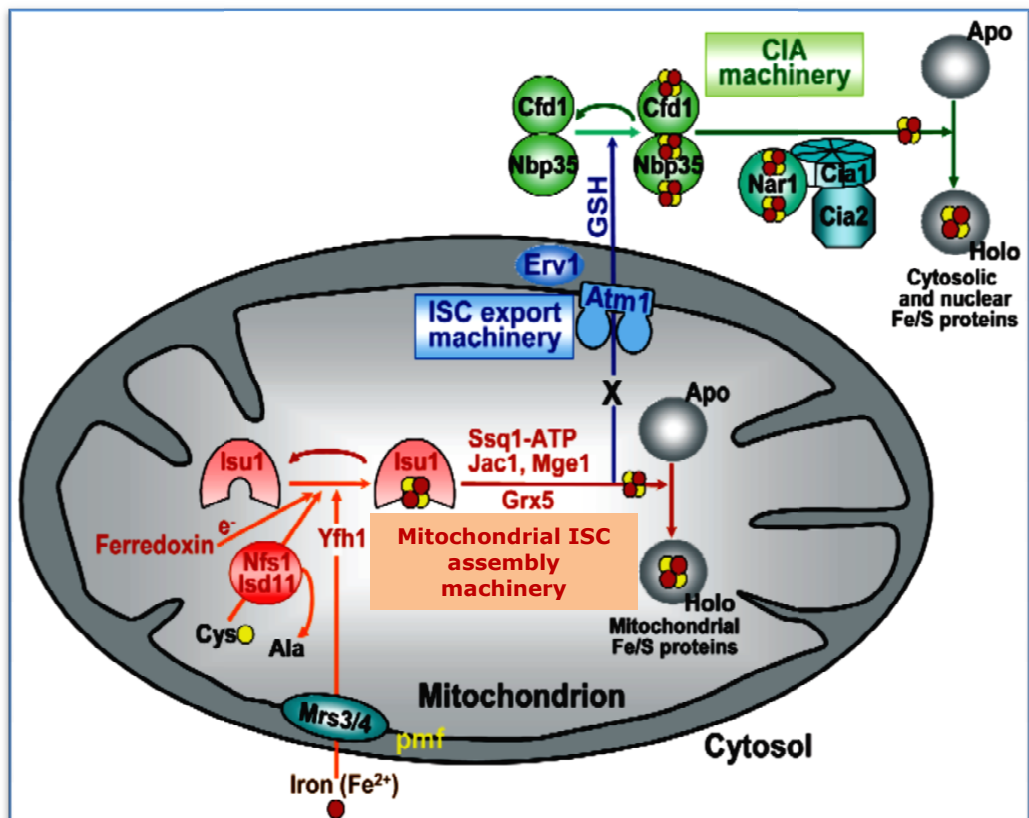


Figure 1.5- A model of Fe-S protein biogenesis in eukaryotes. The biosynthesis of transient Fe-S clusters (red and yellow circles) on scaffold protein Isu1 (orange arrows), is followed by release of clusters from Isu1 and transfer and incorporation into recipient apoprotein (red arrows). This is performed by components of the mitochondrial ISC assembly machinery. Export of an unknown compound (X) by the Atm1 transporter to the cytosol is for utilization in the assembly of Fe-S proteins (blue arrows), with the assistance of both GSH and Erv1 which introduce disulphide bridges to substrates. Maturation of Fe-S proteins is catalyzed by the CIA machinery in the cytosol. The light green arrow refers to the assembly of Fe-S clusters on the Cfd1-Nbp35 complex. Dark green arrows refer to the binding of Fe-S clusters to Cfd1-Nbp35 in a labile fashion. With the assistance of Nar1, Cia1, and Cia2, these clusters can be transferred to target cytosolic and nuclear apoproteins to yield Fe-S holoproteins. Figure adapted from Lill (2007).

1.8 Diseases linked to Fe-S proteins and their biosynthesis

In mammals, defects in components of Fe-S protein biosynthesis or in individual Fe-S proteins are associated with several diseases. Delatycki et al. (2000) showed that Friedreich's ataxia (FRDA), an autosomal recessive neurodegenerative disorder, results from deficiency in the ISC assembly component frataxin (Yfh1). This is associated with a disruption of cellular iron homeostasis and iron accumulation. In addition, defects in the human ISC export protein ABCB7 (Atm1 in yeast) are associated with X-linked sideroblastic anaemia and cerebellar ataxia (Bekri et al., 2000). Defects in the Fe-S protein biosynthesis component glutaredoxin (Grx5), are related to a haematological phenotype named microcytic anaemia (Wingert et al., 2005). This association between Fe-S protein biosynthesis and haematopoiesis was illustrated by the fact that the biogenesis of Fe-S proteins is essential for the maturation of the mammalian cytosolic iron regulatory protein1 (Irp1), which regulates the biosynthesis of many proteins participating in iron uptake, storage and consumption in the cell. Further disease-relevant Fe-S proteins include those involved in DNA repair such as the essential human nuclear Fe-S protein, XPD (Rad3 is the yeast homologue). Inherited mutations in its cluster-coordinating residues may lead to xeroderma pigmentosum, Cockayne syndrome, and trichothiodystrophy (Andressoo et al., 2006).

This project has focused on the essential cytosolic/nuclear Fe-S protein, Rli1. Rli1p carries N-terminal Fe-S clusters and its maturation is reliant on the mitochondrial ISC assembly and export machineries and all four identified CIA components (Kispal et al., 2005; Roy et al., 2003). It was suggested that the essential nature of Fe-S cluster biosynthesis might reflect the essentiality solely of Rli1p (Kispal et al., 2005), although the essential nuclear Fe-S proteins have since been identified.

1.9 The essential Fe-S protein Rli1

Ribonuclease L inhibitor 1 (Rli1) was originally identified for its inhibition of the ribonuclease RNase L protein, which was characterized as a protein that is activated by the interferon system on viral infection in mammalian cells (Bisbal et al., 1995; Bisbal et al., 2001). The yeast Rli1 protein shares 68% amino-acid identity with human RNase L inhibitor (RLI/ABCE1). During viral infection, the synthesis of 2'-5' oligoadenylates (2-5) A is induced by interferon. 2-5 A activates endoribonuclease RNase L by binding with it causing conformational changes and dimerization of the protein (Dong et al., 2001). Activated RNase L cleaves both viral and cellular single-stranded RNA (ssRNA) at the 3' end of sequence, preventing replication of RNA viruses and causing inhibition of protein synthesis. RNase L inhibitor (Rli1) can participate in the regulation of RNase L by preventing 2-5 A binding (Bisbal et al., 1995; Benoit De Coignac et al., 1998; Bisbal et al., 2001). Thus, the expression of Rli1/ABCE1 by some viruses serves as a countermeasure; by inhibiting RNase L (Martinand et al., 1998; Silverman et al., 2007). There is no orthologue of RNase L in either lower eukaryotes or in archaeobacteria. Thus, Rli1p must also fulfil a more general cellular function.

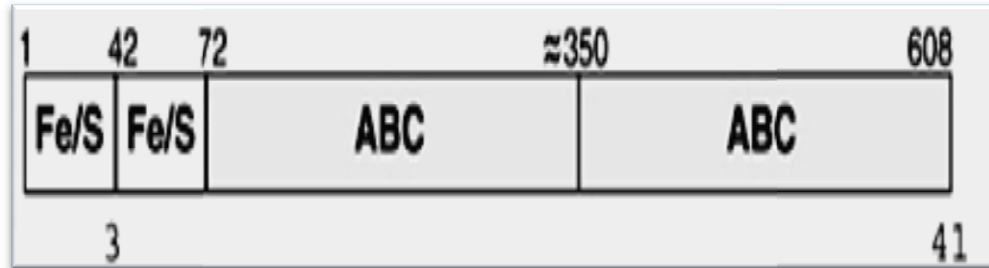
The iron-sulphur (Fe-S) protein Rli1 of yeast is a 68 kDa ABC protein. Rli1p has two cysteine-rich motifs at its N-terminus predicted to associate with two cubic [4Fe-4S] clusters (Fig 1.6) (Kispal et al., 2005). The two [4Fe-4S] clusters of Rli1p (ABCAE1) are predicted to be shielded from solvent and not solvent exposed like certain other ROS sensitive Fe-S proteins that have been described (Karcher et al., 2008). In addition, there are two typical ATP-binding cassette (ABC) domains at the C-terminus of Rli1p, giving Rli1 its alternative name ABCE1 (Chen et al., 2006). These two ABC domains share high sequence homology with members of the ABC protein family (Schuller et al., 2003). Unlike ABC transporters which have transmembrane domains, Rli1p contains a pair of nucleotide binding domains (NBDs) but without connected transmembrane domains (TMDs) (Kerr, 2004; Schuller et al., 2003). Rli1p is thought to convert the chemical energy

of hydrolysis of ATP into a mechanical motion similar to a pair of tweezers where, in the ATP-bound form, contact is made by the NBDs with two ATPs located alongside the interface of dimer. Opening and closing of the two NBDs of the dimer, depending on whether ATP is present, is suggested a mechanism for regulation of ATPase activity to trigger conformational changes in associated function-specific domains (Chen et al., 2003).

Rli1p is highly conserved in evolution and orthologues are not present in eubacteria but present in all eukaryotes as well as archaea, which are single-celled microbes that are classified as a group of prokaryotes based on the sequence of ribosomal RNA genes, and they are members of the Euryarchaeota, Crenarchaeota and Nanoarchaeota (Woese & Fox, 1977; Huber et al., 2002) which live in severe environments such as boiling water and inside volcano, as well some even live in ordinary temperatures, salinities and human gut. Rli1p is an essential protein in all organisms tested (Winzeler et al., 1999; Coelho et al., 2005; Estevez et al., 2004; Schuller et al., 2003). Mutations in critical cysteine residues of Rli1p abolish its association with Fe-S clusters and result in the loss of cell viability, showing that Fe-S clusters of Rli1p are crucial for its activity and hence for cell viability. This makes Rli1 the only known essential cytoplasmic protein that depends on Fe-S cluster biosynthesis in the mitochondria (Kispal et al., 2005; Lill, 2009; Karcher et al., 2008). As detailed previously, the assembly of Fe-S clusters in Rli1p is strongly reliant on several components of the mitochondrial and cytosolic Fe-S protein assembly machineries. Because Rli1p itself is not involved in Fe-S protein biosynthesis, its maturation process may partly explain the indispensable function of mitochondria for viability of yeast cells. In addition, as mitochondrial ISC components such as Nfs1p, Erv1p and Yah1p and cytosolic assembly components such as Cfd1p, Nbp35p and Nar1p are encoded by essential genes, it was previously thought that their essential roles may reflect the assembly of clusters into Rli1p (Kispal et al., 2005). Kispal et al. (2005) showed that in yeast cells Rli1p localization is mostly cytosolic, and partly nuclear. However, Rli1p does not appear to localize to mitochondria.

N-terminus

C-terminus



Sc	DKNSRIAIVS	ADKCKPKKCR	-QECKRSCPV	VKTGKLCIEV
Sp	ESLTRIAIVS	EDKCRPKKCR	-QECRRSCPV	VRTGKLCIEV
Hs	DKLTRIAIVN	HDKCKPKKCR	-QECHKSCPV	VRMGKLCIEV
At	DRLTRIAIVS	SDRCKPKKCR	-QECHKSCPV	VKTGKLCIEV
Ce	DVPLRIAIVE	KDRCKPKKNG	-LACKRACPV	NRQGKQCIIV
Mj	GDFMRLAIID	YDRCQPKKCS	-MECMKYCPG	VRMGEKTIEI
Mt	IKLTRISILD	HDRCPKPKCN	-YVCIKYCPG	VRMDEDTITI
Pa	RK-MRIAVID	YDKCNPDKCG	HFLCERVCPV	NRMGGEAII I
Con	RIA	DRC PKKC	EC CPV	VRMG IE
		↑ ↑	↑ ↑	
	42		71	
Sc	TPTS ⁴² KIAFIS	EILCIGCGIC	VKKCPFD ⁷¹ AIQ	=100%
Sp	NPTDRIA ⁴² FIS	ETLCIGCGIC	VKKCPFGAIN	71%
Hs	TPQSKIA ⁴² WIS	ETLCIGCGIC	IKKCPFGALS	68%
At	TVGSKLAF ⁴² IS	EELCIGCGIC	VKKCPFEAIQ	68%
Ce	EATSTISQ ⁴² IS	EILCIGCGIC	VKKCPYDAIK	62%
Mj	DENTGKPV ⁴² IS	EVLCSGCGIC	VKRCPFKAIS	48%
Mt	DEKTKKPI ⁴² IS	EELCSGCGIC	TKRCPFKAIS	42%
Pa	DEENYKPI ⁴² IQ	EASCTGCGIC	VHKCPFNAIS	47%
Con	IS	E LC GCGIC	VKKCPF AIS	
		↑↑ ↑↑ ↑↑	↑↑	

Figure 1.6- The iron-sulphur domains of Rli1p. Rli1p has two cysteine-rich motifs at its N-terminus predicted to associate with two cubic [4Fe-4S] clusters and two ATP-binding cassette (ABC) domains at the C-terminus. The multi-sequence alignment of the cysteine-rich regions at the N-terminus of Rli1p-like proteins was created by the Multalin program (Corpet, 1988). The different arrows were used to label the conserved cysteine residues. Sc, *S. cerevisiae*; Sp, *Schizosaccharomyces pombe*; Hs, *Homo sapiens*; At, *Arabidopsis thaliana*; Ce, *Caenorhabditis elegans*; Mj, *Methanococcus jannaschii*; Mt, *Methanobacterium thermoautotrophicum*; Pa, *Pyrococcus abyssi*; Con, consensus sequence. Figure adapted from Kispal et al. (2005).

1.9.1 Ribosome biogenesis requires the Fe-S protein Rli1

Rli1p has an essential role in ribosome biogenesis. Yarunin et al. (2005) showed associations between Rli1p and 40S subunits, 80S ribosomes and probably polysomes under low-salt conditions. There was also a minor pool of Rli1p in soluble fractions, demonstrated by sedimentation of TAP-tagged Rli1 on sucrose gradients. Furthermore, depletion of Rli1 in yeast impaired the late step of precursor rRNA processing on both the 40S and 60S subunits and led to defective export of both small and large ribosomal subunits from the nucleus to the cytoplasm. Therefore, Rli1 depletion prevented translation and suppressed growth (Kispal et al., 2005; Yarunin et al., 2005). Zhai et al. (2013) study demonstrated that Lto1, a gene that is overexpressed in cancer, is part of a complex that consists of association of Lto1 with the Fe-S cluster containing Rli1p via Yae1, as well as is required for biosynthesis of the large (60S) ribosomal subunit. Lto1 could convert a nuclear pool of Rli1p to the pathway that makes the rRNA connected with the 60S subunit, where the inhibition of 43S preinitiation complex assembly as well as decrease in polysome content were observed upon depletion of Rli1, similar phenotype was observed when Lot1 function is lost (Zhai et al., 2013). Defective export of ribosomal subunits was also observed in all mutants with defects in components of the CIA machinery, Cfd1, Nbp35 and Nar1 (Yarunin et al., 2005). Kispal et al. (2005) also showed that depletion of Nar1p, required for incorporation of Fe-S clusters to Rli1p, led to nuclear accumulation of ribosomal subunits. Because Rli1p apoprotein occurs at wild type levels under these conditions (Balk et al., 2004), the Kispal et al. (2005) study revealed that the Fe-S clusters of Rli1p are required for its activity in exporting ribosomal subunits from the nucleus. There was no defect in translation as a result of Nar1p depletion, but that does not mean that the Fe-S of Rli1p is not required for translation where Khoshnevis et al. (2010) study showed that the Fe-S cluster of Rli1p is required for its activity in translation termination, supporting the idea that defective nuclear export happened before the arrest of translation. All these data suggest that Rli1p is an essential factor for ribosome biosynthesis (Yarunin et al., 2005; Kispal et al., 2005). In

addition, these data indicated a strong relationship between the function of mitochondria, the assembly of cytosolic Rli1p, and cytosolic biogenesis of ribosomes. These roles of Rli1p are consistent with its localization both to the cytoplasm and nucleus. Moreover, as mentioned previously, a minor fraction of Rli1p is present in the nucleus. The protein is hyper-accumulated in this compartment in nuclear protein export mutants such as *xpo1-1*, which is impaired in export of nuclear export sequence (NES)-containing cargo proteins (Stade et al., 1997). Nuclear accumulation of Rli1p-GFP in *xpo1-1* suggested that Rli1p shuttles between the cytosol and nucleus (Yarunin et al., 2005). Nuclear export of pre-ribosomal subunits (pre40S and pre60S) through the nuclear pore complex (NPC) has been revealed to require the nuclear export receptor, a leucine-rich nuclear export signal-containing protein, exportin (Xpo1p/Crm1p in human), and a functional RanGTPase system (Gadal et al., 2001; Nissan et al., 2002).

1.9.2 Rli1p and translation initiation

The Rli1 protein participates in the process of translation initiation. Dong et al. (2004) showed that Rli1p associates with eukaryotic translation initiation factors that stimulate ribosome loading, such as eIF5, eIF2 and, in particular, the translation initiation complex eIF3. Rli1p can bind with eIF3 and eIF5 independently of its association with the small 40S ribosomal subunit *in vivo*. Moreover, phenotypes such as loss of cell viability, a lesser polysome content, as well as reduced average polysome size were observed *in vivo* as a result of Rli1 depletion. In addition, there was a marked decrease in 40S binding with eIF2 and eIF1, which is consistent with an essential function of Rli1p in translation *in vivo*, by stimulating the assembly of 43S preinitiation complexes (Dong et al., 2004). Furthermore, Yarunin et al. (2005) demonstrated that there was association between Rli1p and both precursor 40S and mature 40S subunits, and with the translation initiation factor complex eIF3 where Hcr1p was visibly associated with Rli1p-TAP. This, together with results of Kispal et al. (2005) that showed association between Rli1p and both ribosomes and

Hcr1p suggests that Hcr1p and Rli1p might associate directly, and Hcr1p might connect Rli1p to the eIF3 complex and thus promote translation initiation. Interestingly, Pisarev et al. (2007) showed a new function of eIF3 in regulating the dissociation of the ribosome after translation termination. The ATP-binding cassette domain of Rli1p (not the Fe-S domain) has been shown to have a direct role in translation initiation.

This was clear from a reduced rate of translation initiation *in vivo* as a result of mutation in this ATP-binding domain. In addition translation of a luciferase mRNA reporter was not promoted by the mutant protein in wild-type cell extracts (Dong et al., 2004). An insufficiency in the free large ribosomal subunit 60S was shown in cells with Rli1 depletion. These results in conjunction with Rli1p localization to the nucleus and cytoplasm collectively suggested that Rli1p may have dual roles in ribosome biogenesis as well as in initiation of translation (Dong et al., 2004).

In light of this, it was further suggested that any Rli1p dysfunction during oxidative stress could be involved in downregulation of both ribosome biogenesis and initiation of translation as part of the adaptation to changing environmental and intracellular conditions (Yarunin et al., 2005).

1.9.3 Rli1p and translation termination and ribosome recycling

Translation termination is mediated by recognition of a stop codon through the eukaryotic release factor1 (eRF1/Sup45 in *S. cerevisiae*) and by the ensuing hydrolysis of the ester bond that binds the tRNA and the polypeptide chain, stimulated by the GTPase activity of eRF3 (Sup35 in *S. cerevisiae*; Jacobson, 2005).

Rli1p interacts with the eukaryotic release factors eRF1/Sup45 and eRF3/Sup35 *in vivo* and *in vitro* (Pisarev et al., 2010; Khoshnevis et al, 2010). In addition, Khoshnevis et al. (2010) showed that in *S. cerevisiae* the association of Rli1p with both Hcr1p and eRF1 is mediated by the second ABC domain of Rli1p, as mutants which were deficient for this domain were defective for association with eRF1 and Hcr1. (Hcr1 interacts with the initiation complex eIF3, an activity

required for translation termination via regulation of ribosome dissociation.) In contrast, *rli1* mutants lacking Fe-S clusters or the first ABC domain were able to associate with eRF1 and Hcr1. Although the Fe-S clusters were not essential for this association, they are considered essential for Rli1p activity in the recognition of a stop codon and thus in translation termination. Thus, an Fe-S cluster mutant of Rli1p did not suppress the read-through defects of a *sup45-2* mutant, suggesting that the Fe-S domain of Rli1p is required for Rli1p activity in translation termination (Khoshnevis et al., 2010). Furthermore, the efficiency of read-through was detected by using a dual reporter assay (Bhattacharya et al., 2000), based on comparison between expression of beta-galactosidase and luciferase open reading frames separated by a stop codon. The assay results showed that Rli1p is crucial for appropriate recognition of the stop codon, because downregulation of *RLI1* caused defects in termination, similar to observations in mutants of the other termination factors (eRF3, eRF1 and Dbp5). *RLI1* overexpression partly repressed the read-through defects of an eRF1 mutant (Khoshnevis et al., 2010).

Biochemical studies have indicated direct functions for eRF1 and eRF3 as well as related proteins such as Dom34 and Hbs1 in downstream ribosome recycling, which are separate processes from peptide release (Pisareva et al., 2011; Shoemaker et al., 2010). Immediately following translation termination, there is still association of eukaryotic 80S ribosomes with messenger RNA (mRNA), P-site deacylated tRNA and eRF1, termed post-termination complexes (post-TCs). Recycling must be performed by separating ribosomes into subunits (Pisareva et al., 2007). The study of Tsuboi et al. (2012) showed that dissociation of a ribosome that is stalled at the 3' end of mRNA is performed by Dom34:Hbs1 complex. Furthermore, this complex is also required for degradation of a 5'-endonucleolytic cleavages of mRNA (NGD), suggesting that degradation of the (NGD) and of nonstop mRNA are stimulated by dissociating stalled ribosome at the 3' end of mRNA.

Interaction of Rli1p with release factors eRF1 and eRF3 is consistent with the finding that eRF1 is essential for Rli1p-mediated

recycling of post-termination ribosomes (Pisarev et al., 2010). Moreover, ABCE1 (Rli1p) and the termination factor pelota (eRF1 paralogue) have been found in eukaryotic and archaeal ribosome recycling complexes (Becker et al., 2012). Furthermore, the Fe-S domain of Rli1p is required for interaction with and stabilization of pelota (in an arrangement that may illustrate the role of Rli1p in stimulating the peptide-release activity of canonical termination factors) (Becker et al., 2012). *In vivo* and *in vitro* there is a direct or indirect interaction of Rli1p with eRF1 and Dom34, as well as the interaction of Dom34 and Rli1p on the ribosome which is relatively stable in yeast (Shoemaker & Green, 2011). Khoshnevis et al. (2010) used nonsense suppression assays to show that *RLI1* overexpression can compensate for inefficient termination produced by mutations in certain release factors, although they did not distinguish whether this was due to the activity of Rli1p in recycling or to a distinctive activity. Numerous studies have implicated the Dom34–Rli1 interaction in humans in splitting free 80S ribosomes or stalled ribosomes at the 3' end of mRNA (Pisareva et al., 2011; Kobayashi et al., 2010; Bhattacharya et al., 2010). Dom34 and Hbs1 are known to act together in splitting ribosomal subunits and dissociating peptidyl-tRNA in yeast; efficient dissociation occurs in the presence of Rli1p and depends on ATP hydrolysis (Pisareva et al., 2011; Shoemaker et al., 2010). Thus, Rli1p increases (>10-fold) the rate of subunit dissociation by Dom34 in a manner that depends on its ATPase activity (the presence of Hbs1 increases the rate by approximately 2.5 fold) (Shoemaker & Green, 2011). Pisareva et al. (2010) showed that dissociation of post-termination complexes to free 60S subunits as well as mRNA- and tRNA- associated 40S subunits can be performed by Rli1p. Hydrolysis of NTP by Rli1p is motivated by post-termination complexes (post-TCs) and is necessary for its activity in recycling. Furthermore, the presence of eRF1/eRF3 (or only eRF1) in post-TCs is required for dissociation of these complexes by Rli1p (Pisareva et al., 2010).

Barthelme et al. (2011) revealed that ATP binding leads to a conformational switch within Rli1 (open-closed) which results in

ribosome dissociation and separation of the peptide release factor aRF1. The Fe-S domain was required for the ribosome splitting. Hydrolysis of ATP was required for releasing Rli1 from the 30S subunit to participate in a new cycle. The results described above collectively describe the role of Rli1 in the final stages of mRNA translation.

1.10 Aims of the current work

Rli1p was the first cytosolic Fe-S protein found to be essential for eukaryotic cell viability. Several studies of Fe-S protein targeting to date have focused on non-essential Fe-S proteins. My interest in Fe-S clusters developed as a result of previous work in the Avery laboratory which showed that methionine sulfoxide reductases (MSRs) have an important role in helping to protect the essential function of Fe-S clusters in oxidatively stressed yeast, where elevated oxidative targeting of Fe-S clusters was observed in *msrΔ* mutants (Sideri et al., 2009). That study also suggested a link between toxicity of the prooxidant metal copper and the cluster integrity of Fe-S proteins in yeast. Those results combined with the notorious ROS-lability of Fe-S clusters and the facts that (i) integrity of the N-terminal [4Fe-4S] cluster domain of Rli1p is crucial for its function in protein synthesis, (ii) Rli1p is one of the most highly conserved proteins across the eukaryotes and archaea (Barthelme et al., 2007; Becker et al., 2012), and (iii) Rli1p is essential in all organisms tested (Winzeler et al., 1999; Coelho et al., 2005; Estevez et al., 2004), made the predominant aim of this study to test the hypothesis that Rli1p could be a primary cellular target of inhibitory ROS action. To test this hypothesis, the project set out to determine whether:

1. The expression level of *RLI1* determines the level of ROS resistance in yeast.
2. Rli1p function (in nuclear export of ribosomal subunits) is sensitive to oxidative stress.
3. An oxidative mechanism is involved in Rli1p-dependent pro-oxidant resistance.
4. Effects of ROS on mRNA translation may be mediated through Rli1.

Chapter 2- Materials and Methods

2.1 Strains and Plasmids

Saccharomyces cerevisiae BY4741 (for genotypes, see Table 1) and the derivative deletion-mutant *sod2Δ* was obtained from Euroscarf (Frankfurt, Germany). A *S. cerevisiae msraΔ/msrbΔ* (*msrΔ*) double mutant in the same background (BY4741) was kindly provided by V. N. Gladyshev (University of Nebraska) and used in a previous study in the Avery laboratory (Sideri *et al.*, 2009). BY4741 was the background used for all experiments except where an alternative background is specified. The wild type W303 and isogenic *tet-RLI1* strains were kind gifts from R. Lill (University of Marburg) (Kispal *et al.*, 2005). Strain R1158 and isogenic strains carrying the following constructs were from Open Biosystems (Lafayette, Colorado): *tet-RLI1*, *tet-RAD3*, *tet-PRI2*, *tet-POL1*, *tet-POL2*, *tet-POL3*. The *S. cerevisiae rli1^{C58A}* mutant was kindly provided by R. Tampe (University of Frankfurt) (Barthelme *et al.*, 2007). An isogenic control strain was constructed in a previous study in the Avery laboratory by inserting the *HIS3* marker alone at *RLI1* locus in strain BY4741. The *S. cerevisiae* L1494 wild type was kindly provided by Dr Susan Liebman (University of Illinois at Chicago) (Chernoff *et al.*, 1994). Plasmid *pRS315-RPS2-eGFP* was kindly donated by E. Hurt (University of Heidelberg) (Milkereit *et al.*, 2003; Kispal *et al.*, 2005). *pCM190-tetRLI1* was constructed in a previous study in the Avery laboratory by PCR amplification of a fragment encompassing the *RLI1* ORF from yeast genomic DNA, and ligating between the *NotI* and *PstI* sites of *pCM190* (Euroscarf, Frankfurt). *pCM190-tetATM1* was constructed in this study using similar procedures (see 2.1.1). This placed *RLI1* or *ATM1* under the control of the *tetO* promoter. The dual-luciferase plasmid containing firefly (FF) and renilla luciferase separated by an in-frame stop codon (*TAA*) was a kind gift from Dr David Bedwell, University of Alabama (Howard *et al.*, 2000). Maps of the plasmids described can be found in (Fig 2.1). Strains that were used in this study are listed in Table 1.

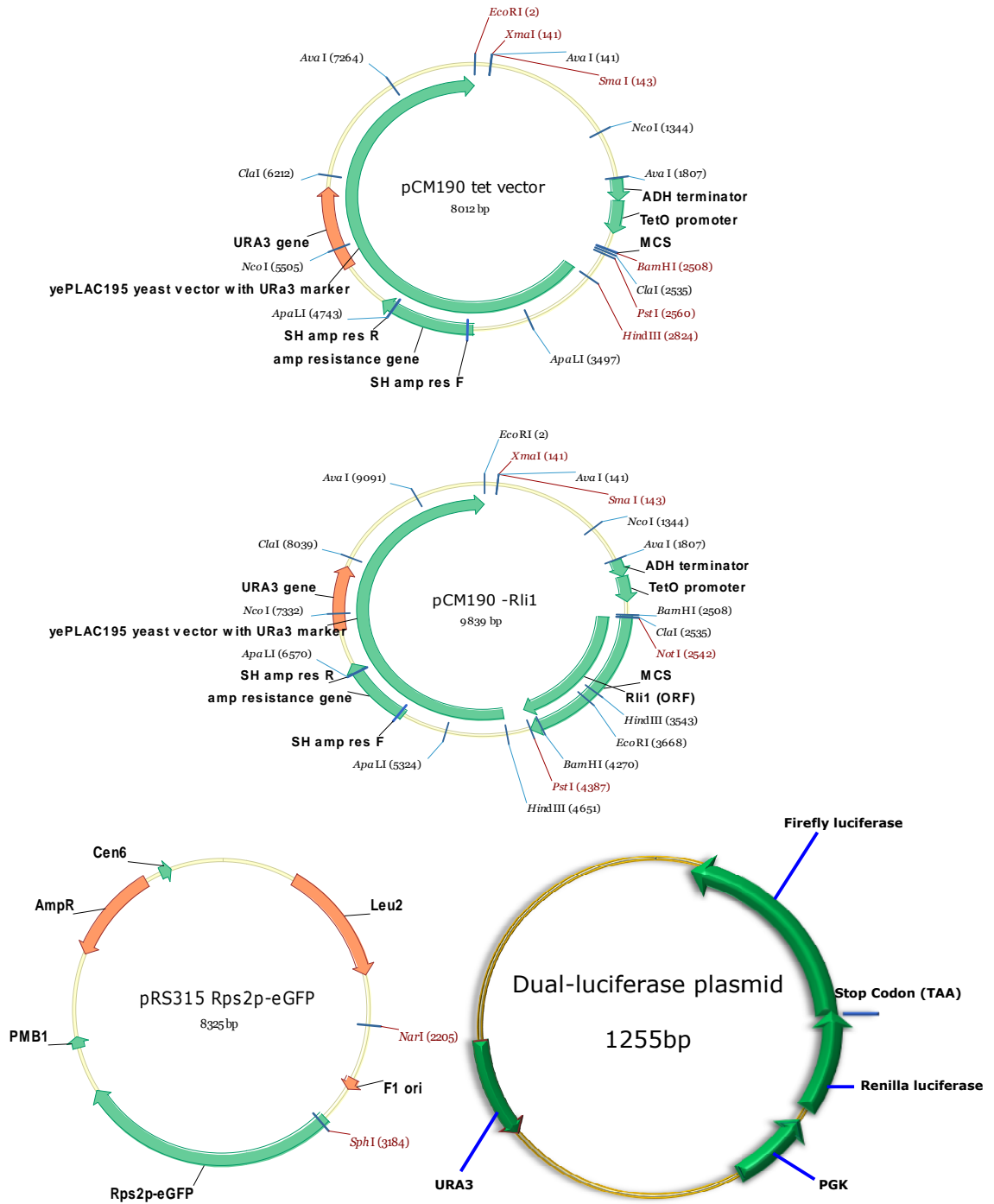


Figure 2.1– Maps of key plasmids utilised during this study. Their construction and/or source are described in section 2.1.

Table 1- *S. cerevisiae* strains used in this study

Strain	Description and Genotype	Source
BY4741 (wild type)	<i>MATα</i> ; <i>his3Δ1</i> ; <i>leu2Δ0</i> ; <i>met15Δ0</i> ; <i>ura3Δ0</i>	Euroscarf (Frankfurt, Germany)
<i>BY4741-ev</i>	BY4741 transformed with empty vector <i>pCM190</i> containing the <i>URA3</i> marker.	This study
<i>BY4741-RLI1</i>	BY4741 transformed with plasmid <i>pCM190</i> -borne <i>tet-RLI1</i> construct. <i>URA3</i> marker.	This study
<i>BY4741-ATM1</i>	BY4741 transformed with plasmid <i>pCM190</i> -borne <i>tet-ATM1</i> construct. <i>URA3</i> marker.	This study
W303 (wild type)	<i>MATα</i> ; <i>ura3-1</i> ; <i>ade2-1</i> ; <i>trp1-1</i> ; <i>his3-11,15</i> ; <i>leu2-3,112</i>	R. Lill (University of Marburg)
<i>W303- pRS315-RPS2-eGFP</i>	W303 transformed with plasmid <i>pRS315</i> borne ribosomal subunit <i>RPS2</i> tagged with green fluorescent protein GFP. <i>LEU2</i> marker.	This study
<i>W303-TAA dual luciferase</i>	W303 transformed with dual-luciferase plasmid containing <i>Firefly</i> and <i>Renilla</i> luciferase genes, separated by a stop codon <i>TAA</i> . <i>URA3</i> marker.	This study
<i>tet-RLI1</i>	<i>RLI1</i> endogenous promoter of strain W303 replaced by titratable <i>TetO</i> promoter, allowing control of the expression levels of <i>RLI1</i> with doxycycline. <i>pRLI1::kanR-tetO7</i> TATA <i>MATα</i> ; <i>ura3-1</i> ; <i>ade2-1</i> ; <i>trp1-1</i> ; <i>his3-11,15</i> ; <i>leu2-3,112</i>	R. Lill (University of Marburg)

<i>tet-RLI1- pRS315-RPS2-eGFP</i>	Strain <i>tet-RLI1</i> transformed with <i>pRS315-RPS2-eGFP</i> . <i>LEU2</i> marker.	This study
<i>tet-RLI1- TAA dual luciferase</i>	Strain <i>tet-RLI1</i> transformed with dual-luciferase plasmid. <i>URA3</i> marker.	This study
<i>msraΔmsrbΔ(msrΔ)</i>	<i>msraΔ/msrbΔ (msrΔ)</i> double mutant in the BY4741 background. <i>MATa</i> ; <i>his3Δ1</i> ; <i>leu2Δ0</i> ; <i>met15Δ0</i> ; <i>ura3Δ0</i> ; <i>msra::kanMX4</i> ; <i>msrb::URA3</i>	V. N. Gladyshev (University of Nebraska)
<i>msraΔmsrbΔ-ev</i>	<i>msrΔ</i> transformed with empty vector <i>pCM190</i> with <i>URA3</i> marker.	This study
<i>msraΔmsrbΔ-ev- pRS315-RPS2-eGFP</i>	<i>msraΔmsrbΔ-ev</i> above was additionally transformed with plasmid <i>pRS315-RPS2-eGFP</i> . <i>LEU2</i> marker.	This study
<i>msraΔmsrbΔ-RLI1</i>	<i>msrΔ</i> above transformed with plasmid <i>pCM190</i> -borne <i>tet-RLI1</i> construct. <i>URA3</i> marker.	This study
<i>msraΔmsrbΔ-RLI1- pRS315-RPS2-eGFP</i>	<i>msraΔmsrbΔ-RLI1</i> above was additionally transformed with plasmid <i>pRS315-RPS2-eGFP</i> . <i>LEU2</i> marker.	This study
<i>sod2Δ</i>	<i>sod2Δ</i> mutant in the BY4741 background. <i>MATa</i> ; <i>his3Δ1</i> ; <i>leu2Δ0</i> ; <i>met15Δ0</i> ; <i>ura3Δ0</i> ; <i>sod2::kanMX4</i>	Euroscarf (Frankfurt, Germany)
<i>sod2Δ-ev</i>	<i>sod2Δ</i> mutant above transformed with empty vector <i>pCM190</i> . <i>URA3</i> marker.	This study
<i>sod2Δ-RLI1</i>	<i>sod2Δ</i> mutant above transformed with plasmid <i>pCM190</i> -borne <i>tet-RLI1</i> construct. <i>URA3</i> marker.	This study
<i>BY4741-HIS3</i>	This strain was created by amplifying the upstream <i>HIS3</i> marker from <i>pRS423</i> plasmid received from (Barthelme et al., 2007), and targeting it upstream of the <i>RLI1</i> genomic locus in wild type strain BY4741, i.e. to the	Avery laboratory

	same location as in the mutant strain <i>rli1</i> ^{C58A} (below), creating a His ⁺ control.	
<i>rli1</i> ^{C58A}	Strain <i>rli1</i> ^{C58A} was created by amplifying the <i>RLI1</i> ^{C58A} coding sequence along with the upstream <i>HIS3</i> marker from <i>pRS423</i> (Barthelme et al., 2007), and targeting this to replace the native <i>RLI1</i> sequence in strain BY4741.	Avery laboratory
<i>rli1</i> ^{C58A} -ev	Strain <i>rli1</i> ^{C58A} transformed with empty vector <i>pCM190</i> . <i>URA3</i> marker.	This study
<i>rli1</i> ^{C58A} - <i>RLI1</i>	Strain <i>rli1</i> ^{C58A} transformed with the plasmid <i>pCM190</i> -borne <i>tet-RLI1</i> construct. <i>URA3</i> marker.	This study
R1158 (wild type)	<i>URA3::CMV-tTA MATa his3-1; leu2-0; met15-0</i> .	Open Biosystems
<i>Tet-RLI1</i>	Strain with the endogenous <i>RLI1</i> promoter replaced by a titratable <i>TetO</i> promoter in the R1158 background. <i>pRLI1::kanR-tet07-TATA URA3::CMV-tTA MATa his3-1 leu2-0 met15-0</i> .	Open Biosystems
<i>Tet-POL1</i>	<i>pPOL1::kanR-tet07-TATA URA3::CMV-tTA MATa his3-1 leu2-0 met15-0</i> .	Open Biosystems
<i>Tet-POL2</i>	<i>pPOL2::kanR-tet07-TATA URA3::CMV-tTA MATa his3-1 leu2-0 met15-0</i> .	Open Biosystems
<i>Tet-POL3</i>	<i>pPOL3::kanR-tet07-TATA URA3::CMV-tTA MATa his3-1 leu2-0 met15-0</i> .	Open Biosystems
<i>Tet-PRI2</i>	<i>pPRI2::kanR-tet07-TATA URA3::CMV-tTA MATa his3-1 leu2-0 met15-0</i> .	Open Biosystems
<i>Tet-RAD3</i>	<i>pRAD3::kanR-tet07-TATA URA3::CMV-tTA MATa his3-1 leu2-0 met15-0</i> .	Open Biosystems

L1494	(<i>MAT</i> α <i>ade1-14(UGA)</i> ; <i>his7-1 (UAA)</i> ; <i>lys2-L864 (UAG)</i> ; <i>leu2-3,112</i> ; <i>trp1Δ1</i> ; <i>ura3-52RDNA</i> <i>pRDN-wt (TRP1, LEU2-d rDNA)</i>).	Dr Susan Liebman (University of Illinois at Chicago)
<i>L1494-ev</i>	L1494 wild type strain above transformed with empty vector <i>pCM190</i> . <i>URA3</i> marker.	This study
<i>L1494-RLI1</i>	L1494 wild type strain above transformed with plasmid <i>pCM190</i> borne <i>tet-RLI1</i> construct. <i>URA3</i> marker.	This study

2.1.1 Construction of *pCM190-tetATM1*

The empty episomal vector *pCM190*, containing the *tetO* promoter and carrying the *URA3* marker, was used for overexpression of *ATM1* under the control of the *tetO* promoter. The -314bp upstream to 1961bp downstream *ATM1* region was amplified from *ATM1* ORF, together with 1kb each of the upstream and downstream genomic sequence using the FWD/*ATM1* and REV/*ATM1* primers listed in Table 2 to generate 2251bp *ATM1* fragment. The PCR reaction was performed using Phusion[®] high-fidelity DNA polymerase (Finzymes) and cycling conditions as described in 2.4.1, Table 4. The PCR fragment was purified by using ethanol precipitation as described in (2.9.1). This fragment was subsequently digested with *NotI* and *PstI* and ligated into the similarly digested plasmid *pCM190-ev*, to generate *pCM190-tetATM1* (Fig 2.2 C). Following transformation into *Escherichia coli* XLI blue as described in 2.10.2, and selection on LB ampicillin plates as described in 2.2, successful ligation was first indicated by diagnostic colony PCR as illustrated in 2.4.4 using FWD/*ATM1* and REV/*ATM1* primers (Figure 2.2 A). Correct ligation was further confirmed by digestion of plasmid DNA with *NotI* and *PstI* to produce bands of ~8kb and ~2kb (Figure 2.2 B). Transformation of *pCM190-tetATM1* into *S. cerevisiae* BY4741 cells followed as described in

2.10.1, with successful transformants selected for on YNB agar minus uracil. Additional confirmation was obtained by isolation of plasmid DNA from transformed yeast followed by diagnostic restriction digests as described above.

Table 2- Primers used to generate ATM1 fragment for insertion in pCM190

Name	Sequence
ATM1-FWD	GATAGCGGCCGCATGCTGCTTCTTCCAAGATGTCCTG
ATM1-REV	GGCCCTGCAGGCGCATGAGCAGTCATTCGGATTC

❖ Underlined sequence corresponds to restriction sites.

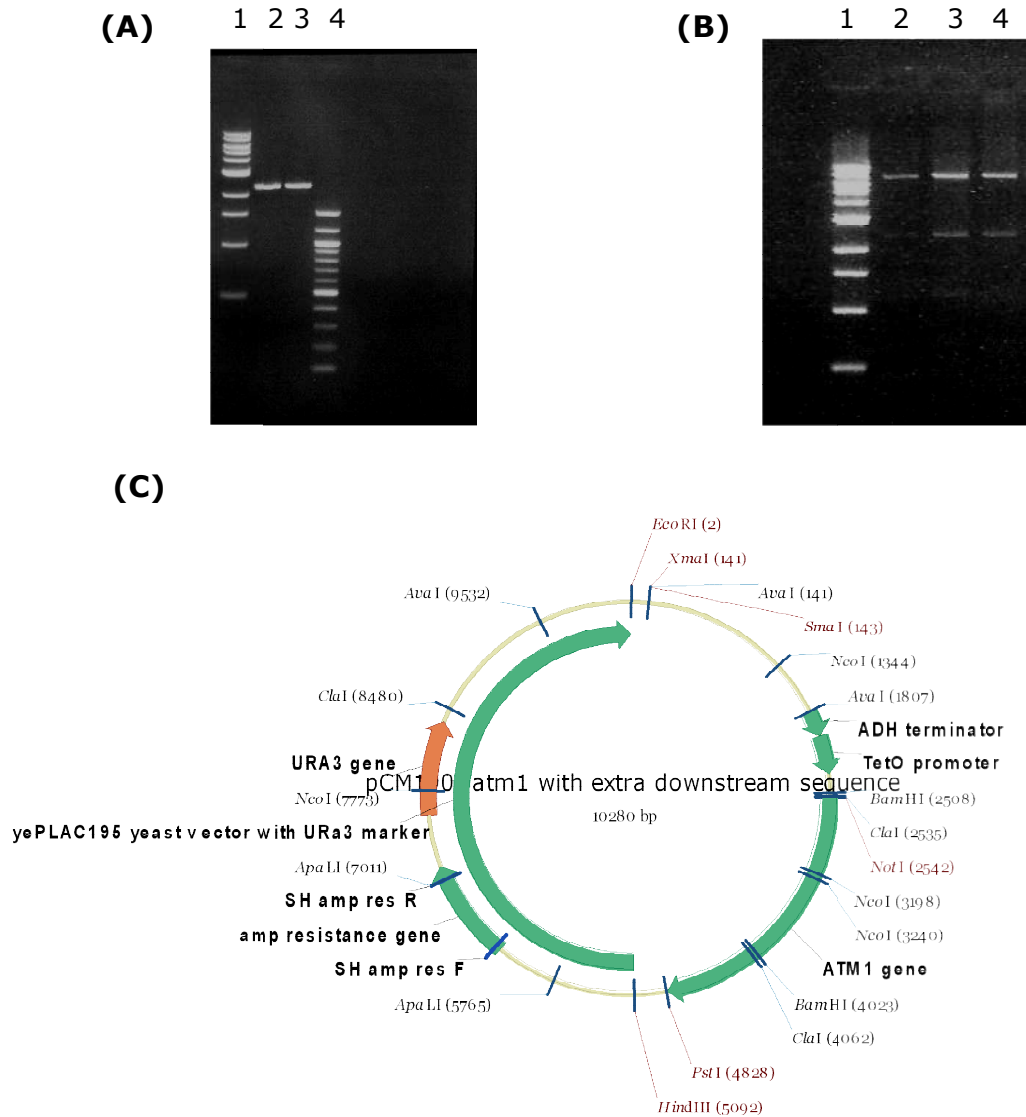


Figure 2.2– Construction of *pCM190-tetATM1*. (A) Amplification of *ATM1* from *pCM190-tetATM1* using FWD/*ATM1* and REV/*ATM1* primers Lane 1, 1Kb DNA ladder; Lanes 2 and 3, *ATM1* PCR product ~2Kb; Lane 4, 100 bp ladder. (B) Digestion of plasmid *pCM190-tetATM1* with *Not1* and *Pst1* to produce bands of ~8kb and ~2kb. Lane 1, 1Kb DNA ladder; Lane 2, vector *pCM190-ev*, ~8Kb; Lanes 3 and 4, ~8kb (vector) and ~2kb (insert) of digested *pCM190-tetATM1*. (C) Map of Plasmid *pCM190-tetATM1* constructed and utilised during this study. Markers: URA3 and amp.

2.2 Growth conditions

Yeast strains were routinely maintained and grown either in yeast extract peptone dextrose (YEPD) broth [1% (w/v) yeast extract, 2% (w/v) bactopectone, 2% (w/v) glucose], or YEPD agar [same but containing 1.6% (w/v) agar], or in yeast nitrogen base (YNB) medium [0.69% yeast nitrogen base without amino acids (Formedium), 2% (w/v) D-glucose] supplemented with the appropriate amino acids, but lacking uracil or leucine as selective markers within plasmids (Ausubel et al., 2007). When necessary, the medium was solidified with 2% (w/v) agar (Sigma). Cultures were grown with shaking at 120 rev/min and 30°C, overnight to stationary phase in standard YEPD or selective YNB broth, before dilution into fresh medium and further growth for 4-5h before experimental use (Holland & Avery, 2009).

In all cases, *E. coli* XLI blue strains were maintained on Luria Bertani (LB) medium (1% tryptone, 0.5% yeast extract, 1% NaCl, with 1.5% agar for plates) (Bertani, 1951) supplemented with ampicillin ($50\mu\text{g ml}^{-1}$) and grown with shaking at 200 rev min^{-1} , 37°C. In order to generate electro-competent cells (2.10.2.1), *E. coli* XLI blue was grown in LB broth supplemented with tetracycline ($50\mu\text{g ml}^{-1}$). All required amino acids and antibiotics are listed in Table 3.

An anaerobic atmosphere for growth assays (using agar plates) was generated with an Oxoid Gas Generating kit (Anaerobic system BR0038B) (Oxoid, Basing-stock, Hampshire, UK). Plates were placed in an anaerobic jar containing Palladium pallets (Anaero Jar, AG 0025A-OXOID), then a BR0038B-OXOID sachet tablet was added which contains sodium borohydride, citric acid and sodium bicarbonate and produces 1800ml H_2 and 350ml CO_2 . Anaerobic indicator strips (BR0055B-OXOID) were included to give a visual indication of anaerobiosis, i.e. a colour change from pink to white.

Short term storage of all yeast and bacterial strains took place at 4°C on the appropriate agar plates. For long term storage glycerol stocks were produced with 20% (w/v) glycerol and kept at -80°C.

Table 3- Amino Acid and Antibiotic Concentrations

Amino Acid Or Antibiotic	Stock Concentration (mg ml⁻¹)	<i>S. cerevisiae</i> Working Concentration (µg ml⁻¹)	<i>E. coli</i> Working Concentration (µg ml⁻¹)
Histidine	10	20	-
Uracil	2	20	-
Leucine	10	100	-
Methionine	10	20	-
Tryptophan	10	20	-
Lysine	10	30	-
Adenine	2	6	-
Ampicillin	50	-	50
Tetracycline	5	-	50
Hygromycin	50	500	-
Doxycycline	1	10	-
Cycloheximide	2.5	50-80	-
Paromomycin	20	100	-

Tetracycline stock solution was made in ethanol. In all other cases, stock solutions were made to the concentrations indicated in dH₂O and filter sterilised. Amino acid stock solutions were stored at 4°C and antibiotic stock solutions were stored at -20°C with the exception of hygromycin which was kept at 4°C.

2.3 Isolation of DNA

In all cases isolated genomic and plasmid DNA was stored at -20°C.

2.3.1 Genomic DNA extraction from *S. cerevisiae*

Cultures (10ml) of *S. cerevisiae* were grown in YEPD overnight at 30°C to stationary phase. 1.5ml of culture was centrifuged at 13000g for 1min. The supernatant was discarded and

the remaining pellet was resuspended in 1ml of sterile dH₂O. The suspension was centrifuged at 13000g for 1min at room temperature and the supernatant was discarded. The cell pellet was resuspended in 200µl breaking buffer [2% (w/v) Triton X-100, 1% (w/v) SDS, 100mM NaCl, 10mM Tris HCl pH 8.0, 1mM EDTA pH 8.0]. 0.3g glass beads (acid washed-Sigma) and 200µl phenol-chloroform (Sigma) were added. A mini bead beater (Biospec products) was used (2x30s shaking with an intervening 2min incubation on ice) to break open the cells. After centrifugation for 5min at 13000g at room temperature, the upper aqueous layer (200µl) was transferred to a clean tube, and 20µl of 3M sodium acetate and 660µl of 100% (v/v) ethanol were added with mixing by inversion. The mixture was incubated on ice for 15min. After centrifugation for 10min, 13000g, 4°C, the supernatant was removed and discarded and the remaining pellet washed in 400µl of (v/v) 70% ethanol by centrifugation for 5min, 13000g at 4°C. Ethanol was removed and the pellet allowed to air dry for 5-10min. The pellet was resuspended in 100µl sterile pure water and incubated at 65°C for 5min in order to dissolve the DNA.

2.3.2 Plasmid DNA extraction from *E. coli*

Plasmid DNA was isolated from *E. coli* from overnight liquid cultures in LB broth, containing ampicillin for plasmid selection (Table 3). Mini preparations of plasmid DNA were with the Zyppy™ Plasmid Miniprep Kit (Zymo Research Corp) as follows: 100µl of Lysis Buffer were added directly to 600µl of overnight bacterial culture. Samples were mixed by inversion four to six times. An aliquot (350µl) of cold Neutralization Buffer was added and samples were mixed by inversion several times to ensure complete neutralisation. After centrifugation at 13000g for 4min, the supernatant, (~900µl), was carefully transferred to a Zymo-Spin™ IIN column. The column was placed in a collection tube and centrifuged for 15s at 13000g, the flow through was discarded and the column placed back in the same collection tube. 200µl of Endo-Wash Buffer was added to the column. Samples were centrifuged at 13000g for 15s followed by the addition of 400µl Zyppy™ Wash Buffer. After centrifugation for 30s at 13000g, columns

were transferred into a clean 1.5ml microfuge tubes and plasmid DNA was eluted by adding 30µl of Zyppy™ Elution Buffer directly to the column matrix. Samples were allowed to stand for 1min at room temperature, and then centrifuged at 13000g for 15s.

2.3.3 Plasmid DNA extraction from *S. cerevisiae*

Yeast colonies containing the plasmid of interest were inoculated in selective YNB broth in 5ml sterile tubes with the appropriate supplements and vortexed for 1min. Cultures were left to grow overnight to stationary phase at 30°C, 120 rev min⁻¹. An aliquot (1.5ml) of culture was centrifuged at 13000g for 5min. The supernatant was discarded by pouring and the pellet resuspended in the residual liquid, ~50µl. 10µl Lyticase (5U/µl) was added and the samples mixed thoroughly by pipetting before being incubated at 37°C, 200 rev min⁻¹ for 1h. Sodium dodecyl sulfate (SDS) [(20µl of 10% (w/v))] was added to the samples which were then vortexed for 1min and frozen at -20°C. Samples were thawed and made up to 600µl with sterile dH₂O. The protocol for plasmid isolation from *E. coli* (2.3.2) was then followed from the point of adding 100µl of Lysis Buffer.

2.4 Polymerase Chain Reaction (PCR)

PCR reactions were performed using a Techne TC-512 gradient thermal cycler. For reactions, Phusion® high-fidelity DNA polymerase (Finzymes) (2.4.1, Table 4) was used when high accuracy was required, or Taq DNA polymerase (New England Biolabs Inc) (2.4.2, Table 5) for diagnostic PCR reactions. PCR reactions using genomic/plasmid DNA and colony PCR (2.4.3, 2.4.4) reactions were carried out in a total volume of 50µl in 0.2ml PCR tubes (Star Lab). The amplification products were analysed by agarose gel electrophoresis (2.6) in the appropriate strength gel. Any PCR products required for cloning were excised from gels and the DNA purified by gel extraction (2.7).

2.4.1 Phusion[®] High-Fidelity DNA polymerase PCR reaction

The standard reaction mixture for PCR reactions utilising Phusion[®] high-fidelity DNA polymerase is detailed in Table 4. Cycling conditions for these reactions were: initial denaturation at 98°C for 30s, followed by 30 cycles of 10s at 98°C, 30s at (*) °C, and 30s per kb of the desired product at 72°C; these 30 cycles were followed by a 10min extension at 72°C before a final hold at 4°C.

*T_m values were calculated using the nearest-neighbor method. Primers > 20nt were annealed at a temperature +3°C of the lower T_m primer. For primers ≤20 nt an annealing temperature equal to the T_m of the lower T_m primer was used.

Table 4- Phusion[®] High-Fidelity DNA Polymerase PCR Reaction Mixture

Component	50µl Reaction
dH ₂ O	Add to 50µl final volume
5X Phusion [®] HF Buffer	10µl (1x)
10mM dNTPs	1µl (200µM final conc.)
Forward primer	2.5µl (0.5µM final conc.)
Reverse Primer	2.5µl (0.5µM final conc.)
Template DNA	1µl (50-250ng)
DMSO (100%)	1.5µl
Phusion [®] DNA Polymerase	0.5µl

2.4.2 Taq DNA Polymerase PCR Reaction

The standard reaction mixture for PCR reactions using Taq DNA polymerase is detailed in Table 5. Cycling conditions for these reactions were: initial denaturation at 95°C for 30s, followed by 30 cycles of 15s at 95°C, 30s at (*)°C, and 1min per kb of the desired product at 72°C; these 30 cycles were followed by a 5min extension at 72°C before a final hold at 4°C.

*T_m values were calculated using the nearest-neighbor method. Primers > 20 nt were annealed at a temperature +3°C of the

lower T_m primer. For primers ≤20 nt an annealing temperature equal to the T_m of the lower T_m primer was used.

Table 5- Taq DNA Polymerase PCR Reaction Mixture

Component	50µl Reaction
dH ₂ O	Add to 50µl final volume
10x Standard Taq or ThermoPol Buffer	5µl (1x)
10mM dNTPs	1µl (200µM final conc.)
Forward primer	2.5µl (0.5µM final conc.)
Reverse Primer	2.5µl (0.5µM final conc.)
Template DNA	1µl (50-500ng)
Taq DNA Polymerase	0.4µl

2.4.3 Yeast Colony PCR

A stock solution of lyticase (L4025 Sigma) was diluted to 50 µl⁻¹ and aliquoted in 50µl quantities. *S. cerevisiae* colonies were picked using either a sterile wooden cocktail stick or pipette tip and added to the 50µl lyticase aliquots (1 colony per aliquot). Samples were then agitated by pipetting and incubated at 30°C for 30min. After incubation at 95°C for 10min, 5µl of each sample was used as template in a 50µl Taq DNA polymerase PCR reaction (2.4.2, Table 5).

2.4.4 Bacterial Colony PCR

In order to ensure the presence of insert into plasmid DNA during cloning, bacterial colony PCR was used where colonies were picked using either a sterile wooden cocktail stick or pipette tip and added to 10µl dH₂O (1 colony per aliquot). Samples were then agitated by pipetting and incubated at 95°C for 15min. Tubes were briefly spun to collect any condensation. 5µl of each sample was then used as template in a 50µl Taq DNA polymerase PCR reaction (2.4.2, Table 5).

2.5 DNA sequencing

High sensitivity DNA sequencing reactions were performed by the University of Nottingham, Medical School Sequencing

laboratory. Analysis was performed using a 3130x1 PRISM Genetic Analyser, with BigDye v3.1. Primers used for sequencing are shown in Table 6. The template concentration used was 100ng μl^{-1} .

Table 6– Sequencing Primers

Primer	Sequence (5'-3')
FWD-SEQ1	GGCATGCATGTGCTCTGTAT
REV-SEQ2	ATAAATAACGTTCTTAATAC

2.6 Digestion of DNA with Restriction Enzymes

Restriction enzymes were used in accordance with the instructions of manufacturer, New England Biolabs Inc. All reactions of restriction digestion were performed in a total volume of 50 μl with incubation at 37°C, overnight. Digestion products were separated by electrophoresis on the appropriate percentage agarose gel (2.7). Where specific digestion products were required for further use (e.g. cloning) the corresponding band was excised from the gel and the DNA purified by gel extraction (2.8).

2.7 DNA Agarose Gel Electrophoresis

Separation of nucleic acids according to size was conducted by electrophoresis using high melting temperature agarose gels. Gels of various concentrations, typically between 0.8-1.5% (w/v) were used depending on the size of nucleic acid fragments to be resolved. Gels were usually prepared using the appropriate amount of agarose (Seakem[®] LE Agarose) in 1x TAE buffer (242g Tris-base, 200ml 0.5M EDTA pH 8.0, 57.1ml CH₃COOH, made up to the volume required with H₂O) followed by heating in a microwave until the agarose had dissolved. Dissolved agarose was left to cool for approximately 15min at which point ethidium bromide was added to a final concentration of 0.5 $\mu\text{g ml}^{-1}$ to allow visualisation of separated DNA. Dissolved agarose was then poured into a specialized tray containing appropriate comb to create wells in the agarose gel, and allowed to set for ~20min to form a solid gel. Gels were placed into the appropriately sized

electrophoresis tank filled with 1x TAE electrophoresis buffer. Bromophenol blue DNA loading dye (50mM Tris-HCl pH 7.6, 100mM EDTA, 15% Ficoll, 0.25% Xylene cyanol, 0.25% Bromophenol blue, dissolved with dH₂O) was added to samples at a final concentration and they were loaded onto the gel along with either a 1kb or 100bp DNA ladder (NEB UK) (Fig 2.3). Gels were run for 40-60min at 80-100V using a Biorad Power-Pac 300. Following electrophoresis, separated DNA was visualised using a Biorad Gel Doc 2000.

2.8 DNA purification from Agarose Gel

The GeneFlow Q-Spin gel Extraction/PCR Purification Kit (GeneFlow) was used to do gel extraction. For DNA extraction from agarose gels, a desired fragment was excised and transferred to a 1.5ml microfuge tube. The gel fragment was weighed and an equivalent (w/v) amount of Binding Buffer was added. For agarose gels greater than 1.5% (w/v), twice the volume of Binding Buffer was used. Samples were incubated at 55°C with occasional vortexing until the gel had completely dissolved. The resulting solution was transferred to a spin column and allowed to stand at room temperature for 3min. Spin columns were centrifuged for 1min at 11000g and flow through in the collecting tube discarded. 500µl of Wash Solution I was added to each column before centrifugation for 15s at 11000g and the flow through discarded. This wash step was then repeated. A longer centrifugation step of 1min at 11000g removed any residual Wash Solution I. Columns were then transferred to new 1.5ml collection tubes and 30-50µl of Elution Buffer added directly to the spin column membrane. Columns were allowed to stand at room temperature for 5min before DNA was eluted by centrifugation for 1min at 11000g. All DNA purified in this way was stored at -20°C.

1Kb ladder

100bp ladder

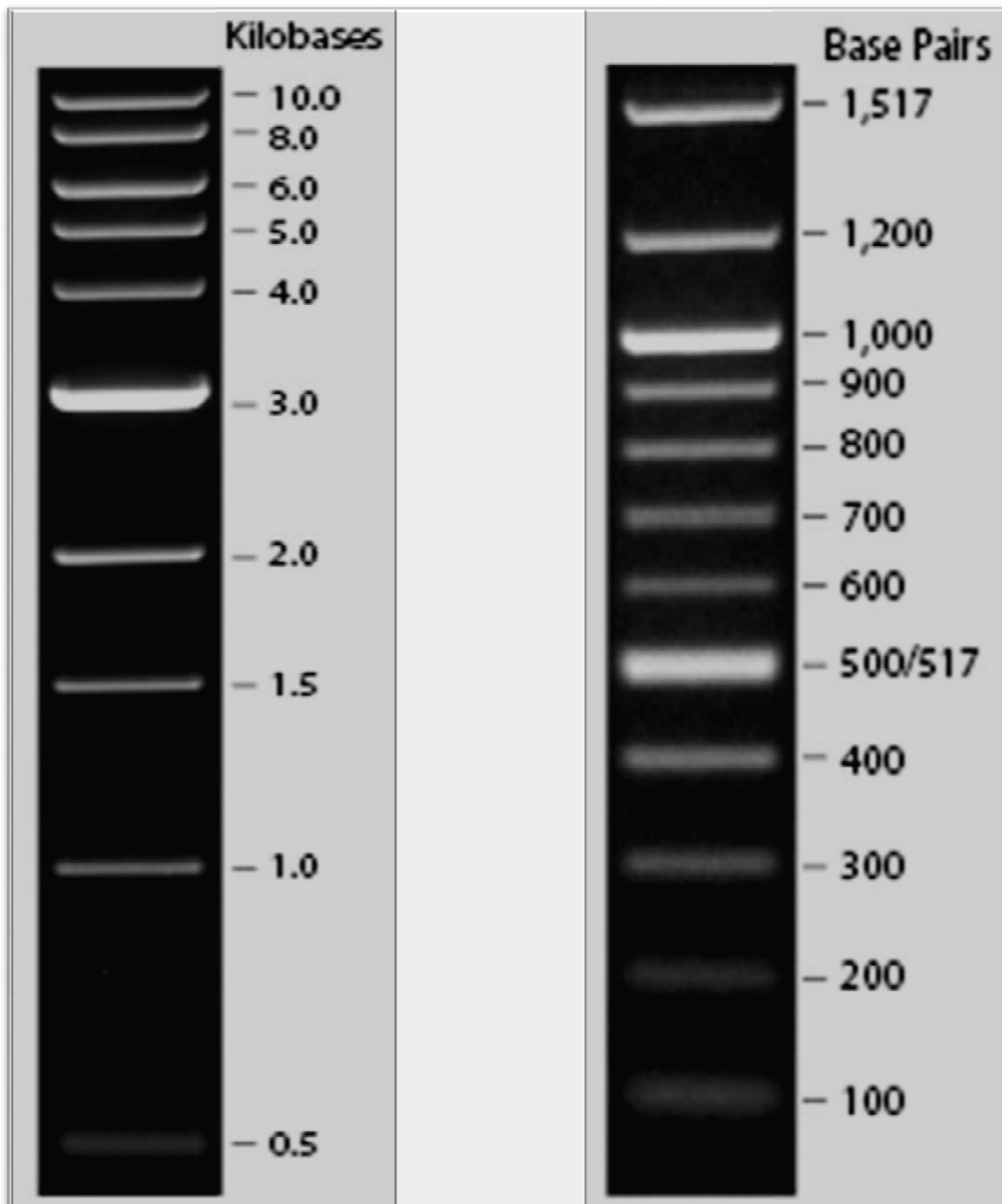


Figure 2.3- DNA ladders 1kb and 100bp used in agarose gel electrophoresis. As shown in Fig 2.2 A and B.

2.9 DNA Ligations

Before ligation, DNA fragments were purified from their either PCR (2.4) or restriction digest (2.6) enzymatic reactions. The CloneJET™ PCR Cloning Kit (K1231 Fermentas Life Sciences) was utilized for cloning of blunt ended Phusion® high-fidelity polymerase (Finnzymes) PCR products into the pJET1.2 blunt cloning vector (Fig 2.4). For this, 50ng of pJET1.2 blunt cloning vector were used per ligation reaction. Ligations not involving pJET1.2 were performed using 100-200ng of the appropriate vector per ligation reaction. DNA concentrations were measured using a Nano-Drop spectrophotometer (NanoDrop Technologies). Dephosphorylation of vector DNA was accomplished using Antarctic Phosphatase (M0289S NEB UK) prior to ligation, to help prevent self ligation via catalyzing the removal 5' phosphate from vector DNA (Sambrook et al., 1989). All DNA ligations were performed at room temperature using T4 DNA Ligase (M0202S NEB UK or supplied with the CloneJET™) after which ligated DNA was prepared for bacterial transformation (2.10.2) by ethanol precipitation (2.9.1). All enzymes were used in accordance with the manufacturer's instructions. A total volume not exceeding 30µl and an insert to vector fragment ratio of 3:1 was used in all cases. In order to calculate the appropriate amount of insert to include in the ligation reaction the following equation was used:

$$\text{Insert Mass (ng)} = \frac{\text{ng Vector} \times \text{Insert Length in bp}}{\text{Vector Length in bp}} \times \text{Insert:Vector Molar Ratio}$$

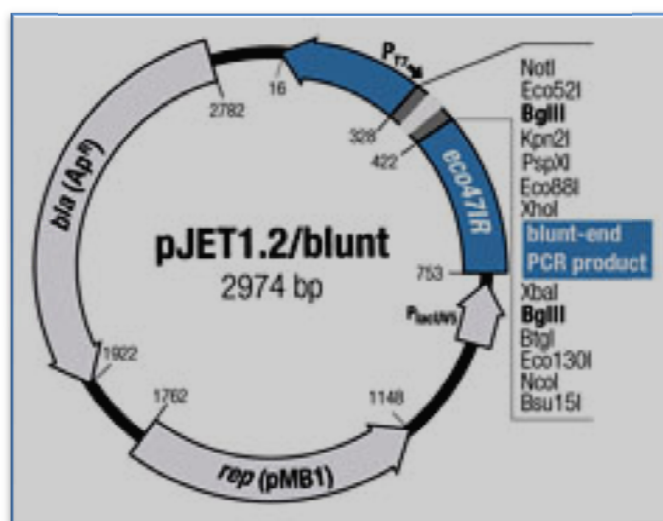


Figure 2.4- Map of pJET1.2/blunt Vector. Location of some restriction enzymes that cut pJET1.2/blunt once are shown. *NotI*: 328, *PstI*: 5. (Source: <http://www.thermoscientificbio.com/ligation>).

2.9.1 Ethanol Precipitation

To purify ligated DNA before transformation, ethanol precipitation was used. A 1/10 volume of 3M sodium acetate was added to ligated DNA in a microfuge tubes, followed by 3x the sample volume of 100% (v/v) ethanol. Samples were then mixed by inversion four to six times and kept on ice for approximately 15min. Samples were centrifuged at 13000g, 4°C, for 10min creating a DNA pellet. The supernatant was carefully removed so as not to disturb the pellet which was then washed with 70% (v/v) ethanol by centrifugation at 13000g, 4°C, for 1min. Ethanol was removed and DNA pellets air-dried, before being resuspended in 10µl dH₂O and incubated at 45°C for 5min in order to dissolve and collect the DNA. All samples were stored at -20°C.

2.10 Transformations

2.10.1 Transformation of plasmid DNA into Yeast

Yeast transformations were performed using the lithium acetate method (Gietz & Woods, 2002). Strains to be transformed were inoculated in liquid YEPD medium and left to grow overnight at 30°C. The cultures were diluted to OD₆₀₀~0.5 in 50ml YEPD and left to

grow at 30°C until OD₆₀₀ ~1. The cells were harvested by centrifugation at 3500g, 3min, and washed in 10ml sterile water. Samples (1ml) of 1x10⁸ cells were transferred to sterile Eppendorf tubes, centrifuged at 13000g, 10s, the supernatant was discarded and the cell pellet resuspended in 1ml of 100mM lithium acetate (LiAc). The suspension was incubated at 30°C for 10min. The suspension was centrifuged and the supernatant was discarded. To the cells was added a newly-prepared transformation mixture, comprising 240µl of 50% (w/v) polyethylene glycol 3350 (PEG), 36µl of 1M LiAc, 52µl of 2mg ml⁻¹ carrier DNA (salmon sperm DNA; 10mg ml⁻¹, Sigma, diluted to 2mg ml⁻¹ and denatured in a boiling water bath for 5min followed by 0-4°C incubation for 5min), 100ng-5µg of plasmid DNA, and sterile pure water up to 360µl final volume. The cell suspension was incubated at 30°C for 30min, then heat shocked by incubation at 42°C for 20min. The cells were centrifuged at 13000g, 10s and harvested. Cells were resuspended in 1ml of sterile dH₂O and allowed to recover for 5min at room temperature before aliquots of the suspension (20, 50, 100, 300µl) were plated on selective YNB agar as described in 2.2.

2.10.2 Preparation of Electro-competent *E. coli* XLI Blue cells

To prepare electro-competent *E. coli* XLI blue cells, cells were grown overnight in 10ml LB broth supplemented with tetracycline (50µg ml⁻¹). This culture was then added to 1L LB broth supplemented with tetracycline and grown to an OD₆₀₀ ~0.5-0.8. Cells were transferred to sterile centrifuge tubes and harvested by centrifugation at 8000g, 4°C for 20min. The supernatant was removed and cells resuspended in 1L of sterile ice-cold 1mM HEPES buffer. Cells were centrifuged at 10000g, 4°C for 15min and again pellets were resuspended in 1L sterile ice-cold 1mM HEPES. Resuspended cells were centrifuged at 10000g, 4°C for 15min before removal of the supernatant and resuspension in 100ml of sterile, ice-cold 1mM HEPES with 10% glycerol. A final centrifugation at 10000g, 4°C for 15min was performed and cells resuspended in 1ml sterile, ice-cold HEPES with 10% glycerol. Aliquots (52µl) of cells were transferred to sterile

screw-cap microfuge tubes and frozen on dry ice. Cells were then stored at -80°C until use.

2.10.2.1 Transformation of plasmid DNA into E. coli

All bacterial transformations were performed by electroporation of XL-1 blue *E. coli* cells. Electro-competent XLI blue cells (50µl) stored at -80°C as described in 2.10.2 were thawed on ice for 5min. Plasmid DNA (1-2µg) was added followed by further incubation on ice for 5min. This mixture was transferred to an electroporation cuvette on ice. The sample was electroporated at 1.8kV using a Biorad electroporator. One millilitre of super-optimal broth with catabolite repression (SOC) medium [2% (w/v) tryptone, 0.5% (w/v) yeast extract, 10mM NaCl₂, 2.5mM KCl, 10mM MgCl₂, 10mM MgSO₄, 20mM glucose] was then immediately added to the electroporation cuvette, and the suspension transferred to a 20ml sterile tube. Cells were allowed to recover by incubation at 37°C with shaking at 200 rev min⁻¹ for 1h. Aliquots (5, 10, 50, 150, 200µl) were spread on to LB agar plates supplemented with 50µg ml⁻¹ ampicillin and incubated overnight at 37°C.

2.11 Measurement of Protein Synthesis Rate

Precipitation of labelled protein using trichloroacetic acid (TCA) after cell incubation in the presence of ³⁵S-methionine enables the measurement of radiolabel incorporation, giving a means to estimate the quantity of protein synthesised in cells. In all cases radio labelled cells and protein extracts were stored at -20°C.

2.11.1 Metabolic labelling with ³⁵S-methionine

To measure the rate of protein synthesis in the absence or presence of cycloheximide or Cu (NO₃)₂, metabolic labelling of yeast cells with [³⁵S] methionine was performed where single colonies were inoculated in YNB media lacking the appropriate supplement (Ura) for plasmid selection and left to grow overnight to stationary phase. Cultures (20ml in 100ml flasks) were diluted to OD₆₀₀~0.05 and left to grow up to OD₆₀₀~0.5. Where indicated, cells were then pre-treated with a final concentration of 80µg ml⁻¹ cycloheximide or 0.35mM Cu

(NO₃)₂, and cultures were incubated for 1h at 30°C with shaking at 120 rev min⁻¹. For subsequent radio-labelling, 15ml of treated or non-treated cells were transferred to sterile tubes and incubated with 0.5µl (500µCi) [³⁵S] methionine (N007 EasyTag™ L-[³⁵S]-Methionine; NEN® Radiochemicals, Boston, MA 02118, USA) for 8min at 30°C with shaking. Cultures were centrifuged at 3500g for 3min. The supernatant was discarded and cells were washed three times in chase medium (YNB medium plus 1mg ml⁻¹ unlabeled methionine, resuspending in 30ml of chase medium and centrifuging at 3500g, 3min each time. Cell pellets resuspended in 1ml of chase medium were transferred to sterile screw-cap microfuge tubes. Cells were centrifuged at 3500g for 5min, the supernatant was discarded and cell pellets stored overnight at -20°C.

2.11.2 Protein extraction from *S. cerevisiae* cells

The method was based on that described by Rand & Grant (2006). Cell pellets (2.11.1) were resuspended in 400µl of lysis buffer, comprising 1.0M potassium phosphate buffer adjusted to pH 7 (Sigma), 0.5M EDTA adjusted to pH 8, 5% (v/v) glycerol, 0.5M phenylmethylsulfonyl fluoride (PMSF), and complete protease inhibitor cocktail tablets from Roche Ltd (diluted according to the manufacturer's instructions). After adding 425-600µm diameter glass beads (Sigma-Aldrich), cells were lysed using a Mini-bead beater for 5 x 20sec (the samples were incubated on ice for 1min between each disruption). Total protein extracts in supernatants were transferred to clean tubes and kept on ice after centrifugation at 6000g for 15min.

2.11.3 Protein quantification with the Bradford assay

Determination of protein concentration was according to Bradford (1976). A 1:5 dilution of the BioRad protein assay dye reagent concentrate (Bio-Rad) was prepared and 1ml was added to 20µl of each protein sample. After 10min, absorbance at 595nm was measured spectrophotometrically. A standard curve was constructed using 0-1mg ml⁻¹ bovine serum albumin (BSA) in the lysis buffer, and the gradient of the BSA standard curve used to determine the protein concentrations in the unknown samples.

2.11.4 Quantification of incorporated [³⁵S] methionine

The same amount of protein was taken from each protein-extract sample after using the method of sample normalization, and transferred to sterile microfuge tubes. 300µl of trichloroacetic acid (20% TCA, Sigma-aldrich) was added to precipitate protein, and the samples mixed thoroughly by pipetting before being incubated on ice for 30min. Vacuum filtration was used to collect the precipitated protein, using ethanol-soaked Whatman GF/C glass microfiber filters positioned at the centre of vacuum flasks and on to which sample was added. Filters were washed with 5ml of 10% TCA followed by 10ml of 95% cold ethanol to dry the filter and prevent quenching. The dry filter was placed into a scintillation vial with 5ml scintillation fluid (Emulsifier Safe, Perkin Elmer, Beaconsfield, Buckinghamshire, UK) and incorporated [³⁵S] methionine was quantified using a Packard Tri-Carb 2100TR liquid scintillation analyzer. Control vials contained 5ml of scintillation fluid only. Incorporation of [³⁵S] methionine was expressed as counts-per-minute (cpm) per µg protein.

2.12 RNA extraction

The RNeasy mini kit from Qiagen was used to extract RNA from cells. Samples containing 1×10^7 cells were transferred to sterile microfuge tubes and centrifuged for 5min, 1000g at 4°C. Cell pellets were resuspended in 100µl of freshly prepared buffer Y1 [1 M sorbitol, 0.1 M EDTA. pH7.4; β-mercaptoethanol (0.1% v/v) and lyticase (50U per 1×10^7 cells) were included just before use]. Samples were then agitated by pipetting and incubated for 15min at 30°C with gentle shaking to generate spheroplasts. 350µl of buffer RLT was added and the samples vortexed vigorously to lyse the spheroplasts. Next, 250µl of 100% ethanol was added and mixed by pipetting. The homogenized lysate was completely transferred to an RNeasy[®] mini spin column, placed in a 2ml collection tube, and centrifuged at 8000g for 15 sec at room temperature. The flow-through was discarded and 700µl Buffer RW1 added before spinning for 15sec at 8000g to wash the spin column membrane. The flow through was again discarded and the column washed with 500µl Buffer RPE supplemented with ethanol by

centrifugation at 8000g for 15sec. This step was repeated with centrifugation at 8000g for 2min. An additional centrifugation step at 13000g for 1min ensured complete removal of Buffer RPE. The columns were transferred to new 1.5ml collection tubes and 50µl of RNase-free water was directly added to the spin column membrane. RNA was finally eluted by centrifugation at 8000g for 1min and stored at -20°C. All RNA was quantified using a Nano-Drop spectrophotometer (NanoDrop Technologies).

2.13 First-strand cDNA synthesis

Reverse transcription reactions were set up using SuperScript™ III Reverse Transcriptase (RT), deoxynucleotide (dNTP) solution mix (10mM each dATP, dCTP, dTTP, dGTP), and Oligo (dT)₂₀ Primer (Invitrogen) according to the manufacturer's instructions. First, 1µl of 2.5µg/µl oligo (dT)₂₀ was added to a nuclease-free microcentrifuge tube, followed by 1µg-5µg total RNA template and 1µl of 10mM dNTP mix. If required nuclease free water dH₂O was added up to a final volume of 13µl. The mixture was heated to 65°C for 5 min followed by incubation on ice for at least 1min. The contents of the microfuge tubes were collected by a brief centrifugation then 4µl of 5X First Strand Buffer, 1µl of 0.1M dithiothreitol (DTT) (Invitrogen), 1µl of 200U.µl⁻¹ SuperScript™ III reverse transcriptase were added. The samples were mixed by gentle pipetting and incubated at 50°C for 1h after which the reaction was inactivated by heating to 70°C for 15 min. The resulting cDNA was then purified using the Geneflow Q-Spin gel Extraction/PCR Purification Kit (Geneflow). In this case an equivalent volume of Binding Buffer was added to cDNA samples and the solutions mixed by gentle pipetting. Samples were then incubated at room temperature for 1min before being transferred to a spin column after which all steps were performed as described for gel extraction in (2.8). All cDNA purified in this way was quantified with a Nano-Drop spectrophotometer (NanoDrop Technologies) and subsequently used for quantitative RT-PCR (qRT-PCR) (2.14). Samples were stored at -20°C.

2.14 Quantitative RT-PCR (qRT-PCR)

qRT-PCR was performed in triplicate reactions, each comprising 30ng purified cDNA, 100nM *RLI1*-specific primers (Table 7), and 1X Fast SYBR[®] Green master mix (Applied Biosystems), made up to 10µl with RNase free water. Reactions were performed in MicroAMP 96-well fast optical plates sealed with optical adhesive film and monitored with a 7500 Fast Real Time PCR System (Applied Biosystems) using 7500 software v2.0.4 (Applied Biosystems). The appropriate annealing temperature was chosen based on gradient PCR reactions using Taq DNA polymerase (2.4.2), and the relevant primer with genomic DNA: the annealing temperature used for *RLI1* was 60°C. A three-step 40-cycle protocol was used, each cycle comprising 20 sec at 95°C, 30 sec at the annealing temperature, and 3sec at 95°C. In all cases a melt curve was included after the amplification stage, where agarose gel electrophoresis and melting-curve analysis were used to confirm a single PCR product. Amplification was quantified from a standard curve constructed from reactions with defined copy numbers of the expected PCR product (2.14.1).

Table 7- qRT-PCR primers

Primer Name	Sequence (5'-3')
RLI1-RT-FWD	CCGGACCTTTAATAGCACGAGGA
RLI1-RT-REV	TACCGCCTTGAAAATCTTAGCCG

2.14.1 Calculation of DNA copy number for qRT-PCR standard curves

As described previously (Halliwell, 2012), determination of copy number for the PCR products to be used in the construction of standard curves was achieved by calculation of the molecular weight (MW) (g mol^{-1}) of dsDNA PCR products and subsequent determination of the number of molecules in 1ng of DNA. The MW of dsDNA PCR products for use in standard curve reactions were calculated using the following equation:

$$MW (g \text{ mol}^{-1}) = (\text{Size of DNA (bp)} \times 607.4) + 157.9$$

The resulting MW ($g \text{ mol}^{-1}$) value was used to determine the number of moles present in 1g of material. Using Avogadro's number ($6.022 \times 10^{23} \text{ molecules mole}^{-1}$), the number of template molecules g^{-1} can be calculated:

$$\text{Molecules } g^{-1} = \text{moles } g^{-1} \times \text{Avogadro's number (molecules mole}^{-1}\text{)}$$

The resulting values can be converted to ng to give the number of molecules (copy number) in 1ng of template DNA.

A Nano-Drop spectrophotometer (NanoDrop Technologies) was used to quantify the template PCR products (cDNA) which were diluted to $1 \text{ ng } \mu\text{l}^{-1}$ before five further serial 10-fold dilutions; 1 μl of each dilution was utilised in standard curve reactions. Therefore a standard curve could be constructed from reactions with defined copy number of the expected PCR product.

2.15 Yeast culture and toxicity assays

2.15.1 Growth curve assay in broth media

For toxicity assays, YNB broth (25ml cultures in 125ml Erlenmeyer flasks) supplemented with appropriate amino acids (Table 1) and glucose (2% w/v) was inoculated from single colonies on agar and incubated with shaking (120 rev min^{-1}) at 30°C for overnight until stationary phase. Cultures were diluted to fresh YNB medium supplemented or not with doxycycline ($10 \mu\text{g ml}^{-1}$, Sigma-aldrich) (Table 1) and incubated with shaking (120 rev min^{-1}) at 30°C for further growth for 4-5h to exponential phase. Samples were diluted to $\text{OD}_{600} \sim 0.02$ and 300 μl aliquots transferred to 48 well plates (Greiner Bio-One) before addition or not of mild concentrations of stressors (Table 8). Cultures were incubated with shaking and OD_{600} recorded continuously in a BioTek 16 Powerwave XS microplate spectrophotometer, as described (Khozoie *et al.*, 2009).

2.15.2 Growth assays on agar

For spotting assays, cultures were prepared as described above. Cultures at $\text{OD}_{600} \sim 2.0$ were diluted in 10-fold series then inoculated as 5 or 8 μl spots from left to right on to YNB agar

supplemented with appropriate amino acids, and supplemented or not with mild concentration of stressors as specified (Table 8). Plates were incubated either under ambient air or anaerobically under H₂ and CO₂ as illustrated in 2.2, at 30°C for 4-5 days before image capture.

2.15.3 Short-term killing assays

Determination of short-term cell killing was according to loss of colony forming ability, as described previously (Sumner *et al.*, 2003). Organisms were cultured in YNB broth as described above. Cultures were diluted to fresh YNB medium and grown for a further 4 h to exponential phase OD₆₀₀~2.0 (zero time) before addition or not of Cu (NO₃)₂ or cycloheximide and incubation for a further 1h. At 0h and 1h, aliquots were diluted in 10-fold series then an appropriate volume (~75µl) containing ~200 cells was spread plated to selective YNB agar plates. Viability was determined after 3-4 days incubation at 30°C by colony forming unit (CFU) counts, and calculated with reference to CFUs formed in the zero-time control incubations. The determination of CFUs after 1h without stressor also allowed any intervening growth to be taken into account. For a similar purpose, cell numbers were determined at the same intervals by haemocytometer counts (improved Neubauer: counting chamber depth, 0.1mm; area, 1 mmx1mm; volume, 0.1µl). Cells were counted under a light microscope within the centre square of the haemocytometer grid (comprising twenty-five smaller squares, each one divided into sixteen further small squares) using the 40x objective:

$$\# \text{cells/ml} = \# \text{ cells within centre square} \times \frac{1 \text{ml}}{\text{Depth X area (0.0001ml)}}$$

Where cell number is expressed as a percentage, this is with reference to cell numbers counted at zero time in the relevant control.

Table 8 – Concentrations of stressors and chemical compounds used during this study

Stressors and Chemical compounds	Stock Concentration (M)	Desired mildly-inhibitory concentration (mM)	Desired lethal concentration (mM)
Copper (II) nitrate Cu (NO ₃) ₂	2.5M	0.35mM	2.5 - 3mM
Chromium(VI)oxide CrO ₃	0.02M	0.05 - 0.1mM	-
Hydrogen peroxide H ₂ O ₂	0.5M	1 - 2mM	-
Paraquat (methyl viologen dichloride hydrate)	1M	4 - 8mM	-
Iron (III) chloride (FeCl ₃)	0.5M	0.7mM	-
Manganese (II) chloride (MnCl ₂)	1M	1mM	-

All stock solutions were made to the concentrations indicated in dH₂O and filter sterilised. Stock solutions were stored at 4°C.

2.16 Assay of nuclear Rps2p-eGFP export

Cells transformed with plasmid *pRS315-RPS2-eGFP* described in (Fig 2.1) were examined for nuclear retention of fluorescence during appropriate treatment with stressors. Overnight cultures in selective YNB broth were diluted to fresh YNB medium and cultured for a further 4-5h with shaking (120 rev min⁻¹) at 30°C to exponential phase (OD₆₀₀~0.2). Cultures were then supplemented with stressor as specified and incubated for further 2 and 4h. Cell nuclei were stained with 10µg ml⁻¹ of 4,6-diamidino-2-phenylindole (DAPI; Sigma) (Pringle et al., 1989) and incubated at 30°C for 30min before being pelleted by centrifugation at 8000g for 3min and resuspended in phosphate buffered saline (PBS). This wash step was then repeated and cells resuspended in 10µl PBS with vortexing. An aliquot (3µl) of stained cells was added to a microscope slide and covered with a

coverslip prior to imaging. Cells were viewed with a Zeiss Axioscope MS fluorescence microscope fitted with a HB050 illuminator. Rps2p-GFP was imaged using the FITC filter while cell nuclei stained with DAPI were observed using the UV filter. Images were captured with a Zeiss AxioCam digital camera.

2.16.1 Doubling time determination

Optical density readings (OD_{600}) were recorded for exponential phase cells (2.16) at initial time t_0 (h) and at final time t (h) in the absence or presence of stressor, using a Pharmacia Biotech/Ultrospec 2000 UV/visible spectrophotometer. Doubling times (Dt) were calculated in the absence (A) or presence (B) of stressor according to the equation:

$$Dt = \frac{-0.301 (t-t_0)}{\text{LogODI-LogODF}}$$

ODI is the optical density of the culture at initial time t_0 (h); ODF is the optical density of the culture at final time t (h), and Dt is the doubling time. The percentage stressor effect on cell doubling time was calculated according to the equation:

$$\% = \frac{Dt (A) - Dt (B)}{Dt (A)} \times 100$$

2.17 Qualitative mRNA mistranslation assay

Determination of mRNA mistranslation in YPD agar was according to suppression of the red pigmentation associated with the *ade1-14* UGA stop codon, thereby producing white colonies as an indicator of mRNA mistranslation (Liu & Liebman, 1996). *S. cerevisiae* L1494 (*ade 1-14*) strain transformed with empty vector *pCM190* or the same plasmid bearing a *tet-RLI1* construct were cultured in selective YNB broth as described above. Exponential-phase cells ($OD_{600} \sim 1.0$), both undiluted and 10-fold diluted, were spotted in 6 μ l aliquots on to YEPD agar supplemented or not with stressor as specified. Plates were incubated aerobically for 4 days at 30°C then images were captured.

2.18 Quantitative mRNA mistranslation assay

Single colonies of wild type (W303) or isogenic *tet-RLI1* strains transformed with the dual-luciferase plasmid (Fig 2.1) were cultured in selective YNB broth as described above. Exponential phase cultures (20ml, at $OD_{600} \sim 0.5$) were treated with stressors as specified. At intervals (2 and 4h), 15ml of cells were pelleted by centrifugation (4000g, 7min) and protein extracted (2.11.2). The subsequent assay was with the dual luciferase assay system (Promega). 5 μ l of protein extract was added to 20 μ l luciferase assay reagent LARII. Samples were read in a Berthold Lumat LB9507 Luminometer for 10s, then 20 μ l of Stop and Glo reagent was added and the luminescence was again read for 10s. The derived ratio of luminescence attributable to the Firefly versus Renilla luciferases indicated the short-term level of mistranslation of the TAA stop codon that separates the two ORFs of *Firefly* and *Renilla* luciferases.

2.19 Statistical Analysis

Statistical analysis of data was performed by Student's t-test using Excel software where data analysis was selected and from the drop-down menu of analysis options I selected t-test: Two-sample assuming unequal variances, and then the averages of all values of our samples were compared to verify whether observed differences were statistically significant. Statistical significance was inferred when resulting p values were below 0.05 ($p < 0.05$) while $p > 0.05$ indicated a lack of significance.

Chapter 3- Rli1p- dependent resistance to oxidative stress

3.1 Introduction

Exposure to reactive oxygen species (ROS) and the oxidative deterioration of protein, lipid and DNA they exert is the harmful consequence that organisms must pay for living an aerobic life. Whereas oxidative damage to cellular macromolecules is very widely reported, just two types of effects are thought potentially to cause ROS toxicity: gain of toxic function, or loss of essential cellular function (Avery, 2011). Furthermore, it is still unknown what is the principal cellular target(s) of ROS that accounts for growth inhibition and/or loss of viability during oxidative stress? There could be more than one such target, the identity of which may depend on the nature of the oxidative stress (Thorpe *et al.*, 2004; Avery, 2011). To establish the identity of an essential protein that is a major ROS target, key criteria that need to be met are that the protein should be modified in an oxidation-dependent manner and exhibit decreased function (which cannot be accounted for by decreased expression) during oxidative stress. Furthermore, knockdown of the relevant protein should produce a ROS-sensitive phenotype and, moreover, overexpression should confer resistance (Avery, 2011).

As described in chapter 1, Fe-S clusters are protein co-factors that are among the most ROS-sensitive structure in biology (Imlay, 2006), yet they have been conserved through evolution and are required for diverse protein functions (Imlay, 2006; Lill, 2009; Py *et al.*, 2011). Several Fe-S proteins are notoriously ROS-labile, although studies of ROS sensitivity to date have focused on non-essential Fe-S proteins (Macomber & Imlay, 2009; Jang & Imlay, 2007; Varghese *et al.*, 2003). The first Fe-S protein identified as essential for eukaryotic cell viability was the multifunctional ABC-family protein, termed Rli1 in the yeast model (ABCE1 in humans and other organisms) (Kispal *et al.*, 2005; Yarunin *et al.*, 2005). Rli1p has roles in translation initiation and termination, and ribosome biogenesis (Kispal *et al.*, 2005; Yarunin *et al.*, 2005; Khoshnevis *et al.*, 2010; Shoemaker & Green, 2011).

More recently, several essential nuclear Fe-S proteins, which include the eukaryotic DNA polymerases Pol1, Pol2, Pol3, a DNA helicase with a function in nucleotide excision repair and transcription, Rad3, and the eukaryotic primase (Pri2), which is essential for RNA primer synthesis, DNA replication and double-strand break repair, have been found to require Fe-S metallocenters (Rudolf et al., 2006; Klinge et al., 2007; Netz et al., 2012).

A strong association of Rli1p with cytosolic ribosomes and Hcr1p, which is involved in the processing of rRNA and translation initiation (Valasek et al., 2001), was found (Kispal et al., 2005). As mentioned in chapter 1, the essential role of Rli1p in translation initiation is via its association with eukaryotic translation initiation factors that stimulate ribosome loading, such as eIF5, eIF2 and, in particular, the translation initiation complex eIF3. Moreover, phenotypes such as loss of cell viability, a lesser polysome content, as well as reduced average polysome size were observed *in vivo* as a result of Rli1 depletion (Dong et al., 2004). Elsewhere, decreased translation initiation and synthesis of protein during ROS stress has been described as an adaptive response which is attained to some extent by phosphorylation of the eukaryotic initiation factor eIF2 by the Gcn2 kinase in yeast (Mascarenhas et al., 2008; Shenton et al., 2006). This response is thought to permit time for a reprogramming of the expressed proteins by the cell after stress is sensed. It has been suggested that reduced Rli1p function owing to probable sensitivity of its Fe-S clusters to ROS could participate in such a response (Yarunin et al., 2005). Nevertheless, the role of Rli1p was not identified in earlier studies of the protein-synthesis response (Mascarenhas et al., 2008; Shenton et al., 2006). Furthermore, results of Kispal et al. (2005) that showed association between Rli1p and both ribosomes and Hcr1p suggests that Hcr1p and Rli1p might associate directly, and Hcr1p might connect Rli1p to the eIF3 complex and thus promote translation initiation. Integrity of the N-terminal [4Fe-4S] cluster of Rli1p is crucial for its function in protein synthesis (Kispal et al., 2005), but despite the Fe-S cluster of Rli1p being not involved in the Rli1p interaction with eRF1 or Hcr1, it is essential for Rli1p activity in

translation termination where mutants of Fe-S cluster of Rli1p do not inhibit the read-through defects of Sup45-2 mutant, as integrity of Fe-S cluster is required for its activity in stop codon recognition (Khoshnevis et al., 2010). In addition, Rli1p has been described as the ribosome recycling factor and Rli1's role is evolutionary conserved (Barthelme et al., 2011; Shoemaker & Green, 2011) where because there are several contacts of NBDs of Rli1p to the ribosomal subunits, ATP stimulated conformational changes between the NBDs could play significant roles in ribosomes recognition and splitting of ribosome (Becker et al., 2012). Rli1p is one of the most highly conserved proteins across the eukaryotes and archaea (Barthelme et al., 2007; Becker et al., 2012). This, together with its essentiality in all organisms tested, but functional dependency on ROS-labile Fe-S clusters in particular the fact that Rli1p function is essential for protein synthesis that hinges on the integrity of its two [4Fe-4S] clusters (Kispal et al., 2005) launched the present hypothesis that Rli1p could be a novel key target of stressor action in cells.

This chapter initiates experiments aiming to test the hypothesis that the essential Fe-S protein Rli1 is a key target accounting for growth inhibition and loss of viability during oxidative stress in *S. cerevisiae*. Manipulation of *RLI1* expression was used to verify whether knockdown of the protein produces a ROS-sensitive phenotype and whether its overexpression confers resistance. This evidence would help corroborate that the effects of oxidative stress are Rli1p-specific, and thereby meet certain key criteria expected of a major protein target of ROS toxicity (Avery, 2011). This was furthered by testing whether other essential nuclear Fe-S proteins (Rad3, Pri2, Pol1, Pol2, and Pol3) may also affect pro-oxidant sensitivity. Furthermore, [Rli1p function in] protein synthesis was assayed to help corroborate whether protein synthesis may be a primary target of ROS.

Results

3.2 Doxycycline controls the expression levels of *RLI1* through tetO promoter

Quantitative RT-PCR (2.14, chapter 2) was used to verify *RLI1* expression levels in yeast cells that were transformed either with the empty vector *pCM190* or with *pCM190* carrying a *tet-RLI1* construct, in which *RLI1* was under the control of the tetracycline-repressible promoter (*tetO*) (Hughes et al., 2000). The yeast cells had been pre-incubated with the tetracycline-related compound doxycycline (Dox; 10 µg ml⁻¹) which represses tetO. Quantitative analysis of *RLI1* mRNA with quantitative RT-PCR (qRT-PCR) using standardized RNA additions in all reactions showed that addition of the doxycycline to cells down-regulated the expression level of *RLI1* by 40-fold in yeast expressing the plasmid borne *tet-RLI1* construct (Fig. 3.1 A). In contrast, *RLI1* expression remained lower and Dox-independent in cells expressing empty vector. On the other hand, relative to the expression level in wild type cells, *RLI1* was up-regulated by >40-fold in yeast expressing a plasmid borne *tet-RLI1* construct in media lacking doxycycline (Fig. 3.1 A). Similar results were obtained with W303 cells or isogenic *tet-RLI1* cells where cells expressing a genome integrated *tet-RLI1* construct (*tet-RLI1*) gave >15-fold higher *RLI1* expression than W303 (WT) cells without *tet-RLI1* construct in the absence of doxycycline (Fig. 3.1 B). This made these cells suitable to test whether *RLI1* expression level determines the level of ROS resistance in yeast.

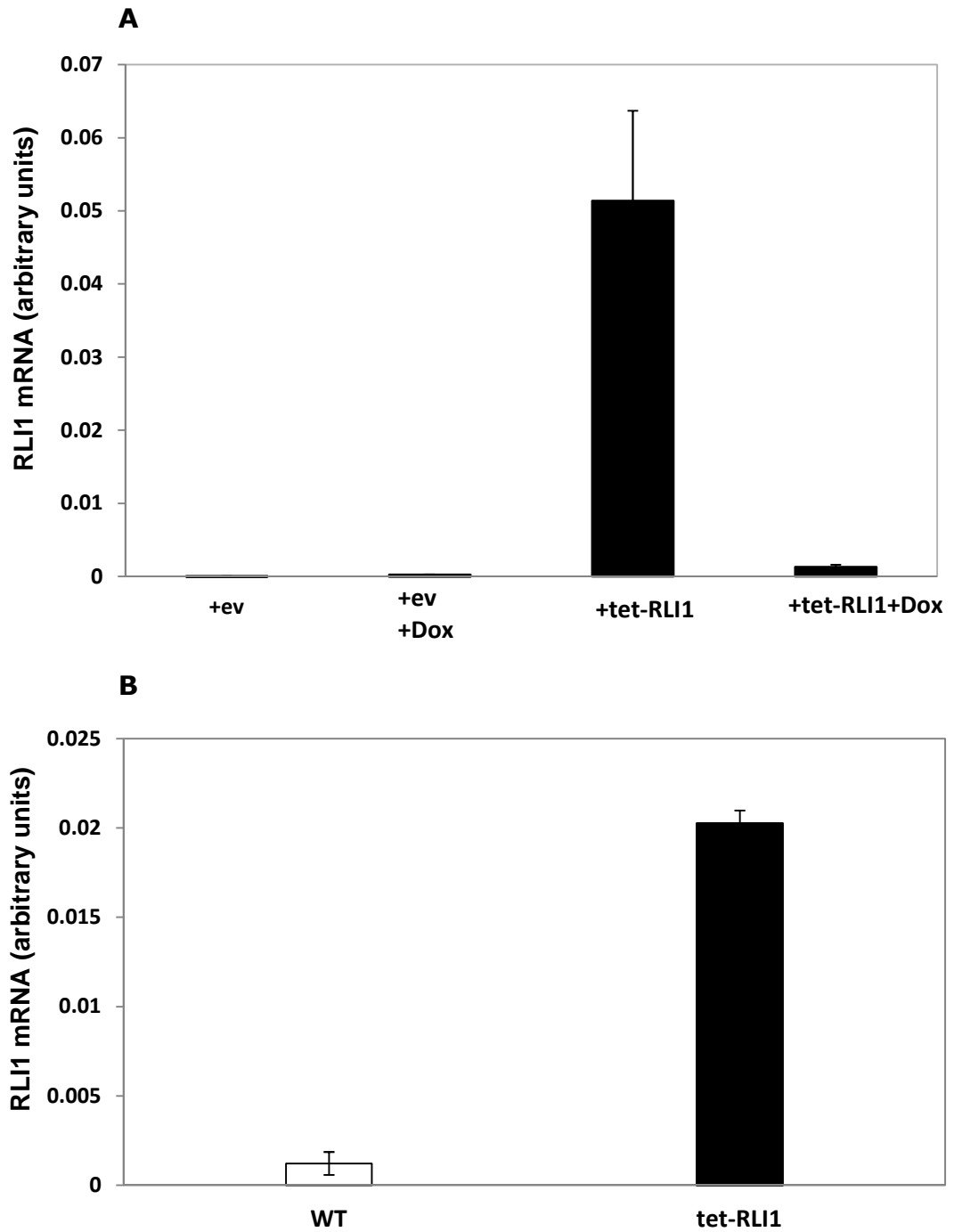


Figure 3.1- qRT-PCR analysis of *RLI1* expression. (A) RNA was extracted from wild type cells transformed with *pCM190* empty vector (+ev) or *pCM190-tetRLI1* (+RLI1) and pre-incubated for 4h in the absence or presence of $10\mu\text{g ml}^{-1}$ doxycycline in YNB medium. *RLI1* mRNA was quantified with qRT-PCR using standardized RNA additions in all reactions, performed in triplicate for each of three independent experiments. Mean data are shown \pm SEM. (B) RNA was extracted from exponential W303 cells or isogenic *tet-RLI1* cells in the absence of doxycycline and analyzed as in (A).

3.3 Rli1p-dependent resistance to oxidative stress

In order to establish the identity of an essential protein that is a major ROS target, key criteria that need to be included are knock-down of the relevant protein (Rli1p) producing a ROS sensitive phenotype and, moreover, overexpression should confer resistance (Avery, 2011). Previous work in the Avery laboratory showed that *RLI1* overexpression fully rescued mild sensitivity of methionine sulphoxide reductase (MSR)-deficient strains to the pro-oxidants Cu, H₂O₂ and paraquat (Sideri, 2007). This resistance with increased Rli1p expression was, therefore, in a mutant predisposed to Fe-S cluster defects. Also that work showed that decreasing *RLI1* expression through use either of a *tet-RLI1* construct in doxycycline-supplemented medium or a heterozygous *RLI1/rli1* strain produced mild Cu (II) sensitivity (Sideri, 2007). It might still be argued that the above phenotypes were all specific to the particular strain defects (*msrΔ* mutant and *RLI1/rli1* strain), whereas Rli1p function may normally protect effectively in wild type cells. Therefore the following experiments focused on overexpressing Rli1p in wild type cells not predisposed to ROS action, as increasing resistance with this approach should be diagnostic that function of the normal toxicity target is being preserved (Avery, 2011). In order to test whether *RLI1* expression level determines the level of ROS resistance in yeast, *S. cerevisiae* BY4741 strains that were transformed either with empty vector *pCM190* or *pCM190-tetRLI1*, were tested for growth in YNB medium supplemented or not with doxycycline and pro-oxidants such as H₂O₂, CrO₃ [Cr(VI)], Cu(II), and paraquat (2.15.1, chapter 2).

3.3.1 *RLI1* expression level determines the level of copper resistance in wild type cells

Only a gene that helps to preserve function of the normal toxicity target should normally increase stress resistance when overexpressed (Avery, 2011). Copper catalyses the formation of ROS (Pinto et al., 2003). To test whether Rli1p could be an essential target accounting for growth inhibition by mild doses of copper stress, BY4741 cells transformed with the empty vector *pCM190* or with

pCM190-tetRLI1 were tested for growth in YNB medium (2.15.1, chapter 2) supplemented or not with doxycycline and with Cu (NO₃)₂. Growth analysis showed comparable growth of both types of cells when incubated in the absence of doxycycline or copper (Fig 3.2 A). However, in medium lacking doxycycline, which gives maximal *RLI1* expression in *pCM190-tetRLI1* transformed cells, but supplemented with copper, a Cu-resistance phenotype was observed. Empty vector-transformed cells that have wild type Rli1p levels showed decreased growth with Cu, whereas elevated *RLI1* expression (minus Dox) conferred relative Cu-resistance in *tet-RLI1* expressing cells (Fig 3.2 B), and these observed differences were statistically significant (P=0.0005, T=2, DF=75) according to Student's t-test. Addition of doxycycline suppressed the Cu-resistance of the *tet-RLI1*-expressing cells, so the Cu resistance could be attributed to Rli1p (Fig 3.2 C). These data are consistent with Rli1p being an essential target of copper stress.

3.3.2 *RLI1* expression level determines the level of chromate resistance in wild type cells

The pro-oxidant metal CrO₃ [Cr (VI)] has an oxidative mode of action involving superoxide (Kubrak et al., 2010; Sumner et al., 2005). Therefore, the same assay (2.15.1, chapter 2) as above with *tet-RLI1* expressing cells was used to test whether Rli1p may be an important target of Cr toxicity. As above, comparable growth of both empty vector and *tet-RLI1* expressing cells was observed in the absence of doxycycline and stressor (CrO₃) (Fig 3.3 A). The addition of 0.1mM CrO₃ gave a Cr-sensitivity phenotype (growth inhibition) in wild type cells with empty vector that have a low level of Rli1p. However, *RLI1* overexpression improved resistance to the test pro-oxidant Cr (VI), restoring cells' growth (Fig 3.3 B), and such observed differences were statistically significant (P=2.61602E-09, T=2, DF=56) according to Student's t-test. Furthermore, doxycycline (Dox) addition suppressed the Cr-resistance of *tet-RLI1* cells. Thus, a Cr-sensitivity phenotype was produced in both types of cell when *RLI1* expression was low (Fig 3.3 C). These data are consistent with Rli1p being a target of chromate stress.

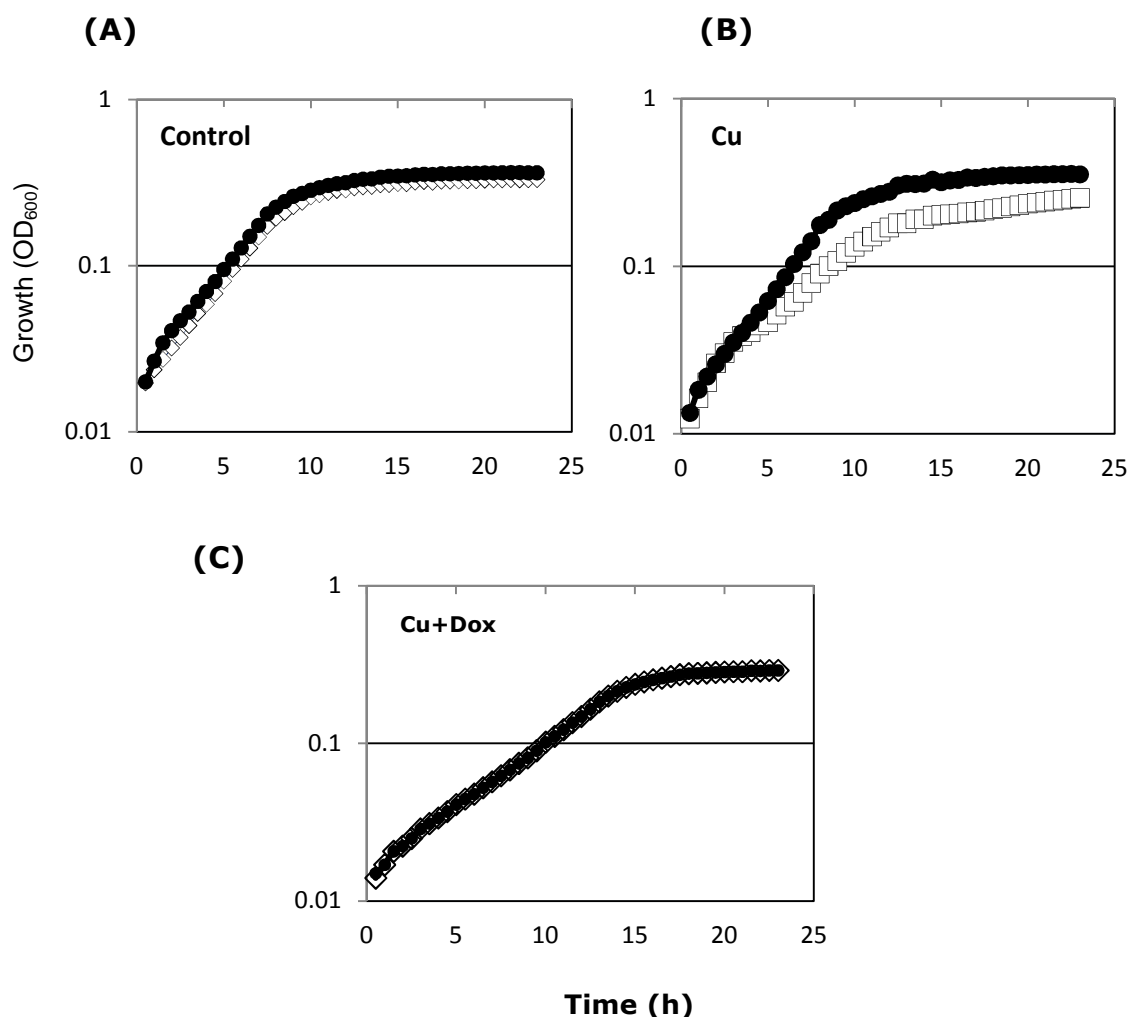


Figure 3.2- *RLI1* expression level determines cellular copper resistance. (A) BY4741 cells transformed with *pCM190* empty vector (□) or with *pCM190-tetRLI1* (●) were cultured in standard YNB medium while incubated in 48-well plates at 30C° in a BioTek power wave microplate spectrophotometer (Gen5) with shaking. (B) As in (A) but with the inclusion of 0.35mM Cu (NO₃)₂. (C) The medium was supplemented both with 0.35mM Cu (NO₃)₂ and with 10µg/ml doxycycline (Dox) (to down-regulate *RLI1* expression in *pCM190-tet-RLI1* transformed cells). SEMs from triplicate independent growth experiments were smaller than the dimensions of the symbols.

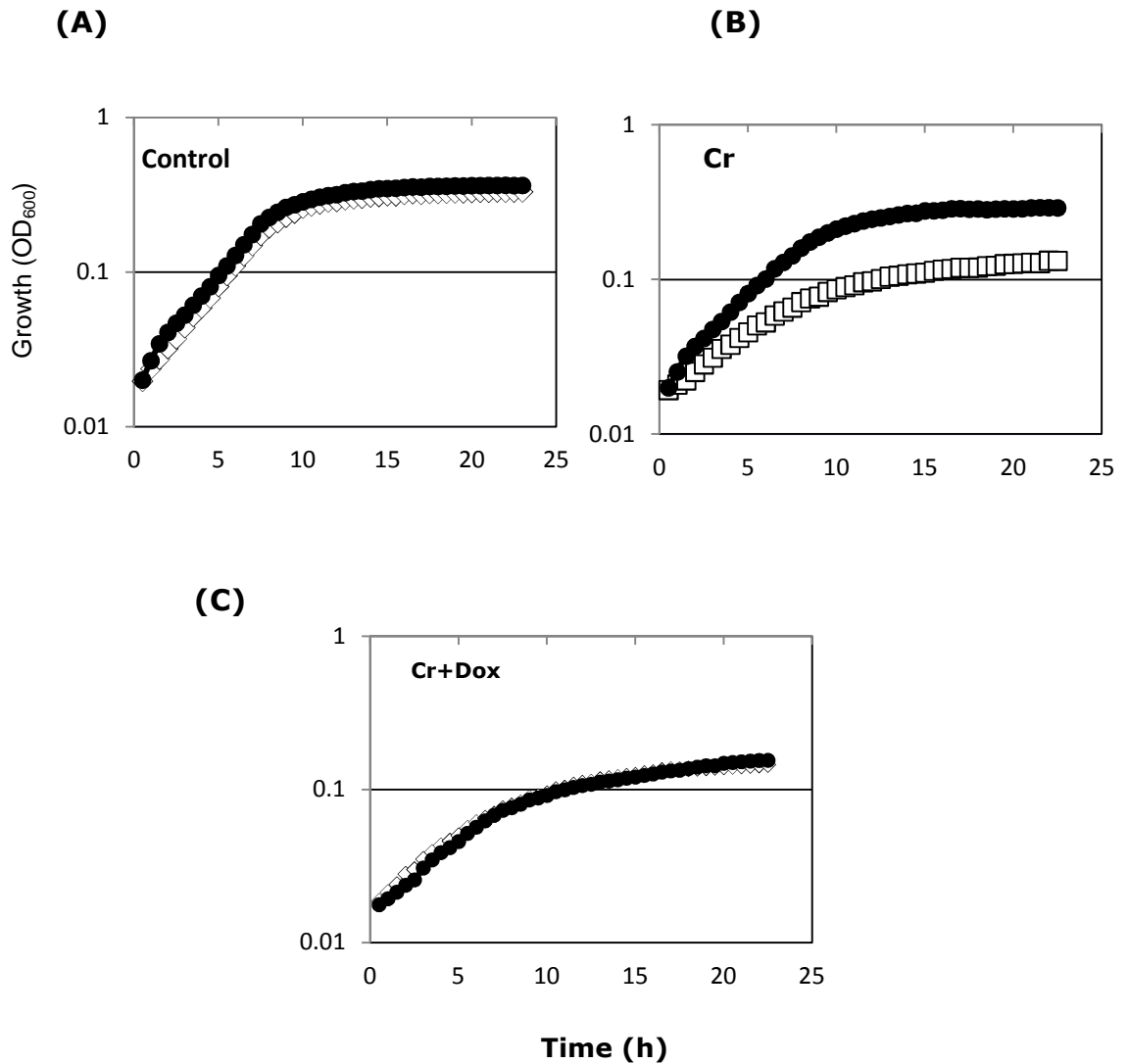


Figure 3.3- *RLI1* expression level determines cellular chromium resistance. (A) BY4741 cells transformed with *pCM190* empty vector (□) or with *pCM190-tetRLI1* (●) were cultured in standard YNB medium while incubated in 48-well plates at 30C° in a BioTek power wave microplate spectrophotometer (Gen5) with shaking. (B) As in (A) but with the inclusion of 0.1mM CrO₃. (C) The medium was supplemented both with 0.1mM CrO₃ and with 10µg/ml doxycycline (Dox) (to down-regulate *RLI1* expression in *pCM190-tetRLI1* transformed cells). SEMs from triplicate independent growth experiments were smaller than the dimensions of the symbols.

3.3.3 *RLI1* expression level determines the level of H₂O₂ resistance in wild type cells

Hydrogen peroxide (H₂O₂) is a toxic reactive oxygen species (Khan & Panda, 2002), primarily due to its conversion to the highly reactive hydroxyl radical OH[•] by interaction with transition metals such as copper and iron (Halliwell et al., 2000). Wild type cells transformed with empty vector showed H₂O₂-sensitive growth in the absence of doxycycline. However, *RLI1* overexpression improved resistance to H₂O₂ (Fig 3.4 B) during growth assays in YNB medium (2.15.1, chapter 2), such observed differences were statistically significant (P=1.1259E-05, T=2, DF=37) according to Student's t-test. As above, the stress-resistance phenotype of *tet-RLI1* expressing cells was suppressed as a result of adding doxycycline to down-regulate *RLI1* expression level (Fig 3.4 C). The data suggested that Rli1p could be an essential target accounting for inhibition of cell growth by H₂O₂.

3.3.4 *RLI1* overexpression confers a very slight effect on paraquat resistance

Paraquat is a potent oxidative stress inducer, as it strongly enhances the production of the superoxide radical O₂^{•-} (Carr et al., 1986). Using the same approach (2.15.1, chapter 2) as above, I tested whether *RLI1* expression may be important for yeast resistance to paraquat stress. Again, growth in standard YNB medium was unaffected by *tet-RLI1* expression versus empty vector (Fig 3.5 A). Moreover, in medium lacking doxycycline but with addition of paraquat, elevated *RLI1* expression appeared to confer a very slight improvement in paraquat resistance relative to empty vector transformed cells (Fig 3.5 B). This phenotypic difference appeared to be abolished by addition of doxycycline which suppressed the paraquat-resistance of the *tet-RLI1*-expressing cells, so the apparent paraquat resistance could be attributed to Rli1p (Fig 3.5 C). These data do not eliminate the possibility that Rli1p is an important target of paraquat stress. In conclusion, the data generally showed that pro-oxidant resistance correlated positively with expression level of Rli1 protein, which fulfilled a key criterion expected of a major protein target of ROS toxicity (Avery, 2011).

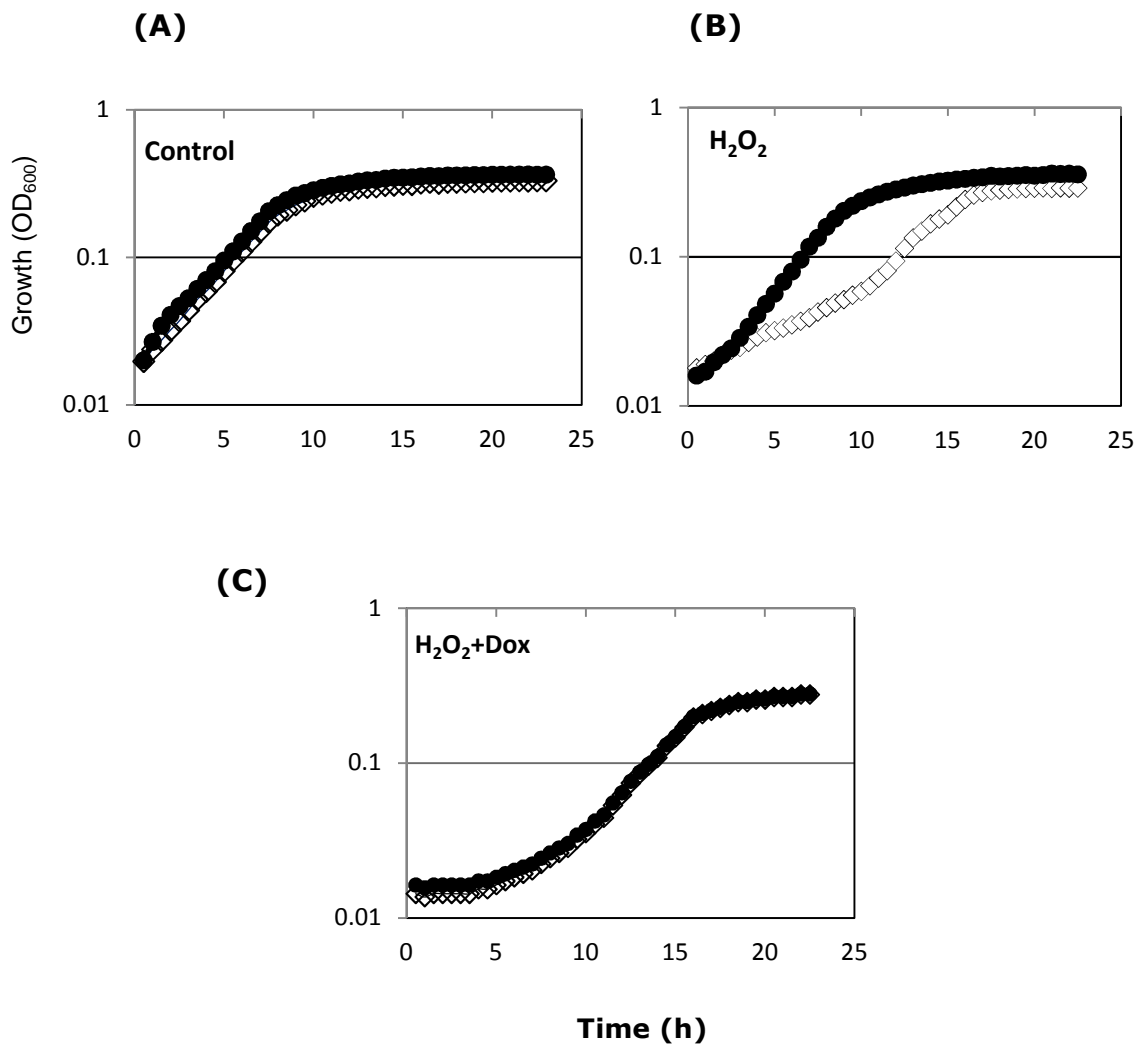


Figure 3.4- *RLI1* expression level determines cellular H₂O₂ resistance. (A) BY4741 cells transformed with *pCM190* empty vector (□) or with *pCM190-tetRLI1* (●) were cultured in standard YNB medium while incubated in 48-well plates at 30C° in a BioTek power wave microplate spectrophotometer (Gen5) with shaking. (B) As in (A) but with the inclusion of 1mM H₂O₂. (C) The medium was supplemented both with 1mM H₂O₂ and with 10μg/ml doxycycline (Dox) (to down-regulate *RLI1* expression in *pCM190-tetRLI1* transformed cells). SEMs from triplicate independent growth experiments were smaller than the dimensions of the symbols.

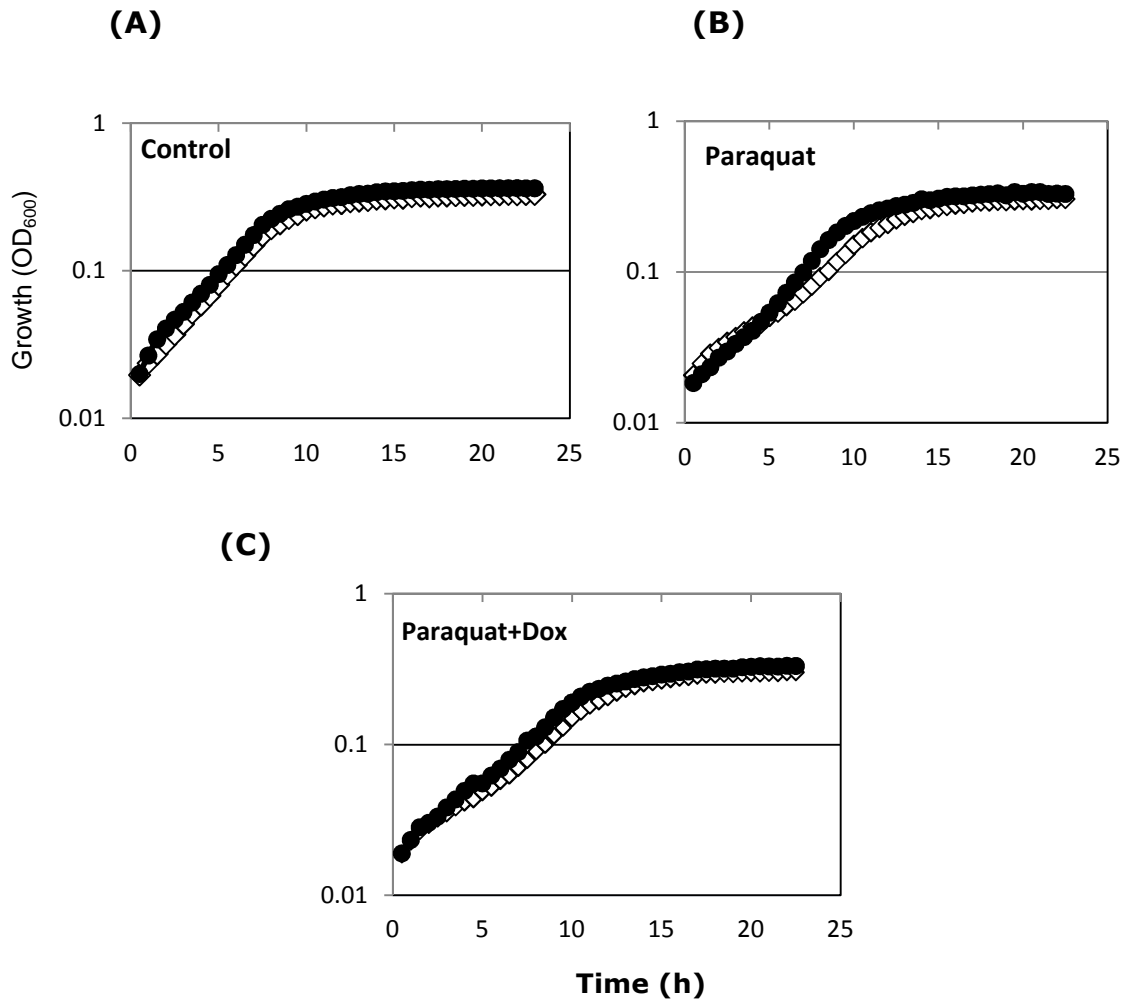


Figure 3.5- *RLI1* expression level determines cellular paraquat resistance. (A) BY4741 cells transformed with *pCM190* empty vector (□) or with *pCM190-tetRLI1* (●) were cultured in standard YNB medium while incubated in 48-well plates at 30 C° in a BioTek power wave microplate spectrophotometer (Gen5) with shaking. (B) As in (A) but with the inclusion of 4mM paraquat. (C) The medium was supplemented both with 4mM paraquat and with 10µg/ml doxycycline (Dox) (to down-regulate *RLI1* expression in *pCM190-tetRLI1* transformed cells). SEMs from triplicate independent growth experiments were smaller than the dimensions of the symbols.

3.4 Stress resistance is specific to Rli1p, among essential Fe-S proteins

Rli1 protein is the only essential cytosolic Fe-S protein (Kispal et al., 2005) known to date. The above results showed that *RLI1* overexpression increased stressor resistance. In order to verify whether stress resistance is specific to Rli1p, growth-curve (2.15.1, chapter 2) and agar spotting assays (2.15.2, chapter 2) were conducted to test whether ROS resistance may also be dependent on essential nuclear Fe-S proteins other than Rli1. These include three eukaryotic DNA polymerases (Pol1, Pol2, Pol3), a DNA helicase with a function in nucleotide excision repair and transcription (Rad3), and the eukaryotic primase (Pri2), which is essential for RNA primer synthesis, DNA replication and double-strand break repair (Rudolf et al., 2006; Klinge et al., 2007; Netz et al., 2012). The R1158 wild type yeast strain was used to represent normal levels of these Fe-S proteins, and compared for stress resistance with isogenic *tet-RLI1*, *tet-Pol1*, *tet-Pol2*, *tet-Pol3*, *tet-Rad3* and *tet-Pri2* strains. In each of these strains, the essential Fe-S protein was under the control of the tetracycline-repressible promoter in a construct integrated in place of the native chromosomal gene. This allows the genes' overexpression when cultured in the absence of doxycycline. In the presence of copper, the wild type strain showed a marked growth inhibition phenotype at 1.5mM Cu (NO₃)₂ (Fig. 3.6). But, according to Student's t-test, Cu-resistance was increased significantly (P=3.41404E-08, T=2, DF=54) in yeast cells expressing the *tet-RLI1* construct with elevated *RLI1* expression (Fig 3.6). Conversely, overexpression of essential nuclear Fe-S proteins did not increase Cu resistance in the tet-fusion strains (Fig 3.6). Results from agar spotting assays (Fig 3.7 A, B) supported the data from growth assay in broth, although there was a suggestion of slight Rad3-dependent Cu resistance on agar. Otherwise, the data showed that stress resistance is specific to Rli1p among the essential Fe-S proteins of yeast. Note that certain additional proteins of the Fe-S biosynthesis pathway may be considered essential, but that is because they are required for eventual delivery of clusters to proteins that have Fe-S-dependent essential functions (like Rli1).

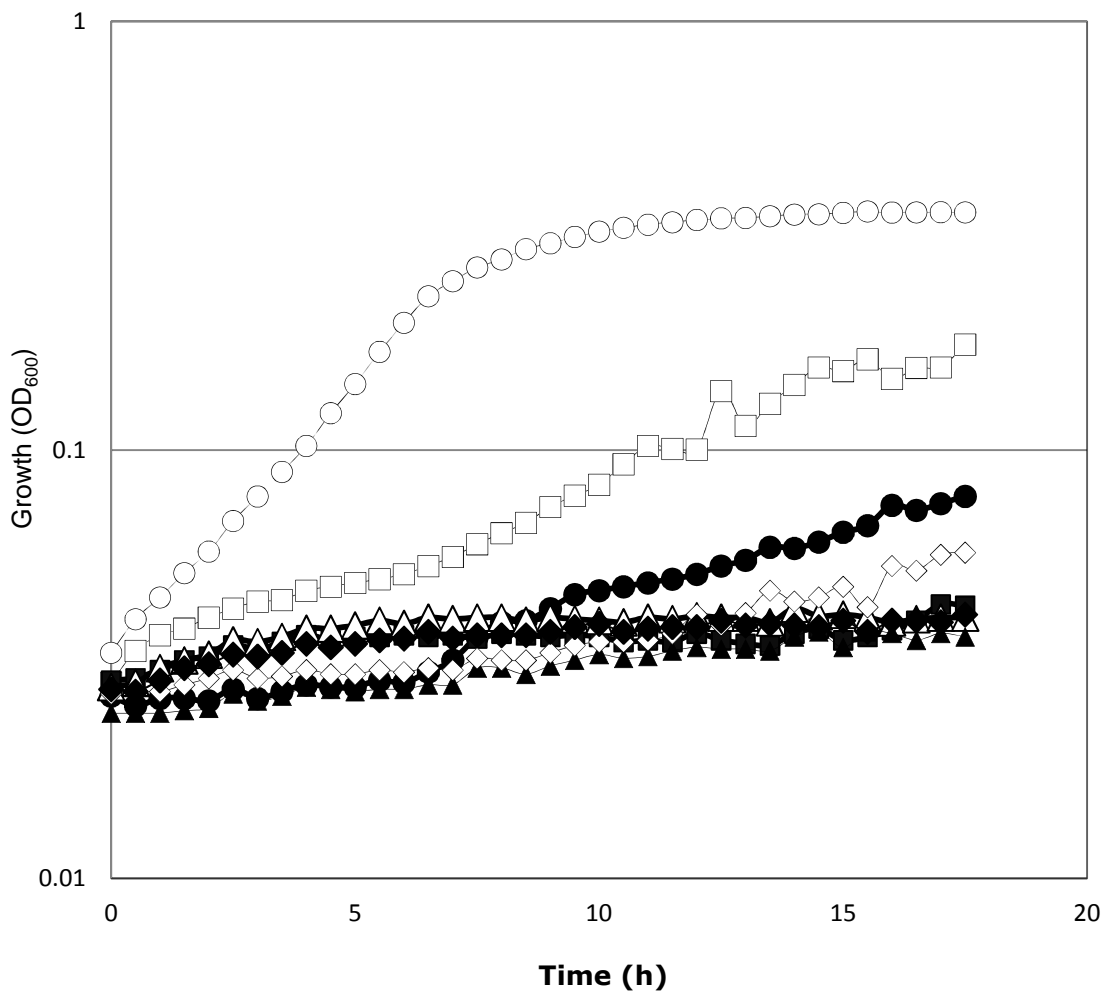


Figure 3.6- Overexpression of essential Fe-S proteins other than Rli1 does not increase stress resistance. The R1158 wild type (●) and isogenic strains *tet-RLI1* (□), *tet-RAD3* (■), *tet-PRI2* (Δ), *tet-POL1* (▲), *tet-POL2* (◇), or *tet-POL3* (◆) were cultured in YNB medium supplemented with 1.5mM Cu (NO₃)₂. (○) Control growth of the wild type in the absence of Cu (NO₃)₂ is shown as a reference [control growth of some *tet*-construct strains was slightly slower than wild type but all were ≥ 2 -fold faster than *tet-RLI1*+copper (□)]. SEMs from triplicate independent experiments were smaller than the dimensions of the symbols.

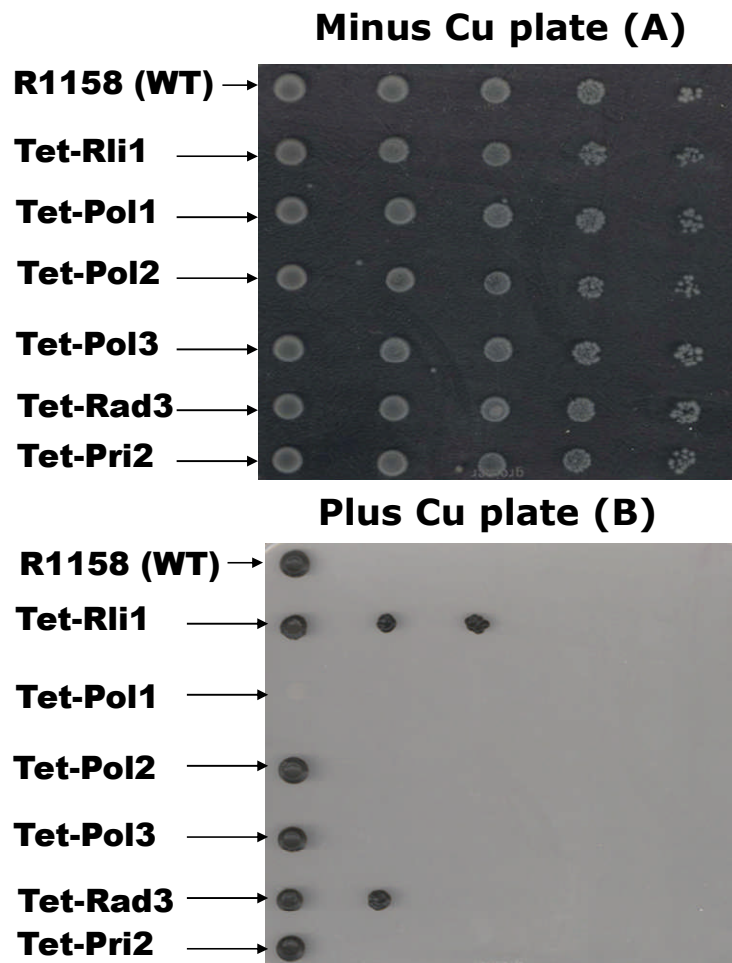


Figure 3.7- Overexpression of essential Fe-S proteins other than Rli1 does not increase stress resistance. (A) Exponential phase cells were collected at $OD_{600} \sim 2.0$, and five serial 10-fold dilutions of the R1158 wild type and isogenic strains *tet-RLI1*, *tet-Pol1*, *tet-Pol2*, *tet-Pol3*, *tet-Rad3* and *tet-Pri2* were spotted from left to right on YNB agar minus copper. (B) As in (A) except that 1mM $Cu(NO_3)_2$ was included in the agar. Plates were incubated for 5 days at 30°C. Typical data from one of three independent experiments are shown.

3.5 *RLI1* overexpression confers resistance to acute short-term killing by copper

The above data showed that *RLI1* overexpression improved resistance to growth inhibitory doses of pro-oxidants. It was decided to test whether Rli1p also protects against killing by copper in the short term (1h), or just against growth-inhibition. First preliminary experiments were conducted (2.15.3, chapter 2) to find a concentration of copper that kills more than 50% of wild type cells in 1h. Kill curves based on preservation of colony forming ability after 1h exposures, showed that concentrations of 2 and 2.5mM Cu (NO₃)₂ achieved this level of viability loss (Fig 3.8). It was reasoned that any culture growth between 0h and 1h in these experiments could probably differ between treatments, so potentially contributing to differences in apparent %viability. It was important to rule out effects of such growth on measurements of killing. Therefore, cells transformed either with the empty vector *pCM190* or *pCM190-tetRLI1* were incubated for 1h in selective YNB broth (2.15.3, chapter 2), in the absence or presence of Cu (NO₃)₂ at the indicated concentrations (Fig 3.8). Using a haemocytometer (cell counting chamber) cell numbers were determined in each condition (2.15.3, chapter 2). Results showed that there was no statistically significant increase in cell number between zero and 1h even in the absence of copper (P=0.113, T=3.2, DF=3) according to Student's t-test (Fig 3.9), indicating that % viability determined with CFUs was reliable (Fig 3.10). Moreover, the persistence of yeast cells during short term exposure to copper depends apparently on the *RLI1* expression level, as numbers of *RLI1* overexpressing cells were higher compared with empty vector cells after 1h exposure to 2.5 or 3mM Cu (NO₃)₂ (Fig 3.9) (P=0.005, T=3.2, DF=3) according to Student's t-test. Presumably the copper stress was such that it disrupted cell integrity entirely, leading to loss of cells distinguishable by microscopy. A similar trend was obtained by colony forming unit (CFU) counts (2.15.3, chapter 2) where *RLI1* overexpression increased considerably resistance to acute short-term killing by copper through increased

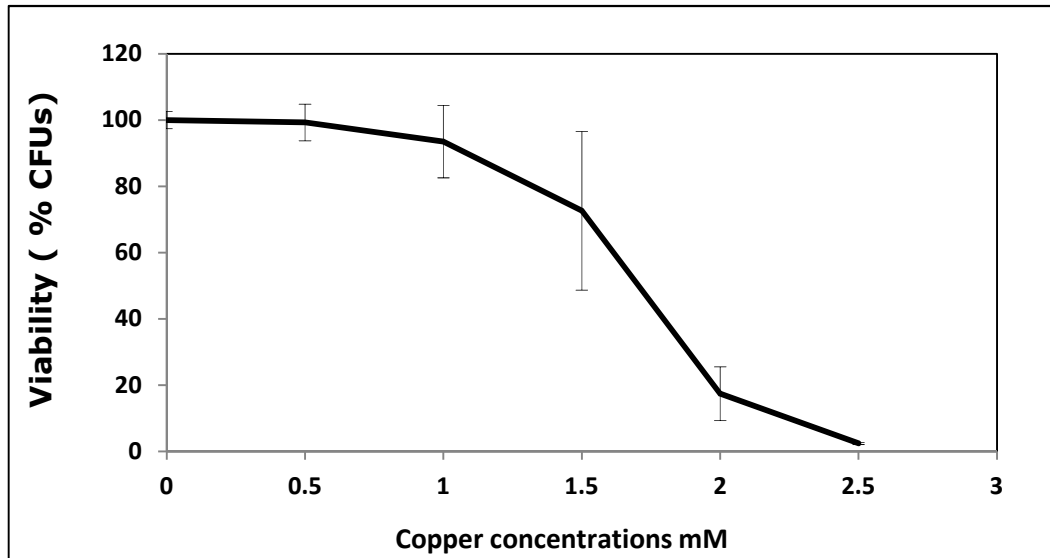


Figure 3.8- Killing concentrations of copper detected by colony forming unit (CFU) counts. Wild type (BY4741) cells were incubated for 1h in YNB broth supplemented or not with different concentrations of $\text{Cu}(\text{NO}_3)_2$ ranging between 0.5 to 2.5mM. Aliquots were diluted and spread to YNB agar. Viability was determined after 3-4 days incubation at 30 C° by colony forming unit (CFU) counts, and calculated with reference to CFUs formed in control (minus copper) incubations. The values in the graph represent the mean of three biological replicates \pm SEM.

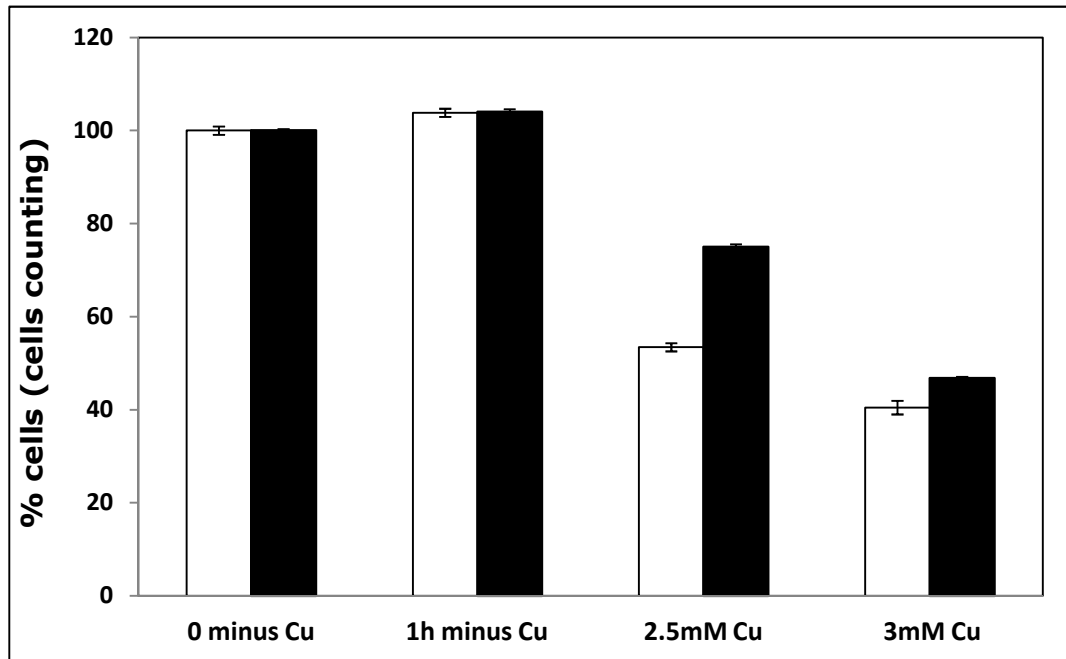


Figure 3.9- *RLI1* overexpression protects against cell killing by Cu. Cells transformed with empty vector *pCM190* (□) or *pCM190-tetRLI1* (■) were incubated for 1h in selective YNB broth, in the absence or presence of copper at the indicated concentrations with shaking at 30C°. After appropriate dilution cells were counted by using a haemocytometer. Percentage cell number was determined by counting cell with a haemocytometer, and calculated with reference to cell numbers counted in the relevant control (+*pCM190* or +*pCM190-tetRLI1*) minus Cu. The values in the graph represent the mean of three biological replicates \pm SEM.

numbers of colonies evident on YNB agar plates post copper exposure, relative to cells carrying the empty vector (Fig 3.10) ($P=0.0004$, $T=3.2$, $DF=3$) according to Student's t-test. It was hypothesized that ROS affected (essential) Rli1p activity. The fact that Rli1p-dependency of ROS resistance was detectable even within 1h above was not inconsistent with that. This is because Rli1 has a relatively short (~ 38 min) half-life (Belle *et al.*, 2006). This means that even if the effect of, say, copper was only to block de novo formation of the active protein (versus an effect on turnover rate also), this would still be sufficient to give a marked loss of Rli1p activity during the above 1h time course. It was also hypothesized that a major effect of any loss of Rli1p function would be decreased protein synthesis, the principal apparent role of Rli1p. However, it was uncertain whether perturbation of protein synthesis alone could be sufficient to explain killing (versus growth inhibition) over a short 1h time scale. Therefore, the protein synthesis inhibitor cycloheximide was tested. First, to determine cycloheximide (CHX) concentrations needed to inhibit protein synthesis in yeast cells under the present conditions, wild-type cells were pre-treated with CHX for 1h in YNB medium before addition of $0.5\mu\text{l}$ of ($500\mu\text{Ci}$) [^{35}S] methionine isotope. Cells extracts were sampled after 8min (2.11.1, chapter 2). Quantification of isotope [^{35}S] methionine per μg filtered protein was measured by scintillation counting (2.11.4, chapter 2) which was expressed as count-per minute (CPM) per μg protein. The results showed that cycloheximide at $80\mu\text{g ml}^{-1}$ inhibited protein synthesis during short term exposure (Fig 3.11). Then the effect of this inhibitory CHX concentration on % viability was tested. Cells transformed with empty vector *pCM190* or *pCM190-tetRLI1* were incubated for 1h in the absence or presence of cycloheximide then CFUs were determined (2.15.3, chapter 2). The results indicated that inhibition of protein synthesis by CHX caused marked loss of viability within 1h. Furthermore, *RLI1* overexpression rescued significantly CHX sensitivity (Fig 3.12) ($P=2.83618\text{E-}06$, $T=2.8$, $DF=4$) according to Student's t-test. The results indicate that rescue of protein synthesis activity could be sufficient to explain rescue by *RLI1* overexpression of ROS-dependent killing.

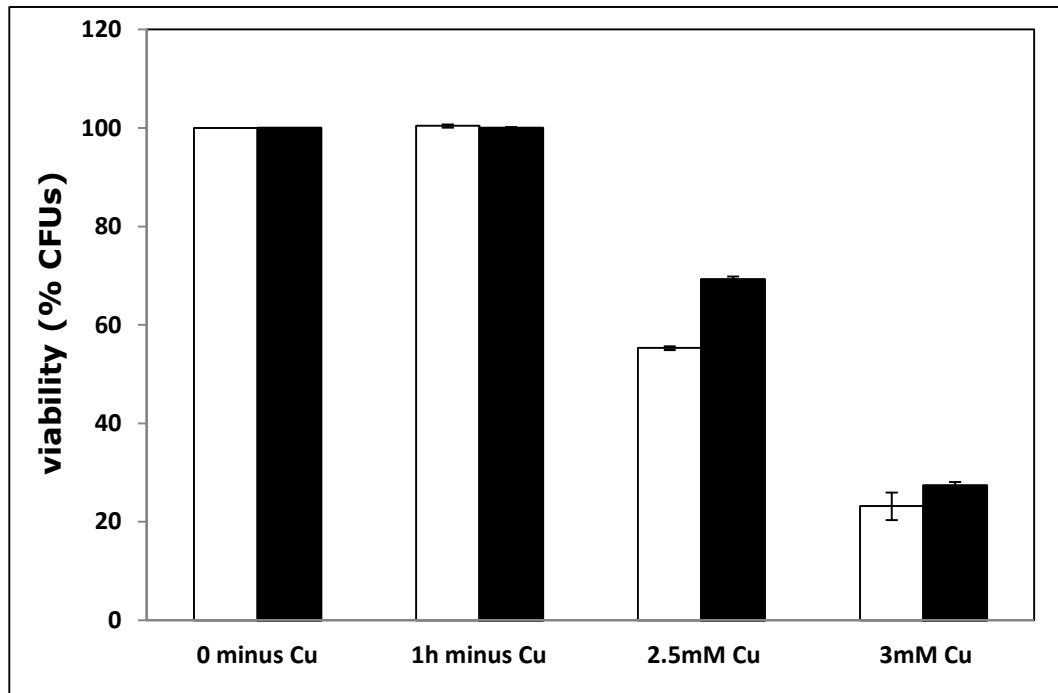


Figure 3.10- *RLI1* overexpression protects against cell killing by Cu. Cells transformed with empty vector *pCM190* (□) or *pCM190-tetRLI1* (■) were incubated for 1h in selective YNB broth, in the absence or presence of copper at the indicated concentrations, then aliquots were diluted and spread to YNB agar. Viability was determined after 3-4 days incubation at 30C° by colony forming unit (CFU) counts, and calculated with reference to CFUs formed in control. The values in the graph represent the mean of three biological replicates \pm SEM.

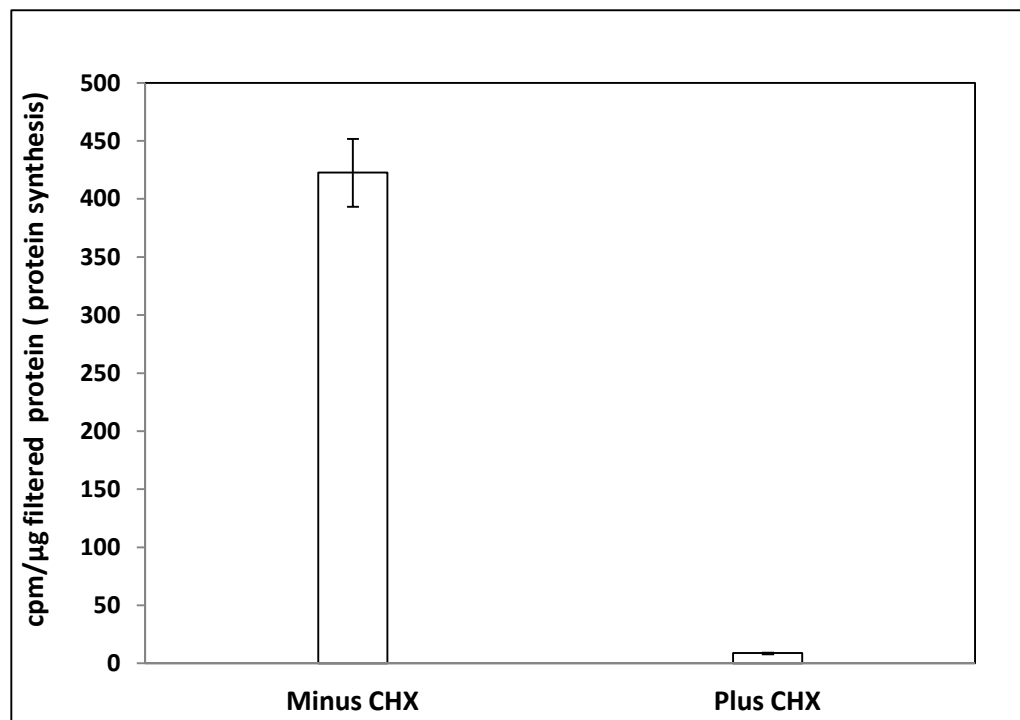


Figure 3.11- Cycloheximide inhibits protein synthesis in a short term exposure. *S. cerevisiae* BY4741 cells were incubated for 1h in YNB broth, supplemented or not with $80\mu\text{g ml}^{-1}$ cycloheximide. Cells were labelled with [^{35}S] methionine for 8min incubation at 30C° . Cells were harvested, washed and proteins were extracted. Quantification of isotope [^{35}S] methionine per μg filtered protein was by scintillation counting which was expressed as counts-per minute (CPM) per μg filtered protein. The values in the graph represent the mean of three biological replicates \pm SEM.

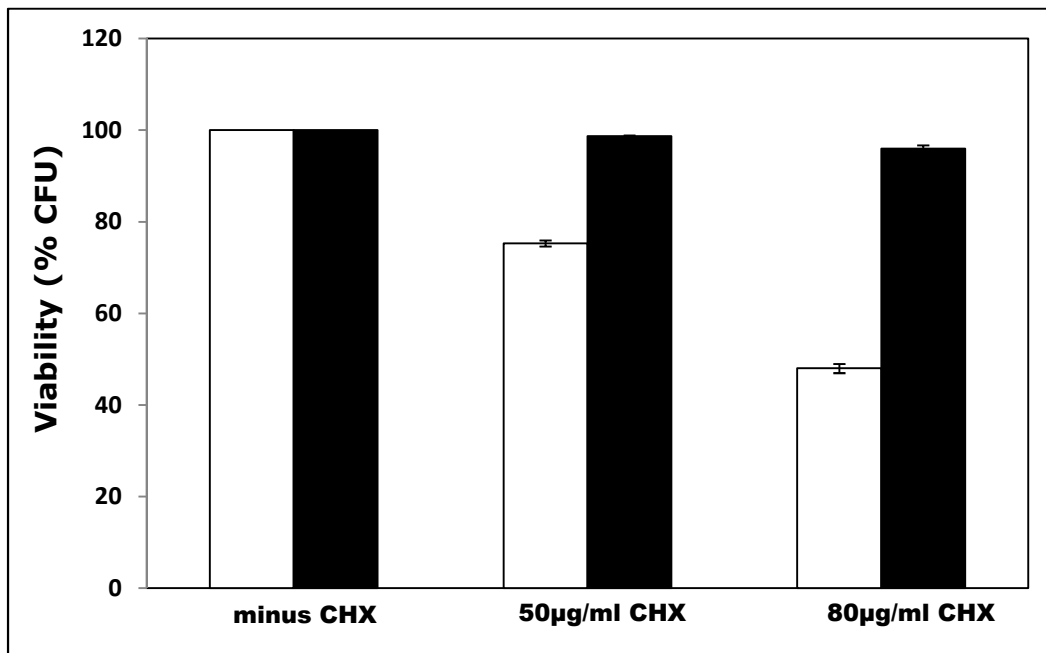


Figure 3.12- *RLI1* overexpression protects against cell killing by cycloheximide. Cells transformed with empty vector *pCM190* (□) or *pCM190-tetRLI1* (■) were incubated for 1h in selective YNB broth, in the absence or presence of cycloheximide at the indicated concentrations, then aliquots were diluted and spread to YNB agar. Viability was determined after 3-4 days incubation at 30C° by colony forming unit (CFU) counts, and calculated with reference to CFUs formed from the relevant minus-CHX control incubation. The values in the graph represent the mean of three biological replicates \pm SEM.

The above results prompted me to test whether Rli1p function in protein synthesis could be a critical target of copper stress. In order to do this, cells transformed either with empty vector *pCM190* or *pCM190-tetRLI1* were first treated or not with a mild dose of copper for 1h. Cells were then radiolabelled (2.11.1, chapter 2) and assayed as above for protein synthesis activity (2.11.4, chapter 2). Results showed that in the presence of copper there was a marked decrease in protein synthesis rate of yeast cells carrying the empty vector (Fig 3.13) ($P=0.02$, $T=2.8$, $DF=4$) according to Student's t-test. In the absence of Cu, *RLI1* overexpressing cells also had a low protein synthesis rate, which could elucidate that it is not necessary increasing *RLI1* expression level will increase its activity, and that may be because there is no an adequate cofactor like Fe-S clusters which are required for Rli1p activity (Kispal et al., 2005), suggesting that wild type-level *RLI1* expression may be optimized for protein synthesis. However, *RLI1* overexpression rescued protein synthesis during copper stress by producing a significant increase in protein synthesis rate compared with yeast cells carrying the empty vector (Fig 3.13) ($P=0.004$, $T=2.8$, $DF=4$) according to Student's t-test. This is consistent with the idea that Rli1p-dependent protein synthesis could be a critical target of copper stress.

In summary, *RLI1* overexpression confers resistance to acute short-term killing by Cu. The resistance to killing was in keeping with Rli1p-dependent protein synthesis being the critical target, as a protein synthesis inhibitor (cycloheximide) is sufficient to cause viability loss. Moreover, a mild dose of copper is sufficient to decrease the protein synthesis rate, an effect partly rescued by *RLI1* overexpression. Together with the growth inhibition data, the results collectively suggested that Rli1p function is a pivotal determinant of growth inhibition by pro-oxidants.

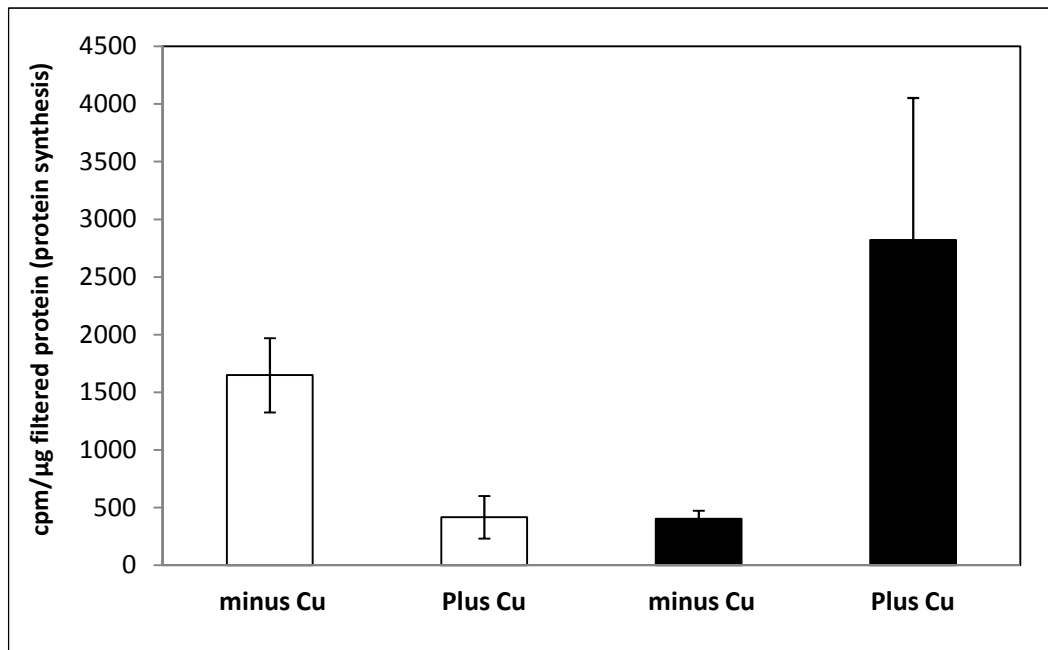


Figure 3.13- *RLI1* overexpression alters protein synthesis rate. Cells transformed with empty vector *pCM190* (□) or *pCM190-tetRLI1* (■) were incubated for 1h in YNB broth, supplemented or not with 0.35 mM Cu (NO₃)₂. Cells were labelled with [³⁵S] methionine for 8min during incubation at 30C°. Cells were harvested, washed and proteins were extracted. Quantification of isotope [³⁵S] methionine per μg filtered protein was by scintillation counting which was expressed as counts-per minute (CPM) per μg filtered protein. The values in the graph represent the mean of three biological replicates ± SEM.

3.6 Discussion

The aim of the studies described in this chapter was to gain some evidence testing the hypothesis that the essential Fe-S protein Rli1 is a key target accounting for growth inhibition and/or loss of viability during oxidative stress in *S. cerevisiae*. In addition, test whether other essential nuclear Fe-S proteins could be targets of ROS or copper action.

As discussed above, in order to establish the identity of an essential protein that is a major ROS target, key criteria that should be fulfilled include that knock-down of the relevant protein should produce a ROS sensitive phenotype and, moreover, overexpression should confer resistance (Avery, 2011). Previous data from the Avery laboratory established ROS sensitivity in Rli1 under-expressing strains (Sideri, 2007). It is well documented that diverse stressors can promote ROS generation; H₂O₂ can be transformed to the highly reactive hydroxyl radical (HO·) in the presence of reduced transition metals such as Cu or Fe (Mohora et al., 2007), whereas paraquat and Cr (VI) act as superoxide-generating agents (Sumner et al., 2005). Therefore, this range of stressors was used to determine the effect of *RLI1* overexpression on ROS resistance and to give insight to a mechanism of action on Rli1p. Superoxide radicals (O₂^{•-}), in particular, have for some time been considered principal antagonists to Fe-S cluster integrity in proteins (Irazusta et al., 2006; Gardner & Fridovich, 1991; Calderon et al., 2009). Here, elevated *RLI1* expression in yeast cells expressing a plasmid borne *tet-RLI1* construct in the absence of doxycycline conferred resistance to all of the test pro-oxidants, particularly H₂O₂, Cr (VI) and Cu (II), whereas a very slight effect was observed on paraquat resistance. The latter result may suggest that Fe-S cluster targeting by O₂^{•-}, generated by paraquat, is not the principal basis of the Rli1p effect. However, Cr (VI) is also thought to have a superoxide-based mode of action and Rli1 exerted a strong phenotype in this case. Abolition of the phenotypes by doxycycline addition corroborated that the effect was due to (tet-regulated) *RLI1* expression. Thus, a first criterion expected

of a key protein target of ROS toxicity (Avery, 2011) was fulfilled according to these results, showing that *RLI1* expression level determines the level of pro-oxidant resistance in yeast cells. Furthermore, stress resistance is specific to Rli1p among essential Fe-S proteins, as the data showed that overexpression of Pri2, Pol1, Pol2 or Pol3 did not increase resistance, whereas Rad3 showed a slight pro-oxidant resistance which was clear from increasing the rate of cells growth during copper exposure comparing with the wild type strain, which could be exploited for further future study. However, measurement of nuclear Fe-S proteins expression levels, which was not conducted in this study, is required via using qRT-PCR. In addition, it is not necessary increasing their level means their activity increased because may be there are no enough cofactor like Fe-S clusters to make them active, therefore, also measure their activities at different levels of their expression during oxidative stress is required to emphasis that overexpression of these essential nuclear Fe-S proteins did not increase pro-oxidant resistance and thereby are not essential target of ROS action.

Rli1p and its orthologs are among the most sequence-conserved proteins known in biology, with essential functions in all organisms tested (Barthelme et al., 2007; Becker et al., 2012). Consequently, preservation of Rli1p function could be a principal determinant of oxidative stress resistance in diverse organisms. The data showed that *RLI1* overexpression improved resistance not only to growth inhibition by the pro-oxidants, but also to killing by copper in the short term (1h). It is well documented that copper promotes ROS generation (Pinto et al., 2003) and that the stability of Fe-S clusters is sensitive to ROS (Macomber & Imlay, 2009). Therefore, copper was used in the short-term experiments as one model of ROS stress. It was hypothesized that ROS affected (essential) Rli1p activity in protein synthesis. The fact that Rli1p-dependency of ROS resistance was detectable even within 1h was not inconsistent with that, as argued in the results section, owing to the relatively short (~38min) half-life of Rli1 (Belle et al., 2006). Resistance to acute short-term killing by Cu was observed in cells expressing *RLI1* overexpression. This resistance

to killing was in keeping with Rli1p-dependent protein synthesis being the critical target, as a protein synthesis inhibitor (cycloheximide) is sufficient to cause viability loss. Moreover, a mild dose of copper is sufficient to decrease the protein synthesis rate, an effect partly rescued by *RLI1* overexpression. This is consistent with the idea that Rli1p-dependent protein synthesis could be a critical target of copper stress and supporting a role for ROS in such targeting. This is particularly likely considering that Rli1p function in protein synthesis hinges on the integrity of the N-terminal [4Fe-4S] clusters (Kispal et al., 2005), the most highly oxidation-sensitive structures known in biological systems (Imlay, 2006). Cu has been reported previously to oxidatively damage Fe-S clusters within other Fe-S proteins (Macomber & Imlay, 2009). The study of Baker et al. (2010) demonstrated that protein damage and the misfolded protein are induced in the presence of copper, and thereby protein translation is downregulated in *Staphylococcus aureus*. Moreover, the positive correlation between *RLI1* expression and stress resistance that was observed in my study counters the possibility that ROS-sensitivity of Fe-S clusters of Rli1p could contribute to decreasing protein synthesis as part of the adaptive response to mild oxidative stress (Yarunin et al., 2005). Therefore, it is likely that any decrease in protein synthesis which is due to Rli1p dysfunction does not represent an adaptive-type response, but may be a deleterious result of ROS targeting and thereby Rli1p dysfunction. Together with the growth inhibition data, my results collectively suggested that pro-oxidant sensitive Rli1p function is a pivotal determinant of growth inhibition by pro-oxidants.

To summarise, the main conclusions from this chapter are that: (i) *RLI1* expression levels determine the level of ROS resistance in yeast cells where *RLI1* overexpression improved resistance to growth inhibitory doses of pro-oxidants and vice versa, (ii) stress resistance is specific to Rli1p among the essential Fe-S proteins of yeast, which was decreased by *RLI1* repression and increased by *RLI1* overexpression, (iii) in *S. cerevisiae*, *RLI1* overexpression protects against killing effect of protein synthesis inhibitor CHX, (iv) *RLI1* overexpression also gave resistance to acute short-term killing by ROS

that was produced by copper, (v) the resistance to killing by ROS was consistent with Rli1p-dependent protein synthesis being a critical target of ROS.

Chapter 4- Mild pro-oxidant stress and Rli1p activity

4.1 Introduction

Protein damage by oxidation has received attention due to its implication in disease and aging (Davies, 2005; Stadtman et al., 2005). A number of proteins have been proven to be inactivated during oxidative conditions and/or by oxidative damage, including a number of Fe-binding proteins (Drake et al., 2002; Avery, 2011). To date, studies of ROS sensitivity of Fe-S proteins have focused on non-essential Fe-S proteins. Some of these proteins that are sensitive to oxidation may be dispensable in some conditions, but required under others. That can be illustrated in metabolic enzymes such as dehydratases, like Fe-S dependent aconitases (Imlay, 2006). Furthermore, biosynthesis of some amino acids (such as valine, lysine and isoleucine) in yeast and bacteria depends on the activity of Fe-S enzymes, and during oxidative stress their effect on cell vitality becomes observable in media lacking these affected amino acids (Carlioz & Touati, 1986; Wallace et al., 2004). To date, these examples provide the evidence that impairment of Fe-S protein function by oxidation has the potential to cause ROS toxicity.

Rli1p is the only known essential, cytosolic Fe-S protein of yeast cells. Its activity in nuclear export of large and small ribosomal subunits and thereby in ribosome biosynthesis depends on the integrity of its Fe-S clusters (Kispal et al., 2005; Yarunin et al., 2005). Translation is also suppressed in *rli1*-depleted cells (Dong et al., 2004). Defects in nuclear export of ribosomes are also observed upon depletion of the protein Nar1, which is required for incorporation of Fe-S clusters to Rli1p, affecting translation (Kispal et al., 2005) where Khoshnevis et al. (2010) study revealed that the Fe-S of Rli1p is required for its activity in translation termination, supporting the idea that defective nuclear export occurred before the arrest of translation. These data indicated a strong relationship between the assembly of cytosolic Rli1p, and cytosolic biogenesis of ribosomes and thereby translation process. These roles of Rli1p are consistent with its localization both to the cytoplasm and nucleus. Therefore, It has been

suggested that the essential nature of Fe-S cluster biosynthesis in cells might reflect the essentiality solely of Rli1p (Kispal et al., 2005).

Whereas loss of an essential Fe-S function could provide one explanation for ROS toxicity, the degradation of ROS-sensitive Fe-S clusters may lead to further toxic ROS production in organisms (Imlay, 2006). The latter would be an example of a gain-of-toxic function mechanism. In either scenario, ROS to which Fe-S clusters are susceptible include H₂O₂ and superoxide (O₂^{•-}) (Lill et al., 2006). Superoxide radicals have been described as principal antagonists to Fe-S cluster integrity in proteins (Irazusta et al., 2006; Gardner & Fridovich, 1991; Calderon et al., 2009), Paraquat and Cr (VI) act as superoxide-generating agents (Carr et al., 1986; Kubrak et al., 2010). In addition, H₂O₂ and Cu are known to damage Fe-S proteins (Macomber & Imlay, 2009; Jang & Imlay, 2007; Varghese et al., 2003). Like other organisms, Fe-S cluster integrity is also extremely sensitive to oxidative stress in *S. cerevisiae*. One study used ⁵⁵Fe-labelling studies to show that Fe-S cluster turnover was accelerated in methionine sulphoxide reductase (MSR)-deficient yeast. This revealed that MSR enzymes can normally protect Fe-S clusters from oxidative damage in cells (Sideri et al., 2009).

Rli1p maturation depends on the functions of the mitochondrial and cytosolic Fe-S protein assembly systems (Lill et al., 2006; Kispal et al., 2005). The ABC transporter Atm1p is a member of the ISC export machinery in yeast which performs an essential function in the generation of Fe-S-replete Rli1 by mediating export of Fe-S cluster precursors synthesized in the mitochondria (Kispal et al., 1999). Depletion of Atm1p results in a strong decrease in the amount of ⁵⁵Fe precipitated with anti-HA antibodies in Rli1-HA expressing cells (Kispal et al., 2005). Furthermore, Sideri et al. (2009) demonstrated that *ATM1* overexpression increased cellular resistance to copper stress in wild type cells. This suggested that an extra-mitochondrial Fe-S protein(s) affects Cu resistance. Increased Cu resistance by *ATM1* overexpression was observed either in rich YEPD medium or minimal medium, indicating that resistance was not due to rescued production of amino acids that require Fe-S protein (e.g. Leu1) activity

for their biosynthesis, as these amino acids are supplied in YEPD. The hypothesis in this thesis is that Rli1p is the key cytosolic determinant of Atm1p-dependent stress resistance. The facts that Cu of the above study is a pro-oxidant and that [4Fe-4S] clusters are notoriously ROS labile suggest an oxidative mode of stressor action against Rli1p. However, non-oxidative [4Fe-4S] cluster damage is also known (Macomber & Imlay, 2009).

This chapter aims to test whether Rli1p function in nuclear export of ribosomal subunits is sensitive to oxidative stress. This will be achieved by applying mild doses of pro-oxidants in conjunction with manipulation of *RLI1* expression to corroborate those effects are Rli1p-specific. In addition, I will attempt to link the previously observed Atm1p-dependent Cu resistance (Sideri et al., 2009) to Fe-S-dependent Rli1p function in nuclear export. Finally, I will test whether integrity of Fe-S clusters within Rli1p is likely to be the critical determinant of cellular sensitivity to oxidative stress by assaying oxygen-dependency of the phenotypes and using an oxygen-labile mutant protein (*rli1*^{C58A}).

Results

4.2 Mild pro-oxidant stress perturbs Rli1p function in nuclear export of Rps2-GFP

4.2.1 Nuclear accumulation of Rps2p-GFP as an indicator of defective Rli1p function

The essential nature of Rli1p function and the fact that pro-oxidant resistance correlated positively with expression level of the protein (Chapter 3) fulfilled two criteria expected of a key protein target of ROS toxicity (Avery, 2011). A third criterion is that the protein function should be susceptible to mild oxidative stress. The principal *in vivo* assay for Rli1p function is of ribosomal subunit export from the nucleus. Nuclear GFP accumulation in cells expressing a GFP fusion with the small ribosomal subunit protein Rps2 is a sensitive indicator of defective Rli1p function (Kispal et al., 2005; Yarunin et al., 2005). Rli1 protein is required for nuclear export of ribosomal subunits, such as (Rps2p). Therefore, in order to assay Rli1p function, a *tet-RLI1*-expressing strain transformed with a plasmid borne construct expressing *Rps2p* tagged with *GFP* (*pRS315-RPS2-eGFP*) (2.10.1, chapter 2) was grown in selective YNB broth medium supplemented or not with 22.5 μ M (10 μ g ml⁻¹) doxycycline. Cells were examined by fluorescence microscopy after 18h incubation. DAPI stain was used to indicate cell nuclei (2.16, chapter 2). Results showed that in the absence of doxycycline (high *RLI1* expression), Rps2-GFP was observed primarily in the cytoplasm of *tet-RLI1* cells, indicating normal nuclear Rps2 export function of Rli1p (Figs 4.1 A). However, treating cells with 10 μ g ml⁻¹ doxycycline (low *RLI1* expression) resulted in the appearance of cells showing strong nuclear accumulation of Rps2-GFP (Figs 4.1. B). These observations were consistent with the previously-reported requirement of Rli1p in nuclear export of ribosomal subunits (Kispal et al., 2005; Yarunin et al., 2005). Therefore, nuclear Rps2p-GFP accumulation was used as a measure of defective Rli1p function here, with rescue of the phenotype by *RLI1* overexpression serving to corroborate Rli1p specificity of phenotypes.

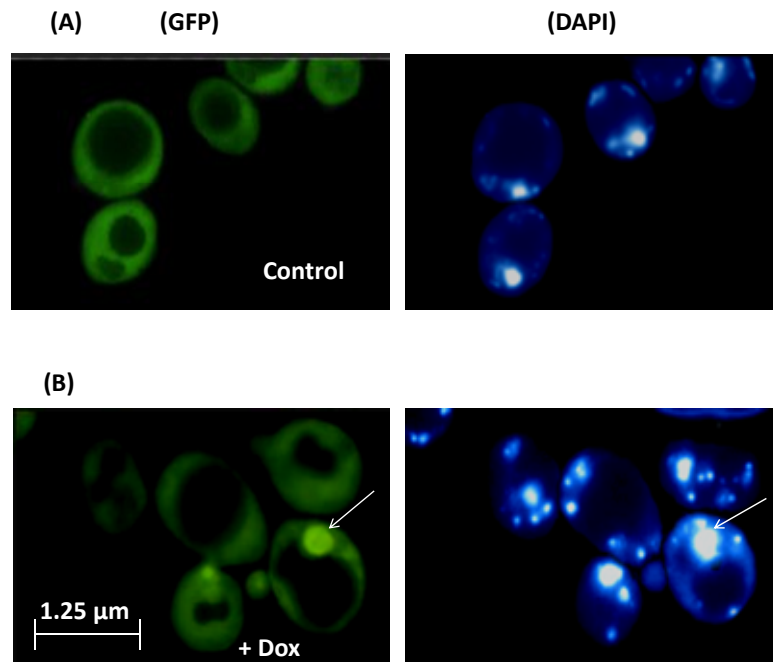


Figure 4.1- Rli1p is required for nuclear export of ribosomal subunits. (A) *tet-RLI1* cells transformed with *pRS315-RPS2-eGFP* were cultured in selective YNB medium lacking doxycycline to allow *RLI1* overexpression, and promoting nuclear export of Rps2p-GFP to the cytoplasm (left panel). Right panel, DAPI staining of cell nuclei. (B) Defective Rli1p function reflected by nuclear accumulation of Rps2p-GFP (left panel) in *tet-RLI1* cells treated with $10\mu\text{g ml}^{-1}$ doxycycline to downregulate *RLI1*. The arrow indicates nuclear Rps2-GFP accumulation. Right panel, DAPI staining of cell nuclei.

4.2.2 ROS sensitivity of Rli1p function in nuclear export of ribosomal subunits

Rli1p is the only Fe-S protein involved in nuclear export of ribosomal subunits, and such activity requires integrity of its Fe-S clusters (Kispal et al., 2005; Yarunin et al., 2005). This dependency on [4Fe-4S] clusters, which are notoriously ROS labile, made Rps2-GFP export activity a suitable assay for ROS sensitive Rli1p function. Therefore, wild type yeast (W303) transformed with *pRS315-RPS2-eGFP* was cultured in selective YNB broth supplemented with a mild dose of 0.35mM Cu (NO₃)₂ (2.16, chapter 2). This dose affected cell doubling time (2.16.1, chapter 2) by <15%. Rps2-GFP was localized primarily to the cytoplasm of control cells where stressor was excluded, indicating normal Rli1p function (Figs 4.2 A). However, exposure to 0.35mM Cu (NO₃)₂ resulted in an increased proportion of cells showing nuclear Rps2p-GFP accumulation, indicating Rli1p dysfunction (Figs 4.2 B).

After that, cells with manipulated *RLI1* expression were assayed during exposure to different stressors. Cells showing nuclear Rps2p accumulation were quantitated with fluorescence microscopy after 2 and 4h incubation with the pro-oxidants (2.16, chapter 2). Here, *RLI1* overexpression was achieved with an isogenic *tet-RLI1* strain which gave >15-fold higher *RLI1* expression than the wild type, in the absence of doxycycline (Fig. 3.1 B, chapter 3). Again, cells were transformed with *pRS315-RPS2-eGFP* and cultured in selective YNB medium; besides copper, the mild doses of stressors assayed were 0.2mM H₂O₂, 1mM paraquat and 0.1mM CrO₃ (2.16, chapter 2). Results showed that in the absence of stressor (control), >99% of cells showed cytosolic Rps2p-GFP localization (Fig 4.3 A). Quantitative analysis of wild type (W303) after 2 and 4h incubation with copper showed that the percentage of cells exhibiting nuclear accumulation of Rps2-GFP was increased significantly by the presence of copper (Fig. 4.3 B) (P=0.004, T=2.5, DF=3) according to Student's t-test. Similar results were obtained with CrO₃ (P=0.007, T=2.8, DF=4), paraquat (P=0.008, T=3.2, DF=3) and H₂O₂ (P=0.01, T=4, DF=2) according to Student's t-test (Figs 4.3 C). This increase was partly suppressed in

the *RLI1*-overexpressing cells, consistent with the effects of pro-oxidants on nuclear Rps2-GFP accumulation being Rli1p specific.

Similar results were verified for Cu (NO₃)₂ stress in a different strain background (BY4741) and with plasmid-borne *tet-RLI1* (Fig 4.4) (P=0.004, T=2.8, DF=4) according to Student's t-test. Cells with visible nuclear fluorescence were a minority of the population in all cases, suggesting there may be a lower limit to the level of nuclear Rps2-GFP accumulation that was detectable.

Collectively, the data indicated that Rli1p function in nuclear Rps2p export is sensitive to mild pro-oxidants, which could be due to ROS targeting of Fe-S clusters within Rli1p. This is consistent with Rli1p being a key target of ROS toxicity, with consequences for Rli1p function in nuclear export of ribosomal subunits and, it can be inferred, for protein synthesis.

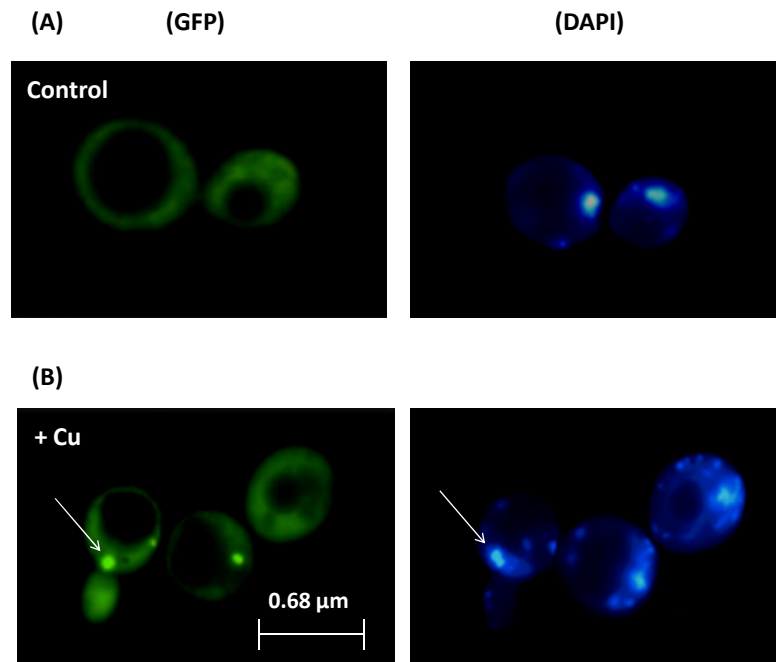


Figure 4.2- Rli1p activity in Rps2p-GFP export is sensitive to mild copper stress. (A) Wild type (W303) cells transformed with *pRS315-RPS2-eGFP* were cultured in selective YNB medium lacking stressors, and showed nuclear export of Rps2p-GFP to the cytoplasm (left panel). Right panel, DAPI staining of cell nuclei. (B) Defective Rli1p function as a result of exposure to 0.35mM Cu (NO₃)₂ was detected as nuclear accumulation of Rps2p-GFP. Similar results were verified in a different strain background (BY4741) and with plasmid-borne *tet-RLI1*. Quantitative results for Cu and other stressors are shown in Fig. 4.3.

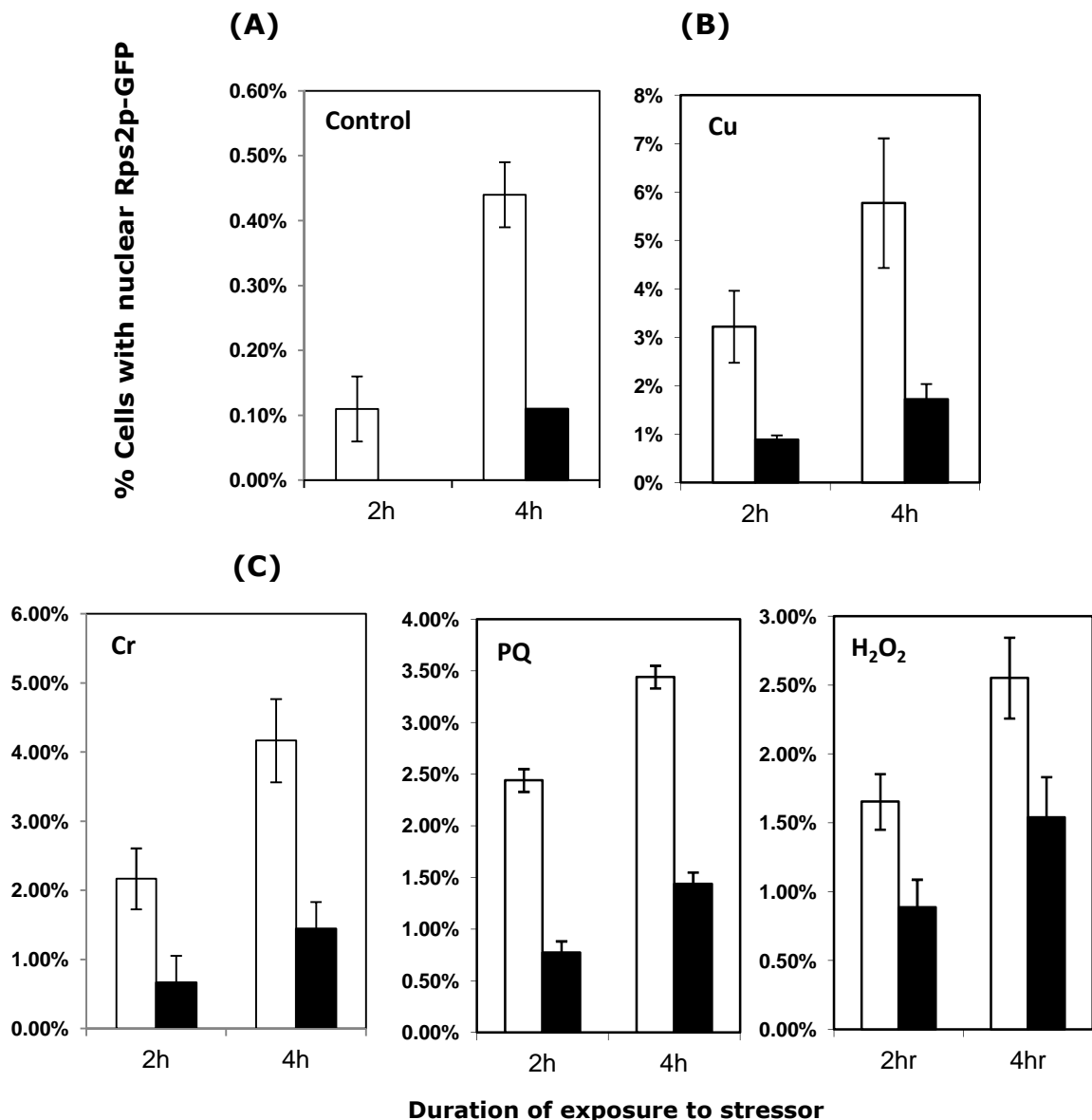


Figure 4.3- Rli1p-dependent activity in ribosomal subunit Rps2p export is decreasing during mild pro-oxidant stress. (A) Wild type (W303) (□) or isogenic *tet-RLI1* overexpression (■) strains transformed with *pRS315-RPS2-eGFP* were cultured in selective YNB medium lacking stressors. The percentage of cells with nuclear accumulation of Rps2-GFP was <1% in both types of cell, according to counts by fluorescence microscopy. (B, C) Strains as above were incubated with 0.35mM Cu (NO₃)₂ (B), or with 0.1mM CrO₃, 1mM paraquat or 0.2mM H₂O₂ (C), for 2 and 4h. These doses affected cell doubling times <15%. Doxycycline was excluded. Values are means from three independent experiments ± SEM between the experiments, with ≥ 300 cells counted under fluorescence microscope in each experiment.

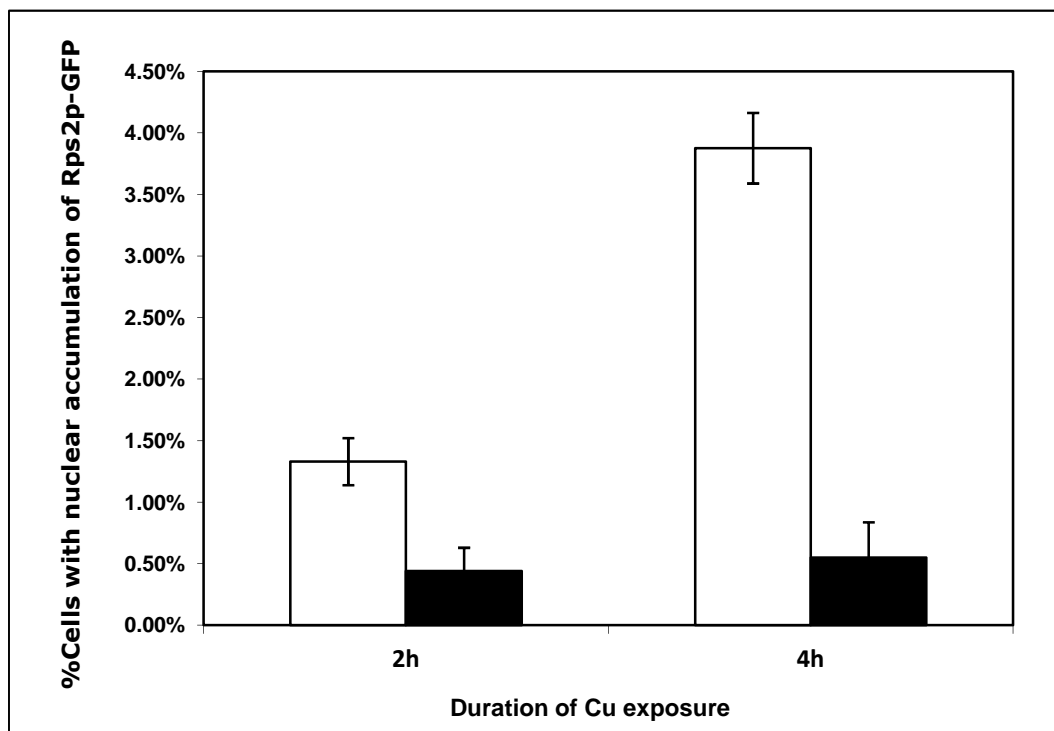


Figure 4.4- Rli1p-dependent activity in ribosomal subunit Rps2p export is decreased during mild copper stress of *S. cerevisiae* BY4741. The BY4741 wild type strain transformed with *pCM190* (□) or *pCM190-tetRLI1* (■) was additionally transformed with *pRS315-RPS2-eGFP* and incubated with 0.35mM Cu (NO₃)₂ for 2 and 4h. Doxycycline was excluded. Values are means from three independent experiments \pm SEM between the experiments, with \geq 300 cells counted under fluorescence microscope in each experiment.

4.3 *ATM1* overexpression restores Rli1p activity in nuclear Rps2- GFP export during copper stress

Maturation of cytosolic and nuclear Fe-S proteins (such as Rli1p) requires the function of both the mitochondrial Fe-S cluster (ISC) assembly machinery as well as a mitochondrial ISC export system (Kispal et al., 1999). As described in the Introduction to this Chapter, the ABC transporter Atm1p of the mitochondrial inner membrane, which is a member of the ISC export machinery, is required to transfer Fe-S cluster precursors that were synthesized by mitochondrial proteins to the cytosol to participate in the assembly of cytosolic Fe-S cluster proteins (Kispal et al., 1999; Cavadini et al., 2007). Sideri et al. (2009) demonstrated that *ATM1* overexpression increased cellular resistance to copper stress, one of the main initial indications that an extra-mitochondrial Fe-S protein(s) affects Cu resistance. To help link Atm1p-dependent Cu resistance to Rli1p function and to test whether Fe-S cluster supply via Atm1p may affect Rli1p-dependent nuclear export (2.16, chapter 2), *pCM190-tetATM1* was constructed to be under the *tetO* promoter regulation as described in (2.1.1, chapter 2). The aim was to test *ATM1* overexpression for restoration of nuclear Rps2-GFP export. Therefore, wild type cells transformed with empty vector *pCM190* or *pCM190-tetATM1* were additionally transformed with *pRS315-RPS2-eGFP* (2.10.1, chapter 2) and incubated for 2 and 4h with a mild dose of Cu (NO₃)₂, which affected cell doubling times by <10% (2.16.1, chapter 2). Quantitative analysis again showed that copper stress increased significantly nuclear accumulation of Rps2-GFP over time (P=0.007, T=3.2, DF=3) according to Student's t-test (Fig 4.5). Moreover, *ATM1* overexpression partly suppressed this nuclear Rps2-GFP export defect (Fig 4.5). This restoration of Rli1p function by *ATM1* overexpression could be due to *ATM1* overexpression supplying more Fe-S clusters to the cytosol (Sideri et al., 2009), and consequently compensating defective Fe-S cluster integrity within Rli1p during Cu stress. This is consistent with Fe-S function being the crucial determinant of continued Rli1p activity during stress.

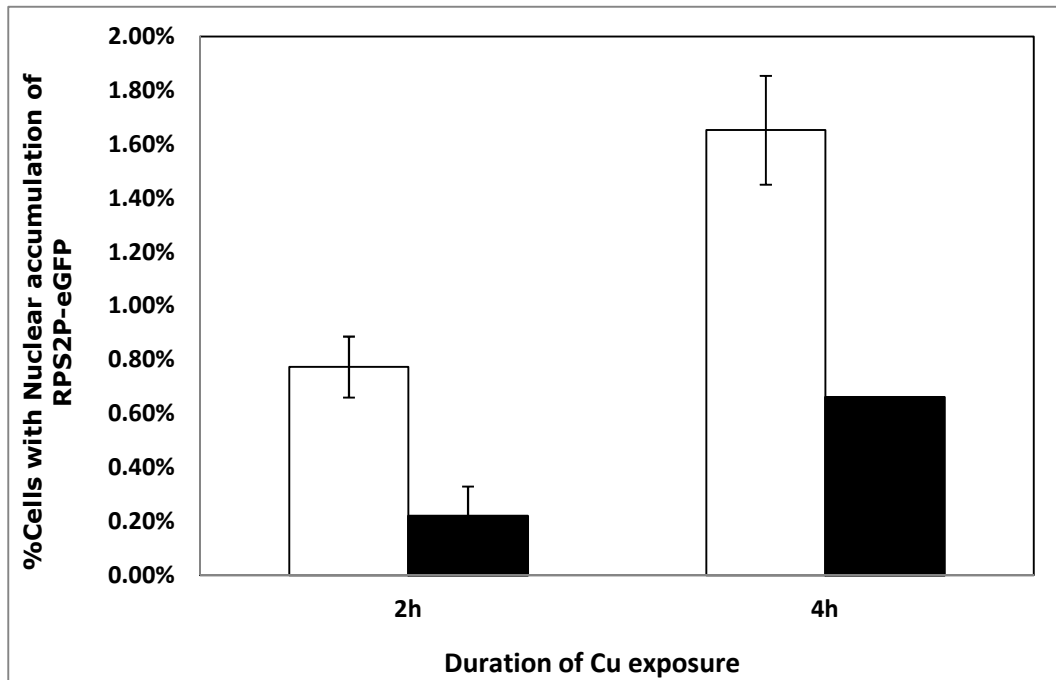


Figure 4.5- *ATM1* overexpression restores Rli1p function during mild copper stress. *S. cerevisiae* BY4741 transformed with *pCM190* (□) or *pCM190-tetATM1* (■) was additionally transformed with *pRS315-RPS2-eGFP* and incubated with 0.25mM Cu (NO₃)₂ for 2 and 4h. Values are means from three independent experiments ± SEM between the experiments, with ≥ 300 cells counted in each experiment.

In conclusion, these results corroborated the idea that Atm1p-dependent Cu resistance (Sideri et al., 2009) was specific to Rli1p and was related to an impact on Rli1p.

4.4 The integrity of Fe-S clusters is required for Rli1p activity during mild oxidative stress

4.4.1 Expression of an iron-sulphur cluster mutant, *rli1*^{C58A}, heightens cellular ROS sensitivity

The recovery of Rli1p function seen in *ATM1* overexpressing cells during mild oxidative stress (Fig 4. 5) was consistent with Fe-S clusters being the specific ROS target relevant to Rli1p. To substantiate this I tested pro-oxidant sensitivity of cells expressing *rli1*^{C58A} by using growth curve assays (2.15.1, chapter 2). This labile version of Rli1p (*rli1*^{C58A}) lacks one of the protein's cluster-coordinating cysteines, via replacement of the cysteine residue 58 of wild type Rli1 with alanine (Barthelme et al., 2007). This yields a labile [3Fe-4S]⁺ cluster which, nevertheless, supports sufficient Rli1p function for cell viability (Barthelme et al., 2007). The cluster's oxygen lability should accentuate any Fe-S centred ROS toxicity. Replacement of wild type Rli1 with the oxygen-labile *rli1*^{C58A} had a little effect on growth rate compared with the wild type in control conditions where stressors were excluded (Fig 4. 6), and such observed differences were not statistically significant (P=0.7, T=2, DF=78) according to Student's t-test. However, the *rli1*^{C58A}-expressing cells were sensitive to the pro-oxidants as evident from decreasing growth rates significantly compared with the wild type (Fig 4.6), particularly to H₂O₂ (P=3.3E-05, T=2, DF=46), Cu (NO₃)₂ (P=7.3E-09, T=2, DF=46) and paraquat (P=0.005, T=2, DF=41), whereas with Cr there was no significant effect on growth rate compared with the wild type (P=0.09, T=2, DF=73) according to Student's t-test. This was consistent with ROS-targeting of Rli1p being centred at one of the protein's Fe-S clusters.

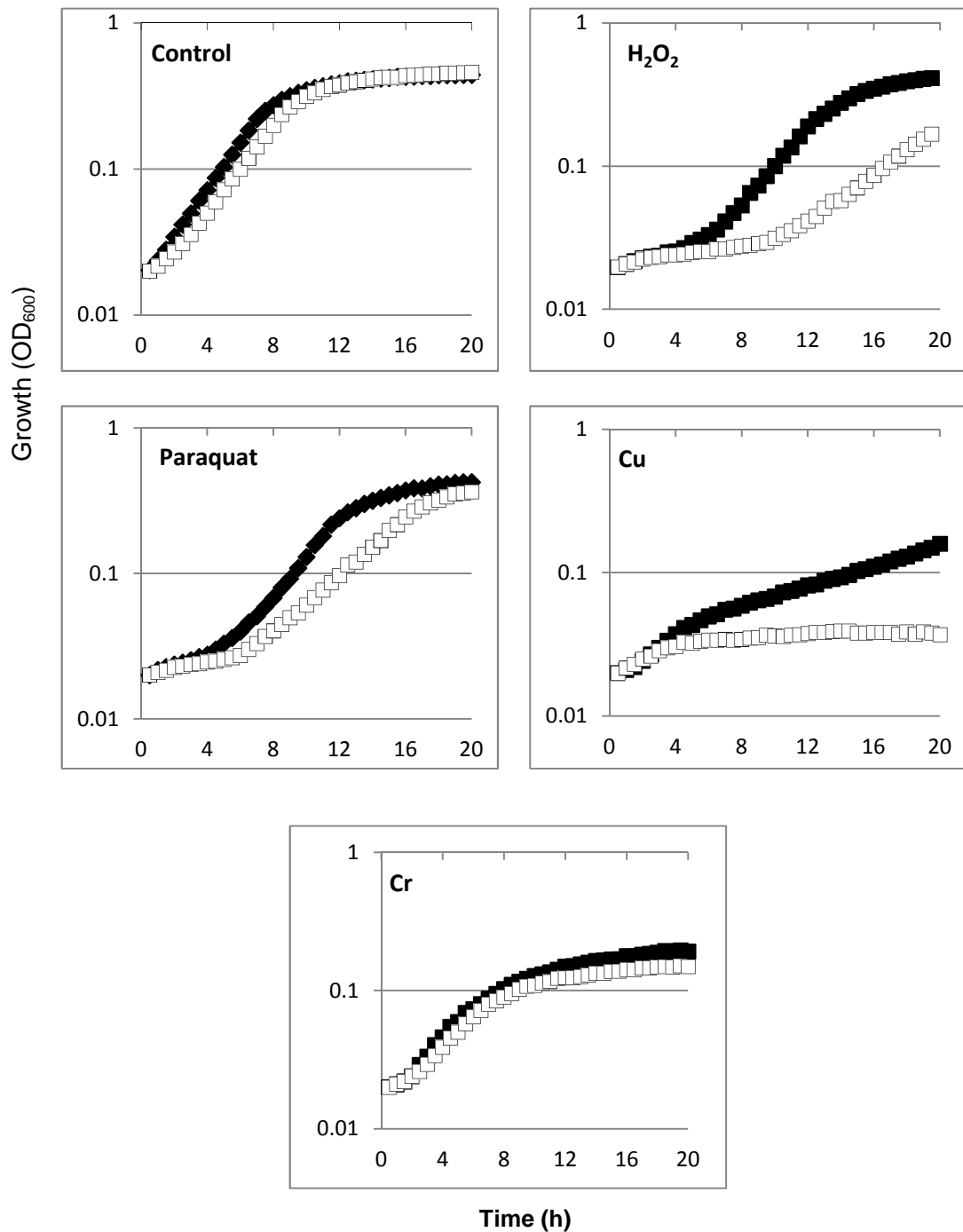


Figure 4.6- Expression of an iron-sulphur (Fe-S) cluster Rli1 mutant (*rli1*^{C58A}) heightens cellular ROS sensitivity. Wild type (■) or *rli1*^{C58A}-expressing cells (□) were cultured in YNB broth in the absence of pro-oxidants (Control), or in the same medium supplemented either with 1mM H₂O₂, 2mM paraquat, 0.5mM Cu (NO₃)₂ or 0.1mM CrO₃. SEMs from triplicate independent experiments were smaller than the dimensions of the symbols.

4.4.2 Expression of *rli1*^{C58A} in place of *Rli1* decreases nuclear *Rps2*-GFP export during copper stress

In order to test whether expression of the Fe-S cluster mutant *rli1*^{C58A} affects Rli1p function in nuclear Rps2-GFP export during stress (2.16, chapter 2), wild type and the *rli1*^{C58A}-expressing cells transformed with *pRS315-RPS2-eGFP* were incubated for 2 and 4h with a mild dose of copper [which affected cell doubling times by <3% (2.16.1, chapter 2)]. Quantitative analysis of the effect of mild copper stress on nuclear export of Rps2p-GFP showed that the effect of copper in causing nuclear accumulation of Rps2p-GFP was accentuated in *rli1*^{C58A}-expressing cells. The proportion of cells exhibiting defective Rps2-GFP export during mild copper stress was ~2-fold greater in *rli1*^{C58A}-expressing cells than in the wild type (Fig 4.7), such observed differences was statistically significant (P=0.03, T=2.8, DF=4) according to Student's t-test. The data are consistent with ROS-targeting of Rli1p function being centred at at-least one of the protein's Fe-S clusters.

4.5 Oxygen-requirement in Rli1p-dependent stress resistance

The fact that the above stressors were pro-oxidants and [4Fe-4S] clusters are notoriously ROS labile pointed to an oxidative mode of action against Rli1p. The above effects were measured over a timescale of hours, which is ample time for oxidative stress caused by the pro-oxidants to take effect (Avery, 2011). However, non-oxidative [4Fe-4S] cluster damage is also known, as reported for copper targeting of Fe-S cluster enzymes (dehydratases) in *E. coli* (Macomber & Imlay, 2009). Therefore, I compared the Rli1p-dependence of stressor resistance under aerobic and anaerobic conditions (2.2, chapter 2) to establish the oxygen dependence of phenotypes. Results from spotting *S. cerevisiae* cells on agar (2.15.2, chapter 2) showed that, as in growth curve assays, *RLI1* overexpression conferred pro-oxidant resistance during aerobic growth (Fig 4.8). On the other hand, in anaerobic conditions, changing the level of *RLI1* expression did not affect the cells' resistances to stressors, which were equally inhibitory

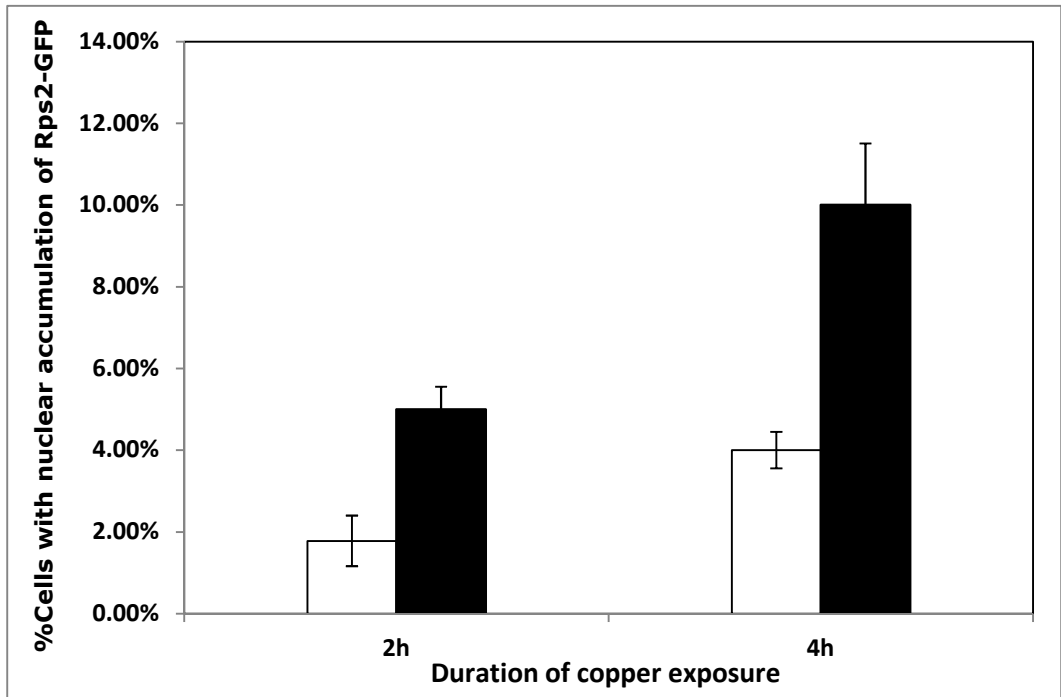


Figure 4.7- Expression of the Fe-S cluster mutant *rli1^{C58A}* heightens defective Rli1p function during copper stress. Wild type (□) or *rli1^{C58A}*-expressing (■) cells transformed with *pRS315-Rps2p-eGFP* were cultured with 0.25mM Cu (NO₃)₂ for 2 and 4h. Values are means from three independent experiment ± SEM, with ≥300 cells counted in each experiment.

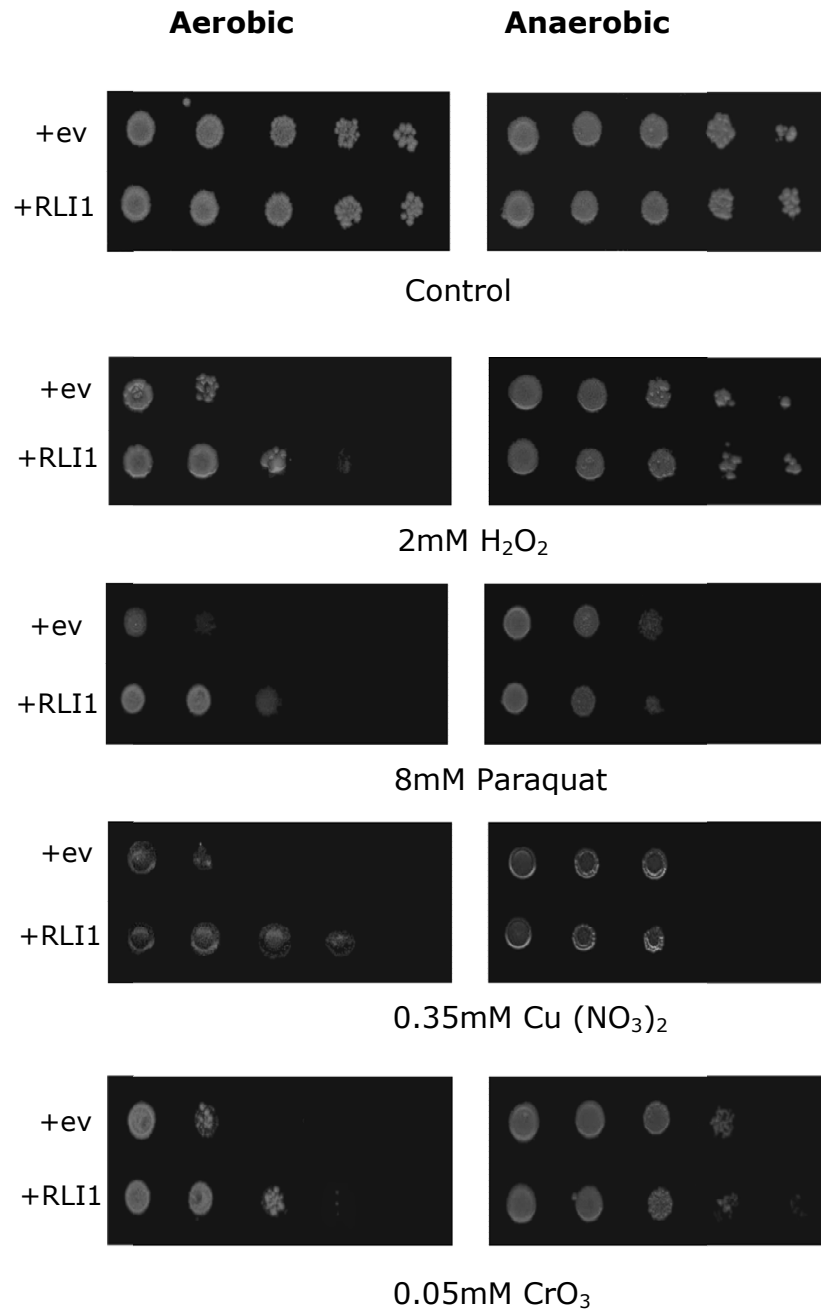


Figure 4.8- Rli1p-dependent resistance to pro-oxidants requires oxygen. *S. cerevisiae* BY4741 transformed with *pCM190* (+ev) or *pCM190-tetRLI1* (+RLI1) were 10-fold serially diluted and spotted from left to right on YNB agar supplemented with stressors as indicated. Plates were incubated for 5 days, either under ambient air or anaerobically under H₂ and CO₂. Typical data from one of several independent experiments are shown.

to wild type or *RLI1* overexpressing cells (Fig 4.8). These data suggested an oxidative mode of Rli1p targeting by stressors.

4.6 Oxygen requirement for the stress sensitivity of *rli1*^{C58A}-expressing cells

The effects of stressors on *rli1*^{C58A}-expressing cells were also compared under aerobic and anaerobic conditions (2.2, chapter 2). As in the earlier growth curve assays, *rli1*^{C58A}-expressing cells were more sensitive to the pro-oxidants than wild type during aerobic growth on agar (2.15.2, chapter 2), consistent with ROS-targeting of Rli1p activity being centred at one of the protein's [4Fe-4S] clusters. However, ROS sensitivity of both types of cell was partly suppressed during anaerobicity (Fig 4.9). This suppression was particularly marked for the *rli1*^{C58A}-expressing cells. The data are consistent with that the [4Fe-4S] clusters of Rli1p could have redox active role after interaction with other components of Rli1 complexe (Rli1/Lto1/Yae1), as Rli1^{C25S} polypeptide, which is free of [4Fe-4S] clusters, can support cells growth in the anaerobic condition, whereas it caused growth inhibition in the aerobic conditions (Zhai et al., 2013). Furthermore, similar to Lto1 and Yae1, the [4Fe-4S] clusters of Rli1p are not necessary in the absence of oxygen, whereas indispensable in the aerobic conditions, this participation in phenotype could reveal a functional interaction between Yae1, Lto1 and the [4Fe-4S] clusters of Rli1p, where Lto1 is crucial in aerobic condition owing to its role in reducing the toxic effect of ROS, therefore, the [4Fe-4S] clusters of Rli1p and LTO1 itself are crucial for preservation of cells growth in the aerobic condition (Zhai et al., 2013). In the cases of paraquat and chromate, anaerobicity fully rescued the relative stress sensitivity of *rli1*^{C58A}-expressing cells. The data suggest that the Fe-S clusters of Rli1p may be specific targets of ROS, and that this is a key mechanism of growth inhibition by the pro-oxidants.

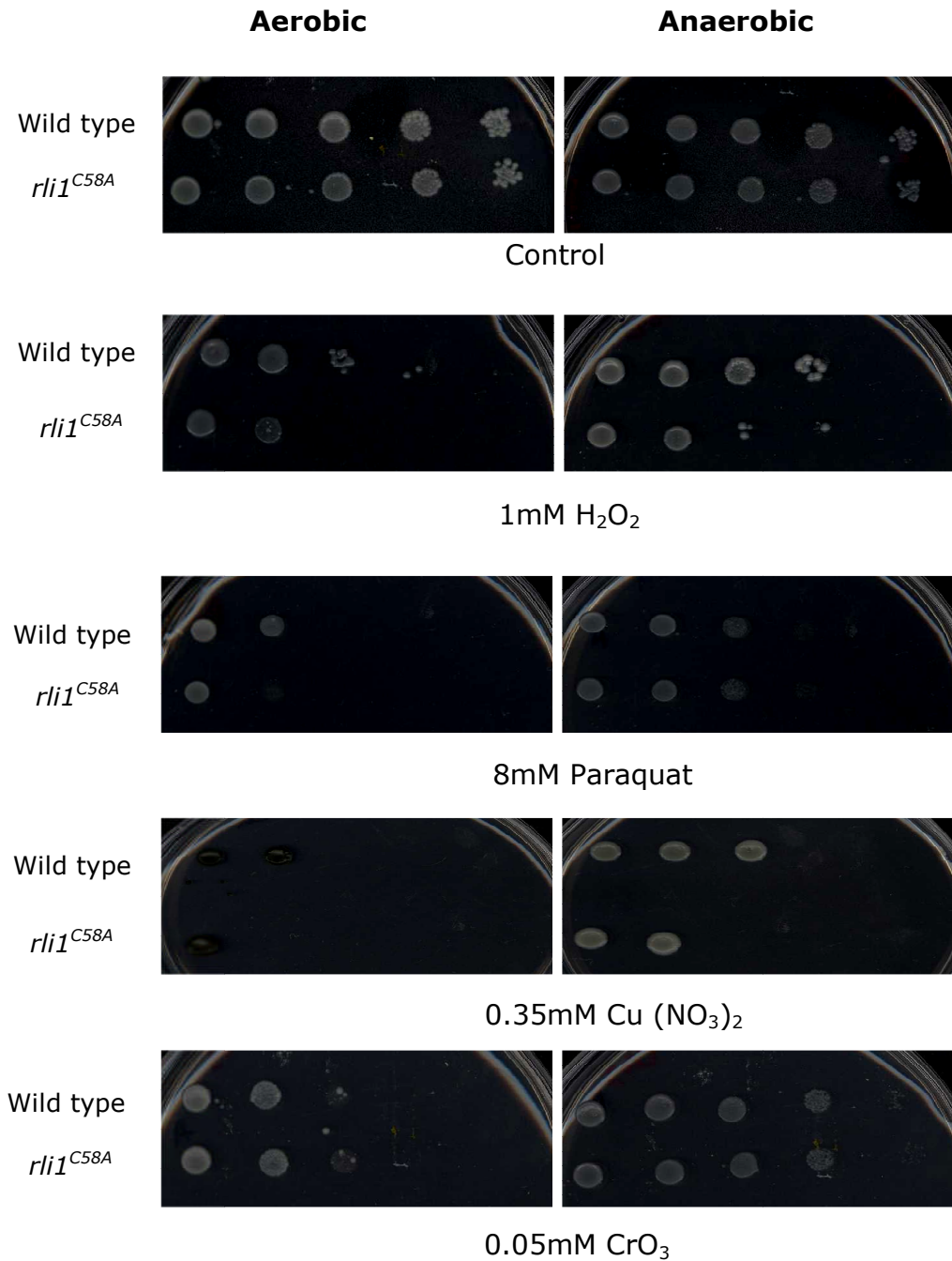


Figure 4.9- Sensitivity of *rli1*^{C58A}-expressing cells to pro-oxidants is suppressed during anaerobicity. *S. cerevisiae* BY4741 and *rli1*^{C58A}-expressing cells were 10-fold serially diluted and spotted from left to right on YNB agar supplemented with stressors as indicated. Plates were incubated for 5 days, either under ambient air or anaerobically under H₂ and CO₂. Typical data from one of two independent experiments are shown.

4.7 Discussion

The main purposes of the studies in this chapter were to test further whether Rli1p is a specific ROS target, via assaying the effect of mild pro-oxidants on Rli1p function. In addition, I tested whether Fe-S cluster supply via Atm1p may be a determinant of continued Rli1p activity during stress, and then that Fe-S clusters within Rli1p specifically are limiting for ROS sensitive Rli1p function. Finally, I aimed to establish the requirement for oxygen in this apparent targeting of Rli1p.

Rli1 is the only essential cytosolic Fe-S protein, required for nuclear export of ribosomal subunits to the cytoplasm among other functions. Strong nuclear accumulation of ribosomal subunits was observed as a result of depleting Rli1p from yeast cells (Kispal et al., 2005; Yarunin et al., 2005). Consequently, nuclear GFP accumulation in cells expressing a GFP fusion with the small ribosomal subunit protein Rps2 was used in this study as a sensitive indicator of defective Rli1p function, a fact further supported by the data in this study. My results indicated that Rli1p function in nuclear export of Rps2-GFP is sensitive to mild oxidative stress. *RLI1* overexpression during pro-oxidant exposure corroborated that the effects were Rli1p-specific, as this manipulation partially restored the nuclear export phenotype. This impact of the level of *RLI1* expression on Rps2-GFP export was consistent with the results of Kispal et al. (2005) and Yarunin et al. (2005) upon depletion of Rli1p. The two [4Fe-4S] clusters of Rli1p are required for its activity in nuclear export of ribosomal subunits (Kispal et al., 2005) and the fact that export was not fully restored by *RLI1* overexpression was expected, as potential issues like defective Fe-S cluster assembly or integrity in Rli1p would still persist. Exporting of Fe-S cluster precursors from the mitochondria to the cytosol through Atm1p is required to generate extra-mitochondrial Fe-S clusters for proteins such as Rli1 (Kispal et al., 1999; Cavadini et al., 2007; Miao et al., 2009). Therefore, to link Atm1p-dependent Cu resistance (Sideri et al., 2009) to Rli1p activity, my data showed restoration of nuclear Rps2-GFP export by *ATM1*

overexpression during mild oxidative stress. This was consistent with recent experiments conducted by Dr. Sara Holland in the Avery laboratory and described in (Alhebshi et al., 2012) which have supported a model in which ROS-targeting of Fe-S clusters prior to their assembly into Rli1p is the critical mechanism of ROS action on Rli1p *in vivo*. In those experiments, HA-tagged Rli1p was immunoprecipitated at intervals from cells incubated with radiolabelled $^{55}\text{FeCl}_3$ under various conditions, and the amount of label retained by Rli1-HA determined. The experiments measured both incorporation and turnover of Fe(S) in Rli1p and showed that some $^{55}\text{Fe-S}$ cluster turnover occurred in purified Rli1-HA during *in vitro* incubation with pro-oxidants. However, that effect was not reproduced *in vivo* at pro-oxidant doses that were just sub-inhibitory to growth, suggesting that Fe-S clusters already inserted into Rli1p are not the main ROS targets *in vivo*. ^{55}Fe incorporation to Rli1p was inhibited by 50-80% in the same conditions, indicating that it is incorporation rather than turnover that is affected by mild oxidative stress. As the toxic action of ROS perturbs the supply of $^{55}\text{Fe-S}$ clusters to Rli1p, it can be inferred that this then affects Rli1p-dependent function in nuclear export. This evidence substantiates that Fe-S function is the crucial determinant of continued Rli1p activity during stress, and that this action at Rli1 provides the explanation for Atm1p-dependent Cu resistance.

Comparing the Rli1p-dependence of stressor resistance under aerobic and anaerobic conditions in wild type cells indicated that whereas high *RLI1* expression confers stress resistance in aerobic conditions, it has no discernible influence in anaerobic conditions, indicating an oxidative mode of Rli1p targeting. To substantiate that Fe-S clusters are specific ROS targets relevant to Rli1p, cells expressing *rli1*^{C58A} were used. *rli1*^{C58A} lacks a [4Fe-4S]-coordinating cysteine, yielding a [3Fe-4S]⁺ cluster. This replacement of wild type Rli1 with an oxygen-labile mutant *rli1*^{C58A} (Barthelme et al., 2007) yielded cells that were sensitive under aerobic conditions to the pro-oxidants. This pro-oxidant sensitivity was in keeping with the mutant protein's (*rli1*^{C58A}) predicted lability (Barthelme et al., 2007), and was also reflected in Rli1p activity, as the proportion of cells exhibiting

defective Rli1p function was higher in *rli1^{C58A}*-expressing cells than in the wild type during stress. This is consistent with the Fe-S clusters being an essential component of Rli1p activity and for yeast cell viability (Kispal et al., 2005). Moreover, comparing sensitivity of *rli1^{C58A}*-expressing cells under aerobic and anaerobic conditions supported the notion that it is Fe-S clusters of Rli1p that are affected by ROS, as *rli1^{C58A}*-expressing cells' pro-oxidant sensitivity was partly suppressed during anaerobicity. The oxygen-dependency here contrasts with a previous report of non-oxidative [4Fe-4S] cluster damage by copper, in which copper inactivated dehydratase Fe-S enzymes by displacement of Fe atoms from the solvent-exposed clusters and binding to the coordinating sulphur atoms (Macomber & Imlay, 2009). The two [4Fe-4S] clusters of Rli1p are predicted to be well shielded from solvent (Karcher et al., 2008) which would be expected to protect them from direct attack by ROS. Thus, the indication that ⁵⁵Fe insertion into Rli1p is the main ROS-sensitive target as discussed above (Alhebshi et al., 2012) resonates with more recent work in bacteria, where cluster assembly on or transfer from scaffold proteins was proposed to underpin oxidant disruption of the ISC system (Jang & Imlay, 2010). Fe-S clusters during transfer are expected to be solvent exposed and thereby ROS-susceptible. This affected Fe-S cluster incorporation to proteins like NADH dehydrogenase I, in which Fe-S clusters are normally well shielded (Jang & Imlay, 2010), like in Rli1p. In the case of Rli1p, targeting of upstream Fe-S cluster assembly or transfer might be most likely to occur in the cytosol, e.g., at cytosolic scaffold or transfer proteins such as Cfd1, Nbp35, Nar1 and Cia1, because Fe-S assembly in the mitochondria is partly shielded from external stress. Nevertheless, the fact that cells expressing *rli1^{C58A}* as their sole Rli1p were ROS sensitive, together with the Fe-S lability of Rli1p seen *in vitro* (Alhebshi et al., 2012), suggests that ROS can cause some Fe-S turnover in Rli1p under particular conditions. The particularly strong sensitivity of *rli1^{C58A}*-expressing cells toward Cu, H₂O₂ and paraquat was commensurate with the fact that Cu (via Fe displacement) (Macomber & Imlay, 2009), H₂O₂ (Jang & Imlay, 2010) and paraquat (Varghese et

al., 2003) can degrade Fe-S clusters beyond the [3Fe-4S]⁺ state, in which the C58A cluster is thought to exist (Barthelme et al., 2007). In contrast, superoxide-generating agent such Cr is not thought to oxidize Fe-S clusters beyond [3Fe-4S]⁺ *in vivo* (Macomber & Imlay, 2009). Therefore, the limited Cr-sensitivity of *rli1*^{C58A}-expressing cells may reflect that only one of the two clusters of the protein remains partly oxidizable by this agent.

To summarise, the main findings in this chapter are that: (i) Rli1p function in nuclear export of Rps2p is sensitive to pro-oxidants, (ii) Atm1p-dependent Cu resistance was specific to Rli1p, presumably determined by mitochondrial export of Fe-S clusters to participate in the generation of Rli1 holoprotein, (iii) Rli1 with heightened ROS-lability accentuates sensitivity of Rli1p function and of cell growth to pro-oxidant stress, consistent with ROS-targeting of Rli1p function being centred at one of the protein's [4Fe-4S] clusters, (v) stressors target essential Rli1p function via an oxidative mode, because Rli1p-dependent stress resistance was suppressed during anaerobicity.

**Chapter 5- Influence of specific gene
deletion and essential metals on Rli1p
function in stress resistance**

5.1 Introduction

Cellular redox balance in biological systems is helped by antioxidant defence systems that neutralize ROS (Manda et al., 2009). Cells have both enzymatic and non-enzymatic defence systems to preserve cellular redox state and to defend their cellular components (Jamieson, 1998). The responses invoked by organisms to counter oxidative stress have received considerable research attention over the last two decades. These include the up-regulation of ROS-scavenging proteins, or enzymes that reverse oxidative damage. Oxidative stress responses are now well characterized in a diverse range of organisms (Imlay, 2008). Methionine sulphoxide reductases (MSRs) are crucial repair enzymes that protect cells by reducing oxidized methionine residues in proteins (Weissbach et al., 2002; Kim & Gladyshev, 2007). Therefore, MSRs help to preserve protein activity during ROS stress (Chen et al., 2007). In addition, Sideri et al. (2009) have shown that MSRs specifically protect Fe-S clusters from inactivation by ROS in the yeast model, possibly through a superoxide scavenging mechanism. Furthermore, Mn-SOD (Sod2p) is a major mitochondrial antioxidant enzyme which acts as superoxide scavenger in mitochondria (Weisiger & Fridovich, 1973) and protects Fe-S clusters from superoxide attack at the mitochondrial location of cluster biosynthesis (Irazusta et al., 2006).

The study of Sideri et al. (2009) with MSR-deficient strains suggested a link between toxicity of copper and the cluster integrity of Fe-S proteins in the yeast model. Fe-S cluster defects in *msrΔ* cells were coincident with sensitization to copper in minimal medium (a Cu-resistance phenotype in rich medium was due to *FET3* upregulation as a result of Fe-S cluster dysfunction, and was growth medium-specific) (Sideri et al., 2009). This was consistent with work in bacteria which showed that Fe-S clusters of dehydratases are primary intracellular targets of copper toxicity, where Fe-S cluster defects occurred by displacement of Fe atoms from the solvent-exposed clusters (Macomber & Imlay, 2009). Other studies have shown that oxidants like H₂O₂ as well as Cu (NO₃)₂ can cause oxidative damage of Fe-S

clusters (Jang & Imlay, 2007; Varghese et al., 2003; Macomber & Imlay, 2009). Sideri et al. (2009) confirmed a ~2-fold increase in Fe-S protein activity in cells overexpressing *SOD2*, and these cells also had increased Cu resistance. As mentioned previously, *ATM1* overexpression also conferred a Cu resistance phenotype as well as increased cytosolic Fe-S protein activity, which indicated that an extra-mitochondrial Fe-S protein(s) affects Cu resistance (Sideri et al., 2009). The preceding chapters of this thesis suggested that the relevant extra-mitochondrial Fe-S protein is Rli1.

The aims of this chapter are (i) to determine whether the role of MSRs in copper resistance may be specific to Rli1p activity; (ii) test whether the role of *SOD2* in copper resistance may involve Rli1p; (iii) verify whether manganese works through *SOD2* in mediating copper resistance; (iv) substantiate that Fe-S cluster defects are responsible for Rli1p-dependent copper resistance.

Results

5.2 Genes that help preserve Rli1p function during oxidative stress

5.2.1 MSRs have a role in Rli1p-dependent nuclear export of ribosomal subunits

In the previous chapter, I showed that Rli1p-dependent function in ribosomal subunit export from the nucleus was compromised during oxidative stress. Here, I tested whether this effect may be accentuated in an MSR-deficient background (*msrΔ*), as MSRs specifically protect Fe-S clusters from inactivation by ROS (Sideri et al., 2009). Previously, it was shown that growth inhibition by copper in an *msrΔ* mutant could be rescued by *RLI1* overexpression (Sideri, 2007). Here, linking MSR activity to Rli1p function would help verify a role for Fe-S cluster targeting being the relevant effect of ROS on Rli1p. Manipulation of *RLI1* expression was used to corroborate that the effects were Rli1p-specific. Therefore, the nuclear Rps2p-GFP export assay (2.16, chapter 2) was performed during mild copper stress in *pRS315-RPS2-eGFP*-transformed *msrΔ* or wild type (BY4741) cells, which were additionally transformed with empty vector or *pCM190-tetRLI1* (for *RLI1* overexpression).

Results showed that, even in the absence of copper, the percentage of *msrΔ* cells with nuclear accumulation of Rps2-GFP (>5%) was considerably higher than that in wild type cells (<1%) (Fig 5.1), and such observed differences were statistically significant ($P=7.72389E-06$, $T=2.8$, $DF=4$) according to Student's t-test. Moreover, this indication of defective Rli1p function in the *msrΔ* mutant was exacerbated during copper stress, where >20% of *msrΔ* cells showed defective nuclear export of Rps2-GFP in comparison with less than 5% of wild type cells, and such differences were statistically significant ($P=0.0002$, $T=3.2$, $DF=3$). *RLI1* overexpression partially restored the nuclear Rps2-GFP export phenotype of both strains during copper stress, corroborating that the effects were Rli1p-specific (Fig 5.1). Considering the elevated oxidative targeting of Fe-S clusters in MSR-deficient cells (Sideri et al., 2009), these results were consistent with Fe-S function being the crucial determinant of continued Rli1p activity during stress.

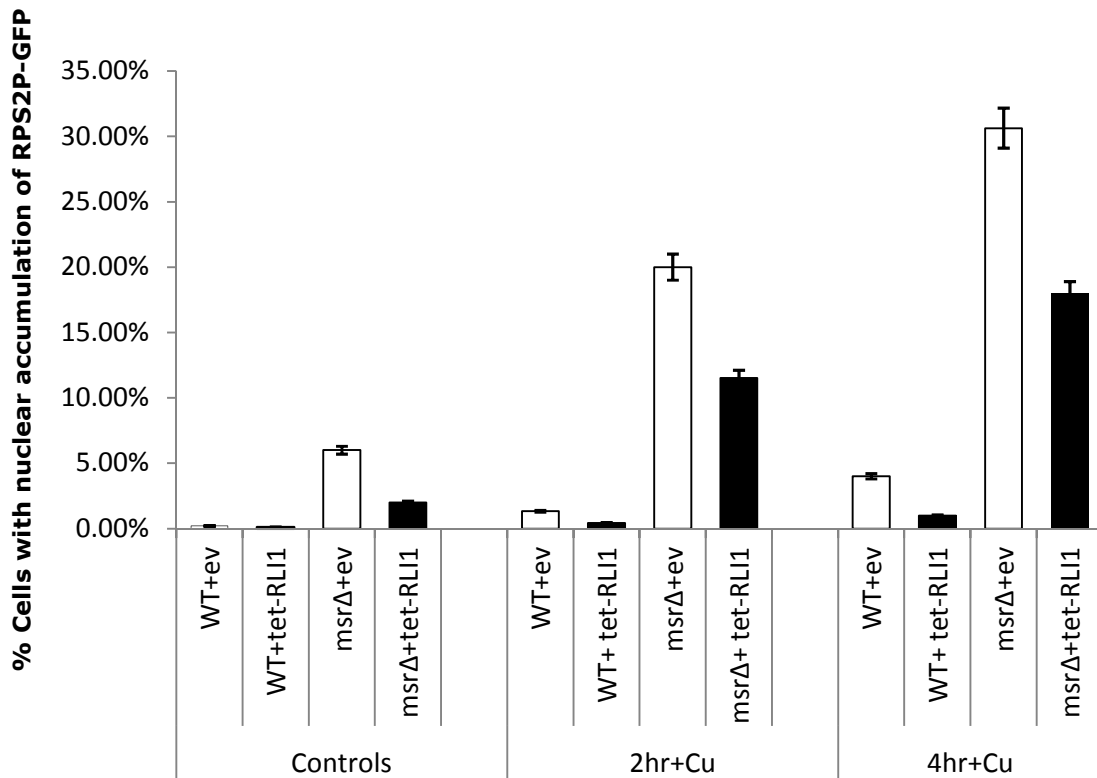


Figure 5.1- Exacerbation of defective Rli1p function in *msrΔ* mutant cells during mild copper stress. The BY4741 wild type and isogenic *msrΔ* double mutant strain transformed with *pCM190* (+ev) (□) or *pCM190-tetRLI1* (■) were additionally transformed with *pRS315-RPS2-eGFP* and cultured in selective YNB medium in the absence or presence of 0.35mM Cu (NO₃)₂ for 2 and 4h, as indicated. Values are means from three independent experiments ± SEM between the experiments, with ≥ 300 cells counted in each experiment.

5.2.2 Sod2 activity is required for Rli1p-dependent pro-oxidant resistance

Previous work in the Avery laboratory showed that Cu resistance of wild type cells was raised by supplementation with $MnCl_2$ or by overexpressing the Mn-SOD encoded by *SOD2* (Sideri et al., 2009). These manipulations promote superoxide scavenging, with superoxide radicals being limiting for cellular Fe-S protein activities generally (Irazusta et al., 2006). In order to determine whether the influence of Sod2 on Cu-resistance could be centred on Rli1p, the effect of *RLI1* overexpression on the Cu-sensitivity phenotype of *sod2Δ* mutant cells was tested.

5.2.2.1 Copper sensitivity phenotype of Sod2 defective cells

In order to verify the copper sensitivity phenotype, *sod2Δ* mutant and wild type cells were cultured in the absence or presence of 1mM $Cu(NO_3)_2$ (2.15.1, chapter 2). Growth results showed the copper sensitivity phenotype of the *sod2Δ* mutant versus wild type cells and there was a statistically significant decrease in growth of *sod2Δ* mutant according to Student's t-test ($P=1.184E-10$, $T=2$, $DF=42$), whereas similar growth of both strains was observed in the absence of copper stress (Fig 5.2) and there were no statistically significant differences in their growth according to Student's t-test ($P=0.9$, $T=2$, $DF=82$). The exacerbated Cu-sensitivity of cells lacking mitochondrial Sod2p suggests an involvement in this phenotype of oxidative stress at the mitochondria, the location of Fe-S cluster biogenesis.

5.2.2.2 Manganese treatment confers Cu-resistance in sod2Δ cells

Work in the Avery laboratory conducted by Dr. Sara Holland has shown that Cu resistance of wild type cells was raised by Mn-superoxide dismutase (Sod2p) overexpression or by supplementation with $MnCl_2$; *Sod2* overexpression was also shown to give a ~2-fold increase in Fe-S protein (aconitase) activity (Alhebshi et al., 2012). Elsewhere, activities of Fe-S mitochondrial proteins such as glutamate synthase, succinate dehydrogenase and the cytosolic Fe-S enzyme isopropylmalate dehydratase have been restored by manganese

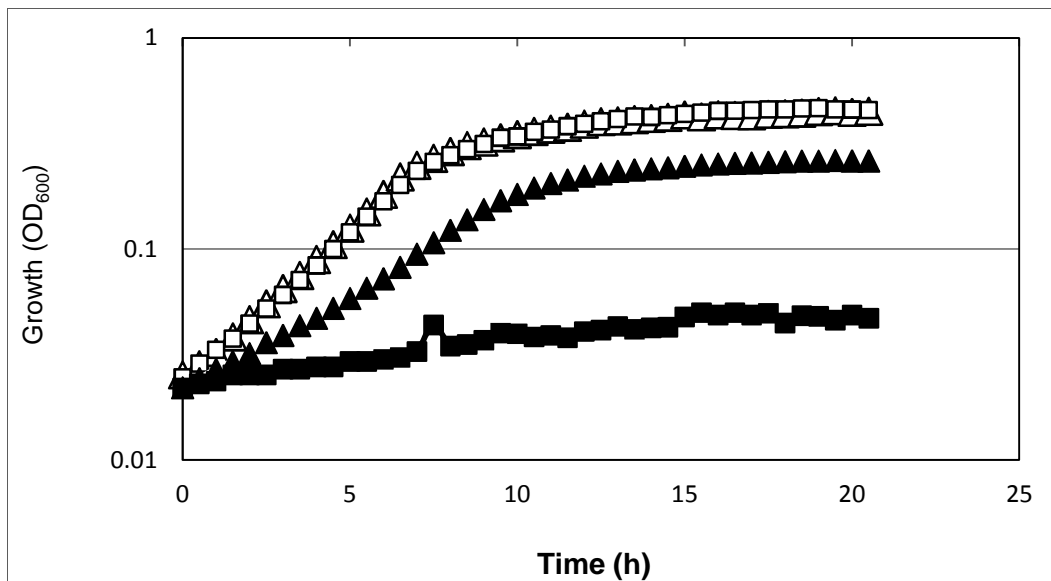


Figure 5.2- Copper sensitivity phenotype of *sod2Δ* mutant cells. *sod2Δ* mutant (□,■) and wild type (△,▲) cells were cultured in YNB medium in the absence (open symbols) or presence (closed) of 1mM Cu (NO₃)₂. SEMs from three independent biological replicates tested were smaller than the dimensions of the symbols.

treatment, which was consistent with a role for Mn-SOD (Sod2) in maintaining activity of these enzymes (Irazusta et al., 2006). To determine whether Mn works through Sod2 in conferring Cu resistance, I tested the effect of adding MnCl₂ on Cu sensitivity in the *sod2Δ* mutant background. The *sod2Δ* mutant and its isogenic wild type (BY4741) were cultured in the absence (Fig 5.3 A) or presence of 1mM Cu (NO₃)₂ alone (Fig 5.3 B) or 1mM Cu (NO₃)₂ plus 1mM MnCl₂ (Fig 5.3 C) (2.15.1, chapter 2). Growth results showed some Cu sensitivity of both strains in the presence of copper alone, with the *sod2Δ* mutant being more sensitive than the wild type (Fig 5.3 B) (P=0.002, T=2, DF=68) according to Student's t-test. However, this sensitivity of the mutant was rescued by addition of MnCl₂ (Fig 5.3 C). Because this protective effect against Cu toxicity in *sod2Δ* cells occurred despite the absence of Sod2p, it is inferred that Mn can compensate for SOD2- deficiency independently of its role as a Sod2p co-factor.

5.2.2.3 *RLI1* overexpression enhances Cu-resistance in *Sod2* defective cells

It is thought that superoxide-scavenging by mitochondrial Sod2p protects Fe-S cluster biogenesis and preserves Fe-S protein activities generally (Irazusta et al., 2006). Therefore, I aimed to test whether the Cu-sensitivity of the *sod2Δ* mutant cells could be pinned to (defects in) Rli1p. To look for suppression of Cu-sensitivity, *RLI1* was expressed under *tetO* regulation in the absence of doxycycline, giving >40-fold overexpression of the *RLI1* mRNA (Fig. 3.1 A, chapter 3).

Transformed *sod2Δ* and wild type strains were cultured in the absence and presence of 1.5mM copper nitrate (2.15.1, chapter 2). The copper hypersensitivity of the *sod2Δ* mutant was confirmed (Fig 5.4 B) and there was a statistically significant decrease in growth of *sod2Δ* mutant compared with the wild type strain (P=1.384E-06, T=2, DF=44) according to Student's t-test. However, *RLI1* overexpression fully rescued this sensitivity (Fig 5.4 A, B) where there were no significant differences in growth in the presence of copper of *sod2Δ* cells transformed with *pCM190-tetRLI1* and its control cells (Fig 5.4 B)

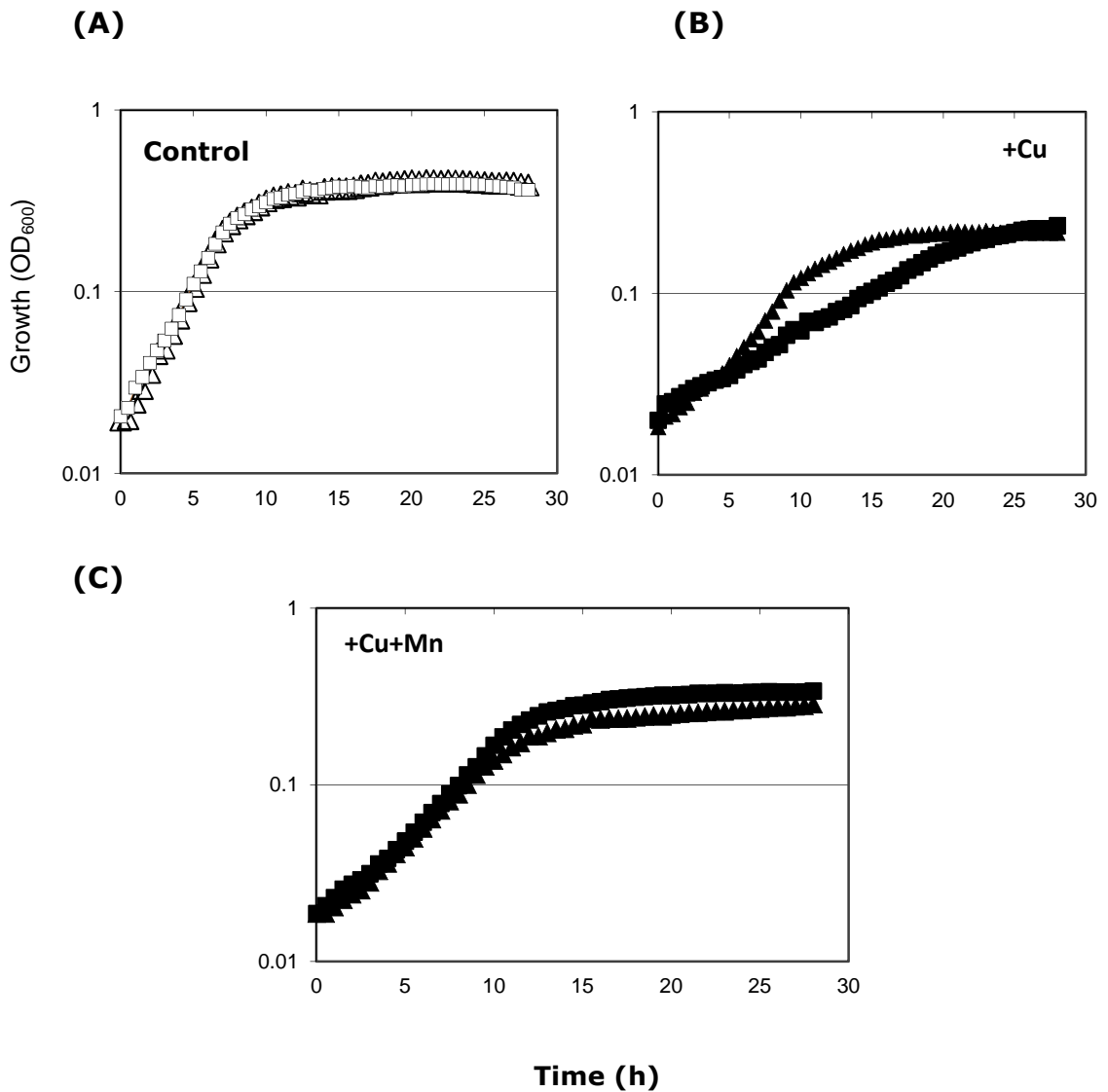


Figure 5.3- Manganese treatment protects against Cu toxicity. *sod2Δ* mutant (\square, \blacksquare) and isogenic wild type BY4741 ($\triangle, \blacktriangle$) cells were cultured in YNB medium in the absence (A) or presence (B) of 1mM $\text{Cu}(\text{NO}_3)_2$ (closed symbols). (C) Cells were incubated with both 1mM $\text{Cu}(\text{NO}_3)_2$ and 1mM MnCl_2 . SEMs from triplicate independent experiments were smaller than the dimensions of the symbols.

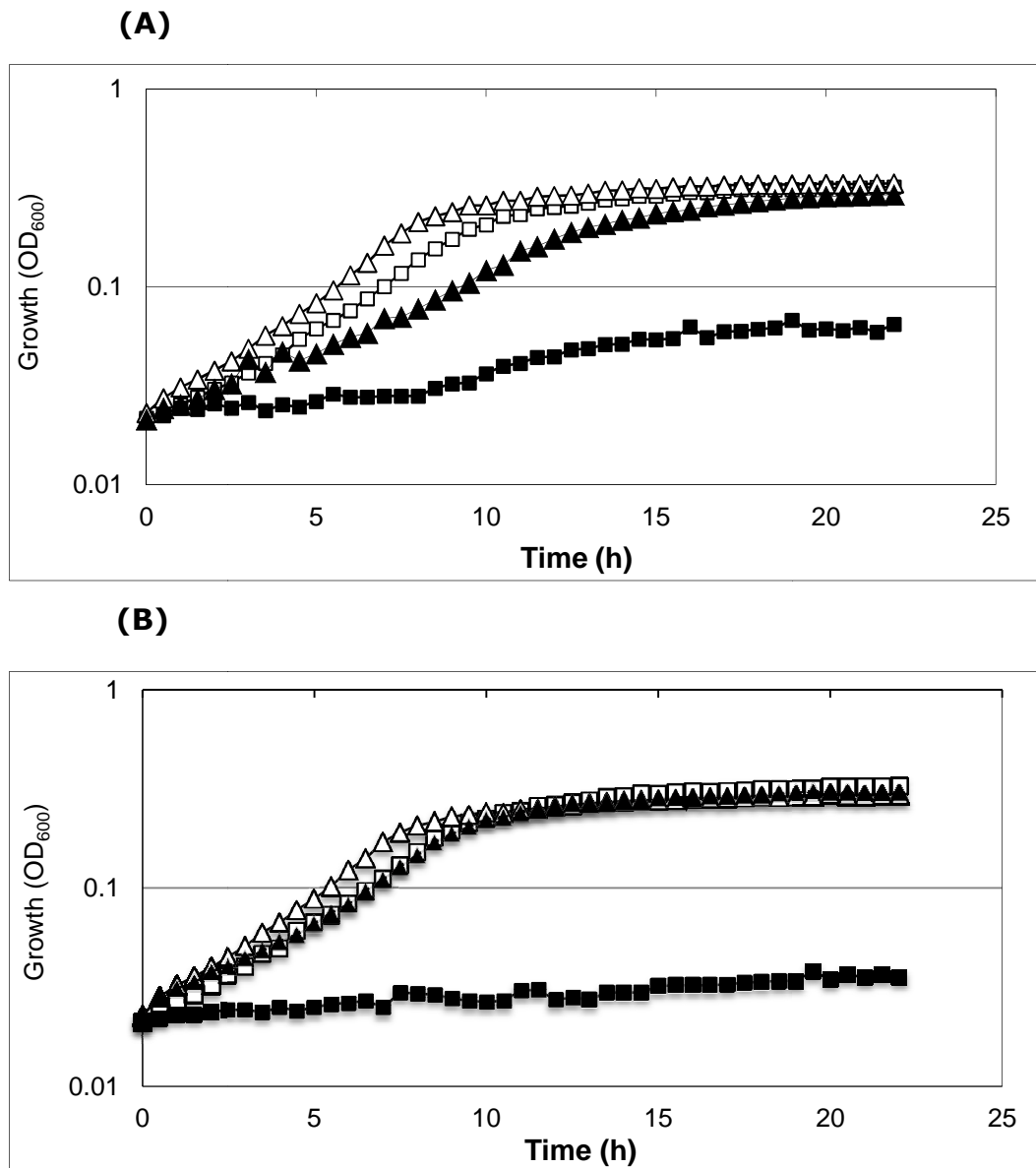


Figure 5.4- *RLI1* overexpression rescues Cu-sensitivity of Sod2p depleted cells. (A) Wild type (BY4741) cells transformed with *pCM190* (\square, \blacksquare) or *pCM190-tetRLI1* ($\triangle, \blacktriangle$) were cultured in the absence (open symbols) or presence (closed) of 1.5mM Cu (NO_3)₂. (B) *sod2Δ* cells transformed with *pCM190* (\square, \blacksquare) or *pCM190-tetRLI1* ($\triangle, \blacktriangle$) were cultured in the absence (open symbols) or presence (closed symbols) of 1.5mM Cu (NO_3)₂. SEMs from triplicate independent growth experiments were smaller than the dimensions of the symbols.

($P=0.3$, $T=2$, $DF=82$) according to Student's t-test. This suggests that the Cu sensitivity of Sod2-deficient cells is mediated through an effect on Rli1p. For example, by defective detoxification of oxygen radicals that target Rli1p. The Cu resistance of *RLI1*-overexpressing *sod2Δ* cells was actually greater than that of overexpressing wild type cells, which could suggest some compensatory gene expression changes in the *sod2Δ* mutant.

5.3 Restoration of Rli1p-dependent stress resistance under conditions that promote Fe-S cluster reconstitution

Oxidative disruption of Fe-S clusters can produce a gain of toxic function effect, since the released Fe (II) may contribute in Fenton reaction and exacerbate oxidative stress (Keyer & Imlay, 1996; Liochev & Fridovich, 1999). This possibility conflicts with what was observed in my previous results (Fig. 3.2-5, chapter 3), as *RLI1* overexpression rescued rather than exacerbated toxicity of pro-oxidants such as $\text{Cu}(\text{NO}_3)_2$, CrO_3 , H_2O_2 and paraquat. As mentioned previously, only a gene that helps to preserve function of the normal toxicity target should normally increase stress resistance when overexpressed (Avery, 2011). Given this evidence that it is loss of essential Rli1p activity which determines stress sensitivity, I sought to substantiate that Fe-S cluster defects cause loss of Rli1p activity during stress. I tested for reversibility of Rli1p inactivation while promoting Fe-S cluster reconstitution (Jang & Imlay, 2007; Varghese et al., 2003; Macomber & Imlay, 2009). Fe-S cluster reconstitution can be stimulated by simple supplementation with ferric chloride as a Fe^{3+} source. This approach was used to restore function *in vivo* of other Fe-S proteins such as aconitase and succinate dehydrogenase in yeast, where prior Fe-S disassembly was the cause of inactivation (Longo et al., 1999; Wallace et al., 2004).

Ferric chloride (FeCl_3) was supplied at a sub-inhibitory concentration (2.15.1, chapter 2). As in previous plots, *RLI1* overexpression did not affect growth in the absence of stressor (Fig 5.5 A), and this was also the case at $700\mu\text{M}$ ferric chloride (Fig 5.5 B). Again, a Cu-sensitivity phenotype of empty vector-transformed cells

was corrected by *RLI1* overexpression (Fig 5.5 C) where there was a statistically significant increase in growth of *RLI1* overexpressing cells ($P=0.004$, $T=2$, $DF=78$) according to Student's t-test. Adding ferric chloride rescued the Cu sensitivity of empty-vector expressing cells, despite the increase pool of labile Fe (Fig 5.5 D).

Similar results were obtained with H_2O_2 stress, where H_2O_2 sensitivity was higher in empty vector-expressing cells compared with *RLI1* overexpressing cells (Fig 5.6 A) ($P=0.04$, $T=2$, $DF=31$) according to Student's t-test. Adding ferric chloride suppressed the H_2O_2 sensitivity of empty vector-expressing cells (Fig 5.6 B).

These data were consistent with the idea that Fe-S cluster defects affect Rli1p activity during stress because toxicity of these pro-oxidants, which can cause decreased ^{55}Fe uptake (Faulkner & Helmann, 2011), was reversed by adding Fe. Nevertheless, further work would be needed to link the Fe-supplementation phenotype specifically to reactivation of Rli1p.

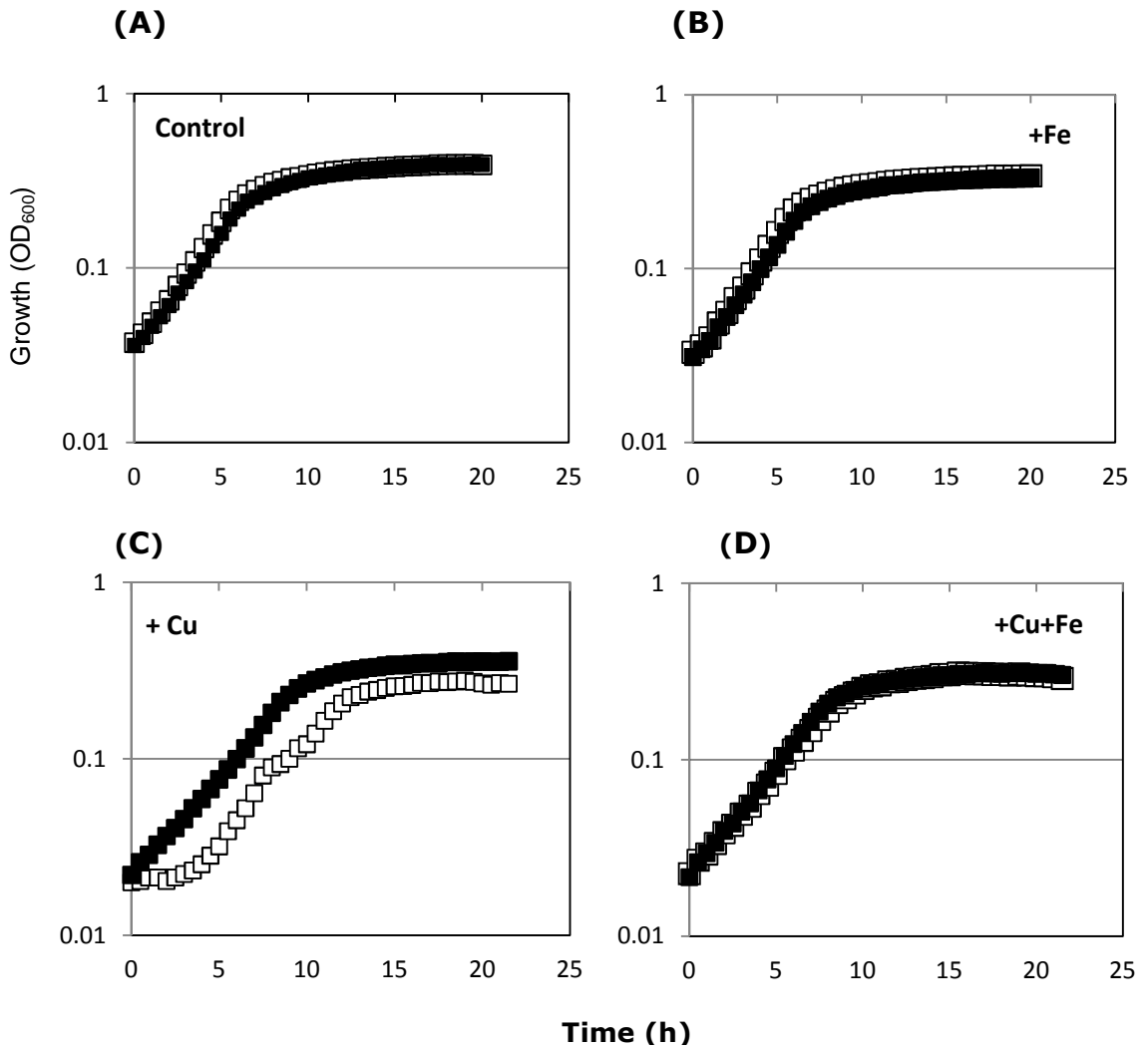
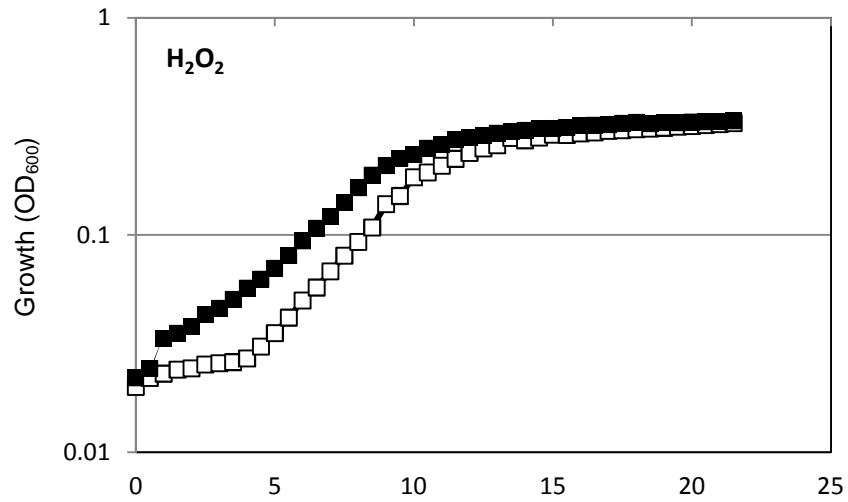


Figure 5.5- Restoration of cellular copper resistance by supplementation with Fe³⁺. BY4741 cells transformed with *pCM190* (□) or *pCM190-tetRLI1* (■) were cultured in YNB medium in the absence of pro-oxidants and ferric chloride (A), in the presence of 700μM FeCl₃ (+Fe) (B), in the presence of 1mM Cu (NO₃)₂ (+Cu) (C), or in the presence of both 700μM FeCl₃ and 1mM Cu (NO₃)₂ (D). SEMs from three independent biological samples were smaller than the dimensions of the symbols.

(A)



(B)

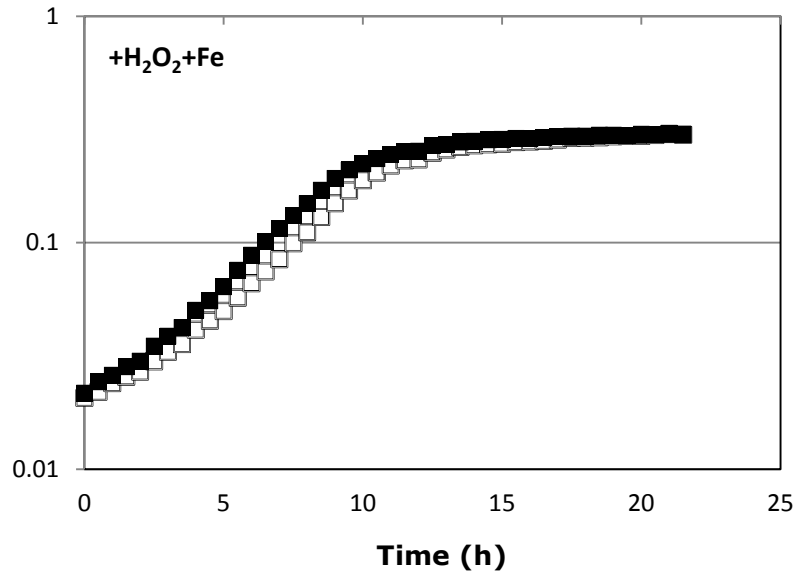


Figure 5.6- Restoration of cellular H₂O₂ resistance by supplementation with Fe³⁺. (A) BY4741 cells transformed with *pCM190* (□) or *pCM190-tetRLI1* (■) were cultured in YNB medium supplemented with 1mM H₂O₂. (B) As in (A) except 700μM FeCl₃ (+Fe) was included. SEMs from three independent biological replicates were smaller than the dimensions of the symbols.

5.4 Discussion

The aim of the studies described in this chapter was to gain evidence showing gene functions and essential metals that could help to preserve Rli1p activity during oxidative stress, considering that Rli1p activity hinges on the integrity of its two [4Fe-4S] clusters.

In *Saccharomyces cerevisiae*, disruption of MSR-encoding genes results in sensitivity to oxidative stress, and leads to defects in Fe-S cluster integrity of Fe-S proteins (Sideri et al., 2009). This could be a consequence of elevated ROS in the absence of MSRs, which would be expected to target FeS-containing proteins (Macomber & Imlay, 2009). A recent study reported degradation of [4Fe-4S] to [2Fe-2S] and creation of cysteine persulfides as cluster ligands during ROS stress in the FNR (Fumarate and Nitrate Reduction) protein of *Thermotoga maritima* (Nicolet et al., 2013). The level of Rli1p is a pivotal determinant of stress resistance in *msrΔ* cells (Sideri, 2007), which is consistent with a role for Fe-S targeting in ROS action on Rli1p. Here, it was demonstrated that MSRs specifically confer protection over the essential function of Rli1p during copper stress. This Rli1p activity in nuclear export of ribosomal subunits is known to depend on integrity of the protein's Fe-S clusters (Kispal et al., 2005).

Experiments performed by Dr. Sara Holland in the Avery laboratory indicated a model in which ROS-targeting of Fe-S clusters prior to their assembly into Rli1p leads to depletion of essential Rli1p function (Alhebshi et al., 2012). To substantiate that the relevant action of ROS is to cause loss of Fe-S function in Rli1p rather than increases in the cellular pool of available Fe, which could provoke further oxidative damage by catalysis of hydroxyl radical production from hydrogen peroxide through the Fenton and Haber-Weiss reactions (Chapter 1, page 16) (Fong et al., 1976; Aisen et al., 2001; Jang & Imlay, 2007; Jian et al., 2011), Fe supplementation was used, as described elsewhere, to promote Fe-S cluster reconstitution (Dutkiewicz et al., 2006; Albrecht et al., 2010). The observed rescue of Cu (NO₃)₂ or H₂O₂ resistance by Fe supplementation, to the level of resistance seen in cells overexpressing *RLI1*, did not support the

possibility that an increased pool of labile Fe was important for Rli1-centred ROS toxicity. Instead, it supported the hypothesis that Fe-S cluster supply to Rli1p is the critical target *in vivo*.

Mn-SOD (Sod2) is involved in superoxide radical detoxification at the mitochondrial location of Fe-S cluster biogenesis (Williams et al., 1998). The study of Imlay (2003) in bacteria indicated that [4Fe-4S] cluster damage in metalloproteins such as the respiratory dehydratase fumarases A and B as well as aconitase B, was caused by superoxide radicals in superoxide dismutase mutants. Furthermore, decreased activities of Fe-S enzymes have been detected in mice lacking Sod2p (Li et al., 1995) and early adult lethality was observed in the absence of Sod2p in *Drosophila* (Kirby et al., 2002; Duttaroy et al., 2003). Cu resistance of wild type cells was raised by supplementation with MnCl₂ or by overexpressing Sod2p (Sideri et al., 2009), agents which promote superoxide scavenging and which are limiting for cellular Fe-S protein activities generally (Irazusta et al., 2006). This supported a role for O₂^{•-} in such Fe-S cluster targeting during Cu stress. In the present study, Rli1p overexpression fully rescued the Cu sensitivity phenotype of the *sod2Δ* mutant and its wild type. This suggested that the Sod2-dependency of Cu resistance could be specific to Rli1p, i.e., caused by depletion of Fe-S supply to active Rli1p following failure of Sod2-mediated detoxification of oxygen radicals at the location of Fe-S cluster biogenesis (Weisiger & Fridovich, 1973). Further previous observations that Mn protects wild type cells against Cu toxicity (Sideri et al., 2009) and that mitochondrial activity (respiration) is sustained in the presence of Mn which maintained both NADH and βNADPH diaphorase oxidative activity, and thereby averted dysfunction of mitochondria (Foglieni et al., 2011) mirrored reports elsewhere of restoration of Fe-S mitochondrial proteins and cytosolic Fe-S enzymes by Mn supplementation (Irazusta et al., 2006). Those results suggested an action of Mn that was mediated through its role as a cofactor for Sod2p. Herein, Mn protected against Cu toxicity in *sod2Δ* mutant cells, indicating that manganese acts independently of Sod2 in protection against Cu toxicity. This is similar to the findings of Tseng et al.

(2001), who demonstrated that Mn accumulation was associated with a protective effect against superoxide stress in *Neisseria gonorrhoeae* which was independent of superoxide dismutase activity and was through quench superoxide anion. Furthermore, addition of Mn to the growth medium protected against oxidative stress in a *sodA* mutant of *Bacillus subtilis* (Inaoka et al., 1999). In addition, there is evidence that complexes of Mn^{2+} with peptides, carbonate, organic acids, and nucleosides able to form catalytic Mn-antioxidants, referring to various metabolic ways to oxidative stress resistance, as well as preserving the activity of repair enzymes in *Lactobacillus plantarum*, which does not have antioxidant enzymes, and in *Deinococcus radiodurans* during its exposure to severe radiation stress, is a crucial role of Mn^{2+} -metabolite defences (Culotta & Daly, 2013). In *sod2Δ* yeast, resistance to oxidative stress was dependent on the presence of Mn ions (Lapinskas et al., 1995). In addition, in both *Lactobacillus plantarum* and *S. cerevisiae*, high levels of intracellular Mn have been shown to substitute functionally for SOD (Archibald & Fridovich, 1981; Chang & Kosman, 1989). The study of Barnese et al. (2008) demonstrated that manganese-phosphate complexes are excellent superoxide dismutase mimics *in vitro*. Furthermore, in *S. cerevisiae*, high Mn levels conferred oxidative stress resistance and suppressed oxidative damage in cells lacking Mn-SOD, indicating that manganese can act independently of Mn-SOD in protection against oxidative damage (Reddi et al., 2009).

To summarise, the main conclusions from this chapter are that (i) Fe-S cluster defects as a result of ROS-mediated targeting are likely to cause Rli1p inactivation, which determines stress sensitivity, (ii) the antioxidant defences against Cu and H_2O_2 represented by MSR enzymes and Sod2p specifically act by preserving (the integrity of Fe-S clusters for) Rli1p function, (iii) manganese can work independently of Sod2 in protection against Cu toxicity.

**Chapter 6- Role of *RLI1* expression level
on translation fidelity during ROS-
induced mRNA mistranslation**

6.1 Introduction

Translation fidelity, which is preserved partly by correct codon-anticodon pairing as well as accurate pairing of each amino acid with its cognate tRNA by the aminoacyl-tRNA synthetase (Ogle & Ramakrishnan, 2005; Ling et al., 2009), is important for the protein synthesis process (Silva et al., 2009) and for accurate protein (hence cell) function (Farabaugh & Bjork, 1999; Ling & Soll, 2010). Mistranslation of mRNA can produce aberrant proteins that misfold or form aggregates (Nystrom, 2005; Drummond & Wilke, 2008). The importance of translation fidelity is highlighted by certain disease states. For instance, misreading of mitochondria-derived mRNA is related to severe myopathies (Ling et al., 2007), dyslipidemia and hypertension (Wilson et al., 2004), while misreading of nucleus-derived mRNA provokes cellular degeneration and apoptosis in mammalian cells (Nangle et al., 2006). Neurodegeneration in a mouse model was due to misfolded proteins arising from errors in protein synthesis (Lee et al., 2006). Misreading of mRNA caused cell cycle defects and loss of viability in *Schizosaccharomyces pombe* (Kimata & Yanagida, 2004).

Mariani et al. (2005) showed that the protein quality control capacity of cells became saturated by large amounts of misfolded proteins during severe oxidative stress, with protein aggregation becoming predominant. In *E. coli*, both *in vitro* and *in vivo*, ROS decreased translation fidelity generally by impairing the editing action of threonyl tRNA synthetase (Ling & Soll, 2010). In that study, H₂O₂ was shown to oxidize cysteine-182 which is important for editing activity, producing Ser-tRNA^{Thr}. The resultant mistranslation impaired growth of *E. coli*. In addition, Holland et al. (2007) showed that pro-oxidants like Cr (VI) lead to accumulation of insoluble and toxic protein aggregates in yeast. Defects in protein synthesis caused by Cr were attributed to mistranslation of mRNA as a novel mode of Cr toxicity in yeast cells. This action was abolished under anaerobic conditions. Among the evidence for Cr action via mistranslation, there was synergistic toxicity between Cr and paromomycin, an aminoglycoside

antibiotic which interferes with normal translation termination (causing readthrough) by binding to a region of the small subunit 16S rRNA decoding A site (Carter et al., 2000; Ogle et al., 2001). This disturbs normal codon-anticodon recognition, affecting translation fidelity. In addition, using 18S ribosomal RNA mutants with differing levels of translation accuracy (Konstantinidis et al., 2006), a yeast strain (L1583) with highly error-prone translation exhibited Cr sensitivity, whereas a strain (L1597) that gives high translational accuracy was Cr resistant (Holland et al., 2007). A further study indicated that depletion of the S-containing amino acids Met and Cys, caused by competition between chromate and sulphate ions for uptake into cells, was the main reason for induction of mRNA mistranslation by Cr (Holland et al., 2010).

Rli1p has a function in translation termination, as discovered through co-immunoprecipitation experiments that showed physical interaction of Rli1p with the translation termination factors eRF1/Sup45 and eRF3/Sup35 in *S. cerevisiae* (Khoshnevis et al., 2010). Furthermore, to test whether decreasing *RLI1* expression level causes defects in stop codon recognition, a dual reporter assay that measures read-through efficiency (Bhattacharya et al., 2000) was used. Such readthrough is seen in cells defective for Sup45, Sup35 or Dbp5, and *RLI1* overexpression suppressed the elevated stop-codon read-through of a *sup45-2* mutant (Khoshnevis et al., 2010). Although the Fe-S clusters of Rli1p are not involved in the protein's interaction with eRF1, which is required for stop codon recognition in *S. cerevisiae* (Khoshnevis et al., 2010; Pisarev et al., 2010), or Hcr1, which is involved in the processing of rRNA and translation initiation via connecting Rli1p to the eIF3 complex (Valasek et al., 2001), the clusters are essential for Rli1p activity in translation termination. Overexpression of an Fe-S cluster mutant of Rli1 did not inhibit the read-through defects of the *sup45-2* mutant (Khoshnevis et al., 2010).

The above insights combined with evidence from my studies to this point suggested a potential involvement of translation fidelity in Rli1p-dependent ROS resistance. My results in Chapter 3 showed that the protein synthesis inhibitor cycloheximide affected viability whereas

RLI1 overexpression protected against this killing effect and increased the protein synthesis rate. This suggested that Rli1p-dependent protein synthesis could be a critical target of ROS. In addition, Rli1p protects against oxygen-dependent Cr toxicity, which is known to involve protein-synthesis defects and mistranslation of mRNA provoked by Cr (Holland et al., 2007). This chapter initiates experiments aiming to test whether translation fidelity could be targeted by pro-oxidants other than chromium and whether such action may be linked to Rli1p dysfunction in protein synthesis. That is, are translation errors produced during pro-oxidant stress an important target accounting for Rli1p-dependent ROS resistance?

Results

6.2 *RLI1* overexpression confers resistance to certain agents that cause mRNA mistranslation

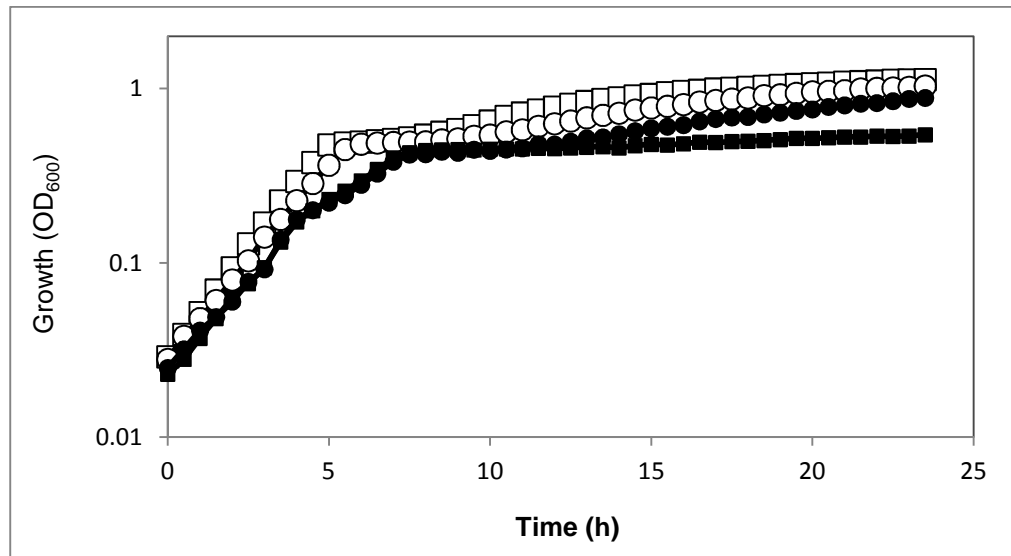
6.2.1 *RLI1* overexpression protects against mistranslation-causing agents

First, different expression levels of *RLI1* were used to indicate whether the action of mistranslation agents in causing loss of translation fidelity could be linked to Rli1p dysfunction. R1158 yeast cells or isogenic *tet-Rli1* cells (expressing a genome integrated *tet-Rli1* construct) were tested for growth in YEPD medium supplemented or not with 6.5 mg ml⁻¹ of the ribosome-targeting drug paromomycin or 0.2mM CrO₃ (2.15.1, chapter 2). Growth analysis showed similar growth of both types of cell when incubated in the absence of paromomycin or CrO₃. In medium supplemented with paromomycin, a paromomycin-sensitivity phenotype was observed in wild type R1158 cells. However, *RLI1* overexpression protected somewhat against this, and according to the last time points (17-23.5h) there was a statistically significant increase in growth of *RLI1* overexpressing cells (P=3E-10, T=2, DF=18) according to Student's t-test (Fig 6.1 A). Similar results were obtained during CrO₃ exposure, consistent with results in Chapter 3 (Fig 3.3 B). A CrO₃-sensitivity phenotype observed in wild type R1158 cells was partly rescued in the *RLI1* overexpressing cells where there was a statistically significant increase in growth of *RLI1* overexpressing cells (P=0.003, T=2, DF=86) according to Student's t-test (Fig 6.1 B). The results were consistent with the growth inhibitory effects of paromomycin and chromium being dependent on Rli1p.

6.2.2 *RLI1* overexpression protects against synergistic toxicity of paromomycin and CrO₃

Paromomycin together with CrO₃ have a strong synergistic toxicity in wild type cells and the additional toxicity due to CrO₃ in this case has been inferred to be due to translation errors (Holland et al., 2007). To test whether *RLI1* overexpression protects against their synergistic toxicity and, it can be inferred, against their effect on translation fidelity, R1158 yeast cells or isogenic *tet-Rli1* cells were tested for growth in YEPD medium supplemented or not with both 1mg

(A)



(B)

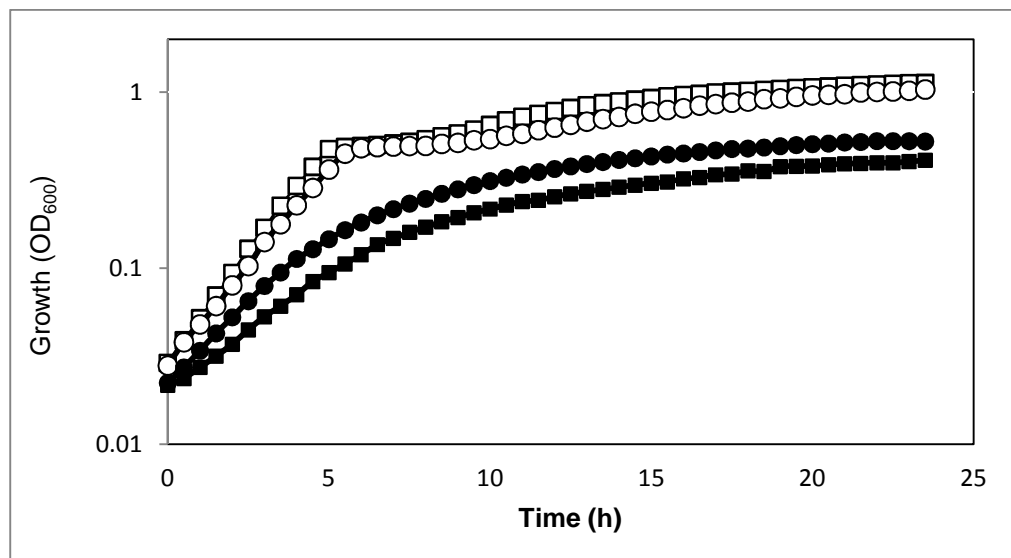


Figure 6.1- *RLI1* overexpression protects against mRNA mistranslation agents. (A) Growth of *S. cerevisiae* R1158 (□,■) and isogenic *tet-RLI1* (○,●) strains in unsupplemented YEPD medium (control; open symbols) or in medium supplemented with 6.5mg ml⁻¹ paromomycin (filled symbols) at 30°C with continuous shaking. (B) As in (A) but where filled symbols refer to medium supplemented with 0.2mM CrO₃. Data presented (A, B) are means of independent triplicate experiments ±SEM.

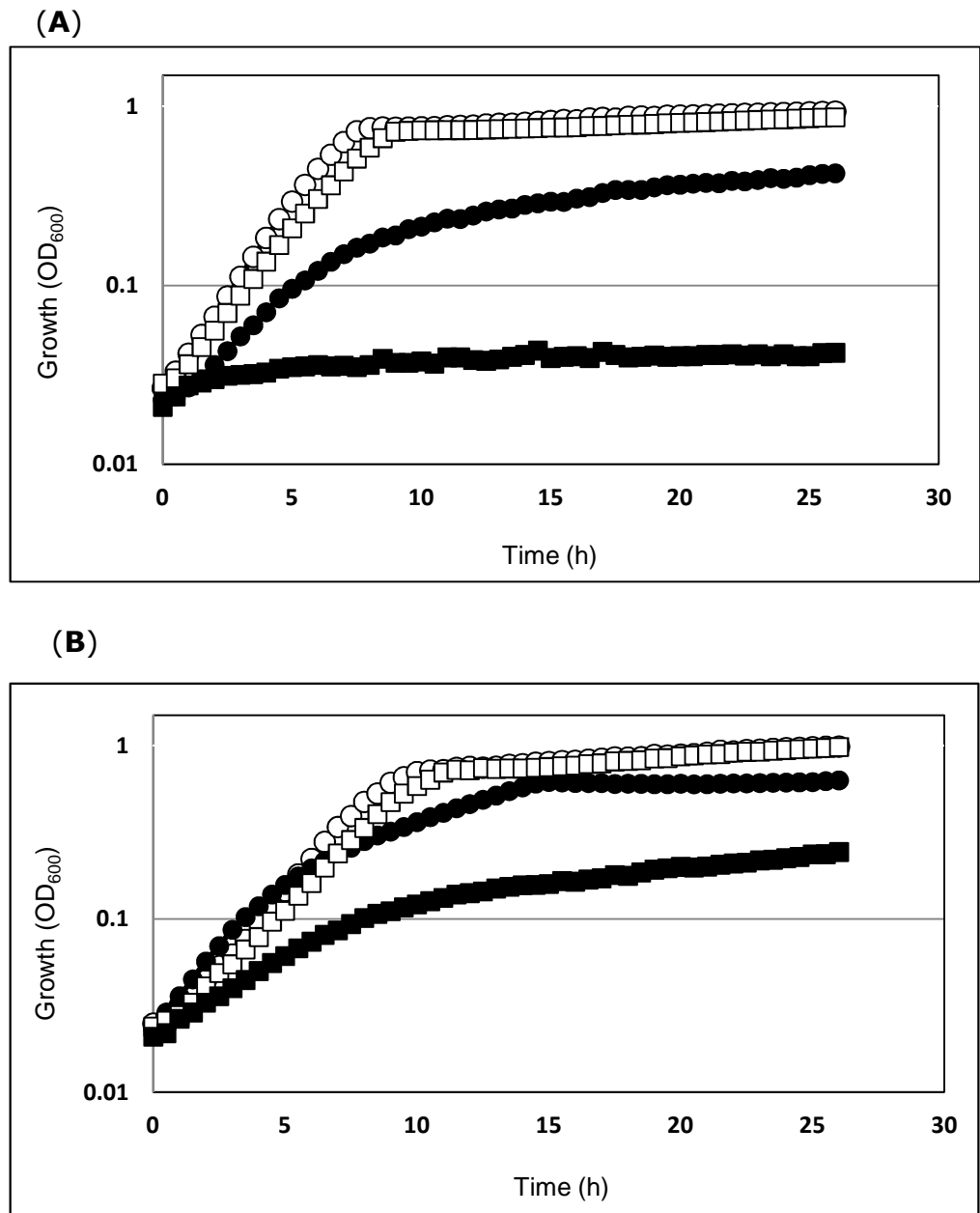


Figure 6.2- *RLI1* overexpression protects against synergistic toxicity of paromomycin and CrO_3 . (A) Growth of wild type *S. cerevisiae* R1158 in unsupplemented YEPD medium (\circ) or in medium supplemented with 0.05mM CrO_3 (\bullet) or 1mg ml^{-1} paromomycin (\square) or both 0.05mM CrO_3 and 1mg ml^{-1} paromomycin (\blacksquare). (B) As in (A) but with the *tet-RLI1* strain (isogenic to R1158). Growth was monitored at 30°C with continuous shaking. Data presented (A, B) are means of three independent biological replicates $\pm\text{SEM}$.

ml⁻¹ paromomycin and 0.05mM CrO₃ (2.15.1, chapter 2). Growth analysis showed similar growth of both types of cells when incubated in the absence of paromomycin and CrO₃. A strong synergistic toxicity of the combination of paromomycin and CrO₃ was observed in wild type cells (Fig 6.2 A) compared with their effect alone where there was a statistically significant decrease in growth with this combination (P=5.2016E-16, T=2, DF=52) according to Student's t-test (Fig 6.2 A). A protective effect of *RLI1* overexpression against this combined toxicity of paromomycin and CrO₃ was observed in yeast cells expressing the *tet-RLI1* construct (Fig 6.2 B) which was clear from a significant increase in growth of *RLI1* overexpressing cells compared with wild type cells in the presence of the combination of paromomycin and CrO₃ (P=5.53816E-15, T=2, DF=53) according to Student's t-test. This was consistent with correction of translation errors being a mechanism by which Rli1p restores growth during stress.

6.3 *RLI1* overexpression corrects mRNA mistranslation

mRNA mistranslation induced by chromium and paromomycin was assayed using a dual-luciferase assay as well as a longer-term qualitative assay (2.17, chapter 2). Both assays are based on (mis)translational read-through of a UAA nonsense (stop) codon (Holland et al., 2007). The aim was to test whether *RLI1* overexpression can protect against misreading of stop codons caused by paromomycin or pro-oxidants.

6.3.1 *RLI1* overexpression protects against paromomycin and CrO₃-induced mRNA mistranslation: qualitative assay

A qualitative assay (2.17, chapter 2) based on red or white colony formation was used to detect mRNA mistranslation during exposure to CrO₃ and paromomycin in wild type (L1494) and *RLI1*-overexpressing cells. This assay is based on read-through of the *ade1-14* UGA premature stop codon, introduced into strain L1494 (2.10.1, chapter 2), and suppression of the red pigmentation associated with this allele to produce white colonies as an indicator of mRNA mistranslation (Liu & Liebman, 1996). L1494 cells transformed with

the empty vector *pCM190* or with *pCM190-tetRLI1* (2.10.1, chapter 2), were pre-grown on selective YNB medium then spotted to YEPD agar supplemented or not with mild doses of 100µg ml⁻¹ paromomycin, or 0.1mM CrO₃, or both together. After 4 days incubation on medium lacking paromomycin or CrO₃, red pigmentation was apparent in both types of cell (Fig 6.3 A), indicative of normal translation termination at the *ade1-14* stop codon. However, the addition of 100µg ml⁻¹ paromomycin led to apparent read through of the stop codon in L1494 cells carrying empty vector, as these produced white colonies (Fig 6.3 B). A protective effect of *RLI1* overexpression was detected against such paromomycin-induced mRNA mistranslation, where red pigmentation was restored in L1494 cells with *pCM190-tetRLI1*, comparable to that observed in the untreated control (Fig 6.3 B). Similar results as above for paromomycin were obtained with 0.1mM CrO₃, which suppressed the red pigmentation associated with *ade1-14* (Fig 6.3 C). This corroborated the result of Holland et al. (2007), where it was shown that mRNA mistranslation is important for chromium toxicity in yeast. Moreover, *RLI1* overexpression restored red pigmentation in Cr-exposed cells (Fig 6.3 C), indicating normal translation termination at high Rli1p levels. In addition, a combination of paromomycin and CrO₃ produced white colonies which were also restored to red pigmentation by *RLI1* overexpression (Fig 6.3 D).

In conclusion, the data supported the hypothesis that chromium toxicity due to mRNA mistranslation could be a result of Cr-targeting of Rli1p function in translation fidelity. Fe-S cluster integrity of Rli1p is essential for its activity in translation termination (Koshnevis et al., 2010).

6.3.2 *RLI1* overexpression protects against ROS-induced mRNA mistranslation: qualitative assay

The preceding results prompted me to find out whether (*RLI1*-suppressible) mRNA mistranslation may be an important cause of other pro-oxidants' toxicities, e.g. Cu (NO₃)₂, H₂O₂ and paraquat. The same *ade1-14* readthrough assay (2.17, chapter 2) as above was used in the first instance. Organisms prepared as described above (6.3.1) were spotted on to YEPD agar supplemented or not with either

0.5mM Cu (NO₃)₂, 1mM paraquat, or 0.5mM H₂O₂; concentrations that were found to be sufficient to give detectable mistranslation without markedly inhibiting growth. As before, media lacking pro-oxidants yielded red colonies in both empty vector- and *pCM190-tetRLI1*-transformed cells (Fig 6.4 A). The addition of 0.5mM Cu (NO₃)₂ appeared to cause mRNA mistranslation in the former case, producing white colonies (Fig 6.4 B). This indication that Cu can cause mRNA mistranslation was reversed by *RLI1* overexpression, which restored red pigmentation (Fig 6.4 B). In the case of paraquat, concentrations of 0.2, 0.3 or 0.4mM did not produce evidence of stop codon readthrough, whereas readthrough (white colonies) was evident at 0.5 or 1mM paraquat (Fig. 6.5). However, *RLI1* overexpression did not seem to protect against such paraquat-induced mRNA mistranslation (Fig 6.5 B). This suggested that the Rli1p-dependence of paraquat resistance, shown earlier in this thesis and also evident from relative colony growth in (Fig. 6.5 B), may be related to a function of Rli1p other than translation fidelity. In addition, to avoid possibility that mRNA mistranslation resulted from random mutation, cells with mRNA mistranslation (white colony) (Fig. 6.5 B) were transferred back to standard YEPD agar, as a result of that, wild type phenotype (red colony) was restored in the absence of stressors, indicating that mRNA mistranslation that was observed is due to target stressor Rli1p specifically, and not as a result of random mutation occurred. Furthermore, mRNA mistranslation could not be detected during the treatment with H₂O₂ in either cell type, despite using different concentrations of H₂O₂ ranging from 0.2-0.7mM, where no obvious change in colony colour compared with untreated control (Fig 6.5 C); higher concentrations such as 0.8 and 1mM were growth inhibitory (not shown). This suggested that Rli1p-dependent H₂O₂ resistance is through a function of Rli1p other than translation fidelity, and that mistranslation may not be so important for H₂O₂ toxicity.

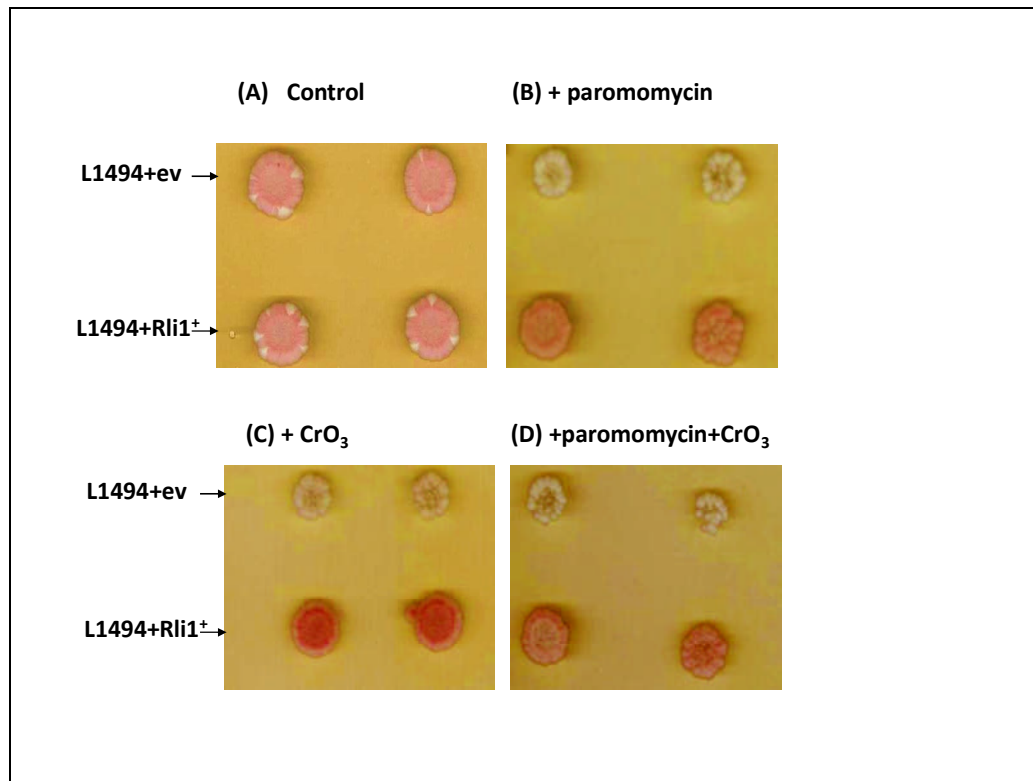


Figure 6.3- *RLI1* overexpression protects against paromomycin and CrO_3 -induced mRNA mistranslation. *S. cerevisiae* L1494 (*ade1-14*) cells transformed with the empty vector (ev) *pCM190* or with *pCM190-tetRLI1* (Rli1^+) were pre-grown to exponential phase in selective YNB medium then spotted to standard YEPD agar (A), or to agar supplemented with $100\mu\text{g ml}^{-1}$ paromomycin (B), or with 0.1mM CrO_3 (C), or both $100\mu\text{g ml}^{-1}$ paromomycin and 0.1mM CrO_3 (D). Plates were incubated aerobically for 4 days at 30°C then images were captured. Typical data from one of three independent experiments are shown.

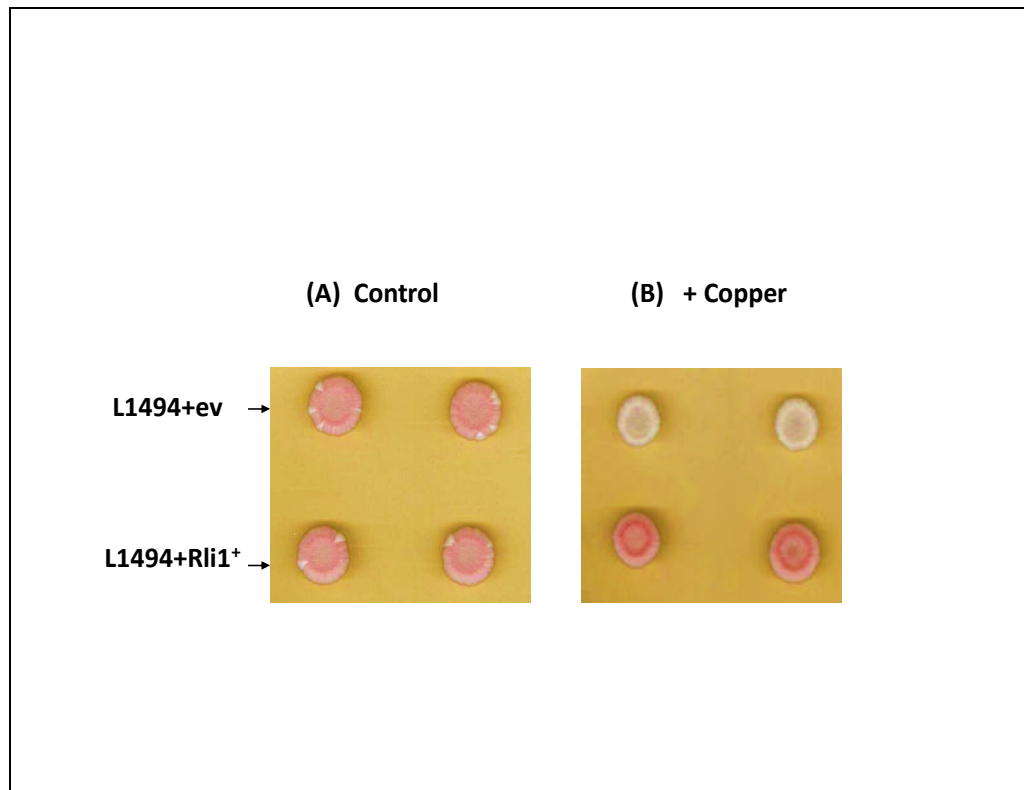


Figure 6.4- *RLI1* overexpression protects against copper-induced mRNA mistranslation. *S. cerevisiae* L1494 (*ade1-14*) cells transformed with the empty vector (ev) *pCM190* or with *pCM190-tetRLI1* (Rli1⁺) were grown to exponential phase in selective YNB medium then spotted to standard YEPD agar (A) or to agar supplemented with 0.5mM Cu (NO₃)₂ (B). Plates were incubated aerobically for 4 days at 30°C then images were captured. Typical data from one of three independent experiments are shown.

6.3.3 *RLI1* overexpression decreased the rate of mRNA mistranslation induced by ROS and paromomycin: quantitative assay

To underline and support the above results, the rate of translational read-through of a TAA nonsense (stop) codon was quantified in a short-term dual-luciferase assay (2.18, chapter 2) at different levels of *RLI1* expression. Here, the ratio of luminescence from firefly versus renilla luciferase indicates the level of translational read-through of the TAA stop codon that separates the two open reading frames (ORFs) of these luciferases within a dual-luciferase plasmid, described in Chapter 2 (Fig 2.1) (Keeling et al., 2004).

Paraquat and H₂O₂ were not included here as *RLI1* overexpression did not protect against paraquat-induced mistranslation of the *ade1-14* stop codon, and stop codon readthrough was not detected with H₂O₂. Wild type (W303) cells or isogenic *tet-RLI1* cells expressing a genome integrated *tet-RLI1* construct (*tet-RLI1*) and transformed with the dual-luciferase plasmid (Keeling et al., 2004), were exposed or not to 80µg ml⁻¹ paromomycin (paro), 0.35mM Cu (NO₃)₂ or 0.05mM CrO₃ in selective YNB medium for 2 and 4h; these concentrations over these time periods were used as they produced comparable degrees of mild inhibition of cell growth (Fig 6.6), as well as mild effects on Rli1p function in nuclear export of ribosomal subunits (Chapter 4, Figs 4.3 B, 4.3 C, 4.4).

The activities of the firefly and renilla luciferases in derived protein extracts were determined in both types of cells luminometrically (2.18, chapter 2). The derived ratio of luminescence attributable to the firefly versus renilla luciferases refers to the level of TAA mistranslation. The results indicated marked increases in the rate of TAA read-through (mistranslation) in cells expressing wild type levels of Rli1 after 2h of exposure to CrO₃ (P=0.002, T=2, DF=8) or paromomycin (paro) (P=4.1E-08, T=2, DF=8) compared with untreated controls, as well as after 4h of CrO₃ exposure (P=1.59E-07, T=2, DF=8) or paromomycin (paro) (P=9.03E-07, T=2, DF=8) according to Student's t-test (Fig 6.7). In the case of Cu (NO₃)₂, mistranslation became evident after 4h incubation where a significant

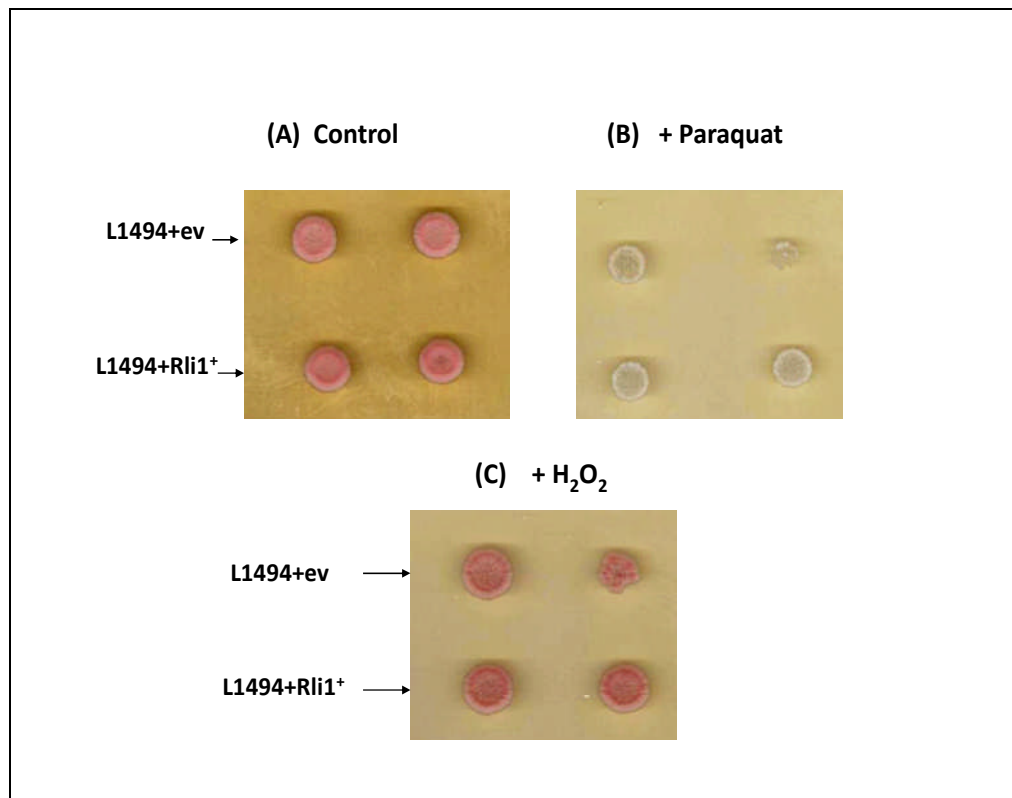


Figure 6.5- *RLI1* overexpression does not appear to protect against paraquat-induced mRNA mistranslation, and H₂O₂ does not cause UGA codon readthrough. *S. cerevisiae* L1494 (*ade1-14*) cells transformed with the empty vector (ev) *pCM190* or with *pCM190-tetRLI1* (*Rli1*⁺) were grown to exponential phase in selective YNB medium then spotted to standard YEPD agar (A), or to agar supplemented with 1mM paraquat (B) or with 0.5mM H₂O₂ (C). Plates were incubated aerobically for 4 days at 30°C then images were captured. Typical data from one of three independent experiments are shown.

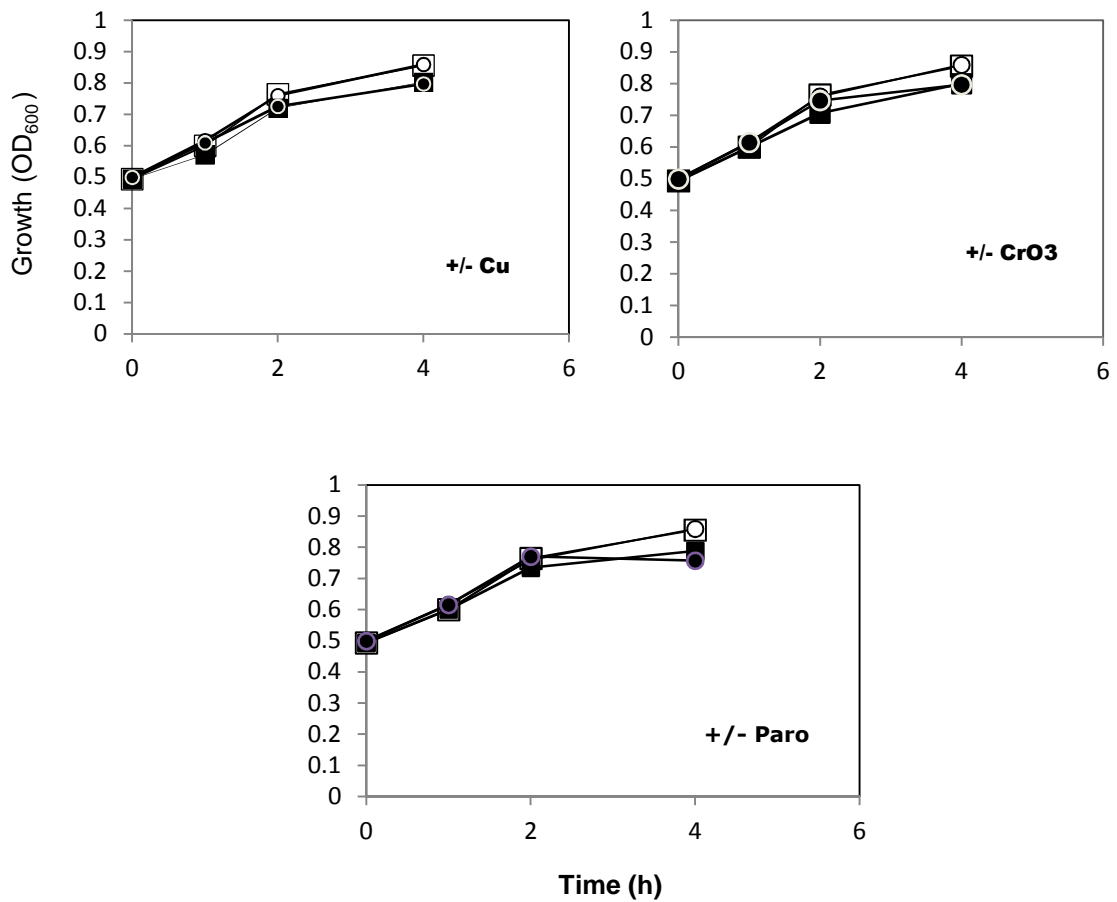


Figure 6.6- Mild effect on yeast growth at concentrations of agents used in short-term dual-luciferase assays. Wild type (W303) cells (□, ■) or isogenic *tet-RLI1* (○, ●) transformed with the dual-luciferase plasmid were cultured in the absence (open symbols) or presence (closed) of 0.35mM Cu (NO₃)₂, 0.05mM CrO₃ or 80μg ml⁻¹ paromomycin (paro) in selective YNB medium and incubated for 4h at 30°C with shaking. Data presented are means of three independent biological replicates ±SEM.

increases in the rate of TAA read-through (mistranslation) in cells expressing wild type levels of Rli1 was observed compared with untreated controls ($P=0.004$, $T=2$, $DF=8$) according to Student's t-test (Fig 6.7), suggesting that copper requires additional time to exert an effect on translation fidelity. *RLI1* overexpression was very effective in protecting against paromomycin-, CrO_3 - and $Cu(NO_3)_2$ -induced mRNA mistranslation, as evident from the ≥ 500 -fold decreased rate of TAA read-through in cells expressing the *tet-RLI1* construct compared with cells expressing wild type levels of Rli1p, such observed decrease was statistically significant with paromomycin ($P=9.03E-07$, $T=2$, $DF=8$), CrO_3 ($P=1.6E-07$, $T=2$, $DF=8$) and $Cu(NO_3)_2$ ($P=0.008$, $T=2$, $DF=8$) according to Student's t-test (Fig 6.7). In the absence of stressor *RLI1* overexpression caused an increase in the readthrough rate, albeit relatively small, consistent with previous findings (Khoshnevis et al., 2010).

In conclusion, results from two independent assays of stop-codon readthrough indicated that such mistranslation, a primary mechanism of Cr toxicity (Holland et al., 2007), may explain the Rli1p-dependency of Cr resistance. In addition, mRNA mistranslation may be among the toxic effects of copper on yeast cells, against which Rli1p protects.

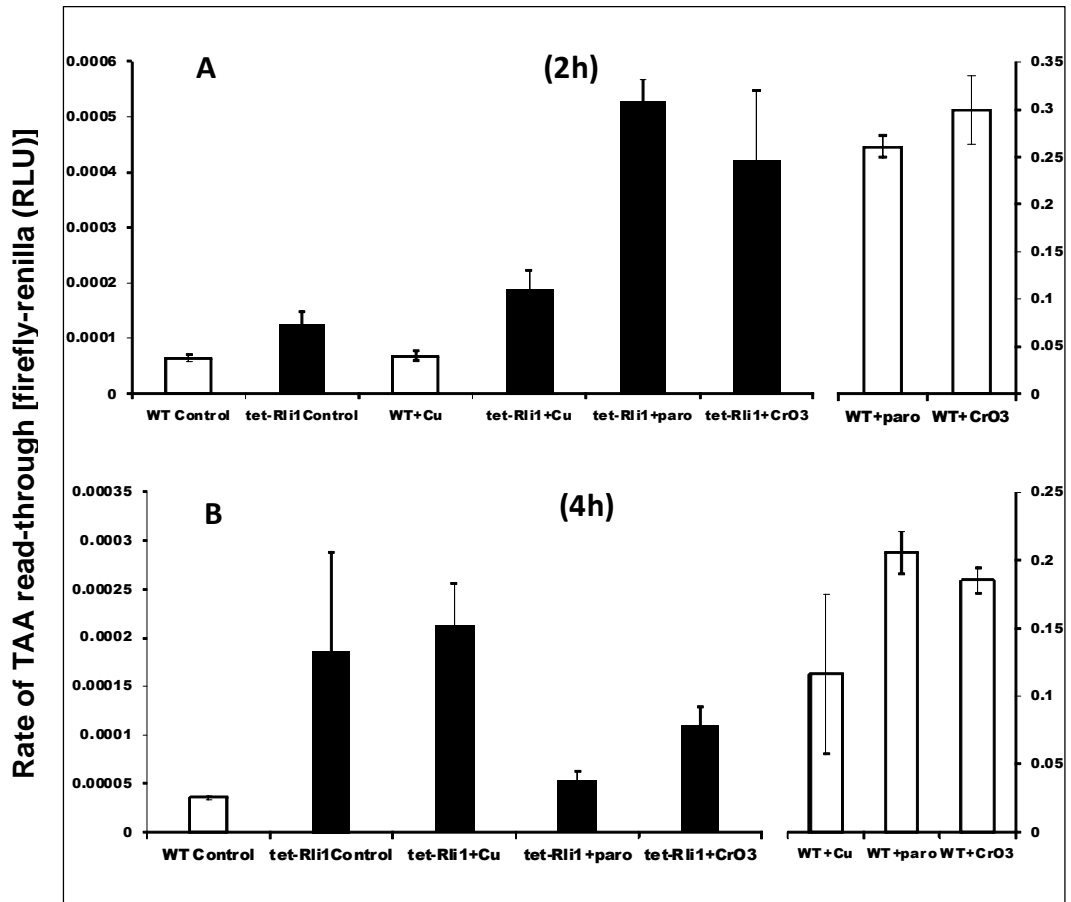


Figure 6.7- *RLI1* overexpression suppresses mRNA mistranslation caused by various stressors. Wild type (WT) cells (□) and isogenic *tet-RLI1* (*tet-Rli1*) (■) transformed with the dual-luciferase plasmid were cultured in the absence (control) or presence of $80\mu\text{g ml}^{-1}$ paromomycin (paro), $0.35\text{mM Cu (NO}_3)_2$ or 0.05mM CrO_3 in selective YNB medium for 2h (A) and 4h (B), as indicated. The activities of the firefly versus renilla luciferase in derived protein extracts were determined in both types of cells luminometrically. The ratio of luminescence from the firefly versus renilla luciferase indicates the short-term level of translational read-through of the *TAA* stop codon that separates the two open reading frames. All values are means \pm standard error of the mean from at least three independent determinations. RLU represents relative light units.

6.4 Discussion

One aim of the studies described in this chapter was to test for induction by pro-oxidants of mistranslation, so potentially indicating a mode of toxic ROS action in yeast. In addition, a key aim was to test whether pro-oxidant action in mRNA mistranslation may be linked to Rli1p dysfunction, thereby indicating a mechanism of Rli1p in protecting against ROS toxicity.

When cells are exposed to oxidative stress some cell constituents are oxidized, which can perturb function of several physiological processes including mRNA translation (Grant, 2011; Shenton et al., 2006). Therefore, as discussed above, this was a motivation to examine a role for translation fidelity in the protective action of Rli1p against pro-oxidants, particularly as my results had shown a further protective role for Rli1p against cycloheximide toxicity which was correlated with increased protein synthesis. The prior evidence suggested that Rli1p-dependent protein synthesis could be a critical target of ROS, and this included the facts that a key protein-synthesis defect provoked by the pro-oxidant Cr is known to be mRNA mistranslation (Holland et al., 2007) and maintenance of translation fidelity is among the known functions of Rli1p in protein synthesis (Khoshnevis et al., 2010). The protein's Fe-S clusters are required for the function of Rli1p in termination of translation: an Fe-S cluster mutant of Rli1p does not suppress the read-through defects of a *sup45-2* mutant whereas wild type Rli1p does (Khoshnevis et al., 2010). Considering also the ROS-sensitivity of Fe-S clusters (Imlay, 2006), the previous evidence collectively suggested a link between the dependency of ROS resistance on Rli1p function and mRNA mistranslation.

The protective effect shown here for Rli1p against chromium toxicity, with a mode of action shown previously to involve mRNA mistranslation (Holland et al., 2007), was linked to mRNA mistranslation. Elevated *RLI1* expression in cells expressing a plasmid borne *tet-RLI1* construct suppressed translation errors during exposure to paromomycin or chromium. Therefore, suppression of

translation errors appears to be a mechanism by which Rli1p function is critical for precluding CrO₃-toxicity, as yeast cell growth can be impaired as a result of mistranslation (Kimata & Yanagida, 2004; Ling & Soll 2010). In contrast to CrO₃, the data showed that mRNA mistranslation was induced by paraquat but *RLI1* overexpression did not seem to protect against this. This suggests that a loss of translation fidelity caused by paraquat is not related to Rli1p. Previously it was shown that oxidized luciferase mRNA was produced in both rabbit reticulocyte lysate and human cells as a result of paraquat exposure, detected by formation of short luciferase polypeptides associated with increased 8-oxoguanosine and resultant translation errors (Tanaka et al., 2006). Formation of 8-oxoguanosine is a mechanism of oxidative mistranslation distinct from others reported in the literature, such as direct oxidation of tRNA synthetases (Ling & Soll, 2010), and such differences could be the basis for some specificity in Rli1p-dependent protection against oxidative mistranslation. Thus, 8-oxoguanosine formation or reading may not be affected by Rli1p function. This lack of effect on paraquat-induced mistranslation may explain why the protective effect of Rli1p against paraquat was slight compared to other stressors (Chapter 3: Fig 3.5 B). It is also consistent with my earlier interpretation that Fe-S cluster targeting by O₂^{•-}, generated by paraquat, is not the principal basis of the Rli1p-dependent phenotypes described here.

In contrast to the other agents tested, treatment with H₂O₂ did not cause mRNA mistranslation according to the qualitative assay used here. This suggests that the toxic effect of H₂O₂ on yeast growth is not related to mistranslation, or stop codon read through, and that a function of Rli1p other than its role in translation fidelity may be important for protection against H₂O₂ toxicity. It was reported that H₂O₂ directly inhibited proteasome activity in human fibroblasts (Reinheckel et al., 1998) which was related to pre-rRNA processing factors that participated in ribosome biogenesis with H₂O₂ slowing the release of mature rRNA from the nucleolus as well as causing depletion of 18S rRNA (Stavreva et al., 2006). It is possible that the protective role of Rli1p against H₂O₂ toxicity could be through its

function in pre-rRNA maturation in the pathway of 18S rRNA synthesis and nuclear export of the small and large ribosomal subunits to the cytosol (Yarunin et al., 2005). On the other hand, copper did provoke mRNA mistranslation, in a manner suppressible by *RLI1* overexpression. As for Cr, these results suggested that Cu-induced mRNA mistranslation may be linked to Cu-dependent loss of Rli1p function. In the quantitative dual-luciferase mistranslation assay, results showed very marked increases in the rate of mRNA mistranslation as a result of copper treatment, while *RLI1* overexpression decreased this by more than 500-fold. Similar results were obtained for CrO₃ and paromomycin. All these results were consistent with the longer-term qualitative assay results. As I mentioned previously, paraquat and H₂O₂ were not included in the quantitative assay.

To summarise, the main conclusions from this chapter are that: (i) translation fidelity, maintenance of which is among the functions of Rli1p in protein synthesis, is sensitive to pro-oxidants, (ii) mRNA mistranslation could have a role in toxic effect of Cu (NO₃)₂ on yeast cells, (iii) translation errors resulting from CrO₃ and Cu (NO₃)₂ exposure are linked to Rli1p, because *RLI1* overexpression helps to protect against these, (iv) mRNA mistranslation that was produced by paraquat does not appear to be related to Rli1p activity because *RLI1* overexpression did not correct it, (v) correcting translation errors could be a key function of Rli1p in protecting against toxicity of certain pro-oxidants.

Chapter 7- Concluding Remarks

7.1 Concluding Remarks

Oxidative stress arises when the generation of ROS such as superoxide radicals, H_2O_2 or hydroxyl radicals (Finkel & Holbrook, 2000; Winter et al., 2008; Jomova & Valko, 2011) exceeds the capability of a biological system to scavenge and inactivate them (Djordjevic, 2004; Trachootham et al., 2008). This thesis refers to the highly evolutionarily-conserved Fe-S protein Rli1 as a novel and essential cellular target of toxicity of various pro-oxidants. This included pro-oxidants with distinct activities, including paraquat and Cr (VI) which act as superoxide-generating agents (Carr et al., 1986; Sumner et al., 2005; Kubrak et al., 2010). Superoxide radicals have been described as principal antagonists to Fe-S cluster integrity in proteins (Irazusta et al., 2006; Gardner & Fridovich, 1991; Calderon et al., 2009), as evident from inactivation by $\text{O}_2^{\cdot-}$ of Fe-S containing dehydratases and aconitase (Winterbourn, 2008). The present results also refer to H_2O_2 and the redox-active metal copper (Pinto et al., 2003; Khan & Panda, 2002; Mohora et al., 2007) which additionally are reported to damage Fe-S proteins (Macomber & Imlay, 2009; Jang & Imlay, 2007; Varghese et al., 2003). H_2O_2 reactivity with proteins is typically with those holding transition metals, such as Fe (D'Autreaux & Toledano, 2007). There are several factors which could explain why Rli1p has not been discovered previously as a potential ROS target and its role in ROS resistance has not been reported earlier. These factors include that its function in protein synthesis has emerged only recently (Kispal et al., 2005; Khoshnevis et al., 2010; Shoemaker & Green, 2011). In addition, because the protein is essential for cell viability under aerobic conditions (Zhai et al., 2013), it is excluded from standard homozygous deletion-mutant screens. Furthermore, Rli1p activities are not readily assayable, particularly *in vivo*. Finally, related work in the Avery laboratory by Dr. Sara Holland indicated that the Fe-S clusters of Rli1p are relatively stable *in vivo* (Alhebshi et al., 2012). This undermined what may have conventionally been considered to be the most likely mechanism of Rli1p inactivation by ROS, i.e. direct attack on the protein's Fe-S clusters by ROS. In fact,

in contrast to ROS-sensitive Fe-S proteins characterised in other studies, the clusters in Rli1p (ABCE1) are not solvent exposed (Karcher et al., 2008).

Rli1 is the only essential cytosolic Fe-S protein under aerobic growth (Kispal et al., 2005; Zhai et al., 2013) reported to date and the essential role of Rli1p in protein synthesis is not conditional (e.g. on the composition of growth medium), making Rli1p unique among the Fe-S proteins that been reported to have ROS-sensitive function. The bacterial dehydratases can be dispensed with, like isopropylmalate isomerase which is strongly sensitive to H₂O₂ but is necessary for growth only in the absence of leucine (Jang & Imlay, 2010). Moreover, earlier studies of Fe-S protein inactivation *in vivo* have predominantly been in cells that are predisposed to Fe-S cluster dysfunction (e.g. mutant strains). In contrast, during this work Rli1p function has been identified as a pro-oxidant target in wild type cells not predisposed to ROS action.

In addition to loss of protein function, disruption of Fe-S clusters by oxidation is known potentially to lead to a gain of toxic function effect, since the released Fe (II) may contribute to Fenton catalysis and aggravate oxidative stress (Keyer & Imlay, 1996; Liochev & Fridovich, 1999). However, my data do not support this latter model for Rli1p, as *RLI1* overexpression rescued rather than exacerbated ROS toxicity. In addition, adding ferric chloride produced stress-resistance despite the increased pool of labile Fe, giving similar protection as *RLI1* overexpression. Furthermore, a similar argument counteracts a previous suggestion that the Fe-S cluster domain of Rli1p could perform a ROS sensing function, as part of the decreased protein synthesis response to oxidative stress (Yarunin et al., 2005; Barthelme et al., 2011). That response is thought to improve ROS resistance, but down regulated *RLI1* expression during this study showed the opposite effect, giving a ROS-sensitivity phenotype. Therefore, it is likely that any decrease in protein synthesis which is due to Rli1p dysfunction does not represent an adaptive-type response, but may be a deleterious result of ROS targeting and

thereby Rli1p dysfunction. Earlier studies did not detect a role for Rli1p in the protein synthesis response (Shenton et al., 2006).

The Fe-S domain of Rli1p seems to have a structural function (Becker et al., 2012) and is not essential for Rli1p binding with the eIF3 component Hcr1p (Kispal et al., 2005; Khoshnevis et al., 2010), or for Rli1-mediated ATP turnover (Barthelme et al., 2011). However, the Fe-S domain of Rli1p is required for nuclear export of ribosomal subunits, translation termination and ribosome splitting (Kispal et al., 2005; Khoshnevis et al., 2010; Shoemaker & Green, 2011; Becker et al., 2012). These Fe-S cluster domains of Rli1p in addition to an ATP-dependent conformational switch of Rli1p are also required for Rli1p activity in ATP hydrolysis and thereby for both ribosome binding and recycling (Barthelme et al., 2011). This need of the Fe-S domain for nuclear export of ribosomal subunits is consistent with the observed sensitivity of this process to oxidative stress and its rescue by elevated *RLI1* expression seen in the present study. The hypothesis that it is the Fe-S clusters of Rli1p that are (indirectly) affected by ROS was further supported by the fact that the proportion of cells exhibiting defective Rli1p function during stress was increased by replacement of wild type Rli1 with *rli1*^{C58A} or in the MSR-deficient *mxrΔ* background. The pro-oxidant sensitivity of the *rli1*^{C58A}-expressing cells was also suppressed during anaerobicity. There are redox roles for the [4Fe-4S] clusters of Rli1p after binding to other components of Rli1 complex (Rli1/Lto1/Yae1), which responds to oxidative damage of the 60S ribosomal subunit, therefore, The [4Fe-4S] clusters of Rli1p and LTO1 itself are required for maintenance of cells growth in the aerobic not anaerobic conditions (Zhai et al., 2013). In addition, the rescue by *RLI1* overexpression of *sod2Δ*-mutant sensitivity to oxidative stress supported the critical nature of Fe-S cluster integrity for Rli1p activity during such stress, as Fe-S clusters are known to be targeted more readily in *sod2Δ* cells (Longo et al., 1999). Thus, Fe-S cluster defects are likely to cause Rli1p dysfunction, which determines stress sensitivity. MSR enzymes and Sod2p are two functions that have some specific roles in preserving the integrity of Fe-S clusters and thereby Rli1p activity during oxidative stress. The apparent Fe-S requirement

for Rli1p function in terminating translation correctly is a further function of this protein that is susceptible to ROS action.

Fe-S cluster turnover mediated by ROS has been described as the mechanism of protein inactivation during previous studies on proteins with solvent exposed Fe-S clusters (Flint et al., 1993; Macomber & Imlay, 2009). The study of Karcher et al. (2008) showed that the two [4Fe-4S] clusters of Rli1p (ABCE1) are predicted to be well shielded from solvent. Thus, despite only one or two reports of successful purification of active Rli1p (Shoemaker & Green, 2011), the protein's Fe-S clusters are remarkably stable in Rli1-HA immunoprecipitations (Kispal et al., 2005). My data showed restoration of nuclear Rps2-GFP export by *ATM1* overexpression during mild oxidative stress. As Atm1 functions in FeS delivery to cytosolic proteins upstream of Rli1, this result was consistent with experiments conducted by Dr. Sara Holland in the Avery laboratory and described in Alhebshi et al. (2012). These suggested that oxidative targeting of Fe-S clusters destined for incorporation into Rli1p is the main, albeit indirect, mechanism of ROS action on Rli1p. The Fe-S clusters already inserted in Rli1p are not the key targets *in vivo*. *In vitro*, using purified Rli1-HA, some ⁵⁵Fe-S turnover was observed. However, that effect was not reproduced *in vivo* at pro-oxidant doses that were just sub-inhibitory, whereas 50-80% inhibition of ⁵⁵Fe incorporation to Rli1p was observed in the same conditions. The indication that ⁵⁵Fe incorporation to Rli1p is the primary ROS-sensitive target *in vivo* mirrors work in bacteria, where cluster assembly on or transfer from scaffold proteins was proposed to support oxidant disruption of the ISC system (Jang & Imlay, 2010), as Fe-S clusters are expected to be solvent exposed and thereby ROS-susceptible during transfer. This affected Fe-S cluster incorporation to proteins similar to Rli1p, such as NADH dehydrogenase I, in which Fe-S clusters are well shielded (Jang & Imlay, 2010). Because Fe-S cluster assembly inside mitochondria is partly shielded from external stress, targeting of Fe-S cluster assembly or transfer upstream of Rli1p would seem most likely to occur in the cytosol; for instance, at scaffold or transfer proteins such as Cfd1, Nbp35, Nar1 and Cia1.

The possibility of Fe-S cluster turnover in Rli1p *in vivo* may be more important for ROS toxicity in cells expressing *rli1*^{C58A} as their sole Rli1p. Pro-oxidant sensitivity that was observed in these cells was in keeping with the predicted lability of *rli1*^{C58A} (Barthelme et al., 2007). *rli1*^{C58A} lacks a [4Fe-4S]-coordinating cysteine, yielding a [3Fe-4S]⁺ cluster which, despite that, sustains Rli1p function for cell viability. The other coordinating cysteines are predominantly essential (Kispal et al., 2005; Barthelme et al., 2007). The observed strong Cu- and H₂O₂-sensitivity phenotype of *rli1*^{C58A}-expressing cells in this study was in keeping with the fact that Cu [via Fe displacement (Macomber & Imlay, 2009)] and H₂O₂ (Jang & Imlay, 2010, Djaman et al., 2004) can decompose Fe-S clusters beyond the [3Fe-4S]⁺ state that is thought to exist in the C58A cluster (Barthelme et al., 2007). In contrast, there is not thought to be degradation of Fe-S clusters beyond [3Fe-4S]⁺ *in vivo* by superoxide-generating agents such as paraquat and Cr (Varghese et al., 2003; Jervis et al., 2009; Macomber & Imlay, 2009), which could explain the lower relative paraquat-and Cr-sensitivity of *rli1*^{C58A}-expressing cells. Here, only one of the two clusters of the protein may remain partly oxidizable by these agents.

Rli1p is an essential Fe-S protein in yeast and its orthologues are present in all characterised archaea and eukaryotes. Its function is highly conserved through evolution and essential in all organisms tested (Winzeler et al., 1999; Coelho et al., 2005; Estevez et al., 2004; Schuller et al., 2003; Barthelme et al., 2007; Becker et al., 2012). Fe-S clusters of Rli1p are crucial for its activity and hence for cell viability under aerobic conditions, whereas are not necessary in the absence of oxygen, as the Rli1^{C255} polypeptide, which is free of [4Fe-4S] clusters, can support cells growth in the anaerobic condition, whereas it caused growth inhibition in the aerobic conditions (Zhai et al., 2013). This study of Zhai et al. (2013) suggested a redox active role for the [4Fe-4S] clusters of Rli1p. This makes Rli1 the only known essential cytoplasmic protein under aerobic growth that depends on Fe-S cluster biosynthesis in the mitochondria (Kispal et al., 2005; Lill, 2009; Karcher et al., 2008). Therefore, maintenance of Rli1p activity in cells may be a key determinant of ROS resistance in diverse

organisms. This comprises chronic and acute oxidative stress, because mild effects on growth and severe short-term effects on viability were rescued by *RLI1* overexpression in this project. Furthermore, effects of pro-oxidants on translation fidelity were corrected by *RLI1* overexpression, which could reflect a key mechanism for Rli1p in conferring oxidative stress resistance.

Ultimately, further research on the mechanism of Rli1p in protecting against oxidative stress is required. For example, further investigation at the molecular level is required to delineate the mechanism of Rli1p-suppressible copper action in inducing mRNA mistranslation. As I mentioned previously, the study of Ling & Soll, (2010) showed that oxidation of the Cys¹⁸² editing site of threonyl-tRNA synthetase by H₂O₂ caused mRNA mistranslation, resulting in protein misfolding and growth defects in *E. coli*. Furthermore, the eukaryotic translation initiation factor eIF4e was detected as a target for cadmium toxicity in human cell lines, and the mechanism was proposed to be ROS-mediated (Othumpangat et al., 2005). In contrast, at the present time, there is no report of a component of the translation machinery targeted by Cr or Cu. Loss of Rli1p function provides a novel plausible target accounting for mRNA mistranslation during stress by these agents.

References

- Abbott, D. A., Suir, E., Duong, G. H., Hulster, E. D., Pronk, J. T., Maris, A. J. A. V. (2009). Catalase overexpression reduces lactic acid-induced oxidative stress in *Saccharomyces cerevisiae*. *Appl. Environ. Microbiol.* 75: 2320-2325.
- Adam, A. C., Bornhovd, C., Prokisch, H., Neupert, W., Hell, K. (2006). The Nfs1 interacting protein Isd11 has an essential role in Fe/S cluster biogenesis in mitochondria. *Embo. J.* 25: 174–183.
- Adamo, G. M., Brocca, S., Passolunghi, S., Salvato, B., Lotti, M. (2012). Laboratory evolution of copper tolerant yeast strains. *Microbial. Cell. Factories.* 11: 1.
- Ahn, J., Nowell, S., Mccann, S. E., Yu, J., Carter, L., Lang, N. P., Kadlubar, F. F., Ratnasinhe, L. D., Ambrosone, C. B. (2006). Associations between catalase phenotype and genotype: modification by epidemiologic factors. *Cancer. Epidemiol. Prev.* 15: 1217-1222.
- Ahn, D. U., Wolfe, F. H., Sim, J.S. (1993). The effect of metal chelators, hydroxyl radical scavengers, and enzyme systems on the lipid peroxidation of raw turkey meat. *Poultry. Sci.* 72: 1972-1980.
- Albrecht, A. G., Netz, D. J. A., Miethke, M., Pierik, A. J., Burghaus, O., Peuckert, F., Lill, R., Marahiel, M. A. (2010). SufU is an essential iron-sulfur cluster scaffold protein in *Bacillus subtilis*. *J. Bacteriol.* 192: 1643-1651.
- Alhebshi, A., Sideri, T. C., Holland, S. L., Avery, S. V. (2012). The essential iron-sulfur protein Rli1 is an important target accounting for inhibition of cell growth by reactive oxygen species. *Mol. Biol. Cell.* 23: 3582-3590.
- Altmann, K., Durr, M., Westermann, B. (2007). *Saccharomyces cerevisiae* as a model organism to study mitochondrial biology. *Biol. Med. Sci.* 372: 81-90.
- Andressoo, J. O., Hoeijmakers, J. H., Mitchell, J. R. (2006). Nucleotide excision repair disorders and the balance between cancer and aging. *Cell. Cycle.* 24: 2886-2888.
- Andrew, A. J., Dutkiewicz, R., Knieszner, H., Craig, E. A. & Marszalek, J. (2006). Characterization of the interaction between the J-protein Jac1 and the scaffold for Fe-S cluster biogenesis, Isu1. *J. Biol. Chem.* 281: 14580–14587.

- Aisen, P., Enns, C., Wessling-Resnick, M. (2001). Chemistry and biology of eukaryotic iron metabolism. *Int. J. Biochem. Cell. Biol.* 33: 940-959.
- Archibald, F. S., Fridovich, I. (1981). Manganese and defenses against oxygen toxicity in *Lactobacillus plantarum*. *J. Bacteriol.* 145: 422-451.
- Ausubel, F.M., Brent, R., Kingston, R.E., Moore, D.D., Seidman, J.G., Struhl, K. (2007). *Current protocols in molecular biology*. John Wiley & Sons: New York.
- Avery, A. M., Avery, S. V. (2001). *Saccharomyces cerevisiae* expresses three phospholipid hydroperoxide glutathione peroxidases. *J. Biol. Chem.* 276: 33730-33735.
- Avery, S. V. (2011). Molecular targets of oxidative stress. *Biochem. J.* 434: 201-210.
- Avery, S. V. (2001). Metal toxicity in yeast and the role of oxidative stress. *Adv APP1. Microbiol.* 49: 111-142.
- Avery, S. V., Howlett, N. G., Radice, S. (1996). Copper toxicity towards *Saccharomyces cerevisiae*: dependence on plasma membrane fatty acid composition. *Appl. Environ. Microbiol.* 62: 3960-3966.
- Ayala-Castro, C., Saini, A., Outten, F. W. (2008). Fe-S cluster assembly pathways in bacteria. *Microbiol. Mol. Biol. Rev.* 72: 110-125.
- Baker, J., Sitthisak, S., Sengupta, M., Johnson, M., Jayaswal, R. K., Morrissey, J. A. (2010). Copper stress induces a global stress response in *Staphylococcus aureus* and represses *sae* and *agr* expression and biofilm formation. *Appl. Environ. Microbiol.* 76: 150-160.
- Balk, J., Pierik, A. J., Aguilar, Netz, D., Muhlenhoff, U., Lill, R. (2004). The hydrogenase-like Nar1p is essential for maturation of cytosolic and nuclear iron-sulfur proteins. *Embo. J.* 23: 2105-2115.
- Bandyopadhyay, S., Chandramouli, K., Johnson, M. K. (2008). Iron-sulfur cluster biosynthesis. *Biochem. Soc. Trans.* 36: 1112-1119.
- Bansal, A. K., Bilaspuri, G. S. (2009). Antioxidant effect of vitamin E on motility, viability and lipid peroxidation of cattle spermatozoa under oxidative stress. *Animal. Sci. Pap. Rep.* 27: 5-14.

- Barnese, K., Gralla, E. B., Cabelli, D. E., Valentine, J. S. (2008). Manganous phosphate acts as a superoxide dismutase. *J. Am Chem. Soc.* 130: 4604-4606.
- Barras, F., Loiseau, L., Py, B. (2005). How *Escherichia coli* and *Saccharomyces cerevisiae* build Fe/S proteins. *Adv. Microb. Physiol.* 50: 41-101.
- Barthelme, D., Dinkelaker, S., Albers, S. V., Londei, P., Ermler, U., Tampe, R. (2011). Ribosome recycling depends on a mechanistic link between the FeS cluster domain and a conformational switch of the twin-ATPase ABCE1. *Proc. Natl. Acad. Sci. USA.* 108: 3228–3233.
- Barthelme, D., Scheele, U., Dinkelaker, S., Janoschka, A., MacMillan, F., Albers, S. V., Driessen, A. J. M., Stagni, M. S., Bill, E., Klauke, W. M., Schunemann, V., Tampe, R. (2007). Structural organization of essential iron-sulfur clusters in the evolutionarily highly conserved ATP-binding cassette protein ABCE1. *J. Biol. Chem.* 282: 14598-14607.
- Bayot, A., Santos, R., Camadro, J. M., Rustin, P. (2011). Friedreich's ataxia: the vicious circle hypothesis revisited. *BMC. Med.* 9: 112.
- Becker, T., Franckenberg, S., Wickles, S., Shoemaker, C. J., Anger, A. M., Armache, J. P., Sieber, H., Ungewickell, C., Berninghausen, O., Daberkow, I., Karcher, A., Thomm, M., Hopfner, K. P., Green, R., Beckmann, R. (2012). Structural basis of highly conserved ribosome recycling in eukaryotes and archaea. *Nat.* 482: 501-508.
- Beinert, H. (2000). "Iron-sulfur proteins: ancient structures, still full of surprises." *J. Biologic. Inorg. Chem.* 5: 2–15.
- Beinert, H., Holm, R. H., Münck, E. (1997). Iron-sulfur clusters: nature's modular, multipurpose structures. *Sci.* 277: 653–659.
- Bekri, S., Kispal, G., Lange, H., Fitzsimons, E., Tolmie, J., Lill, R., Bishop, D. F. (2000). Human ABC7 transporter: gene structure and mutation causing X-linked sideroblastic anemia with ataxia (XLSA/A) with disruption of cytosolic iron-sulfur protein maturation. *Blood.* 96: 3256–3264.
- Belle, A., Tanay, A., Bitincka, L., Shamir, R., O'Shea, E.K. (2006). Quantification of protein half-lives in the budding yeast proteome. *Proc. Natl. Acad. Sci. USA.* 103: 13004-13009.
- Bencze, K. Z., Kondapalli, K. C., Cook, J. D., McMahon, S., Millan-Pacheco, C., Pastor, N., Stemmler, T. (2006). The structure and function of frataxin. *Crit. Rev. Biochem. Mol. Biol.* 41: 269–291.

- Benoit De Coignac, A., Bisbal, C., Lebleu, B., Salehzada, T. (1998). cDNA cloning and expression analysis of the murine ribonuclease L inhibitor. *Gene*. 209: 149–156.
- Bertani, G. (1951). Studies on lysogenesis. I. The mode of phage liberation by lysogenic *Escherichia coli*. *J. Bacteriol.* 62: 293–300.
- Bharadwaj, P., Martins, R., Macreadie, I. (2010). "Yeast as a model for studying Alzheimer's disease." *Fems. Yeast. Res.* 10: 961–969.
- Bhattacharya, A., McIntosh, K. B., Willis, I. M., Warner, J. R. (2010). Why Dom34 stimulates growth of cells with defects of 40S ribosomal subunit biosynthesis. *Mol. Cell. Biol.* 30: 5562–5571.
- Bhattacharya, A., Czaplinski, K., Trifillis, P., He, F., Jacobson, A., Peltz, S. W. (2000). Characterization of the biochemical properties of the human *Upf1* gene product that is involved in nonsense-mediated mRNA decay. *RNA*. 6: 1226–1235.
- Bigelow, D. J., Squier, T. C. (2005). Redox modulation of cellular signaling and metabolism through reversible oxidation of methionine sensors in calcium regulatory proteins. *Biochimica. Biophys. Acta. (BBA)- Proteins & Proteomics*. 21703: 121–134.
- Bisbal, C., Salehzada, T., Silhol, M., Martinand, C., Le Roy, F., Lebleu, B. (2001). The 2–5A/RNase L pathway and inhibition by RNase L inhibitor (RLI) *Methods. Mol. Biol.* 160: 183–198.
- Bisbal, C; Martinand, C; Silhol, M; Lebleu, B; Salehzada, T. (1995). Cloning and characterization of an RNase L inhibitor. A new component of the interferon-regulated 2-5 A pathway. *J. Biol. Chem.* 270: 13308–13317.
- Biteau, B., Labarre, J., Toledano, M. B. (2003). ATP-dependent reduction of cysteine-sulphinic acid by *S. cerevisiae* sulphiredoxin. *Nat.* 425: 980–984.
- Bjornstedt, M., Kumar, S., Bjorkhem, L., Spyrou, G., Holmgren, A. (1997). Selenium and the thioredoxin and glutaredoxin systems. *Biomed. Environ. Sci.* 10: 271–279.
- Bjornstedt, M., Xue, J., Huang, W., Akesson, B., Holmgren, A. (1994). The thioredoxin and glutaredoxin systems are efficient electron donors to human plasma glutathione peroxidase. *J. Biol. Chem.* 269: 29382–29384.
- Bolotin-Fukuhara, M., Dumas, B., Gaillardin, C. (2010). "Yeasts as a model for human diseases." *Fems. Yeast. Res.* 10: 959–960.

- Bors, W., Langebartels, C., Michel, C., Sandermann, J. H. (1989). Polyamines as radical scavengers and protectants against ozone damage. *Phyto. chem.* 28: 1589–1595.
- Boveris, A. (1984). Determination of the production of superoxide radicals and hydrogen peroxide in mitochondria. *Methods. Enzy. Mol.* 105: 429–435.
- Bradford, M. (1976). A rapid and sensitive method for quantitation of microgram quantities of protein utilizing the principle of protein-dye binding. *Anal. Biochem.* 72: 248–254.
- Bramley, P. M., Elmadfa, I., Kafatos, A., Kelly, F. J., Manios, Y., Roxborough, H. E., Schuch, W., Sheehy, P. J. A., Wagner, K. H. (2000). Vitamin E. *J. Sci. Food. Agric.* 80: 913–938.
- Burritt, D. J. (2008). The polycyclic aromatic hydrocarbon phenanthrene causes oxidative stress and alters polyamine metabolism in the aquatic liverwort *Riccia fluitans* L. *Plant. Cell. Envir.* 31: 1416–1431.
- Bushweller, J. H., Billeter, M., Holmgren, A., Wuthrich, K. (1994). The nuclear magnetic resonance solution structure of the mixed disulfide between *Escherichia coli* glutaredoxin (C14S) and glutathione. *J. Mol. Biol.* 235: 1585–1597.
- Cabiscol, E., Piulats, E., Echave, P., Herrero, E., Ros, J. (2000). Oxidative stress promotes specific protein damage in *Saccharomyces cerevisiae*. *J. Biol. Chem.* 275: 27393–27398.
- Calderon, I. L., Elias, A. O., Fuentes, E. L., Pradenas, G. A., Castro, M. E., Arenas, F. A., Perez, J. M., Vasquez, C. C. (2009). Tellurite-mediated disabling of [4Fe-4S] clusters of *Escherichia coli* dehydratases. *Microbiol.* 155: 1840–1846.
- Calinescu, C., Mondovi, B., Federico, R., Ispas-Szabo, P., Mateescu, M. A. (2012). Carboxymethyl starch: chitosan monolithic matrices containing diamine oxidase and catalase for intestinal delivery. *Interna. J. Pharma.* 428: 48–56.
- Carlioz, A., Touati, D. (1986). Isolation of superoxide dismutase mutants in *Escherichia coli*: is superoxide dismutase necessary for aerobic life. *Embo. J.* 5: 623–630.
- Carp, H., Janoff, A., Abrams, W., Weinbaum, G., Drew, R. T., Weissbach, H., Brot, N. (1983). Human methionine sulfoxide-peptide reductase, an enzyme capable of reactivating oxidized alpha-1-proteinase inhibitor *in vitro*. *Am. Rev. Respir. Dis.* 127: 301–305.
- Carr, R. J. G., Bilton, R. E. Atkinson, I. (1986). Toxicity of paraquat to microorganisms. *Appl. Environ. Microbiol.* 52: 1112–1116.

- Carter, A. P., Clemons, W. M., Brodersen, D. E., Morgan-Warren, R. J., Wimberly, B. T., Ramakrishnan, V. (2000). Functional insights from the structure of the 30S ribosomal subunit and its interactions with antibiotics. *Nature*. 407: 340–348.
- Cavadini, P., Biasiotto, G., Poli, M., Levi, S., Verardi, R., Zanella, I., Derosas, M., Ingrassia, R., Corrado, M., Arosio, P. (2007). RNA silencing of the mitochondrial ABCB7 transporter in HeLa cells causes an iron-deficient phenotype with mitochondrial iron overload. *Blood*. 109: 3552–3559.
- Chan, M. K., Kim, J., Rees, D.C. (1993). The nitrogenise FeMo-cofactor and p-cluster pair: 2. 2 A resolution structures. *Sci*. 260: 792-794.
- Chance, B., Sies, H., Boveris, A. (1979). Hydroperoxide metabolism in mammalian organs. *Physiol. Rev.* 59: 527–605.
- Chandramouli, K., Unciuleac, M. C., Naik, S., Dean, D. R., Huynh, B. H., Johnson, M. K. (2007). Formation and properties of [4Fe-4S] clusters on the IscU scaffold protein. *Biochem*. 46: 6804–6811.
- Chang, E. C., Kosman, D. J. (1989). Intracellular Mn (II) associated superoxide scavenging activity protects Cu, Zn superoxide dismutase deficient *Saccharomyces cerevisiae* against dioxygen stress. *J. Biol. Chem.* 264: 12172–12178.
- Chelikani, P., Fita, I., Loewen, P. C. (2004). Diversity of structures and properties among catalases. *Cell. Mol. Life. Sci.* 61: 192–208.
- Chen, B., Markillie, L. M., Xiong, Y., Mayer, M. U., Squier, T. C. (2007). Increased catalytic efficiency following gene fusion of bifunctional methionine sulfoxide reductase enzymes from *Shewanella oneidensis*. *Biochem*. 46: 14153-14161.
- Chen, J., Lu, G., Lin, J., Davidson, A. L., Quioco, F. A. (2003). A tweezers-like motion of the ATP-binding cassette dimer in an ABC transport cycle. *Mol. Cell*. 12: 651–661.
- Chen, Z. Q., Dong, J., Ishimura, A., Daar, I., Hinnebusch, A. G., Dean, M. (2006). The essential vertebrate ABCE1 protein interacts with eukaryotic initiation factors. *J. Biol. Chem.* 281: 7452–7457.
- Chernoff, Y. O., Vincent, A., Liebman, S.W. (1994). Mutations in eukaryotic 18s ribosomal RNA affect translational fidelity and resistance to aminoglycoside antibiotics. *Embo. J.* 13: 906-913.
- Chillappagari, S., Seubert, A., Trip, H., Kuipers, O. P., Marahiel, M. A., Miethke, M. (2010). Copper stress affects iron homeostasis by

- destabilizing iron-sulfur cluster formation in *Bacillus subtilis*. J. Bacteriol. 192: 2512-2524.
- Circu, M. L., Aw, T. Y. (2010). Reactive oxygen species, cellular redox systems, and apoptosis. Free. Rad. Biol. Med. 48: 749-762.
- Coelho, C. M., Kolevski, B., Bunn, C., Walker, C., Dahanukar, A., Leever, S. J. (2005). Growth and cell survival are unevenly impaired in *pixie* mutant wing discs. Development. 132: 5411-5424.
- Corpet, F. (1988). Multiple sequence alignment with hierarchical clustering. Nucleic. Acids. Res. 16: 10881-10890.
- Costa, V. M. V., Amorim, M. A., Quintanilha, A., Ferreira, P. M. (2002). Free. Radic. Biol. Med. 33: 1507-1515.
- Crampton, N., Kodiha, M., Shrivastava, S., Umar, R., Stochaj, U. (2009). Oxidative stress inhibits nuclear protein export by multiple mechanisms that target FG nucleoporins and Crm1. Mol. Biol. Cell. 20: 5106-5116.
- Culotta, V. C., Joh, H. D., Lin, S. J., Slekar, K. H., Strain, G. (1995). A physiological role of *Saccharomyces cerevisiae* copper/zinc superoxide dismutase in copper buffering. J. Biol. Chem. 270: 29991-29997.
- Culotta, V. C., Daly, M. J. (2013). Manganese complexes: diverse metabolic routes to oxidative stress resistance in prokaryotes and yeast. Antiox. Redox. Signal. 19: 933-944.
- Daily, D., Vlamis-Gardikas, A., Offen, D., Mittelman, L., Melamed, E., Holmgren, A., Barzilai, A. (2001). Glutaredoxin protects cerebellar granule neurons from dopamine-induced apoptosis by dual activation of the ras-phosphoinositide 3-kinase and jun N-terminal kinase pathways. J. Biol. Chem. 276: 21618-21626.
- Dam, B. V., Hinsbergh, V. W. M.V., Stehouwer, C. D. A., Versteilen, A., Dekker, H., Buytenhek, R., Princen, H. M., Schalkwijk, C. G. (2003). Vitamin E inhibits lipid peroxidation-induced adhesion molecule expression in endothelial cells and decreases soluble cell adhesion molecules in healthy subjects. Oxford. J. Med. Cardiovas. Res. 57: 563-571.
- D'Autreaux, B., Toledano, M. B. (2007). ROS as signalling molecules: mechanisms that generate specificity in ROS homeostasis. Nat. Rev. Mol. Cell. Biol. 8: 813-824.
- Davies, M. J. (2005). The oxidative environment and protein damage. Biochimica. et. Biophysica. Acta. 1703: 93-109.

- Dawes, I. W. (1999). Stress responses. In the metabolism and molecular physiology of *Saccharomyces cerevisiae* (Dickinson, J. R., Schweizer, M., eds). 277-326.
- Delatycki, M. B., Williamson, R., Forrest, S.M. (2000). Friedreich ataxia: an overview. *J. Med. Genet.* 37: 1.
- Djaman, O., Outten, F.W., Imlay, J. A. (2004). Repair of oxidized iron-sulfur clusters in *Escherichia coli*. *J. Biol. Chem.* 279: 44590-44599.
- Djordjevic, V. B. (2004). Free radicals in cell biology. *Inter. Rev. Cyto.* 237: 57-89.
- Dong, B., Niwa, M., Walter, P., Silverman, R. H. (2001). Basis for regulated RNA cleavage by functional analysis of RNase L and Ire1p. *RNA.* 7: 361-373.
- Dong, J., Lai, R., Nielsen, K., Fekete, C. A., Qiu, H., Hinnebusch, A. G. (2004). The essential ATP-binding cassette protein RLI1 functions in translation by promoting preinitiation complex assembly. *J. Biol. Chem.* 279: 42157-42168.
- Doudican, N. A., Song, B., Shadel, G. S., Doetsch, P. W. (2005). Oxidative DNA damage causes mitochondrial genomic instability in *Saccharomyces cerevisiae*. *Mol. Cell. Biol.* 25: 5196-5204.
- Drake, S. K., Bourdon, E., Wehr, N. B., Levine, R. L., Backlund, P. S., Yergey, A. L., Rouault, T. A. (2002). Numerous proteins in mammalian cells are prone to iron-dependent oxidation and proteasomal degradation. *Dev. Neuro. Sci.* 24: 114-124.
- Drummond, D. A., Wilke, C. O. (2008). Mistranslation-induced protein misfolding as a dominant constraint on coding-sequence evolution. *J. Cell.* 134: 341-352.
- Dutkiewicz, R., Marszalek, J., Schilke, B., Craig, E. A., Lill, R., Muhlenhoff, U. (2006). The Hsp70 chaperone Ssq1p is dispensable for iron-sulfur cluster formation on the scaffold protein Isu1p. *J. Biol. Chem.* 281: 7801-7808.
- Duttaroy, A., Paul, A., Kundu, M., Belton, A. (2003). A *sod2* null mutation confers severely reduced adult life span in *Drosophila*. *Genetics.* 165: 2295-2299.
- Eckers, E., Bien, M., Stroobant, V., Herrmann, J. M., Deponte, M. (2009). Biochemical characterization of dithiol glutaredoxin 8 from *Saccharomyces cerevisiae*: the catalytic redox mechanism redux. *Biochem.* 48: 1410-1423.

- England, K., Cotter, C. T. (2005). Direct oxidative modifications of signalling proteins in mammalian cells and their effects on apoptosis. *Redox. Report.* 10: 237–245.
- Estevez, A. M., Haile, S., Steinbuchel, M., Quijada, L., Clayton, C. (2004). Effects of depletion and overexpression of the *Trypanosoma brucei* ribonuclease L inhibitor homologue. *Mol. Biochem. Parasitol.* 133: 137–141.
- Farabaugh, P. J., Bjork, G. R. (1999). How transitional accuracy influences reading frame maintenance. *Embo. J.* 18: 1427-1434.
- Faraci, F. M., Didion, S. P. (2004). Superoxide dismutase isoforms in the vessel wall. *Arterioscler. Thromb. Vasc. Biol.* 24: 1367-1373.
- Faulkner, M. J., Helmann, J.D. (2011). Peroxide stress elicits adaptive changes in bacterial metal ion homeostasis. *Antiox. Redox. Signal.* 15: 175-189.
- Fernandes, A. P., Holmgren, A. (2004). Glutaredoxins: glutathione-dependent redox enzymes with functions far beyond a simple thioredoxin backup system. *Antiox. Redox. Signal.* 6: 63-74.
- Ferraro, D. J., Gakhar, L., Ramaswamy, S. (2005). Rieske business: structure-function of Rieske non-heme oxygenases. *Biochem. Biophys. Res. Commun.* 338: 175-90.
- Finkel, T., Holbrook, N. J. (2000). Oxidants, oxidative stress and the biology of ageing. *Nat.* 408: 239–247.
- Flint, D. H., Tuminello, J. F., Emptage, M. H. (1993). The inactivation of Fe–S cluster containing hydro-lyases by superoxide. *J. Biol. Chem.* 268: 22369-22376.
- Flohe, L., Gunzler, W. A., Schock, H. H. (1973). Glutathione peroxidase: a selenoenzyme. *Febs. Lett.* 32: 132–134.
- Flora, S. J. S., Bhadauria, S., Kannan, G. M., Singh, N. (2007). Arsenic induced oxidative stress and the role of antioxidant supplementation during chelation: a review. *J. Environ. Biol.* 28: 333-347.
- Foglieni, C., Cavarelli, M., Piscopiello, M., Fulgenzi, A., Ferrero, M. E. (2011). Mn bioavailability by polarized Caco-2 cells: comparison between Mn gluconate and Mn oxyprolinate. *Nutrition. J.* 10: 77.
- Fong, K. L., Mccay, P. B., Poyer, J. L. (1976). Evidence for superoxide-dependent reduction of Fe³⁺ and its role in enzyme-generated hydroxyl radical formation. *Chem. Biol. Interact.* 15: 77-89.

- Fontecave, M. (2006). Iron-sulfur clusters: ever-expanding roles. *Nat. Chem. Biol.* 2: 171-174.
- Fontecave, M., Ollagnier-de-Choudens, S. (2008). Iron-sulfur cluster biosynthesis in bacteria: mechanisms of cluster assembly and transfer. *Arch. Biochem. Biophys.* 474: 226-237.
- Foury, F. (1997). Human genetic diseases: a cross-talk between man and yeast. *Gene.* 195: 1-10.
- Freeman, H. C. (1975). *Inorganic biochemistry* (Eichhorn G. L., ed) Elsevi. Sci. Inc. New York. 1: 153-156.
- Fridovich, I. (1995). Superoxide radical and superoxide dismutases. *Annu. Rev. Biochem.* 64: 97-112.
- Friedlich, A. L., Smith, M.A., Zhu, X., Takeda, A., Nunomura, A., Moreira, P. I., Perry, G. (2009). Oxidative stress in parkinson's disease. *Open. Patho. J.* 3: 38-42.
- Gadal, O., Strauss, D., Kessl, J., Trumppower, B., Tollervey, D. Hurt, E. (2001). Nuclear export of 60s ribosomal subunits depends on Xpo1p and requires a nuclear export sequence-containing factor, Nmd3p, that associates with the large subunit protein Rpl10p. *Mol. Cell. Biol.* 21: 3405-3415.
- Gajewska, E., Bernat, P., Dlugonski, J., Sklodowska, M. (2012). Effect of nickel on membrane integrity, lipid peroxidation and fatty acid composition in wheat seedlings. *J. Agrono. Crop. Sci.* 198: 286-294.
- Gardner, P. R., Fridovich, I. (1991). Superoxide sensitivity of the *Escherichia coli* 6-phosphogluconate dehydratase. *J. Biol. Chem.* 266: 1478-1483.
- Gardner, P. R., Fridovich, I. (1991). Superoxide sensitivity of the *Escherichia coli* aconitase. *J. Biol. Chem.* 266: 19328-19333.
- Gerber, J., Muhlenhoff, U., Lill, R. (2003). An interaction between frataxin and Isu1/Nfs1 that is crucial for Fe/S cluster synthesis on Isu1. *Embo. Rep.* 4: 906-911.
- Giacco, F., Brownlee, M. (2010). Oxidative stress and diabetic complications. *Circ. Res.* 107: 1058-1070.
- Gietz, R. D., Woods, R. A. (2001). Genetic transformation of yeast. *Bio. Techniq.* 30: 816-831.
- Gietz, R. D., Woods, R. A. (2002). Transformation of yeast by lithium acetate/single stranded carrier DNA/polyethylene glycol method. *Methods. Enzymol.* 350: 87-96.

- Grant, C. M. (2001). Role of the glutathione/glutaredoxin and thioredoxin systems in yeast growth and response to stress conditions. *Mol. Microbiol.* 39: 533–541.
- Grant, C. M. (2011). Regulation of translation by hydrogen peroxide. *Antiox. Redox. Signal.* 15: 191–203.
- Green, J., Bennett, B., Jordan, P., Ralph, E. T., Thomson, A. J., Guest, J. R. (1996). Reconstitution of the [4Fe-4S] cluster in FNR and demonstration of the aerobic-anaerobic transcription switch *in vitro*. *Biochem. J.* 316: 887–892.
- Gueldener, U., Heck, S., Fielder, T., Beinhauer, J., Hegemann, J. H. (1996). A new efficient gene disruption cassette for repeated use in budding yeast. *Nucleic. Acids. Res.* 24: 2519-2524.
- Gueldener, U., Heinisch, J., Koehler, G. J., Voss, D., Hegemann, J. H. (2002). A second set of loxP marker cassettes for Cre-mediated multiple gene knockouts in budding yeast. *Nucleic. Acids. Res.* 30. 6: e23.
- Hagensee, M. E., Moses, R. E. (1989). Multiple pathways for repair of hydrogen peroxide-induced DNA damage in *Escherichia. coli*. *J. Bacteriol.* 171: 991-995.
- Halliwell, B., Clement, M. V., Long, L. H. (2000). Hydrogen peroxide in the human body. *Febs. Lett.* 486: 10–13.
- Halliwell, B., Gutteridge, J. M. C. (1999). *Free radicals in biology and medicine*, 3rd. ed. Oxford University Press. Midsomer Norton. Avon. England.
- Halliwell, S. C. (2012). Cell individuality in adhesin expression of *Candida glabrata*. PhD thesis. University of Nottingham. pp: 83-84.
- Hausmann, A., Netz, D. J. A., Balk, J., Pierik, A. J., Muhlenhoff, U., Lill, R. (2005). The eukaryotic P-loop NTPase Nbp35: an essential component of the cytosolic and nuclear iron-sulfur protein assembly machinery. *Proc. Natl. Acad. Sci. USA.* 102: 3266–3271.
- Hazra, T. K., Hill, J. W., Izumi, T., Mitra, S. (2001). Multiple DNA glycosylases for repair of 8-oxoguanine and their potential *in vivo* functions. *Prog. Nucleic. Acid. Res. Mol. Biol.* 68: 193-205.
- Hentze, M. W., Muckenthaler, M. U., Andrews, N. C. (2004). Balancing acts: molecular control of mammalian iron metabolism. *Cell.* 117: 285–297.

- Herbette, S., Roeckel-Drevet, P., Drevet, J. R. (2007). Seleno-independent glutathione peroxidases. More than simple antioxidant scavengers. *Febs. J.* 274: 2163–2180.
- Herrero, E., de la Torre-Ruiz, M. A. (2007). Monothiol glutaredoxins: a common domain for multiple functions. *Cell. Mol. Life. Sci.* 64: 1518–1530.
- Holland, S. L., Avery, S. V. (2009). Actin-mediated endocytosis limits intracellular Cr accumulation and Cr toxicity during chromate stress. *Toxicol. Sci.* 111: 437-46.
- Holland, S. L., Ghosh, E. and Avery, S. V. (2010). Sulfur starvation and mRNA mistranslation in yeast are linked in a common mechanism of chromate toxicity. *Toxicol. In vitro.* 24: 1764–1767.
- Holland, S., Lodwig, E., Sideri, T., Reader, T., Clarke, I., Gkargkas, K., Hoyle, D. C., Delneri, D., Oliver, S. G., Avery, S. V. (2007). Application of the comprehensive set of heterozygous yeast deletion mutants to elucidate the molecular basis of cellular chromium toxicity. *Genome. Biol.* 8. R268.
- Holmgren, A. (1989). Thioredoxin and glutaredoxin systems. *J. Biol. Chem.* 264: 13963-13966.
- Holmgren, A., Johansson, C., Berndt, C., Lonn, M. E., Hudemann, C., Lillig, C. H. (2005). Thiol redox control via thioredoxin and glutaredoxin systems. *Biochem. Soc. Trans.* 33: 1375–1377.
- Howard, M. T., Shirts, B. H., Petros, L. M., Flanigan, K. M., Gesteland, R. F., Atkins, J. F. (2000). Sequence specificity of aminoglycoside-induced stop codon readthrough: potential implications for treatment of duchenne muscular dystrophy. *Ann. Neurol.* 48: 164-169.
- Howlett, N. G., Avery, S. V. (1997). Relationship between cadmium sensitivity and degree of plasma membrane fatty acid unsaturation in *Saccharomyces cerevisiae*. *Appl. Microbiol. Biotechnol.* 48: 539–545.
- Huber, H., Hohn, M. J., Rachel, R., Fuchs, T., Wimmer, V. C., Stetter, K.O. (2002). "A new phylum of archaea represented by a nanosized hyperthermophilic symbiont". *Natur.* 417. 6884: 27–28.
- Hughes, T.R., Marton, M.J., Jones, A.R., Roberts, C.J., Stoughton, R., Armour, C.D., Bemmett, H.A., Coffrt, E., Dai, H., He, Y.D., Kodd, M.J., King, A.M., Meyer, M.R., Slade, D., Lum, P.Y., Stepaniants, S.B., Shoemaker, D.D., Gachotte, D., Chahraburty, K., Simon, J., Bard, M., Friend, S.H. (2000).

Functional discovery via a compendium of expression profiles. *Cell*. 102: 109–126.

- Humphries, K. M., Deal, M. S., Taylor, S. S. (2005). Enhanced dephosphorylation of cAMP-dependent protein kinase by oxidation and thiol modification. *J. Biologic. Chem.* 280: 2750–2758.
- Hutchinson, F. (1985). Chemical changes induced in DNA by ionizing radiation. *Prog. Nucleic. Acid. Res.* 32: 116-154.
- Imlay, J. A. (2003). Pathways of oxidative damage. *Annu. Rev. Microbiol.* 57: 395-418.
- Imlay, J. A. (2006). Iron-sulphur clusters and the problem with oxygen. *Mol. Microbiol.* 59: 1073-1082.
- Imlay, J. A. (2008). Cellular defences against superoxide and hydrogen peroxide. *Ann. Rev. Biochem.* 77: 755-776.
- Imlay, J. A., Linn, S. (1986). Bimodal pattern of killing of DNA-repair-defective or anoxically grown *Escherichia. coli* by hydrogen peroxide. *J. Bacteriol.* 166: 519-527.
- Inaoka, T., Matsumura, Y., Tsuchido, T. (1999). SodA and manganese are essential for resistance to oxidative stress in growing and sporulating cells of *Bacillus subtilis*. *J. Bacteriol.* 181: 1939-1943.
- Irazusta, V., Cabisco, E., Reverter-Branchat, G., Ros, J., Tamarit, J. (2006). Manganese is the link between frataxin and iron-sulfur deficiency in the yeast model of Friedreich ataxia. *J. Biol. Chem.* 281: 12227-12232.
- Jacobson, A. (2005). The end justifies the means. *Nat. Struct. Mol. Biol.* 12: 474–475.
- Jamieson, D. J. (1998). Oxidative stress responses of the yeast *Saccharomyces cerevisiae*. *Yeast.* 14: 1511-1527.
- Jang, S. J., Imlay, J. A. (2010). Hydrogen peroxide inactivates the *Escherichia coli* Isc iron-sulphur assembly system, and OxyR induces the Suf system to compensate. *Mol. Microbiol.* 78: 1448-1467.
- Jang, S., Imlay, J. A. (2007). Micromolar intracellular hydrogen peroxide disrupts metabolism by damaging iron-sulfur enzymes. *J. Biol. Chem.* 282: 929-937.
- Janke, C., Magiera, M. M., Rathfelder, N., Taxis, C., Reber, S., Maekawa, H., Moreno-Borchart, A., Doenges, G., Schwob, E., Schiebel, E., Knop, M. (2004). A versatile toolbox for PCR-based

tagging of yeast genes: new fluorescent proteins, more markers and promoter substitution cassettes. *Yeast*. 21: 947-962.

- Jervis, A. J., Crack, J. C., White, G., Artymiuk, P.J., Cheesman, M. R., Thomson, A. J., Brun, N. E. L., Green, J. (2009). The O₂ sensitivity of the transcription factor FNR is controlled by Ser24 modulating the kinetics of [4Fe-4S] to [2Fe-2S] conversion. *Proc. Natl. Acad. Sci.* 106: 4659-4664.
- Ji, L., La, J. H. (2000). Antioxidant defense: effects of aging and exercise. In: *Free Radicals in Exercise and Aging*, edited by Radak, Z., Champaign, I. L. Human Kinetics. pp: 35-72.
- Jian, J., Yang, Q., Dai, J., Eckard, J., Axelrod, D., Smith, J., Huang, X. (2011). Effects of iron deficiency and overload on angiogenesis and oxidative stress—a potential dual role for iron in breast cancer. *Free. Radic. Biol. Med.* 50: 841-847.
- Johnson, D. C., Dean, D. R., Smith, A. D., Johnson, M. K. (2005). Structure, function, and formation of biological iron-sulfur clusters. *Annu. Rev. Biochem.* 74: 247-281.
- Johnson, D., Travis, J. (1979). The oxidative inactivation of human alpha-1-proteinase inhibitor. Further evidence for methionine at the reactive center. *J. Biologic. Chem.* 254: 4022-4026.
- Jomova, K., Valko, M. (2011). Advances in metal-induced oxidative stress and human disease. *Toxicol.* 283: 65-87.
- Kagi, J. H. R., Vallee, B. L. (1960). Metallothionein: a cadmium- and zinc-containing protein from equine renal cortex. *J. Biol. Chem.* 235: 3460-3465.
- Kalinina, E. V., Chernov, N. N., Saprin, A. N. (2008). Involvement of thio-, peroxi-, and glutaredoxins in cellular redox-dependent processes. *Bio. Chem.* 73: 1493-1510.
- Kang, Y. J. (2006). Metallothionein redox cycle and function. *Exp. Biol. Med.* 231: 1459-1467.
- Karcher, A., Schele, A., Hopfner, K. P. (2008). X-ray structure of the complete ABC enzyme ABCE1 from *Pyrococcus abyssi*. *J. Biol. Chem.* 283: 7962-7971.
- Keeling, K. M., Lanier, J., Du, M., Salas-Marco, J., Gao, L., Kaenjak-Angeletti, A., Bedwell, D. M. (2004). Leaky termination at premature stop codons antagonizes nonsense-mediated mRNA decay in *S. cerevisiae*. *RNA*. 10: 691-703.
- Kennedy, M. C., Stout, C. D. (1992). Aconitase: an iron-sulfur enzyme. *Adv. Inorg. Chem.* 38: 323-339.

- Kerr, I. D. (2004). Sequence analysis of twin ATP binding cassette proteins involved in translational control, antibiotic resistance, and ribonuclease L inhibition. *Biochem. Biophys. Res.* 315: 166-173.
- Keyer, K., Imlay, J. A. (1996). Superoxide accelerates DNA damage by elevating free-iron levels. *Proc. Natl. Acad. Sci. USA.* 93: 13635-13640.
- Khan, M. H., Panda, S. K. (2002). Induction of oxidative stress in roots of *Oryza sativa* L. in response to salt stress. *Biol. Plant.* 45: 625 – 627.
- Khor, H. K., Jacoby, M. E., Squier, T. C., Chu, G. C., Chelius, D. (2010). Identification of methionine sulfoxide diastereomers in immunoglobulin gamma antibodies using methionine sulfoxide reductase enzymes. *J. Mabs.* 2: 299-308.
- Khoroshilova, N., Beinert, H., Kiley, P. J. (1995). Association of a polynuclear iron-sulfur center with a mutant FNR protein enhances DNA binding. *Proc. Natl. Acad. Sci. USA.* 92: 2499–2503.
- Khoshnevis, S., Gross, T., Rotte, C., Baierlein, C., Ficner, R., Krebber, H. (2010). The iron-sulphur protein RNase L inhibitor functions in translation termination. *Embo. Rep.* 11: 214–219.
- Khozoie, C., Pleass, R.J., Avery, S.V. (2009). The antimalarial drug quinine disrupts Tat2p-mediated tryptophan transport and causes tryptophan starvation. *J. Biol. Chem.* 284: 17968-17974.
- Kiley, P. J., Beinert, H. (2003). The role of Fe-S proteins in sensing and regulation in bacteria. *Curr. Opin. Microbiol.* 6: 181–185.
- Kim, H. Y., Gladyshev, V. N. (2007). Methionine sulfoxide reductases: selenoprotein forms and roles in antioxidant protein repair in mammals. *Biochem. J.* 407: 321-329.
- Kim, I. S., Sohn, H. Y., Jin, I. (2011). Adaptive stress response to menadione-induced oxidative stress in *Saccharomyces cerevisiae* KNU5377. *J. Microbiol.* 49: 816–823.
- Kimata, Y., Yanagida, M. (2004). Suppression of a mitotic mutant by tRNA-Ala anticodon mutations that produce a dominant defect in late mitosis. *J. Cell. Sci.* 117: 2283–2293.
- King, G. L., Loeken, M. R. (2004). Hyperglycemia-induced oxidative stress in diabetic complication. *Hist. Chem. Cell. Biol.* 122: 333-338.

- Kirby, K., Hu, J., Hilliker, A. J., Phillips, J. P. (2002). RNA interference-mediated silencing of Sod2 in drosophila leads to early adult-onset mortality and elevated endogenous oxidative stress. *Proc. Natl. Acad. Sci. USA.* 99: 16162–16167.
- Kirkman, H. N., Gaetani, G. F. (2007). Mammalian catalase: a venerable enzyme with new mysteries. *Trends. Biochem. Sci.* 32: 44–50.
- Kispal, G., Csere, P., Prohl, C., Lill, R. (1999). The mitochondrial proteins Atm1p and Nfs1p are required for biogenesis of cytosolic Fe/S proteins. *Embo. J.* 18: 3981–3989.
- Kispal, G., Sipos, K., Lange, H., Fekete, Z., Bedekovics, T., Janaky, T., Bassler, J., Aguilar Netz, D.J., Balk, J., Rotte, C., Lill, R. (2005). Biogenesis of cytosolic ribosomes requires the essential iron-sulphur protein Rli1p and mitochondria. *Embo. J.* 24: 589–598.
- Kitada, M., Igarashi, K., Hirose, S., Kitagawa, H. (1979). Inhibition by polyamines of lipid peroxide formation in rat liver microsomes. *Biochem. Biophys. Res. Commun.* 87: 388–394.
- Klatt, P., Molina, E. P., DeLacoba, M. G., Padilla, A. C., Martinez-Galisteo, E., Barzena, J. A., Lamas, S. (1999). Redox regulation of c-Jun DNA binding by reversible S-glutathiolation. *Faseb. J.* 13: 1481–1490.
- Klinge, S., Hirst, J., Maman, J. D., Krude, T., Pellegrini, L. (2007). An iron-sulfur domain of the eukaryotic primase is essential for RNA primer synthesis. *Nat. Struct. Mol. Biol.* 14: 875–877.
- Klinner, U., Schafer, B. (2004). Genetic aspects of targeted insertion mutagenesis in yeasts. *Fems. Microbiol. Rev.* 28: 201–223.
- Kobayashi, K., Kikuno, I., Kuroha, K., Saito, K., Ito, K., Ishitani, R., Inada, T., Nureki, O. (2010). Structural basis for mRNA surveillance by archaeal Pelota and GTP-bound EF1alpha complex. *Proc. Natl. Acad. Sci. USA.* 107: 17575–17579.
- Koc, A., Gasch, A. P., Rutherford, J. C, Kim, H. Y., & Galdyshev, V. N. (2004). Methionine sulphoxide regulation of yeast lifespan reveals reactive oxygen species-dependent and-independent components of aging. *Proc. Natl. Acad. Sci. USA.* 101: 7999–8004.
- Kohen, R., Moor, E., Oron, M. (2003). Measurements of biological reducing power in health and diseases by voltammetric methods. In: *Redox genome interaction in health and disease*, Fuchs, J., Packer, L. (eds). Marcel Decker Inc., New York (in press).

- Konstantinidis, T. C., Patsoukis, N., Georgiou, C. D., Synetos, D. (2006). Translational fidelity mutations in 18S rRNA affect the catalytic activity of ribosomes and the oxidative balance of yeast cells. *Biochem.* 45: 3525-3533.
- Krinsky, N. I., (1998). The antioxidant and biological properties of the carotenoids. *Ann. Acad. Sci.* 854: 443-447.
- Kubrak, O.I., Lushchak, O.V., Lushchak, J.V., Torous, I.M., Storey, J.M., Storey, K.B., Lushchak, V.I. (2010). Chromium effects on free radical processes in goldfish tissues: comparison of Cr (III) and Cr (VI) exposures on oxidative stress markers, glutathione status and antioxidant enzymes. *Comp. Biochem. Physiol. C.* 152: 360–370.
- Kusano, T., Berberich, T., Tateda, C., Takahashi, Y. (2008). Polyamines: essential factors for growth and survival. *Planta.* 228: 367-381.
- Lange, H., Kispal, G., Kaut, A., Lill, R. (2000). A mitochondrial ferredoxin is essential for biogenesis of intra-and extra-mitochondrial Fe/S proteins. *Proc. Natl. Acad. Sci. USA.* 97: 1050–1055.
- Lapinskas, P. J., Cunningham, K. W., Liu, X. F., Fink, G. R., Culotta, V. C. (1995). Mutations in PMR1 suppress oxidative damage in yeast cells lacking superoxide dismutase. *Mol. Cell. Biol.* 15: 1382.
- Lee, B. C., Le, D. T., Gladyshev, V. N. (2008). Mammals reduce methionine-*S*-sulfoxide with MsrA and are unable to reduce methionine-*R*-sulfoxide, and this function can be restored with a yeast reductase. *J. Biol. Chem.* 283: 28361-28369.
- Lee, J. W., Beebe, K., Nangle, L.A., Jang, J., Longo-Guess, C. M., Cook, S. A., Davisson, M. T., Sundberg, J. P., Schimmel, P., Ackerman, S. L. (2006). Editing-defective tRNA synthetase causes protein misfolding and neurodegeneration. *Nat.* 443: 50–55.
- Lefevre, S., Brossas, C., Auchere, F., Boggetto, N., Camadro, J.M., Santos, R. (2012). Apn1 AP-endonuclease is essential for the repair of oxidatively damaged DNA bases in yeast frataxin-deficient cells. *Hum. Mol. Genet.* 21: 4060–4072.
- Levine, R. L., Moskovitz, J., Stadtman, E. R. (2000). Oxidation of methionine in proteins: roles in antioxidant defense and cellular regulation. *Iubmb. Life.* 50: 301–307.
- Li, Y., Huang, T. T. Carlson, E. J. Melov, S. Ursell, P. C., Olson, J.L., Noble, L.J., Yoshimura, M.P., Berger, C., Chan, P.H., Wallace,

- D.C., Epstein, C.J. (1995). Dilated cardiomyopathy and neonatal lethality in mutant mice lacking manganese superoxide dismutase. *Nat. Genet.* 11: 376–381.
- Lill, R. (2009). Functional and biogenesis of iron-sulphur proteins. *Nat.* 460: 831-838.
- Lill, R. (2007). Iron-sulfur clusters: basic building blocks for life. *Zellbiologie. Aktuell.* 33: 17-20.
- Lill, R., Dutkiewicz, R., Elsässer, H. P., Hausmann, A., Netz, D. J., Pierik, A. J., Stehling, O., Urzica, E., Mühlenhoff, U. (2006). Mechanisms of iron-sulfur protein maturation in mitochondria, cytosol and nucleus of eukaryotes. *Biochem. Biophys. Acta.* 1763: 652-667
- Lill, R., Fekete, Z., Sipos, K., Rotte, C. (2005). Is there answer? Why are mitochondria essential for life? *Iubmb. Life.* 57: 701-703.
- Lill, R., Muhlenhoff, U. (2006). Iron-sulfur protein biogenesis in eukaryotes: components and mechanisms. *Annu. Rev. Cell. Dev. Biol.* 22: 457–486.
- Lill, R., Mühlenhoff, U. (2008). Maturation of iron-sulfur proteins in eukaryotes: mechanisms, connected processes, and diseases. *Annu. Rev. Biochem.* 77: 669–700.
- Lillig, C. H., Berndt, C., Holmgren, A. (2008). Glutaredoxin systems. *Biochim. Biophys. Acta.* 1780: 1304–1317.
- Lillig, C. H., Holmgren, A. (2007). Thioredoxin and related molecules— from biology to health and disease. *Antioxid. Redox. Signal.* 9: 25–47.
- Limon-Pacheco, J., Gonsebatt, M.E. (2009). The role of antioxidants and antioxidant-related enzymes in protective responses to environmentally induced oxidative stress. *Mutat. Res.* 674: 137-147.
- Ling, J., Soll, D. (2010). Severe oxidative stress induces protein mistranslation through impairment of an aminoacyl-tRNA synthetase editing site. *Proc. Natl. Acad. Sci.* 107: 4028-4033.
- Ling, J., Reynolds, N., Ibba, M. (2009). Aminoacyl-tRNA synthesis and translational quality control. *Annu. Rev. Microbiol.* 63: 61–78.
- Ling, J., Roy, H., Qin, D., Rubio, M. A., Alfonzo, J. D., Fredrick, K., Ibba, M. (2007). Pathogenic mechanism of a human mitochondrial tRNAPhe mutation associated with myoclonic epilepsy with ragged red fibers syndrome. *Proc. Natl. Acad. Sci. USA.* 104: 15299-15304.

- Liochev, S.I., Fridovich, I. (1999). Superoxide and iron: partners in crime. *Iubmb. Life.* 48: 157-161.
- Liu, R., Liebman, S. W. (1996). A translational fidelity mutation in the universally conserved sarcin/ricin domain of 25S yeast ribosomal RNA. *RNA.* 2: 254-263.
- Longo, V. D., Gralla, E. B., Valentine, J. S. (1996). Superoxide dismutase activity is essential for stationary phase survival in *Saccharomyces cerevisiae*. Mitochondrial production of toxic oxygen species *in vivo*. *J. Biol. Chem.* 271: 12275–12280.
- Longo, V. D., Liou, L. L., Valentine, J. S., Gralla, E. B. (1999). Mitochondrial superoxide decreases yeast survival in stationary phase. *Arch. Biochem. Biophys.* 365: 131-142.
- Macomber, L., Imlay, J. A. (2009). The iron-sulfur clusters of dehydratases are primary intracellular targets of copper toxicity. *Proc. Natl. Acad. Sci. USA.* 106: 8344-8349.
- Macomber, L., Rensing, C., Imlay, J. A. (2007). Intracellular copper does not catalyze the formation of oxidative DNA damage in *Escherichia. coli*. *J. Bacteriol.* 189: 1616–1626.
- Malkin, R., Rabinowitz, J. C. (1966). The reconstitution of clostridial ferredoxin. *Biochem. Biophys. Res. Commun.* 23: 822–827.
- Manda, G., Nechifor, M. T., Neagu, T. M. (2009). Reactive oxygen species, cancer and anti-cancer therapies. *Curr. Chem. Biol.* 3: 342-366.
- Marchler, G., Schuller, C., Adam, G., Ruis, H. (1993). A *Saccharomyces cerevisiae* UAS element controlled by protein kinase A activates transcription in response to a variety of stress conditions. *Embo. J.* 12: 1997-2003.
- Margoshes, M., Vallee, B. L. (1957). A cadmium protein from equine kidney cortex. *J. Am. Chem. Soc.* 79: 4813-4814.
- Mariani, E., Polidori, M.C., Cherubini, A., Mecocci, P.(2005).Oxidative stress in brain aging, neurodegenerative and vascular diseases: An overview. *J. Chromatogr. B.* 827: 65–75.
- Maritim, A. C., Sanders, R. A., Watkins, J. B. (2003). Diabetes, oxidative stress, and antioxidants. *Rev. j. Biochem. Mol. Toxicol.* 17: 24-38.
- Maroz, A., Anderson, R. F., Smith, R. A., Murphy, M. P. (2009). Reactivity of ubiquinone and ubiquinol with superoxide and the hydroperoxyl radical: implications for *in vivo* antioxidant activity. *Free. Radic. Biol. Med.* 46: 105-109.

- Martinand, C., Salehzada, T., Silhol, M., Lebleu, B., Bisbal, C. (1998). The 2-5 A /RNase L pathway in encephalomyocarditis-virus-(EMCV)-infected cells. *Fur. J. Biochem.* 254: 248-55.
- Martinez, A., Portero-Otin, M., Pamplona, R., Ferrer, I. (2010). Protein targets of oxidative damage in human neurodegenerative diseases with abnormal protein aggregates. *Brain. Pathol.* 20: 281–297.
- Martins, V., Manfredini, V., Benfato, M. S. (2005). High levels of catalase in SOD mutants of *Saccharomyces cerevisiae* in high aeration conditions. *Brazilian. J. Microbiol.* 36: 347-351.
- Mascarenhas, C., Edwards-Ingram, L. C., Zeef, L., Shenton, D., Ashe, M. P., Grant, C. M. (2008). Gcn4 is required for the response to peroxide stress in the yeast *Saccharomyces cerevisiae*. *Mol. Biol. Cell.* 19: 2995–3007.
- Mattie, M. D., Freedman, J. H. (2001). Protective effects of aspirin and vitamin E (α -tocopherol) against copper-and cadmium-induced toxicity. *Biochem. Biophys. Res. Commun.* 285: 921-925.
- Matuszewska, E., Kwiatkowska, J., Kuczynska-Wisnik, D., Laskowska, E. (2008). *Escherichia coli* heat-shock proteins IbpA/B are involved in resistance to oxidative stress induced by copper. *Microbiol.* 154: 1739–1747.
- May, J. M., Qu, Z. C., Mendiratta, S. (1998). Protection and recycling of alpha-tocopherol in human erythrocytes by intracellular ascorbic acid. *Arch. Biochem. Biophys.* 349: 281–289.
- McCord, J. M., Keele, B., Fridovich, I. (1971). An enzyme based theory of obligate anaerobiosis: the physiological function of SOD. *Proc. Natl. Acad. Sci.* 68: 1024–1027.
- Medicherla, B., Goldberg, A. L. (2008). Heat shock and oxygen radicals stimulate ubiquitin-dependent degradation mainly of newly synthesized proteins. *J. Cell. Biol.* 182: 663–673.
- Mehta, J. L., Rasouli, N., Sinha, A. K., Molavi, B. (2006). Oxidative stress in diabetes: a mechanistic overview of its effects on atherogenesis and myocardial dysfunction. *Int. J. Bio. Chem. Cell. Bio.* 38: 794–803.
- Mendez, J. I., Nicholson, W. J., Taylor, W. R. (2005). SOD isoforms and signaling in blood vessels: evidence for the importance of ROS compartmentalization. *Arterioscler. Thromb. Vasc. Biol.* 25: 887-888.
- Mesecke, N., Spang, A., Deponte, M., Herrmann, J. M. (2008). A novel group of glutaredoxins in the cis-Golgi critical for oxidative stress resistance. *Mol. Biol. Cell.* 19: 2673–2680.

- Mesecke, N., Terziyska, N., Kozany, C., Baumann, F., Neupert, W., Hell, K., Herrmann, J. M. (2005). A disulfide relay system in the intermembrane space of mitochondria that mediates protein import. *Cell*. 121: 1059–1070.
- Meyer, J. (2008). Iron-sulfur protein folds, iron-sulfur chemistry, and evolution. *J. Biol. Inorg. Chem.* 13: 157–170.
- Miao, R., Kim, H., Koppolu, U. M., Ellis, E. A., Scott, R. A., Lindahl, P. A. (2009). Biophysical characterization of the iron in mitochondria from Atm1p-depleted *Saccharomyces cerevisiae*. *Biochem.* 48: 9556-9568.
- Milkereit, P., Strauss, D., Bassler, J., Gadai, O., Kuhn, H., Schutz, S., Gas, N., Lechner, J., Hurt, E., Tschochner, H. (2003). A Noc complex specifically involved in the formation and nuclear export of ribosomal 40 S subunits. *J. Biol. Chem.* 278: 4072-4081.
- Mills, G. C. (1957). Hemoglobin catabolism. I. Glutathione peroxidase, an erythrocyte enzyme which protects hemoglobin from oxidative breakdown. *J. Biol. Chem.* 229: 189–197.
- Mnaimneh, S., Davierwala, A.P., Haynes, J., Moffat, J., Peng, W.-T., Zhang, W., Yang, X., Pootoolal, J., Chua, G., Lopez, A., Trochesset, M., Morse, D., Krogan, N.J., Hiley, S.L., Li, Z., Morris, Q., Grigull, J., Mitsakakis, N., Roberts, C.J., Greenblatt, J.F., Boone, C., Kaiser, C.A., Andrews, B.J., Hughes, T.R. (2004). Exploration of essential gene functions via titratable promoter alleles. *Cell*. 118: 31-44.
- Mohora, M., Greabu, M., Muscurel, C., Duja, C., Totan, A. (2007). The sources and the targets of oxidative stress in the etiology of diabetic complications. *J. Bio. Phys.* 17: 63-84.
- Morimoto, N., Miyazaki, K., Kurata, T., Ikeda, Y., Matsuura, T., Kang, D., Ide, T., Abe, K. (2012). Effect of mitochondrial transcription factor a overexpression on motor neurons in amyotrophic lateral sclerosis model mice. *J. Neurosci. Res.* 90: 1200–1208.
- Moskovitz, J., Berlett, B. S., Poston, J. M., & Stadtman, E. (1997). The yeast peptide-methionine sulphoxide reductase functions as an antioxidant *in vivo*. *Proc. Natl. Acad. Sci. USA.* 94: 9585-9589.
- Moskovitz, J., Flescher, E., Berlett, B. S., Azare, J., Poston, J. M., Stadtman, E. R. (1998). Overexpression of peptide-methionine sulfoxide reductase in *Saccharomyces cerevisiae* and human T cells provides them with high resistance to oxidative stress. *Proc. Natl. Acad. Sci. USA.* 95: 14071–14075.

- Muhlenhoff, U., Gerber, J., Richhardt, N., Lill, R. (2003). Components involved in assembly and dislocation of iron-sulfur clusters on the scaffold protein Isu1p. *Embo. J.* 22: 4815–4825.
- Muhlenhoff, U., Lill, R. (2000). Biogenesis of iron-sulfur proteins in eukaryotes: a novel task of mitochondria that is inherited from bacteria. *Biochem. Biophys. Acta.* 1459: 370-82.
- Nangle, L. A., Motta, C. M., Schimmel, P. (2006). Global effects of mistranslation from an editing defect in mammalian cells. *Chem.Biol.* 13: 1091-1100.
- Nayvelt, I., Hyvonen, M. T., Alhonen, L., Pandya, I., Thomas, T., Khomutov, A. R., Vepsalainen, J., Patel, R., Keinanen, T. A., Thomas, T. J. (2010). DNA condensation by chiral alpha-methylated polyamine analogues and protection of cellular DNA from oxidative damage. *Bio. macro. molecu.* 11: 97-105.
- Netz, D. J., Pierik, A. J., Stümpfig, M., Mühlenhoff, U., Lill, R. (2007). The Cfd1-Nbp35 complex acts as a scaffold for iron-sulfur protein assembly in the yeast cytosol. *Nat. Chem. Biol.* 3: 278–286.
- Netz, D. J., Stith, C. M., Pierik, A. J. (2012). Eukaryotic DNA polymerases require an iron-sulfur cluster for the formation of active complexes. *Nat. Chem. Biol.* 8: 125-132.
- Nicolet, Y., Rohac, R., Martin, L., Fontecilla-Camps, J. C. (2013). X-ray snapshots of possible intermediates in the time course of synthesis and degradation of protein-bound Fe₄S₄ clusters. *Proc. Natl. Acad. Sci.* 110: 7188-7192.
- Nissan, T. A., Baszler, J., Petfalski, E., Tollervey, D., Hurt, E. (2002). 60S pre-ribosome formation viewed from assembly in the nucleolus until export to the cytoplasm. *Embo. J.* 21: 5539–5547.
- Nordstrand, K., Aslund, F., Holmgren, A., Otting, G., Berndt, K. D. (1999). NMR structure of *Escherichia coli* glutaredoxin 3-glutathione mixed disulfide complex: implications for the enzymatic mechanism. *J. Mol. Biol.* 286: 541-552.
- Nystrom, T. (2005). Role of oxidative carbonylation in protein quality control and senescence. *Embo. J.* 24: 1311–1317.
- Ogle, J. M., Brodersen, D. E., Clemons, W. M., Tarry, M. J., Carter, A. P., Ramakrishnan, V. (2001). Recognition of cognate transfer RNA by the 30S ribosomal subunit. *Sci.* 292: 897–902.
- Ogle, J. M., Ramakrishnan, V. (2005). Structural insights into translational fidelity. *Annu. Rev. Biochem.* 74: 129–177.

- Oliver, S., Eva, F. (2009). Spectroscopic characterization of Cicer arietinum metallothionein1. *Inorganica. Chimica. Acta.* 362: 714-724.
- Othumpangat, S., Kashon, M., Joseph, P. (2005). Eukaryotic translation initiation factor 4E is a cellular target for toxicity and death due to exposure to cadmium chloride. *J. Biol. Chem.* 1280: 25162-25169.
- Parent, S. A., Bostian, K. A. (1995). Recombinant DNA technology: yeast vectors, p. 121-178. In Wheals, A. E., Rose, A. H., Harrison, J. S. *The yeasts. 6. Yeast genetics.* Acad. Press. London. U. K.
- Park, S., You, X., Imlay, J. A. (2005). Substantial DNA damage from submicromolar intracellular hydrogen peroxide detected in Hpx-mutants of *Escherichia coli*. *Proc. Natl. Acad. Sci. USA.* 102: 9317-9322.
- Pekmezci, D. (2011). Vitamins and the immune system: Vitamin E and immunity. ISBN: 978-0-12-386960-9. 86: 179-215.
- Penkowa, M., Keller, P., Keller, C., Hidalgo, J., Giralt, M., Pedersen, B. K. (2005). Exercise-induced metallothionein expression in human skeletal muscle fibres. *Exp. Physiol.* 90: 477-486.
- Pinto, E., Sigaud-Kutner, T.C.S., Leitao, M.A., Okamoto, O.K., Morse, D., Colepicolo, P. (2003). Heavy metal-induced oxidative stress in algae. *J. Phycol.* 39: 1008-1018.
- Pisarev, A. V., Hellen, C. U., Pestova, T. V. (2007). Recycling of eukaryotic posttermination ribosomal complexes. *Cell.* 131: 286-299.
- Pisarev, A. V., Skabkin, M. A., Skabkin, M. A., Pisareva, V. P., Pisareva, V. P., Skabkina, O. V., Skabkina, O. V., Rakotondrafara, A. M., Rakotondrafara, A. M., Hentze, M. W., Hentze, M. W., Hellen, C. U. T., Hellen, C. U. T., Pestova, T. V., Pestova, T. V. (2010). The role of ABCE1 in eukaryotic posttermination ribosomal recycling. *Mol. Cell.* 37: 196-210.
- Pisareva, V. P., Skabkin, M. A., Hellen, C. U., Pestova, T. V., Pisarev, A. V. (2011). Dissociation by pelota, Hbs1 and ABCE1 of mammalian vacant 80S ribosomes and stalled elongation complexes. *Embo. J.* 30: 1804-1817.
- Priault, M., Bessoule, J. J., Grelaud-Coq, A., Camougrand, N. and Manon, S. (2002). Bax-induced cell death in yeast depends on mitochondrial lipid oxidation. *Eur. J. Biochem.* 269: 5440-5450.

- Pringle, J. R., Preston, R. A., Adams, A. E. M., Stearns, T., Drubin, D. G., Haarer, B. K., Jones, E. W. (1989). Fluorescence microscopy methods for yeast. *Methods. Cell. Biol.* 31: 357-435.
- Py, B., Moreau, P. L., Barras, F. (2011). Fe-S clusters, fragile sentinels of the cell. *Curr. Opin. Micro. Biol.* 14: 218-223.
- Qiu, X., Brown, K., Hirschey, M. D., Verdin, E., Chen, D. (2010). Calorie restriction reduces oxidative stress by SIRT3-mediated SOD2 activation. *Cell. Metab.* 12: 662-667.
- Rand, J., Grant, C. M. (2006). The thioredoxin system protects ribosomes against stress-induced aggregation. *Mol. Cell.* 17: 387-401.
- Ranquet, C., Ollagnier-de-Choudens, S., Loiseau, L., Barras, F., Fontecave, M. (2007). Cobalt stress in *Escherichia coli*: the effect on the iron-sulfur proteins. *J. Biol. Chem.* 282: 30442-30451.
- Rao, A. K., Ziegler, Y. S., Mcleod, I. X., Yates, J. R., Nardulli, A. M. (2008). Effects of Cu/Zn superoxide dismutase on estrogen responsiveness and oxidative stress in human breast cancer cells. *Mol. Endocrinol.* 22: 1113-1124.
- Raulfs, E. C., O'Carroll, I. P., Dos Santos, P. C., Unciuleac, M. C., Dean, D. R. (2008). *In vivo* iron sulfur cluster formation. *Proc. Natl. Acad. Sci. USA.* 105: 8591-8596.
- Reddi, A. R., Jensen, L. T., Naranuntarat, A., Rosenfeld, L., Leung, E., Shah, R., Culotta, V. (2009). The overlapping roles of manganese and Cu/Zn SOD in oxidative stress protection. *Free. Radic. Biol. Med.* 46: 154-162.
- Reed, T. T. (2011). Lipid peroxidation and neurodegenerative disease. *Free. Radic. Biol. Med.* 51: 1302-1319.
- Reekmans, R., Smet, K. D., Chen, C., Hummelen, P. V., Contreras, R. (2005). Old yellow enzyme interferes with Bax-induced NADPH loss and lipid peroxidation in yeast. *Fems. Yeast. Res.* 5: 711-725.
- Reinheckel, T., Sitte, N., Ullrich, O., Kuckelkorn, U., Davies, K. J. A., Grune, T. (1998). Comparative resistance of the 20S and 26S proteasome to oxidative stress. *Biochem. J.* 335: 637-642.
- Rice-Evans, C. A., Burdon, R. H. (1994). *New comprehensive biochemistry: free radical damage and its control.* 28. Elsevi. Sci. Amsterdam.
- Rider, J. E., Hacker, A., Mackintosh, C. A., Pegg, A. E., Woster, P. M., Casero, R. A. (2007). Spermine and spermidine mediate

- protection against oxidative damage caused by hydrogen peroxide. *Amino. Acids* .33: 231-240.
- Roberts, R. A., Laskin, D. L., Smith, C. V., Robertson, F. M., Allen, E. M. G., Doorn, J. A., Slikkerk, W. (2009). Nitrate and oxidative stress in toxicology and disease. *Toxicol. Sci.* 112: 4-16.
- Rodriguez-Manzanque, M. T., Tamarit, J., Belli, G., Ros, J., Herrero, E. (2002). Grx5 is a mitochondrial glutaredoxin required for the activity of iron/sulfur enzymes. *Mol. Biol. Cell.* 13: 1109-1121.
- Roy, A., Solodovnikova, N., Nicholson, T., Antholine, W., Walden, W. E. (2003). A novel eukaryotic factor for cytosolic Fe-S cluster assembly. *Embo. J.* 22: 4826-4835.
- Ruan, H., Tang, X. D., Chen, M. L., Joiner, M. L., Sun, G., Brot, N., Weissbach, H., Heinemann, S. H., Iverson, L., Wu, C. F., Hoshi, T. (2002). High-quality life extension by the enzyme peptide methionine sulfoxide reductase. *Proc. Natl. Acad. Sci. USA.* 99: 2748 -2753.
- Rudolf, J., Makrantonis, V., Ingledew, W. J., Stark, M. J., White, M. F. (2006). The DNA repair helicases XPD and FancJ have essential iron-sulfur domains. *Mol. Cell.* 23: 801-808.
- Ruzicka, F. J., Beinert, H. (1978). The soluble "high potential" type iron-sulfur protein from mitochondria is aconitase. *J. Biol. Chem.* 253: 2514-2517.
- Rypniewski, W. R., Breiter, D. R., Benning, M. M., Wesenberg, G., Oh, B. H., Markley, J. L., Rayment, I., Holden, H. M. (1991). Crystallization and structure determination to 2.5-Å resolution of the oxidized [2Fe-2S] ferredoxin isolated from *Anabaena* 7120. *Biochem.* 30: 4126-4131. Pdb 1fxa.
- Salmon, T. B., Evert, B. A., Song, B. W., Doetsch, P.W. (2004). Biological consequences of oxidative stress-induced DNA damage in *Saccharomyces cerevisiae*. *Nucleic. Acids. Res.* 32: 3712-3723.
- Sambrook, J., Fritsch, E. F., Maniatis, T. (1989). *Molecular cloning: a laboratory manual*. (2nd ed). 5: 72.
- Schafer, F. Q., Buettner, G. R. (2001). Redox environment of the cell as viewed through the redox state of the glutathione disulfide/glutathione couple. *Free. Radic. Biol. Med.* 30: 1191-1212.
- Schilke, B., Williams, B., Knieszner, H., Puksza, S., Silva, P. D., Craig, E. A., Marszalek, J. (2006). Evolution of mitochondrial chaperones utilized in Fe-S cluster biogenesis. *Curr. Biol.* 16: 1660-1665.

- Schneider, D., Schmidt, C. L. (2005). Multiple rieske proteins in prokaryotes: where and why?. *Biochim. Biophys. Acta* . 1710: 1-12.
- Schuller, C., Bauer, B. E., Kuchler, K. (2003). Inventory and evolution of fungal ABC protein genes. In *ABC Proteins: from bacteria to man*, Holland, B. I., Cole, S. P. C., Kuchler, K., Higgins, C. F (eds). pp: 279–293. Amsterdam: Academic. Press.
- Shadel, G. S. (1999). Yeast as a model for human mtDNA replication. *Am. J. Hum. Genet.* 65: 1230-1237.
- Sharma, P., Jha, A. B., Dubey, R.S., Pessaraki, M. (2012). Reactive oxygen species, oxidative damage, and antioxidative defense mechanism in plants under stressful conditions. *J. Botan.* 2012: 26.
- Sharov, V. S., Ferrington, D. A., Squier, T.C., Schöneich, C. (1999). Diastereoselective reduction of protein-bound methionine sulfoxide by methionine sulfoxide reductase. *Febs. Lett.* 455: 247–250.
- Sharov, V. S., Schöneich, C. (2000). Diastereoselective protein methionine oxidation by reactive oxygen species and diastereoselective repair by methionine sulfoxide reductase. *Free. Radic. Biol. Med.* 29: 986–994.
- Sheff, M. A., Thorn, K. S. (2004). Optimized cassettes for fluorescent protein tagging in *Saccharomyces cerevisiae*. *Yeast.* 21.8: 661-670.
- Sheftel, A., Stehling, O., Lill, R. (2010). Iron–sulfur proteins in health and disease. *Trends. Endocrinology. Metabolism.* 21: 302–314.
- Shen, S., Callaghan, D., Juzwik, C., Xiong, H., Huang, P., Zhang, W. (2010). ABCG2 reduces ROS-mediated toxicity and inflammation: a potential role in Alzheimer's disease. *J. Neuro. Chem.* 114: 1590-604.
- Shenton, D., Smirnova, J. B., Selley, J. N., Carroll, K., Hubbard, S. J., Pavitt, G. D., Ashe, M. P., Grant, C. M. (2006). Global translational responses to oxidative stress impact upon multiple levels of protein synthesis. *J. Biol. Chem.* 281: 29011–29021.
- Shestivska, V., Adam, V., Prasek, J., Macek, T., Mackova, M., Havel, L., Diopan, V., Zehnalek, J., Hubalek, J., Kizek, R. (2011). Investigation of the antioxidant properties of metallothionein in transgenic tobacco plants using voltammetry at a carbon paste electrode. *Int. J. Electro. Chem. Sci.* 6: 2869-2883.

- Shimpuku, H., Tachi, Y., Shinohara, M., Ohura, K. (2000). Effect of vitamin E on the degradation of hydrogen peroxide in cultured human umbilical vein endothelial cells. *Life. Sci.* 68: 353–359.
- Shoemaker, C. J., Eyler, D. E., Green, R. (2010). Dom34:Hbs1 promotes subunit dissociation and peptidyl-tRNA drop-off to initiate no-go decay. *Sci.* 330: 369-372.
- Shoemaker, C. J., Green, R. (2011). Kinetic analysis reveals the ordered coupling of translation termination and ribosome recycling in yeast. *Proc. Natl. Acad. Sci. USA.* 108: E1392–E1398.
- Sideri, T. C. (2007). Role of MSR activity and protein aggregation in metal toxicity in yeast. PhD thesis. University of Nottingham.
- Sideri, T. C., Willetts, S. A., Avery, S. V. (2009). Methionine sulphoxide reductases protect iron-sulphur clusters from oxidative inactivation in yeast. *Microbiol.* 155: 612-623.
- Sies, H. (1997). "Oxidative stress: oxidants and antioxidants. *Experimental. Physio.* 82: 291-295.
- Silva, R., Duarte, I., Paredes, J., Lima-Costa, T., Perrot, M., Boucherie, H., Goodfellow, B., Gomes, A., Mateus, D., Moura, G., Santos, M. (2009). The yeast PNC1 longevity gene is up-regulated by mRNA mistranslation. *Plos. One.* 4: e5212.
- Silverman, R.H. (2007). Viral encounters with OAS and RNase L during the IFN antiviral response. *J. Virol.* 10: 01471-07.
- Skoneczny, M., Chelstowska, A., Rytka, J. (1988). Study of the coinduction by fatty acids of catalase A and acyl-CoA oxidase in standard and mutant *Saccharomyces cerevisiae* strains. *Eur. J. Biochem.* 174: 297-302.
- Sonntag, V. (1987). *The chemical basis of radiation biology.* Taylor and Francis. New York.
- Srinivasan, V., Netz D. J., Webert H., Mascarenhas J., Pierik A. J., Michel H., Lill R. (2007). Structure of the yeast WD40 domain protein Cia1, a component acting late in iron-sulfur protein biogenesis. *Structure.* 15: 1246–1257.
- Stade, K., Ford, C. S., Guthrie, C., Weis, K. (1997). Exportin 1 (Crm1p) is an essential nuclear export factor. *Cell.* 90: 1041–1050.
- Stadtman, E. R. (2001). Protein oxidation in aging and age-related diseases. *Ann. N. Y. Acad. Sci.* 928: 22-38.

- Stadtman, E. R., Remmen, H. V., Richardson, A., Wehr, N. B., & Levine, R. L. (2005). Methionine oxidation and aging. *Biochem. Biophys. Acta.* 1703: 135-140.
- Stavreva, D. A., Kawasaki, M., Dundr, M., Koberna, K., Muller, W. G., Tsujimura-Takahashi, T., Komatsu, W., Hayano, T., Isobe, T., Raska, I, Misteli, T., Takahashi, N., McNally, J. G. (2006). Potential roles for ubiquitin and the proteasome during ribosome biogenesis. *Mol. Cell. Biol.* 26: 5131-5145.
- Stephen, D. W. S., Jamieson, D. J. (1996). Glutathione is an important antioxidant molecule in the yeast *Saccharomyces cerevisiae*. *Fems. Microbiol. Lett.* 141: 207-212.
- Stoyanovsky, D. A., Osipov, A. N., Quinn, P. J., Kagan, V. E. (1995). Ubiquinone-dependent recycling of vitamin-E radicals by superoxide. *Arch. Biochem. Biophys.* 323: 343-351.
- Sumner, E. R., Avery, A. M., Houghton, J. E., Robins, R. A., Avery, S. V. (2003). Cell cycle- and age-dependent activation of Sod1p drives the formation of stress resistant cell subpopulations within clonal yeast cultures. *Mol. Microbiol.* 50: 857-870.
- Sumner, E. R., Shanmuganathan, A., Sideri, T. C., Willetts, S. A., Houghton, J. E., Avery, S. V. (2005). Oxidative protein damage causes chromium toxicity in yeast. *Microbiol.* 151: 1939-1948.
- Susani, M., Zimniak, P., Fessl, F., Ruis, H. (1976). Localization of catalase A in vacuoles of *Saccharomyces cerevisiae*: evidence for the vacuolar nature of isolated "yeast peroxisomes". *Hoppe Seylers Z Physiol. Chem.* 357: 961-970.
- Szaleczky, E., Prechl, J., Feher, J., Somogyi, A. (1999). Alterations in enzymatic antioxidant defence in diabetes mellitus-a rational approach. *Post. Med. J.* 75: 13-17.
- Tadolini, B. (1988). Polyamine inhibition of lipid peroxidation. *Biochem. J.* 249: 33-36.
- Taisuke, Y., Emiko, T., Hiroya, Y., Yasuyoshi, S. (2009). Yap1-regulated glutathione redox system curtails accumulation of formaldehyde and reactive oxygen species in methanol metabolism of *Pichia pastoris*. *Eukaryot. Cell.* 8: 540-549.
- Tamai, K. T., Gralla, E. B., Ellerby, L. M., Valentine, J. S., Thiele, D. J. (1993). Yeast and mammalian metallothioneins functionally substitute for yeast copper-zinc superoxide dismutase. *Proc. Natl. Acad. Sci. USA.* 90: 8013-8017.
- Tanaka, T., Izawa, S., Inoue, Y. (2005). GPX2, encoding a phospholipid hydroperoxide glutathione peroxidase homologue,

codes for an atypical 2-Cys peroxiredoxin in *Saccharomyces cerevisiae*. J. Biol. Chem. 280: 42078–42087.

- Tanaka, M., Chock, P. B., Stadtman, E. R. (2006). Oxidized messenger RNA induces translation errors. Proc. Natl. Acad. Sci. 104: 66-71.
- Thorpe, G.W., Fong, C.S., Alic, N., Higgins, V.J., Dawes, I.W. (2004). Cells have distinct mechanisms to maintain protection against different reactive oxygen species: oxidative-stress-response genes. Proc. Natl. Acad. Sci. USA. 101: 6564-6569.
- Tong, W. H., Rouault, T. A. (2006). Functions of mitochondrial ISCU and cytosolic ISCU in mammalian iron-sulfur cluster biogenesis and iron homeostasis. Cell. Metab. 3: 199–210.
- Tonks, N. K. (2006). Protein tyrosine phosphatases: from genes, to function, to disease. Nat. Rev. Mol. Cell. Biol. 7: 833–846.
- Tracey, A. R., Tong, W. H. (2008). Iron-sulfur cluster biogenesis and human disease. Rev. Cell. press. 24: 398-407.
- Tracey, A., Rouault, T.A., Tong, W. H. (2008). Iron-sulfur cluster biogenesis and human disease. Rev. Mol. Med. Genet. 24: 398-407.
- Trachootham, D., Alexander, J., Huang, P. (2009). Targeting cancer cells by ROS-mediated mechanisms: a radical therapeutic approach. Nat. Rev. 8: 579-591.
- Trachootham, D., Lu, W., Ogasawara, M. A., Valle, N.R-D., Huang, P. (2008). Redox regulation of cell survival. Antiox. Redox. Signal. 10: 1343-1374.
- Tseng, H. J., Srikhanta, Y., McEwan, A. G., Jennings, M. P. (2001). Accumulation of manganese in *Neisseria gonorrhoeae* correlates with resistance to oxidative killing by superoxide anion and is independent of superoxide dismutase activity. Mol. Microbiol. 40: 1175–1186.
- Tsuboi, T., Kuroha, K., Kudo, K., Makino, S., Inoue, E., Kashima, I., Inada, T. (2012). Dom34:hbs1 plays a general role in quality-control systems by dissociation of a stalled ribosome at the 3' end of aberrant mRNA. Mol. Cell. 46. 4: 518-529.
- Tudek, B., Speina, E. (2012). Oxidatively damaged DNA and its repair in colon carcinogenesis. Mut. Res. 736: 82-92.
- Tudek, B., Winczura, A., Janik, J., Siomek, A., Foksinski, M., Olinski, R. (2010). Involvement of oxidatively damaged DNA and repair in cancer development and aging. Am. J. Transl. Res. 2: 254-284.

- Unciuleac, M. C., Chandr, A.K., Nailk, S., Mayer, S., Huynh, B. H., Johnson, M. K., Dean, D. R. (2007). *In vitro* activation of apo-aconitase using a [4Fe-4S] cluster-loaded form of the IscU [Fe-S] cluster scaffolding protein. *J. Biochem.* 46: 6812–6821.
- Valasek, L., Hasek, J., Nielsen, K. H., Hinnebusch, A. G. (2001). Dual function of eIF3j/Hcr1p in processing 20S pre-rRNA and translation initiation. *J. Biol. Chem.* 276: 43351–43360.
- Varghese, S. M., Tang, Y., Imlay, J. A. (2003). Contrasting sensitivities of *Escherichia coli* aconitases A and B to oxidation and iron depletion. *J. Bacteriol.* 185: 221-230.
- Viarengo, A., Burlando, B., Ceratto, N., Panfoli, I. (2000). Antioxidant role of metallothioneins: a comparative overview. *Cell. Mol. Biol.* 46: 407-417.
- Vijayanathan, V., Thomas, T., Thomas, T.J. (2002). DNA nanoparticles and development of DNA delivery vehicles for gene therapy. *Bio. chem.* 41: 14085-14094.
- Vogt, W. (1995). Oxidation of methiononyl residues in proteins: tools, targets, and reversal. *Free. Radic. Biol. Medic.* 18: 93–105.
- Volbeda, A., Charon, M. H., Piras, C., Hatchikian, E. C., Frey, M., Fontecilla-Camps, J.C. (1995). Crystal structure of the nickel-iron hydrogenase from *Desulfovibrio gigas*. *Nat.* 373: 580-587.
- Wach, A., Brachat, A., Alberti-Segui, C., Rebischung, C., Philippsen, P. (1997). Heterologous *HIS3* marker and GFP reporter modules for PCR targeting in *Saccharomyces cerevisiae*. *Yeast.* 13: 1065-1075.
- Wallace, M. A., Liou, L. L., Martins, J., Clement, M. H. S., Bailey, S., Longo, V. D., Valentine, J. S., Gralla, E. B. (2004). Superoxide inhibits 4Fe-4S cluster enzymes involved in amino acid biosynthesis: cross-compartment protection by CuZn-superoxide dismutase. *J. Biol. Chem.* 279: 32055–32062.
- Wang, T., Craig, E. A. (2008). Binding of yeast frataxin to the scaffold for Fe-S cluster biogenesis. *Isu. J. Biol. Chem.* 283: 12674–12679.
- Waris, G., Ahsan, H. (2006). Reactive oxygen species: role in the development of cancer and various chronic conditions. *J. Carcinog.* 5: 14.
- Weisiger, R. A., Fridovich, I. (1973). Mitochondrial superoxide dismutase. Site of synthesis and intramitochondrial localization. *J. Biol. Chem.* 248: 4793-4796.

- Weissbach, H., Etienne, F., Hoshi, T., Heinemann, S. H., Lowther, W. T., Matthews, B., St. John, G., Nathan, C., Brot, N. (2002). Peptide methionine sulfoxide reductase: structure, mechanism of action, and biological function. *Arch. Biochem. Biophys.* 397: 172–178.
- Weissbach, H., Resnick, L., and Brot, N. (2005). Methionine sulfoxide reductases: history and cellular role in protecting against oxidative damage. *Biochim. Biophys. Acta.* 1703: 203-212.
- Wiedemann, N., Urzica, E., Guiard, B., Muller, H., Lohaus, C., Meyer, H. E., Ryan, M. T., Meisinger, C., Muhlenhoff, U., Lill, R., Pfanner, N. (2006) . Essential role of Isd11 in iron-sulfur cluster synthesis on Isu scaffold proteins. *Embo. J.* 25: 184–195.
- Williams, M. D., Remmen, H. V., Conrad, C. C., Huang, T. T., Epstein, C. J., Richardson, A. (1998). Increased oxidative damage is correlated to altered mitochondrial function in heterozygous manganese superoxide dismutase knockout mice. *J. Biol. Chem.* 273: 28510-28515.
- Wilson, F. H., Hariri, A., Farhi, A., Zhao, H., Petersen, K. F., Toka, H. R., Nelson-Williams, C., Raja, K. M., Kashqarian, M., Shulman, G. I., Scheinman, S. J., Lifton, R. P. (2004). A cluster of metabolic defects caused by mutation in a mitochondrial tRNA. *Sci.* 306: 1190-1194.
- Wingert, R. A., Galloway, J. L., Barut, B., Foott, H., Fraenkel, P., Axe, J. L., Weber, G. J., Dooley, K., Davidson, A. J., Schmid, B., Paw, B. H., Shaw, G. C., Kingsley, P., Palis, J., Schubert, H., Chen, O., Kaplan, J., Zon, L. I. (2005). Deficiency of *glutaredoxin 5* reveals Fe–S clusters are required for vertebrate haem synthesis. *Nat.* 436: 1035-1039.
- Winterbourn, C. C. (2008). Reconciling the chemistry and biology of reactive oxygen species. *Nat. Chem. Biol.* 4: 278-286.
- Winzler, E. A., Shoemaker, D. D., Astromoff, A., Liang, H., Anderson, K., Andre, B., Bangham, R., Benito, R., Boeke, J. D., Bussey, H., Chu, A. M., Connelly, C., Davis, K., Dietrich, F., Dow, S. W., El Bakkoury, M., Foury, F., Friend, S. H., Gentalen, E., Giaever, G., Hegemann, J. H., Jones, T., Laub, M., Liao, H., Liebundguth, N., Lockhart, D. J., Lucau-Danila, A., Lussier, M., M'Rabet, N., Menard, P., Mittmann, M., Pai, C., Rebischung, C., Revuelta, J. L., Riles, L., Roberts, C. J., Ross-MacDonald, P., Scherens, B., Snyder, M., Sookhai-Mahadeo, S., Storms, R. K., Veronneau, S., Voet, M., Volckaert, G., Ward, T. R., Wysocki, R., Yen, G. S., Yu, K., Zimmermann, K., Philippsen, P., Johnston, M., Davis, R. W. (1999). Functional characterization of the *S. cerevisiae*

genome by gene deletion and parallel analysis. *Sci.* 285: 901–906.

- Winter, J., Ilbert, M., Graf, P.C., Ozcelik, D., Jakob, U. (2008). Bleach activates a redox-regulated chaperone by oxidative protein unfolding. *Cell.* 135: 691–701.
- Woese, C., Fox, G. (1977). Phylogenetic structure of the prokaryotic domain: the primary kingdoms. *Proc. Natl. Acad. Sci. USA.* 74. 11: 5088-5090.
- Wolfe-Simon, F., Starovoytoy, V., Reinfelder, J. R., Schofield, O., Falkowski, P. G. (2006). Localization and role of manganese superoxide dismutase in a marine diatom. *Plant. Physio.* 142: 1701-1709.
- Yarunin, A., Panse, V., Petfalski, E., Tollervey, D., Hurt, E. (2005). Functional link between ribosome formation and biogenesis of iron-sulfur proteins. *Embo. J.* 24: 580-588.
- Young, I. S., McEneny, J. (2001). Lipoprotein oxidation and atherosclerosis. *Biochem. Soc. Trans.* 29: 358-362.
- Youseff, B. H., Holbrook, E. D., Smolnycki, K. A., Rappleye, C. A. (2012). Extracellular superoxide dismutase protects *Histoplasma* yeast cells from host-derived oxidative stress. *Plos. Pathog.* 8: e1002713.
- Yuen, K. S., Halliday, G. M. (1997). Alpha-tocopherol, an inhibitor of epidermal lipid peroxidation, prevents ultraviolet radiation from suppressing the skin immune system. *Photo. Chem. Photo. Biol.* 65: 587-592.
- Zhai, C., Li, Y., Mascarenhas, C., Lin, Q., Li, K., Vyrides, I., Grant, C.M., Panaretou, B. (2013). The function of ORAOV1/LTO1, a gene that is overexpressed frequently in cancer: essential roles in the function and biogenesis of the ribosome. *Onc.* 10. 1038.
- Zhang, X. H. (2010). Regulation of protein function by residue oxidation. *Proteomics. Insights:* 317–324.
- Zhang, X-H., Weissbach, H. (2008). Origin and evolution of the protein-repairing enzymes methionine sulphoxide reductases. *Biologic. Rev.* 83: 249–257.
- Zou, T., Rao, J. N., Liu, L., Xiao, L., Cui, Y. H., Jiang, Z., Ouyang, M., Donahue, J. M., Wang, J. Y. (2012). Polyamines inhibit the assembly of stress granules in normal intestinal epithelial cells regulating apoptosis. *Am. J. Phys. Cell. Phys.* 303: 102-111.